

2000

The thermal properties of cob buildings of Devon

Goodhew, Steven Michael Rhyder

<http://hdl.handle.net/10026.1/594>

<http://dx.doi.org/10.24382/3826>

University of Plymouth

All content in PEARL is protected by copyright law. Author manuscripts are made available in accordance with publisher policies. Please cite only the published version using the details provided on the item record or document. In the absence of an open licence (e.g. Creative Commons), permissions for further reuse of content should be sought from the publisher or author.

THE THERMAL PROPERTIES OF COB BUILDINGS OF DEVON

by

STEVEN MICHAEL RHYDER GOODHEW

**A thesis submitted to the University of Plymouth
in partial fulfilment for the degree of**

DOCTOR OF PHILOSOPHY

**School of Architecture
Faculty of Technology**

September 2000

Copyright Statement.

'This copy of the thesis has been supplied on condition that anyone who consults it is understood to recognise that its copyright rests with its author and that no quotation from the thesis and no information derived from it may be published without the author's prior consent.'

Steven Michael Rhyder Goodhew.

The Thermal Properties of Cob Buildings of Devon.

Abstract

Little has been published concerning the thermal properties of existing unbaked earth walls. In order to model the thermal behaviour of a building constructed using traditional cob walls, the thermal conductivity and thermal diffusivity need to be established.

The Centre for Earthen Architecture (CEA), based at the University of Plymouth's School of Architecture has carried out research into various aspects of cob architecture typical to the Devon area. This study supplements other work concerning the moisture content, structure and pathology of cob as a building material.

This research concentrates upon the development of a time dependent probe technique for the measurement of the thermal conductivity and thermal diffusivity of cob. The literature concerning the technique is reviewed. Methods of obtaining thermal data from the results are discussed. Particular emphasis is placed upon the measurement of the probe's thermal contact conductance with the test material. A series of laboratory tests and results from specific test materials are described. From this work, a link between the improvement of the thermal contact between the probe and the specimen and the accuracy of the thermal diffusivity values is established.

The development of field test apparatus is described and the results from three field tests are examined. Values for thermal conductivity, diffusivity and the probe thermal contact conductance are established. These results are used in a thermal simulation of a cob dwelling. The output from the simulation is compared with results from a modern timber-frame house of identical dimensions and use. The thermal response of the modern timber-frame house was found to be similar to that of the cob dwelling. However, generally, the range of internal air temperature was found to be higher in the interior spaces of the timber framed dwelling than the cob dwelling.

List of Contents

	Section
Copyright Statement.....	(II)
Abstract.....	(III)
List of Contents.....	(IV)
List of Illustrations.....	(VI)
List of Tables.....	(VI)
List of Graphs.....	(X)
Acknowledgements.....	(XIII)
Authors declaration.....	(XIV)
Nomenclature.....	(XV)
Glossary.....	(XVI)

Chapter	Page
1 Introduction to Unbaked Earth Materials.....	1
Description of the unbaked earth walling materials that are the main focus of the study.	
2 The Thermal Properties of Unbaked Earth Building.....	10
Materials.	
A review of work focusing upon the thermal behaviour of different earth walling systems.	
3 Review of literature concerning thermal.....	17
conductivity measurement methods including the thermal probe technique.	
A review of work concerning transient thermal conductivity measurement techniques including the time dependent	

thermal probe method.

4	Apparatus and procedure	29
	Description of the laboratory apparatus and conditions surrounding materials and probes.	
5	Measurement Theory	36
	Description of theory, results, time, power, probe conductance and other pertinent factors including the background behind the following techniques; * rate analysis, * long time analysis, * short time analysis, * iterative solutions.	
6	Laboratory measurements and results	55
	Tables of results with discussions concerning the representative nature of the measurements carried out upon the following materials: wax, glycerine, phenolic foam, lightweight aerated concrete block, cobblocks, mudstud and wychert.	
7	Field measurements and results	94
	Tables of results with brief discussions concerning the measurements carried out at the following field studies: cob barn, Rezare; a summerhouse, Bovey Tracey and a dwelling, Frogmire in Sandford, mid-Devon.	
8	Discussion	122
	A discussion of the results from the laboratory and field studies, with reference to the general aims and objectives of the research.	
9	Thermal modelling and results	135
	Review of previous simulations. Description of the two simulation models and internal conditions used. The results of modelling, graphs and diagrams.	
10	Conclusions and Future Work	146
	Discussion of the use of the probe technique in view of the previously stated aims. The validity of the in-situ/lab-based testing regimes. Debate around the results of the thermal modelling and recommendations as to the future direction of follow-on work.	
	References and Bibliography	156
	Appendix A	170

Explores the background and application of the Solver routine, found in the Microsoft Office Excel 97 spread sheet package, which was used to determine the thermal properties of some of the samples studied in this work.

Appendix B.....178

Diagram of the thermal probe.

List of Illustrations

Page

Figure 1.1 Marker Cottage..... 4

Figure 1.2 Demonstration cob wall..... 5

Figure 1.3 French rammed earth wall..... 6

Figure 1.4 Indian earth blocks..... 7

Figure 1.5 Example of wattle and daub construction.....8

Figure 2.1 The modifying effects of earth walling upon
external temperature variations..... 14

Figure 4.1 Diagram of probe and instrumentation..... 30

Figure 5.1 Summary of Laboratory and Field Measurements..... 37

Figure 7.1 Field equipment in cob barn, Rezare, NR Launceston.....95

Figure 7.2 Cob barn, Rezare, NR Launceston.....98

Figure 9.1 ModelIT CAD representation of the domestic model used for
the two simulations.....138

List of Tables

Page

Table 2.1 Shows the thermal characteristics of soils (Minke, 1994).....11

Table 3.1 Shows the dimensions, thermal properties and time intervals
for cylindrical probes (de Vries & Peck, 1958)..... 21

Table 5.1 Shows the results from the rate analysis of wax
(runcode Wx2t1400)..... 46

Table 5.2 Shows the range of variables used for Solver2..... 48

Table 5.3	Shows the results for the published and measured values of three thermal variables of glycerine compared with those obtained using Solver2 of the long time analysis expression.....	50
Table 5.4	Shows the range of variables, Solver4 on cobblock data.....	51
Table 6.1	Summary of long time analysis results for initial study of paraffin wax with single thermocouple and air filled probe.....	58
Table 6.2	Summary of long time thermal conductivity, paraffin wax, twin thermocouple probes.....	61
Table 6.3	Summary of the short time analysis, paraffin wax, twin thermocouple probe.....	62
Table 6.4	Shows the results of rate analysis for paraffin wax.....	63
Table 6.5	Summary of the rate analysis for paraffin wax.....	64
Table 6.6	Shows a summary of the long time analysis for the glycerine studies.....	67
Table 6.7	Summary of the Blackwell short time results for the glycerine.....	68
Table 6.8	Summary of long time analysis results, phenolic foam with a single thermocouple and air filled probe.....	70
Table 6.9	Summary of long time analysis results for phenolic foam with HTSP heat sink-filled probe.....	71
Table 6.10	Summary of the short time results, phenolic foam.....	73
Table 6.11	Shows the location of the different probe types in lightweight aerated concrete block shown in graphs 6.9 and 6.10.....	74
Table 6.12	Summary of the long time results of the laboratory studies of lightweight aerated concrete block.....	75
Table 6.13	Summary of short-time results, lightweight aerated concrete block.....	76

Table 6.13A	Summary of the measured results and published values of thermal properties of laboratory studies.....	77
Table 6.14	Summary of long time results for initial studies on mudstud walling with single thermocouple and air filled probe.....	79
Table 6.15	Summary of the long time results, of the laboratory studies, mudstud.....	80
Table 6.16	Summary of short time results, mudstud.....	81
Table 6.17	Summary of rate analysis studies on mudstud.....	82
Table 6.18	Summary of long time results for initial studies on wychert with single thermocouple air filled probe.....	83
Table 6.19	Summary of the long time analysis of the laboratory studies of wychert.....	84
Table 6.20	Summary of short time analysis results, wychert.....	85
Table 6.21	Summary of rate analysis studies on wychert.....	86
Table 6.22	Summary of long time results for initial studies of cob block with single thermocouple air filled probe.....	87
Table 6.23	Summary of long time results for initial studies of cobwool with single thermocouple air filled probe.....	87
Table 6.24	Summary of the long time results of the second series of measurements upon cob blocks.....	89
Table 6.25	Summary of the long time results for cobwool blocks.....	89
Table 6.26	Summary of the short time results, cob blocks.....	90
Table 6.27	Summary of the short time results, cobwool blocks.....	91
Table 6.28	Summary of the rate results, cobwool blocks.....	92
Table 6.29	Summary of mean thermal conductivity and diffusivity values from the laboratory work.....	93

Table 7.1	Summary of the Rezare studies.....	99
Table 7.2	Summary of the long time results, Rezare.....	101
Table 7.3	Summary of the short time results, Rezare.....	102
Table 7.4	Shows the input values of the three parameters for Solver2 routine, Rezare cob.....	103
Table 7.5	Shows the typical Solver2 values for Rezare cob.....	103
Table 7.6	Summary of the values generated by Solver2 iterative routine for Rezare cob.....	104
Table 7.7	Summary of the summerhouse measurements series.....	106
Table 7.8	Summary of the long time results for the Bovey studies.....	106
Table 7.9	Shows the short time results for Bovey cob.....	108
Table 7.10	Shows the Excel Solver2 values which influence graph 7.9,.....	109
Table 7.11	Summary of the Solver2 results for Bovey cob, series 2.....	110
Table 7.12	Summary of the heater power and probe conditions for the measurements undertaken at Frogmire.....	112
Table 7.13	Summary of the long time results, Frogmire.....	115
Table 7.14	Summary of the short time results , Frogmire.....	117
Table 7.15	Shows the values used in Solver2 to generate, Table 7.16.....	118
Table 7.16	Shows the chosen values using Solver2.....	118
Table 7.17	Summary of the Solver2 values for Frogmire cob.....	119
Table 7.18	Summary of the best values using the long and short time methods for the three field studies.	121
Table 8.1	Summary of the thermal properties of the field test results.....	131
Table 9.1	Summary of the minimum, maximum and mean air temperatures from the two models simulated using Apache Sim...	144
Table 10.1	Summary of the results from the laboratory and field studies.....	152

List of Graphs

Page

Graph 5.1	Shows typical long time behaviour, phenolic foam.....	41
Graph 5.2	Shows the typical short time analysis for cob block with HTSP heat sink material in the sample hole and in the probe.....	43
Graph 5.3	Shows the rate of change of probe temperature as a function of probe to specimen temperature difference.....	45
Graph 5.4	Shows an Iterative solution showing theoretical and measured data for glycerine using Excel Solver2.....	49
Graph 5.5	Shows an Iterative solution using Excel Solver 4, coblock, theoretical and measured data for an air filled probe.....	52
Graph 6.1	Shows the variation of measured thermal conductivity of paraffin wax with maximum probe temperature.....	58
Graph 6.2	Shows the long time behaviour of twin thermocouple probes in wax with various 'fillings'.....	60
Graph 6.3	Shows a typical rate analysis of paraffin wax.....	63
Graph 6.4	Shows the probe conductance, H, from the rate analysis, variation with heater power, paraffin wax.....	65
Graph 6.5	Shows the long time behaviour, glycerine.....	67
Graph 6.6	Shows the Blackwell short time analysis parameter Y against root t, glycerine.....	68
Graph 6.7	Shows a typical long time result, phenolic foam.....	71
Graph 6.8	Shows a typical short time analysis for phenolic foam.....	72
Graph 6.9	Shows the long time behaviour of an air filled probe and heat-sink filled probe in a lightweight aerated concrete block.....	74
Graph 6.10	Shows the long time behaviour of the probes shown in graph 6.9, interchanged in the same lightweight aerated	

	concrete block.....	75
Graph 6.11	Shows the short time behaviour, lightweight aerated concrete block, heat sink material in probe and hole.....	76
Graph 6.12	Shows the variation of thermal conductivity of mudstud with heater power.	78
Graph 6.13	Shows the long time behaviour of mudstud block with heat sink material in the probe and hole.	80
Graph 6.14	Shows the short time analysis, mud-stud.....	81
Graph 6.15	Shows a long time behaviour, wychert, HTSP heat sink in the probe and in the hole.....	84
Graph 6.16	Shows the short time analysis, whycert, HTSP heat sink in the probe and the hole.....	84
Graph 6.17	Shows the long time behaviour of a cob block, combinations of heat sink material in the probe and the hole.....	88
Graph 6.18	Shows the short time analysis of cob blocks with heat sink material in various positions.....	90
Graph 7.1	Shows the ambient and probe temperature variations during a typical field test.....	96
Graph 7.2	Shows a range of long time analysis curves measured using different heater power settings.....	96
Graph 7.3	Shows the rise in probe temperature fluctuating at low probe heater settings.....	97
Graph 7.4	Shows a typical long time behaviour, field study, Rezare.....	100
Graph 7.5	Shows the short time analysis, Rezare.....	101
Graph 7.6	Shows Solver2 results, Rezare field study.....	104
Graph 7.7	Shows the effects of introducing heat-sink material, short time analysis,	

	within the probes and test holes Bovey cob.....	107
Graph 7.8	Shows the measured values matched against the Solver2 values with a probe conductance of $198 \text{ W m}^{-2}\text{K}^{-1}$, Bovey cob.....	109
Graph 7.9	Shows the long time curves for two probes each with different fillings, Frogmire.....	113
Graph 7.10	Shows the long time behaviour for air filled interchanged probes Frogmire.....	114
Graph 7.11	Shows a probe filled with heat sink compound, sample hole with and without heat sink compound , Frogmire.....	115
Graph 7.12	Shows the short time analysis, different heat-sink fillings in probes, Frogmire.....	116
Graph 7.13	Shows Solver2 solution against measured data for Frogmire cob.....	119
Graph 8.1	Shows a comparison of the field measurements with published data, indicating various thermal conductivities at different densities.....	132
Graph 9.1	Shows the internal downstairs air temperatures for the cob and timber frame models over a six month period.....	141
Graph 9.2	Shows a comparison of upstairs and down stairs, January, internal air temperatures for the cob model.....	142
Graph 9.3	Shows a comparison of upstairs and down stairs, January, internal air temperatures timber frame model.....	142
Graph 9.4	Shows a comparison of upstairs and down stairs, July, internal air temperatures for the cob model.....	143
Graph 9.5	Shows a comparison of upstairs and down stairs, July, internal air temperatures, timber frame model.....	144

Acknowledgements

I am most grateful to my supervisor and director of studies, Dr Richard Griffiths for his knowledgeable advice and vital encouragement throughout this study.

I would like to thank Linda Watson and Dave Short for opportunities to better my knowledge of cob buildings and for general advice. I am also grateful for the advice and support of my colleagues during the research, especially Paul Murray who assisted in many ways.

Finally, I am indebted to my family who may be seeing more of me.

Author's Declaration.

At no time during the registration for the degree of Doctor of Philosophy has the author been registered for any other University award.

Relevant seminars and conferences were attended at which work was presented. A visit was made in April 1997 to ENTEPE, Lyons, France to investigate different methods of obtaining the thermal conductivity of building materials.

Presentations:

"The reasoning behind the Investigation into Thermal Properties of Cob Walling." Out of Earth II, Dartington May 1995.

Conferences Attended:

Out of Earth, Dartington, May 1994.

Out of Earth II, Dartington May 1995.

Papers Presented:

"Some Preliminary Studies of the Thermal Properties of Devon Cob Walls." Terra 2000, (8th International Conference on the Study and Conservation of Earthen Architecture).

English Heritage, May 2000.

Signed.....

Date.....

Nomenclature

λ is the thermal conductivity of the specimen, $\text{Wm}^{-1}\text{K}^{-1}$,

α is the thermal diffusivity of the studied material, m^2s^{-1} ,

H is the outer conductivity of the probe, $\text{Wm}^{-1}\text{K}^{-1}$,

Q is the heat supplied per unit length of probe, Wm^{-1} ,

t is the elapsed time of the measurement in seconds,

θ is the temperature of the probe, K

m is the mass per unit length of the probe, kgm^{-1} ,

c is the specific heat capacity of the probe, $\text{Jkg}^{-1}\text{K}^{-1}$,

r_0 is the external radius of the probe, m ,

r_1 is the internal radius of the probe, m ,

α_p is the thermal diffusivity of the of the probe material, m^2s^{-1} ,

W is the rate of energy arrival, where $W = Ql$.

l is the length of the probe, m .

Glossary

Adobe

Adobe is a Spanish word meaning sun-dried brick and describes a technique of building using unbaked clay blocks. Most adobe blocks are produced using moulds and a moist mixture of subsoil and sometimes chopped straw. The greatest concentration in the UK of examples of this technique can be found in East Anglia, where they are referred to as 'clay lump'.

Cob

Cob is a monolithic (built as one unit) form of earth wall construction. Cob walls are made from a mixture of subsoil, straw, water and in some instances manure. These walls are very thick often up to 650mm, and built upon a stone plinth. Cob walls are native to the South West of England and can be found in large manor houses, a variety of dwellings and small agricultural buildings.

It is difficult to accurately describe the constituents of a cob wall because of the accepted practise of using the local soils and adjusting the building technique accordingly. Clough Williams-Ellis refers to this trait when describing cob buildings techniques ' The soil itself suggested the construction'. However, some soils are more suitable for use in cob walls and Clough Williams-Ellis describes an analysis of a typical piece of old cob walling.

Stones	24.2%
Coarse sand	19.7%
Fine sand	32.5%
Clay	20.6%
Straw	1.25%
Water	1.55%

(It is assumed that these figures represent the mass of each constituent rather than the volume although this isn't entirely clear from Clough Williams-Ellis's account).

Further more detailed descriptions of the constituents of contemporary cob and other monolithic walling techniques are described in a number of texts including Earth Construction by Hugo Houben and Hubert Guillaud, Earth Construction Handbook by Gernot Minke, and Conservation of Clay and Chalk buildings by Gordon T. Pearson. These volumes are described more fully in the References and Bibliography sections of this work.

L. Keefe discusses the behavioural characteristics of cob used in walls in Chapter 4 of an M Phil thesis (Keefe,1998), An Investigation into the Causes of Structural Failure in Traditional Cob Buildings. Keefe assesses the compressive strength of some samples of cob at different moisture contents concluding that samples with a straw content of 1.5% straw, by mass show a decrease in strength from 750kN/m² at 3.5% equilibrium moisture content, (e.m.c.) to 40 kN/m² at 20% e.m.c. The density of the cob used for these measurements had an average of value of 1790kg/m³ and it would be expected that as the density of the cob increases, the compressive strength will increase (Minke, 1994).

Measurements taken by Trotman and Keefe have indicated that the equilibrium moisture content at the foot of a cob wall of an occupied building should be between 3.5 to 5.0% dry weight, and that an e.m.c. can be as little as 1.5 to 2.0% dry weight can be expected higher up the wall (Trotman,1993).

All of the measured and estimated values that are used to describe or classify cob, must be viewed with caution as the properties of cob vary according to the subsoil, construction technique and individual builder.

Cob block.

Cob blocks or cobblock (as referred to in the text), use the same earth, straw and water mixture as monolithic cob but moulds are used to produce separate blocks similar in dimensions to standard concrete blocks, (typical dimensions 210mm x 430mm x 100mm). The blocks are either laid wet to produce a homogeneous wall or allowed to dry and joined using a clay mortar. Cobwool blocks are a variation of this technique, using waste wool in place of the straw.

Earth Bermed

Earth bermed refers to the practice of raising the level of the earth surrounding a building or structure, bringing it into contact with some or all of the exterior wall surfaces. Earth berming has often been associated with deliberate attempts to increase the thermal mass of a building.

Mud and Stud, (referred in the text as Mudstud).

Form of earth building found in Lincolnshire. Based upon a heavyweight timber framework, infilled with very thick daub often up to 300mm thick, (see Wattle and Daub), giving the appearance of a building constructed in a monolithic manner.

Rammed Earth.

Rammed earth, or 'pise de terre', describes a walling technique where earth is placed between shutters and manually or mechanically compacted. Henry Holland introduced it to the British Isles following a study of French methods in 1797. In Australia the earth often has cement added as a stabiliser before being rammed between shutters.

Stabilised Earth.

The stabilisation of earth refers to the addition of different materials that will shorten the hardening period or confer other properties to an earth wall. Stabilising agents include cement, lime and bitumen. Stabilising materials will often be used when an earth material is being used in very exposed conditions or when a wall is being produced during winter months. Different stabilising agents confer different set times and must be used in quantities and circumstances that will not detract from the original properties of the unstabilised earth wall.

Wattle and daub.

Wattle and daub is a walling technique based upon a woven wooden framework. Earth, often with a clay content, in a wet consistency is forced into the framework to produce a thin wall suitable for partitions. Often used as a technique to produce infill panels in the external walls of older timber frame buildings.

Wychert

A monolithic form of walling made from a natural mixture of decayed limestone and very stiff clay. Most buildings of this type are found along the northern edge of the Chiltern hills, Buckinghamshire. The name originates from a dialect term meaning white earth.

Chapter 1

Introduction to unbaked earth building materials.

Introduction

The Centre for Earthen Architecture (CEA), based within the University of Plymouth School of Architecture, has carried out research into the various aspects of vernacular architecture typical of the Devon area. The local monolithic form of unbaked walling, known as Cob, has featured in several projects investigated by the CEA. The relationship between the moisture content of these walls and their structural properties have been investigated (Greer, 1997). The pathology of structural failure of cob walls has also been researched and patterns of failure have been analysed (Keefe, 1998). Links have been made between the age, building form and the geographical location of cob buildings using Geographic Information Systems (GIS), (Ford, unpublished). A study, concerning the effects of straw content upon the mechanical properties of cob walls, is on going and will be complete soon, (Coventry, unpublished). However, the thermal properties of cob walls have not been studied and this work is concerned with this aspect of the behaviour of cob buildings in Devon. The thermal characteristics of similar earth walling systems are also explored.

There are two thermal properties of building materials that affect the thermal performance of a building, (i) the thermal conductivity, (λ), and (ii) the thermal capacity, (c). When studying the thermal performance of a building material, both the rate of heat transfer and the quantity of heat required to raise the temperature of the material need to be known.

This work will explore the application of a time dependent probe technique to measure these two thermal properties. The measurement technique must satisfy five criteria:

- (i) the technique must be non-destructive,
- (ii) it must not influence the material being measured,
- (iii) it must give representative values for both the thermal conductivity, λ and thermal diffusivity, α^* ,
- (iv) it should be rapid and affordable and
- (v) allow *in-situ* testing.

*It is interesting to note that the thermal capacity, c , is not directly accessible using this probe method. However, the thermal behaviour of buildings is often studied using the volumetric heat capacity of the materials, or ρc , rather than just c , where ρ is the density. Since both α and λ are available via the probe technique, then we may determine ρc from the relationship, $\alpha = \lambda/\rho c$.

A time-dependent thermal probe technique theoretically meets the five required criteria. For example, if a small diameter probe is used, then it may be assumed that one 3mm diameter hole of 70mm in length will not damage a wall that may have a thickness as large as 650mm. The measurements can be carried out with a sufficient delay as not to be affected by previous readings or affect future measurements. The probe technique has the advantage that it will theoretically give values for both thermal conductivity and thermal diffusivity.

Previous researchers have used periods of heating of less than an hour with relatively inexpensive equipment (See chapter 3). The short test periods required for measurements, allied with the low power inputs needed, allow a small test apparatus with a self-contained power supply to be used. This gives the technique the unique advantages of affordability, portability and flexibility in carrying out *in-situ* tests.

Previous research (see chapter 3), using a time-dependent thermal probe technique has provided a number of solutions to many of the theoretical problems that are inherent in the successful use of the technique. However, one vital element is still an obstacle to obtaining realistic thermal data from *in-situ* tests, that of the interface between the probe and the material being examined. The effect of this constraint, the thermal probe conductance (H) and the different power levels supplied to the probe are explored in this work. A series of exploratory studies are carried out in laboratory conditions culminating in 3 series of *in-situ* field measurements. The measured data is used in a dynamic thermal simulation.

Unbaked earth building materials.

Earth was, and in some cases still is, one of the most widely used of all building materials used for walling. Today the use of earth construction continues in areas where labour is cheap and abundant and where other transported materials are expensive or unobtainable. In most instances the use of earth in western developed countries is confined to walls only, but walls can sometimes constitute quite a small percentage of the structure of a building. In many developing countries where the properties of earth construction are more widely appreciated, earth is utilised in the construction of floors and roofs, in addition to walls.

Worldwide, traditional earth construction techniques are variously known as cob, pise de terre, adobe, clay lump (and its close relation wattle and daub). All of these techniques have been used successfully according to the local conditions, customs, and materials. Different techniques have been used to provide long lasting, appropriate and comfortable dwellings, (further details can be found in the glossary).



Figure 1.1 Marker cottage, constructed from cob

Cob walling may be seen as perhaps the most unsophisticated method of building in unbaked earth, relying as it does on a mixture of subsoil and straw, laid in layers, one on the other, with no support from formwork.

Traditionally local sub-soil would be dug (making sure that it was free of organic impurities such as vegetation, humus or topsoil) and inspected to ensure that it contained the correct proportion of constituents and not an excess of clay or chalk (Williams-Ellis, 1947). The preparation can vary considerably depending upon geography, geology and tradition. In many parts of Devon labourers would then beat the chosen subsoil with an implement such as a heavy prong to ensure the lumps were broken down and then the larger stones could be picked out.

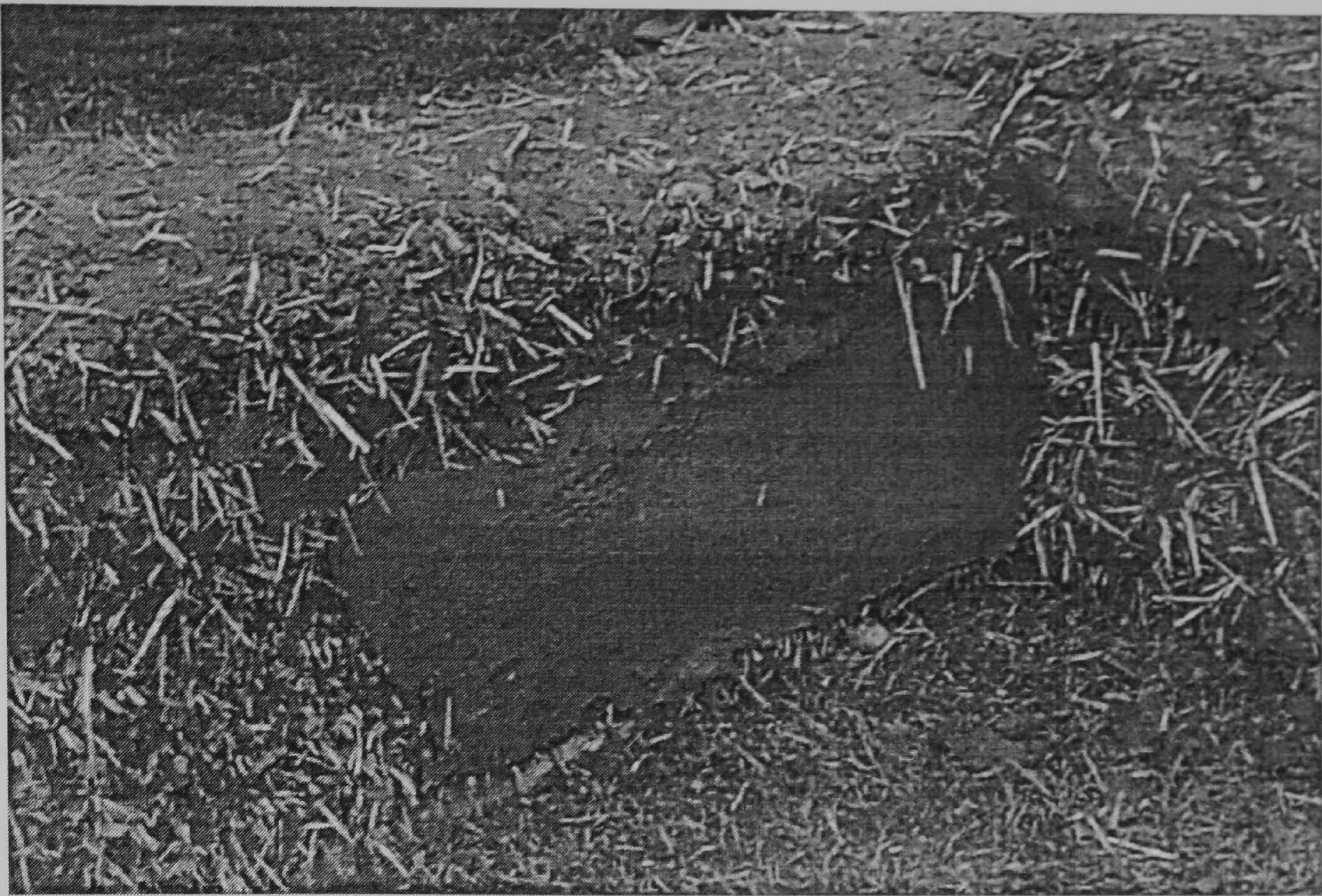


Figure 1.2 Demonstration cob wall, showing earth rendering

A bed of the soil, often circular and around 300mm high by 6m across (McCann, 1983) would then be prepared and if necessary, sprinkled with water. The bed would be trodden by labourers, or by horses or cattle where they were available or for larger projects. At this point straw would be added with a fork by one labourer, whilst another would turn the mix and regulate the amount of water added, to ensure a consistent product. The finished mix would then be mounded in a compact heap and covered with straw to decrease moisture loss until ready for use.

To raise the cob wall above ground level and to protect it from rain splash and rising damp, a pinning, plinth or foundation wall of varying thickness and would be prepared. This would be made from stone or other impervious material.

The layers of cob would be laid upon the pinning at a little over the same thickness of the stone plinth itself, which normally measured between 0.6 m - 1.2 m (Egeland, 1988). This thickness often tapered towards the top of the wall and was often emphasised by the 'paring down' or 'coaxing' of the walls, where the labourers would cut back the excess material at

the wall's edges to make the vertical sides straight. The height of each 'lift', or layer, and the thickness of the walls themselves vary considerably according to the locality, the soil type, the use of the building, the cob mason, and the use of the building.

Cob buildings are abundant in the South West of England and can be found between Cornwall and some parts of Hampshire, although they are most numerous in parts of North and Mid Devon. This investigation measures the thermal properties of cob in these locations. A chalk-rich regional variation, wychert or wichert, from Buckinghamshire and an infill material, mud and stud from Linconshire are also investigated.

Another form of unbaked earth walling is *pise de terre*. *Pise de terre* is French for rammed earth and refers to mechanically compressing earth between climbing shuttering, allowing continuous construction until the wall has reached the required height. Semi-dry earth, without straw or other fibre is rammed between boards. Each course is added directly on to the previous, without intervals for drying, sometimes reaching roof height in one day. Figure 1.3 shows a gable-end wall of a traditional French dwelling, (located near Lyon), constructed from *pise de terre*.



Figure 1.3 French rammed earth, '*pise de terre*', (single storey dwelling).

When compared to cob walling, rammed earth tends to produce a more durable wall than cob, and often of reduced thickness. This is normally due to the higher density of the *pise de terre* walling material.

Adobe, a Spanish word for mud, is an alternative walling technique to monolithic construction and describes the technique of forming separate earth blocks, often sun dried, and layering them like bricks. This form of construction is common in Mexico and is often practiced in California and in South West America, where other materials for building are scarce and where the resulting structures have great durability as a result of the semi-arid climate. Adobe avoids the requirement for a climbing shutter, but does have the disadvantage of producing vulnerable joints. A near relative of adobe, compressed block, is produced using mechanical compression of relatively dry earth. The properties of compressed blocks can be different from adobe blocks, because of adobe's use of a wetter mix.

Clay lump is the regional form of adobe found in East Anglia. The clay is mixed with straw and similar to the adobe method, is formed into blocks by pressing into wooden forms. The mix is then left in the sun to dry, and is laid in a liquefied clay mortar in a similar manner to brick or blockwork. Another regional variation of unbaked earth blocks can be found in India where the blocks are cut from the ground. Figure 1.4 shows a number of these blocks awaiting transportation, cut from the surrounding strata, near Goa, Western India.



Figure 1.4, Indian earth blocks.

Wattle and Daub is a composite form of construction and often can be one of the simplest and cheapest forms of walling. It utilises a framework of interlaced rods and twigs of,

depending what is available, reeds, withies or bamboo which are woven horizontally between posts that are imbedded in the ground, to form a lattice. Mud is then applied to the wall on both the inside and the outside, at a sufficiently wet consistency for it to be squeezed between the gaps in the framework. Because of this method of construction, in contrast to cob walls, the finished partition is very thin. To ensure that the adhesion of the soil to the framework is acceptable at this range of thickness, the soil needs to be very moist and to contain a large proportion of clay.

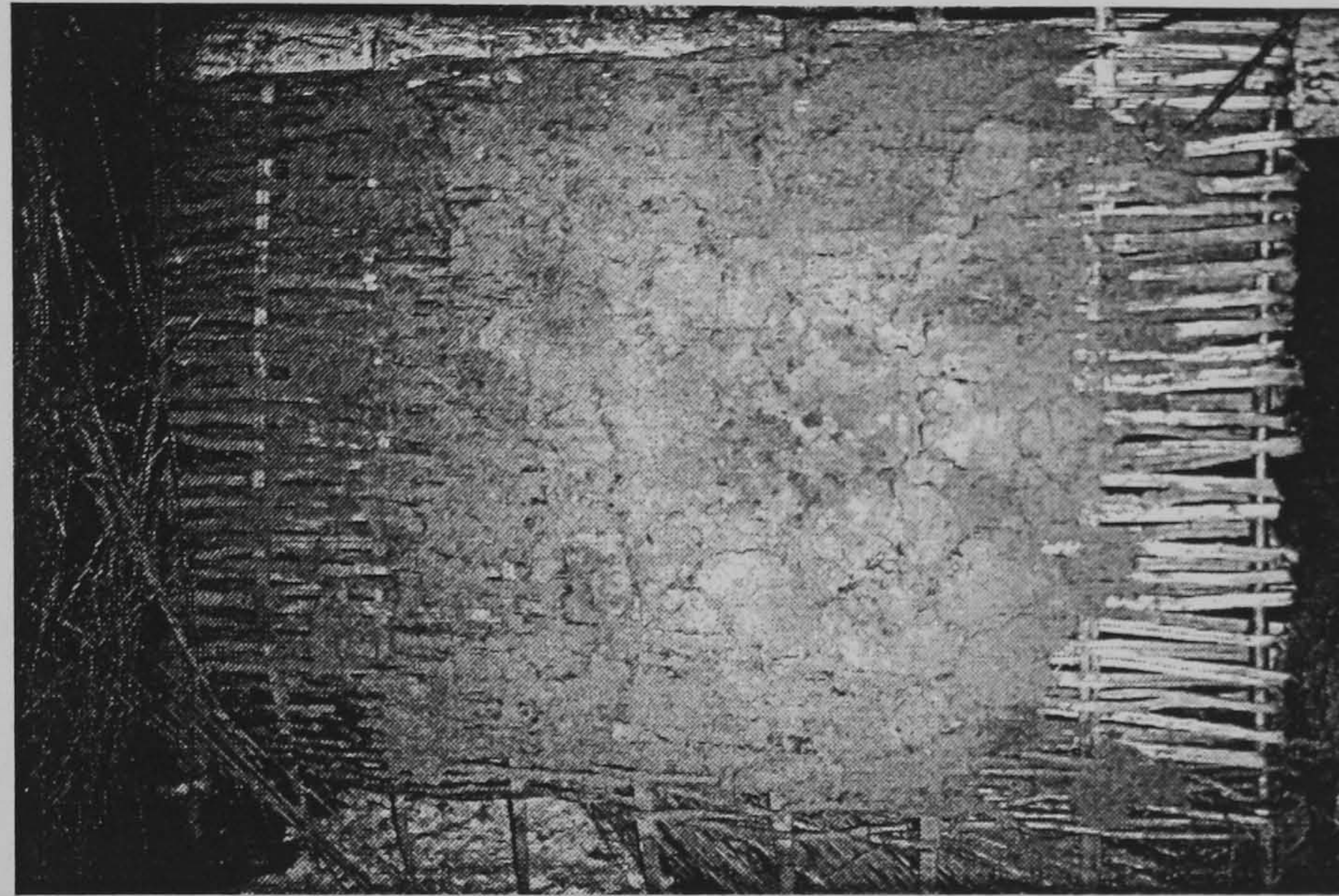


Figure 1.5 Example of wattle and daub construction.

The large movements associated with the changes in moisture content in clay soils are almost completely negated by the influence of the framework. To further reduce the instance of cracking of the mud layers, vegetable fibres, straw or animal hair are sometimes added to the soil as it is being mixed, thus binding all parts of the wall together. The wall is then finally finished off with a layer of plaster, usually mud based, to try and improve the wall's appearance and weathering qualities. Variations exist of wattle and daub used as an infill material, 'lath and daub' or 'stud and mud' are similar to many of the infill panels found in medieval timber frame housing. These panels are normally constructed of riven oak staves which are slotted into the frame at both ends, around which hazel withies 7/8 to 1 inch (22 to 25mm) thick (Wright, 1980) are horizontally woven. The daub used for infill panels is very similar to that employed for complete walls, but for the possible addition of cow dung to the mixture of clay and straw, which is believed to increase the strength of the mix and provide a degree of protection against damp penetration (Wright, 1980).

The earth used in the various construction techniques may be stabilised with cement, lime or bitumen. The type of stabiliser depends upon the type of clay present in the subsoil and the desired modification of built properties. Appropriate stabilisers will normally increase the strength and therefore, often improve the durability of the final product. This is particularly important in areas that experience particularly inclement weather and often allow the wall to acquire a greater strength more quickly. Inappropriate or incorrectly stabilisers however, can have negative effects upon the properties of an earth wall.

Conclusions

Cob walling systems are one part of a range of unbaked earth technologies used in different guises around the world. Variations exist in the UK leading to specific vernacular traits. All of the techniques can be environmentally benign using little energy in production and for transportation. The materials readily breakdown after use, with little consequence to the environment.

Little information is available pertinent to the thermal characteristics of cob and other earth building techniques. Chapter 2 reviews the existing knowledge concerning the thermal behaviour of various types of unbaked earth walling.

Chapter 2

The Thermal Properties of Unbaked Earth Walling.

The thermal properties of soils, especially at high moisture contents, are well documented, many to the extent of allocating special moisture factors to allow for changes in those thermal properties with different moisture contents (EDSL, 1989). The values for the thermal conductivity of cob walling however remains the subject of guided estimates mostly based upon the CIBSE guide figures for mud or soil. For example for ' *Clay with 11% moisture content, the thermal conductivity is 1.1W/mK*', (CIBSE, 1985). Descriptions concerning the thermal capacity and thermal diffusivity of materials similar to cob are rare. For this reason, comparisons with many of the materials studied using the probes are made after the account of each measurement. Conclusions pertaining to the thermal diffusivity of all the unbaked materials are discussed in chapters 8, 9 and 10. The relationship $\alpha = \lambda / \rho c$ allows the calculation of c , the specific heat capacity of a material, given that the thermal diffusivity, α , the thermal conductivity, λ and the density, ρ of the material are known. It is important to know the value of the specific heat capacity of cob, as in combination with a known value of cob's thermal conductivity, it has a large influence upon the time-dependent thermal behaviour of cob buildings.

Published Data Relating to the Thermal Properties of Earth Walling.

Clough Williams Ellis estimates the thermal conductivity of earth walls as follows,

"..since the thermal conductivity is related to the density of the material ,and since the density of earth walls approximates to that of a gravel concrete, at about 130lb./cu.ft.,their thermal conductivity would be expected to be no more than that of the concrete; that is, about 7 B.Th.U./per hour/per sq. ft./per deg. F." (Williams Ellis, et al., 1947)

(The reader should bear in mind that this estimate was made over 50 years ago and its current validity could be questioned).

If a factor of 0.144 (EDSL, 1989) is used to convert this figure to $\text{Wm}^{-1} \text{K}^{-1}$ then the following is obtained; $7 * 0.144 \text{ B.Th.U./per hour/per sq. ft./per deg. F.}$, is approximately $1 \text{ Wm}^{-1} \text{K}^{-1}$

The Building Research Establishment makes a general comment concerning comfort levels;

"The outstanding fact to be noted in reference to cob buildings is the frequent reference to their comfort. From this we may infer that the temperature was equitable, warm in winter and cool in summer, and that the wall was able to resist the penetration of damp from without. These characteristics were probably in large measure due to the great thickness of walls." (BRE, 1922)

A more precise estimate can be found in the December Edition 1990 of "Architect and Surveyor" magazine;

"..... a cob wall well insulated with straw, sawdust and woodshavings, is likely to have a 'U' value of $0.35 \text{ Wm}^{-2}\text{K}^{-1}$ for a 625mm thickness and a 'U' value of $0.48 \text{ Wm}^{-2}\text{K}^{-1}$ for 460mm thickness. External render and internal plaster have been assumed in both cases. Such low values could make the material suitable for modern use." (Gooch, 1990)

Therefore according to Gooch, the thermal conductivity of a cob will be approximately $1.0 \text{ Wm}^{-1}\text{K}^{-1}$, very similar to the value approximated by Williams Ellis. The ramifications of the likely thermal transmission values quoted by Gooch are discussed at the end of chapter 8.

Gordon Pearson in his book "Conservation of Clay and Chalk Buildings" quotes from several historical texts as to the warmth of earth buildings. This is backed up by figures taken from the CIBSE guide (CIBSE, 1985) and states;

"The tables confirm the beliefs of the cottagers that earth buildings were warmer than stone".(Pearson, 1992)

Pearson concludes ;

" It is interesting to compare a 600mm thick earth wall with a modern cavity wall of brickwork and blockwork and note that the former has a lower (i.e. better) U value thereby confirming the warmth of the old mud cottage".* (Pearson, 1992)

* (the reader should note that a cob wall will be less likely to have a lower 'U' value than a cavity wall built to conform to the 1995 building regulations, Part L, Conservation of Fuel and Power).

Minke (1994) refers to many properties of soils and their behaviour when constituted into unbaked earth walling systems. Minke discusses the relationship between the density of the soil used and the thermal conductivity of the resulting wall. The following table, table 2.1, summarises that relationship;

Soil	Density (kgm ⁻³)	Thermal Conductivity (Wm ⁻¹ K ⁻¹)
Heavy	2000	0.93
Medium Density	1200-1700	0.70
Lightweight	1200	0.47

Table 2.1, Thermal Characteristics of Soils (Minke, 1994).

Very lightweight clay blocks have formed a topic of preliminary research at the Helsinki University of Technology within the Architecture Research Unit for the Built Environment. Mikael Westermarck has co-ordinated research into the manufacture and use of a range of naturally based materials for production in rural areas in Nordic countries. The availability of raw materials was an important part of this study and those that could be readily sourced from forestry and agricultural areas typified the choice of materials. The base or filling materials ranged from different varieties of timber, fibres, humus and straws to more inert materials such as stones, soils, silts and sand. Each 'base' or 'filling' material was utilised with or without a binding agent to produce a saleable building product. The lighter earth based blocks used clay as a binder and used a base material of straw, reeds or flax. These blocks were produced with a thickness of 400mm and have a density of less than 350 kgm⁻³. The preliminary research document produced by this group describes the blocks as;

“providing according to calculations, an external wall with the required heat insulation standards set for residential building.” (Westermarck, 1997.)

If the densities of the blocks are categorised according to Minke's values in table 2.1 it can be observed that the thermal conductivity of the lightweight clay blocks will be less than 0.47 Wm⁻¹K⁻¹. From a chart published Volhard and Westermarck(1994), earth based building materials of densities between 300 and 400 kg m⁻³ will have a thermal conductivity of between 0.1 and 0.12 Wm⁻¹K⁻¹. Allowing for only the thermal resistance provided by the lightweight block, that is ignoring the surface resistances, then for a thickness of 0.4m the thermal transmission value or U value will be approximately:

$$'U' \text{ value} = \lambda / l = 0.3 \text{ Wm}^2\text{K}^{-1}, \text{ (where } l = \text{width, m)}.$$

This value complies with the current thermal transmission value for walls of $0.45 \text{ Wm}^{-2}\text{K}^{-1}$ stipulated by the UK Building Regulations Part L, 1995.

The Devon Earth Building Association have published an advice sheet concerning "*Cob and the Building Regulations*", within which the thermal properties of cob walling are discussed in connection with the UK Building Regulations Part L, Conservation of Fuel and Power. The UK Building Regulations will apply to all newly built cob buildings that serve the same purposes as a qualifying conventionally constructed building. In addition to this qualification any building, such as a cob barn, that will undergo a material change of use (when that use is deemed to be controlled, such as conversion to a dwelling), will require the regulations to be applied to both the existing structure and any new services and other building work.

Earth Walling in Hot Climates

Earth walling systems are used extensively and successfully in hotter parts of the world where testaments to their thermal behaviour can be found:

" Even in an Australian summer climate it is almost impossible for an earth house to get really heated as the best brick building can during a heat wave. It is always cool in summer and warm in winter" (Knox, 1978).

This is confirmed by a series of notes produced by the Commonwealth Experimental Building Station (CEBS), Sydney, who, when referring to a resurgence in the use of earth walling materials state:

"This increase is due mainly to shortages of normal building materials, but partly also to an appreciation of the superior thermal performance of earth walls; owing to their density and thickness, such walls are particularly suitable for hot climates." (CEBS, 1950).

The important thermophysical effect of earth walling is to damp the thermal variations of the external environment. This thermal inertia is beneficial for buildings in hot countries and tests undertaken in Egypt have concluded that a well-made mud brick can provide more thermal damping than a hollow concrete block. According to William Facey;

“ ..it has only recently been scientifically demonstrated beyond doubt that earth’s perceived superiority is indeed real, notably in tests carried out by two engineers, one British and one Saudi Arabian, Dr David Webb and Dr Salih bin ‘Abd al-Rahman al-Ajlan.” (Facey, 1997).

The benefits of the thermal properties of earth have also been utilised within various types of buildings that use passive solar energy, including a number of adobe based dwellings in the United States of America. The thermal mass of these buildings is sometimes further enhanced by the use of insulation as a backing to earth walling and flooring to store heat over long time periods. (Yellott, 1975)

Volhard and Westermarck use the following diagram to suggest how earth walls moderate exterior change in temperatures over a 24hour period.

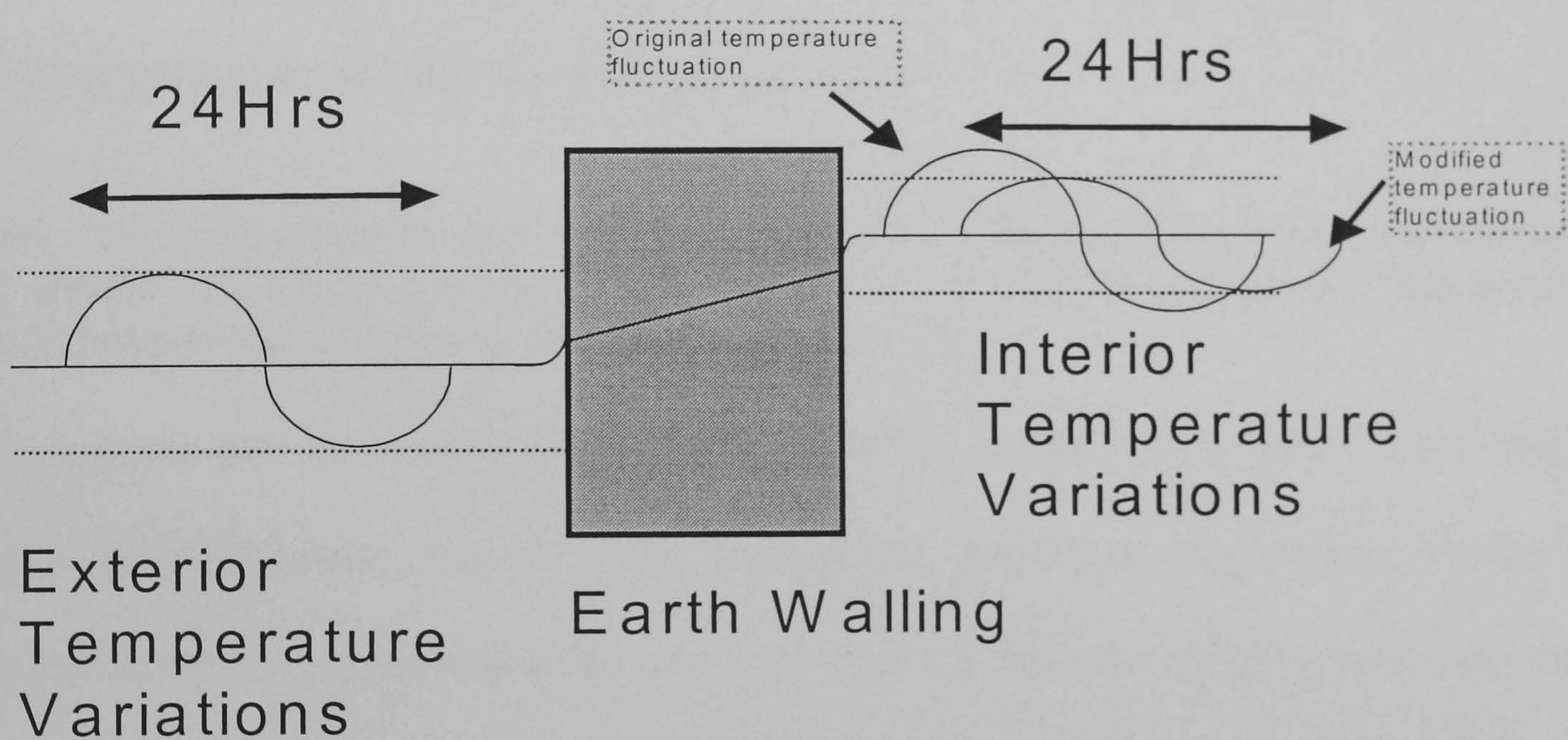


Figure 2.1 The modifying effects of earth walling upon internal temperature variations over a typical 24hour-time period. (Based upon Volhard, F. and Westermarck, M., 1994.)

Effects such as those shown above will moderate against large variations in external temperature, whether the variations are large differences of low or high temperatures.

Cob Walling and moisture

The moisture content of building materials can alter their structural and thermal properties including their thermal conductivity. Cob walls tend to be slightly hygroscopic in nature (Trotman, 1993) and thus readily absorb moisture from the surroundings unless some form of barrier, such as a vapour check, prevents this.

Tim Padfield has analysed the behaviour of earth walling with a view to introducing this construction technique into museums for use as a humidity buffer using some properties of earth walls previously investigated by Gernot Minke, (Minke, G., 1994). Padfield modelled the behaviour of an earth wall using a computer simulation basing the required initial data upon a series of measured results from a climate chamber. When discussing the water absorbent properties of materials such as cob, he states ;

“In recent times this property has been disregarded, or even viewed as a disadvantage, allowing condensation and damage within the wall. A subtler analysis shows that porosity can in fact prevent condensation damage.” (Padfield, 1998)

Padfield suggests that the moisture absorbing properties of earth walls are, in part, related to the ‘open grained’ nature of its structure. This is then investigated by utilising a scanning electron micrograph to give a greatly enlarged view of an area of approximately 1mm across. This view of an earth wall is contrasted with a similar view of a cellular concrete block and the nature of the grain and pore structure is compared. Padfield comments upon the earth wall’s *“..microscopic fissures, which give it a large accessible surface”*, which would present any moist air with a large surface area, thus promoting good absorption of moisture. In contrast the cellular concrete showed *“ ...gas bubbles mostly far apart with only occasional interconnections.”* The result of this isolated or more closed cell structure is to dramatically reduce the ability of the cellular concrete to absorb moisture when compared with the earth walling material. However, the isolation of the pores do give cellular concrete better thermal insulation qualities than earth walling materials. Because the thermal conductivity of cob walls may vary *in-situ* this leads to a requirement for thermal conductivity

studies to be carried out in a more realistic situation than laboratory testing can provide. Field studies are essential to generate a database.

Conclusion

Much anecdotal evidence exists suggesting that buildings constructed from unbaked earth maintain a 'steady' internal thermal environment. However, very little work has been carried out measuring this behaviour. Earth sheltered buildings have been the subject of some simulations, the findings of which suggest that unbaked earth walls may act to damp the variations in ambient temperatures. These findings are discussed in chapter 9.

Many values used to represent the thermal conductivity of unbaked earth walling are often approximations derived from other materials of a similar density. The attempts to categorise any unbaked earth walling materials, such as cob, to ensure their compliance with current building regulations have used these approximations.

The use of earth walling materials for damping variations in temperature within buildings hints at the importance of establishing the value of the thermal capacity of unbaked walling. The investigation of the behaviour of any such buildings using dynamic thermal analysis is dependent upon the establishment of a firm value for this thermal property. The varying moisture content of the walling is confirmed, suggesting that an *in-situ* transient thermal measuring technique would be best suited to measure a representative figure for the thermal conductivity and thermal capacity. Chapter 3 focuses upon the development of this transient technique, the many variations of the technique that have been investigated and suggests an appropriate experimental procedure for this study.

Chapter 3

Review of literature concerning thermal conductivity measurement methods including the thermal probe technique.

Techniques used to measure the thermal characteristics of materials conform to two broad types, steady state and transient methods. Steady state methods include measurement systems such as the guarded hot plate method, (CIBSE Guide A,1985). Transient techniques include measurement systems such as the hot wire method which has a number of variations. This chapter describes these measurement techniques in relation to their historical development and their suitability to determining the thermal conductivity and other thermal properties of cob walling in Devon.

The majority of thermal conductivities, that are used to calculate the air to air thermal transmission values that enable buildings to satisfy the UK Building Regulations, are obtained from the guarded hot plate method (CIBSE Guide A,1985). This method places a thin sample of the material being studied in an apparatus that constantly heats one side of the sample and cools the other. The energy required to maintain the temperature difference between the two sides enables an assessment of the thermal conductivity of the sample. In this method the sample needs to come to an equilibrium state where the heat flow across the material is constant. This constant heat flow with steady temperatures is only achieved after a period of many hours . Any heating/cooling over this length of time will alter the moisture distribution in the sample.

As the moisture content of the sample varies, so will the sample's thermal properties, including its thermal conductivity. Most building materials employed in buildings operate in conditions that normally have a moisture content higher than those samples tested within the guarded hot plate method. This means that the values for the thermal conductivity obtained by the hot plate method, are lower than the thermal conductivity of materials that

are in use in real buildings. To establish the thermal conductivity values of any building material that is *in-situ* requires a technique that enables the material to be studied without a considerable variance in the moisture content of the sample.

As alluded to within the CIBSE guide, there is a time dependent thermal probe technique that requires a period of several hundred seconds to obtain a set of data, rather than the 24 hours or so for the guarded hot plate method. Because of the short time periods required for the probe measurements and the relatively small temperature rise used, the sample moisture content is relatively undisturbed. Furthermore the steady-state guarded hot plate method only measures the thermal conductivity value, and is unable to give the thermal diffusivity of a sample. Transient or time dependent techniques can measure both the thermal conductivity and diffusivity.

The Time Dependent Thermal Probe Technique

The time-dependent thermal probe technique uses a probe, or other instrument, which approximates to a line heat source of constant strength. This probe is placed into a homogeneous sample, assumed to be of infinite size and at a known uniform temperature, and allowed to come into thermal equilibrium with the specimen. On establishing a constant heat input, the rise in temperature of the probe is recorded and analysed to give the thermal characteristics of the sample, (see chapter 5).

A transient heat method was suggested as early as 1888 by Schleiermacher, who proposed the use of a cylindrical probe. Independently a similar probe was described by Stalhane and Pyk (1931). This method was developed and used for measuring the thermal conductivity of liquids by Weishaupt (1940) and by van der Held and van Drunen (1949). The technique has been used more recently by Vilcu and Ciochina (1980), Watanabe (1997) and Fuji *et al* (1997) to simultaneously measure the thermal conductivity and thermal diffusivity in a range of different liquids such as toluene, pure

water, carbon tetra-chloride and *n*-heptane.

An instrument was first developed for use with soils and building insulation materials by Hooper and Lepper (1950). This instrument was intended to determine the thermal conductivity of moist soils and other wet and dry solids in their natural location. The probe had an outside diameter of approximately 2mm, was 460mm long and constructed from aluminium with a steel conical tip. Near the centre of the probe body were located two or more thermocouples connected in series using external cold junctions, which would measure the increase in temperature due to an axial constantan heater supplied with constant power. The electrical source of power was a battery, as the use of direct current avoided induction effects, and allowed the instrument to be portable. The portability of the instrument is only mentioned briefly and no indications of the practical difficulties of using the instrument *in-situ* are discussed. Measurements were taken over a period of 420 seconds and reproducibility of 0.5% was claimed.

D'Eustachio and Schreiner (1952) used the basic criterion utilised by Hooper and Lepper, but after constructing and testing a number of probes concluded that a reduction in outside diameter and therefore, a redesign of the probe was necessary to enable the effective use of small temperature rises. These re-designed probes were 100mm long using a bifilar coil heater and following Hooper and Lepper, thermocouples connected in series were placed at the probe midpoint. The smaller constant power of 0.011 Watts supplied to the heater resulted in temperature rises in the specimen of approximately 1 to 3 degrees Celsius, but no indication of the time-period required for this temperature-rise was given. D'Eustachio and Schreiner observed that an air space between the probe and the sample being tested, equal to 50% of the diameter of the probe, did not seem to affect the results obtained when the power input was 'sufficiently' low. The heat flow axially along the probe was also investigated and in the central portion was less than 0.1% of the heat input. From this they concluded that the average axial flow during the measured

interval was less than this and therefore the end losses from the probe were assumed to be negligible.

The different investigators, engineers and soil scientists that are interested in time dependent thermal conductivity measurements are described by de Vries and Peck (1958). De Vries and Peck used the expressions derived by Blackwell (1954) to take account of the finite probe length and any boundary conditions. The internal heater wire was modified by encasing the wire within a glass capillary tube with an external diameter of approximately 0.5mm and an internal diameter slightly larger than the wire. This enabled the steepest temperature gradients to be found in the glass rather than in a soil test sample and therefore reduced the probability of moisture migration. From this first development a probe for measuring the thermal conductivity of soil was developed. The diameter of this probe was approximately 1.1mm and a length of 130mm. The outer construction of the probe consisted of metallic gauze impregnated with paraffin wax. Within the wax a glass capillary tube, similar to the earlier version was located close to a thermocouple-junction. The end of the probe was sealed with plastic and capped with an insulating cover. Most of the thermal properties that de Vries and Peck measured were taken at a start temperature of 20 degrees Celsius, and concentrated upon materials such as copper, glass, quartz, air and various different moist and dry soils. A test carried out upon a sample of dry coarse sand used a maximum temperature increase of 0.8 °C measuring both the time required for the sample to increase in temperature and also the time taken to cool after the heater was switched off. The cooling 'branch' time was counted from the end of the heating section onwards and each point was said to have been corrected for the influence of the previous heating. With the large variations in external ambient temperature that can be expected when using any transient thermal conductivity measuring technique in a climate such as the UK, it is likely that temperature rises of less than 1°C will be affected by outside influences when carrying out *in-situ* measurements. With this correction applied, the two lines, heating and cooling, could be

seen to be straight and coincide with each other. Errors in the thermal conductivity values following from the probe experiments were discussed by de Vries (1952), and were found to be approximately +/- 5%. This error can be confirmed by examining the plotted lines for both the heating and the cooling branches of the temperature curve, where their deviation should coincide with the expected error. Mention is also made of the use of a check that should be made upon the magnitude of the contact resistance between the probe and the sample that is described in chapter 5. The thermal conductivity values measured by de Vries and Peck for dry quartz sand were found to be in close agreement with results on similar materials using steady state methods by Smith and Byres (1938). De Vries extends the investigation to examine the range of different methods of utilising variations upon the 'hot wire thermal probe' dynamic technique. Table 3.1, allows the reader to view the various thermal probe designs and the typical time taken for each measurement.

Authors	Diameter (mm)	Length (mm)	Time of first Reading t_0 (sec)	Time of Heating t_1 (sec)
Skeib(1950)	1.1	250	50	100
Hopper and Lepper(1950)	4.8	460	180	420
deVries(1952)	1.1	130	10	180
D'Eustachio and Schieiner(1952)	0.76	100	—	—
Mason and Kurtz(1952)	6.3	600	60	1500
Buettner(1955)	0.7	25	1	10
Bullard <i>et al</i> (1956)	0.86	63.4	5	600
Mann and Forsyth (1956)	1.4	100	20	120
Makowski and Mochlinski (1956)	4.8	460	40	1200

Please note, the table and other authors mentioned in the table have been referenced de Vries & Peck, 1958. The full reference for this work is located in the reference section at the end of this study.

Table 3.1 shows the dimensions, thermal properties and time intervals for cylindrical probes (de Vries & Peck, 1958)

Table 3.1 shows that the time taken and the first reading for each of the measurements varies for different researchers. As is discussed in chapter 5, the time of first reading and the measurement of the probes' thermal fit in a test hole are linked.

In 1958 the Division of Building Research, Canadian National Research Council, published data concerning testing of moist clay, snow, silica aerogel and sawdust using a probe with a thermocouple attached to the outer surface of the sheath at mid-height (Woodside, 1958). The test materials were placed in an aluminium cylinder of internal diameter 150mm and internal height 370mm. The experiment time lasted about 15 minutes, but the frequency of the data collection was described as being delayed by enough as to allow the sample to attain thermal equilibrium. The temperature rose within the samples (varying according to the material), 10°F for snow and 59°F for silica aerogel. The test results upon moist sawdust showed a reduction of the initial conductivity to approximately a fifth less in magnitude assumed to be caused by the partial drying out of the sample. This investigation concluded that moisture migration within test samples could be minimised by increasing the probe radius, contrary to previous developments that tended to advocate smaller probes. As the heater powers used in the investigation are small and one of the major factors to be overcome is the establishment of a good thermal contact of the probe in a sample hole, the author is minded to choose a probe of smaller radius.

Wechsler and Glaser (1965) developed a probe to investigate the thermal conductivity of solid, porous and powdery rocks and minerals. This study was undertaken with the view that similar probes could be used on lunar surface materials. The probe used for the study was constructed with a stainless steel sheath, welded shut at the measurement end, 140mm long and with a diameter of 1.24mm. The probe utilised straight and bifilar coil heaters (wound from 0.025mm constantan wire) and a copper-constantan thermocouple detected the temperature rise at the centre of the probe. External chromel-alumel thermocouples were also used. The use of the probe is described by Wechsler and Glaser, as:

“(1) Inserting the probe into the sample to be tested; (2) allowing thermal and pressure conditions to come to equilibrium and then supplying power to the heater at a level that the temperature of the sensor increases from 2°C to 10°C over a 20 minute period; (3) recording the transient response of the temperature sensor and (4) measuring

the heater power.”

A refinement used by Wechsler and Glaser for their probe was to use small diameter glass supports for the wires in the apparatus to reduce any heat leaks to the lowest possible levels. The results obtained agreed well with published data and so it was concluded that:

“ The line heat source and thermal conductivity probe, are reliable and versatile apparatus for measurement of thermal conductivity of rocks and minerals in solid vesicular and powder form.”

Banaszkiewicz *et al* (1997) have produced an algorithm to obtain thermophysical properties from interstellar bodies such as the moon, Titan or comets such as Wirtanen.

The object of the new method of data interpretation is to allow accurate measurements of thermal conductivity and thermal diffusivity under difficult conditions. The available resources for space experiments are very extensive and so it is prudent to be able to extract as much as possible from available data and to design the experiment in the most optimal way. The probe was constructed from a 1mm radius hollow aluminium cylinder with a copper wire (radius 0.03mm) tightly wound round it. The wire serves as a heat source and simultaneously as a resistance type temperature sensor. To improve the thermal contact between the probe and the medium being measured, the free space around the probe had been filled with pump oil, which the authors considered to be a perfect conductor due to the convection effect. This method uses constant power for supplying the heater rather than the constant current supply that is more normally utilised, since the changing resistance is required to give the temperature rise. It was estimated that given 0.01K accuracy in temperature data, then any thermal diffusivity determinations should have an accuracy of about 5%.

Various transient methods for the determination of the thermal conductivity and thermal diffusivity.

In 1950 Clarke and Kingston published an account of the use of a 'variable state' method

of simultaneously determining the thermal conductivity and thermal diffusivity of insulating materials (Clarke & Kingston,1950). The apparatus used thin strips of shim steel as heaters providing constant heat input through blocks of the sample whose properties were to be measured. The blocks were arranged so that the heaters sandwiched the interface at which the temperature rise was measured. Ebonite slabs were used to partially isolate the sample. The whole test block was housed in a constant temperature cabinet maintaining a temperature within a variation of approximately +/- 0.05°C. The procedure used heating time-periods of about 270 seconds with a cooling time of about 155 minutes. The authors evaluated various sources of error, including the thermal capacity of the heater, the thermal capacity of the apparatus, heat losses from the pile and the thermal contact resistance of the heater, the total error being approximated as +/- 2.5%. The apparatus was felt to be suitable for the determination of the thermal properties of heat insulating materials available in sheet form.

Transient plane source or transient hot strip method

This technique is a development of the hot wire method, whose initial use was to help determine the thermal conductivity and thermal diffusivity of soils when designing and optimising earth based heat pump systems, (Gustafsson,1979). The technique utilises a metal strip both as a continuous plane heat source and as a sensor of the temperature increase in the strip itself. Solid materials are investigated by pressing the strip between two flat surfaced samples of the material. The thermal properties are obtained by a similar technique to the probe method. A constant current is supplied to the metal strip. The subsequent voltage increase between the ends of the strip is monitored over a short period of time after the current was switched on. Gustafsson and Karawacki (1979) carried out a series of studies on various materials including granite and quartz and glycerine. The thermal conductivity values for granite gave a mean value of 3.680 $\text{Wm}^{-1}\text{K}^{-1}$ with a standard deviation of 0.007 $\text{Wm}^{-1}\text{K}^{-1}$. The thermal diffusivity for the same material gave a mean figure of $1.541 \times 10^{-6} \text{m}^2 \text{s}^{-1}$ with a standard deviation of 0.020 $\text{m}^2 \text{s}^{-1}$.

Glycerine gave results of $0.2855 \text{ Wm}^{-1}\text{K}^{-1}$ as a mean value of thermal conductivity with a standard deviation of 0.0019. The mean thermal diffusivity was found to be $9.42 \times 10^{-6} \text{ m}^2\text{s}^{-1}$ with a standard deviation of 0.22×10^{-6} (This thermal diffusivity is reported as $\dots \times 10^{-2}$ but is inconsistent with other values contained in a similar nearby table.... a value of $\times 10^{-8}$ is consistent and I strongly believe that this was a typographical error). These results give good agreement with results of experimentation undertaken by the author see chapter 6. An evolution of the technique used a series of 'square' pulses rather than the single transient heating of the metallic thin film. This development reduced the need for '*expensive electronic equipment*' (Gustafsson, 1983).

A new ring source device is described by Sattel as a time dependent method, with the time for one measurement being not longer than one minute (Sattel, 1980). This method used the centre of a heated ring to give the time-dependent temperature values of thermal conductivity, thermal diffusivity and volumetric specific heat. Samples of different sediments under pressures of up to 400 bar were measured in layers that enabled study of the different heat flow characteristics, both perpendicular and parallel to the layers. This method helps explain the negative slope of temperature gradients within boreholes in situations such as oilfields.

In 1990 Gustafsson published information concerning a variation of the transient plane source technique by using two experimental arrangements referred to as the hot square and hot disk. The two transient plane source elements are made of $10\mu\text{m}$ nickel foil covered with $25\mu\text{m}$ Kapton. These elements were used to measure the thermal properties of materials as cold as liquid nitrogen and for metals and insulators at temperatures of 200°C . These two configurations allowed maximum applicability whilst still combining both the heat source and the temperature sensor. The plane source elements were also used by Izhar-ul-Haq et al (1991) to investigate the thermophysical properties of marble

stone building materials. The measured values of thermal diffusivity of the marble samples were in close agreement with similar values obtained by the transient hot strip method.

Further refinements of the transient plane source method include the dynamic plane source technique that has been used for studying poor thermal conductors with thermal conductivities equal or below $2 \text{ Wm}^{-1}\text{K}^{-1}$, such as rubber and polycarbonate, (Karawacki et al 1992).

A re-evaluation of the Transient Hot Strip method was undertaken by Song et al (1993), who investigated the thermophysical properties of granular materials and proposed a new technique for evaluating data over a long time period. The transient hot strip method was also used by Song et al (1993) to determine the thermal conductivity, thermal diffusivity and specific heat of slags containing iron oxides. Sabuga and Hammerschmidt (1995) used a 'standard' transient hot strip technique to investigate the thermophysical properties of Pyrex glass 7740, but used an individual weighting factor to account for systematic errors in the data. This procedure is intended to yield valid thermal conductivity and thermal diffusivity measurements.

Red-sand bricks, glycerine and mercury were investigated using the Transient Plane Source technique by Maqsood et al (1994). The source of heat was a hot disc made from bifilar spirals and similar to that used by Izhar-ul-Haq et al and Karawacki et al. Similar investigations were undertaken on thin samples of metallic materials, (Gustavsson et al, 1994) and on silicate and carbonate based rocks (Saxena,1994). The measured values for the thermal transport properties of glycerine at room temperature gave a thermal conductivity of $0.314 \text{ Wm}^{-1}\text{K}^{-1}$ and a thermal diffusivity of $1.1 \times 10^{-7} \text{ m}^2 \text{ s}^{-1}$. These figures compare well with measurements carried out by the author, (details in chapter 6, laboratory measurements.)

The transient copper disc sample method

This technique uses a preheated copper disc that is brought into contact with a disc shaped sample. The sample is initially at a uniform temperature and surrounded by a thick layer of insulation. The copper disc has the same surface area as the sample and is assumed to be brought into perfect contact with the whole upper face of that sample. exponents of this technique also assumed that the copper disc is a perfect conductor and that there is no heat loss from the system and therefore the total quantity of heat in the system remains constant. Thermal conductivity, diffusivity and specific heat capacity variables can be obtained from this technique.

This method relies on the prompt application of the preheated disc onto the sample in a definite and rapid manner, combined with a sufficiently low thermal contact resistance as to not affect the measured temperature transients. To this end, silicon grease was used to improve the thermal contact between the copper disc and the sample. The silicon grease had to fulfil the following requirements: -

- (i) not to soak into the sample,
- (ii) to yield easily at the points of contact as the copper disc is brought into contact with the sample, but to have lower mobility thereafter and
- (iii). to possess a high thermal conductivity.

In this work, the use of silicon based contact heat sink compound is discussed in chapters 4 and 5. The results of the laboratory and field studies use of silicon heat sink compound are described in chapters 6 and 7.

Conclusion

The reader may recall that to satisfy the requirements for studying the thermal properties of cob walling (as described in chapter one),

- (i) the technique must be non-destructive,
- (ii) it must not influence the material being measured,
- (iii) it must give representative values for both (λ) and (α),
- (iv) it should be rapid and affordable and
- (v) allow *in-situ* testing.

As can be seen in the previous review, many transient thermal measurement techniques have been developed to provide thermal information for different materials. These methods can provide values for the thermal diffusivity and allow data collection with minimal disruption. Some of the methods are, however, best suited to the laboratory or require such extensive development that they will be unsuitable for *in-situ* testing of cob walling. The thermal probe technique is simple and robust which makes it suitable for *in-situ* testing. However, the varying conditions that will be encountered by the unpredictable nature of the measurement environment and lack of any sample preparation do raise several critical questions. The technique will have to provide consistent results in the field, where there may be considerable variations in the probe hole temperature. The walling structure and hole surface properties will vary considerably, introducing difficulties in maintaining adequate thermal contact between the probe and the sample. These issues will be discussed and potential solutions developed and reviewed.

Chapter 4

Apparatus and procedure.

Two different arrangements of apparatus have been used during this project to measure the thermal properties of cob samples. The first measurements were taken using a laboratory-based system on samples of cob material and other specimens. A second portable system was developed from the first, which was suitable for the field studies. This chapter describes the two sets of test apparatus.

The thermal probe method of measuring the thermal properties has been selected as the most promising technique, as it can meet the criteria set earlier in this work. The probe used can be small, thus enabling measurements to be taken without large-scale disruption of the specimen. The equipment required to power the probe heater and to record any data is relatively simple and can be powered from a portable DC supply. The sample times are commendably small, in the order of a thousand seconds, although much longer periods are required between measurements, so that thermal equilibrium in the sample can be regained. With modern developments in telemetry, simple automated data collection could soon be possible (see conclusions and future work).

The design of the thermal probe used in this work was based upon that developed by the University of Cranfield, (Batty et al, 1984). The final version of the probe produced by the University of Cranfield was made from a stainless steel tube of external radius (r_0), 1.3×10^{-3} m, (a diagram of the probe can be found in appendix B). The hairpin heater was made from doubled mild steel wire and ran nearly the whole length of the probe. The temperature sensor was a type E thermocouple attached to the centre of the heater, and therefore at the centre of the probe. Two small section cables lead from the thermocouple to a measurement point located in a datalogger. Current and potential leads were

attached to the heater and a Farnell Instruments Ltd L30 stabilised DC power supply was used in the laboratory studies. The potential difference across a standard resistance, in series with the probe heater, was used to determine the heater current. The potential differences, across the probe heater and a 1Ω standard resistance, were measured and recorded by the data logger. The probe was sealed at one end with an inert fast-setting epoxy resin adhesive. At the other, a plastic grommet protects the cabling as it leaves the probe.

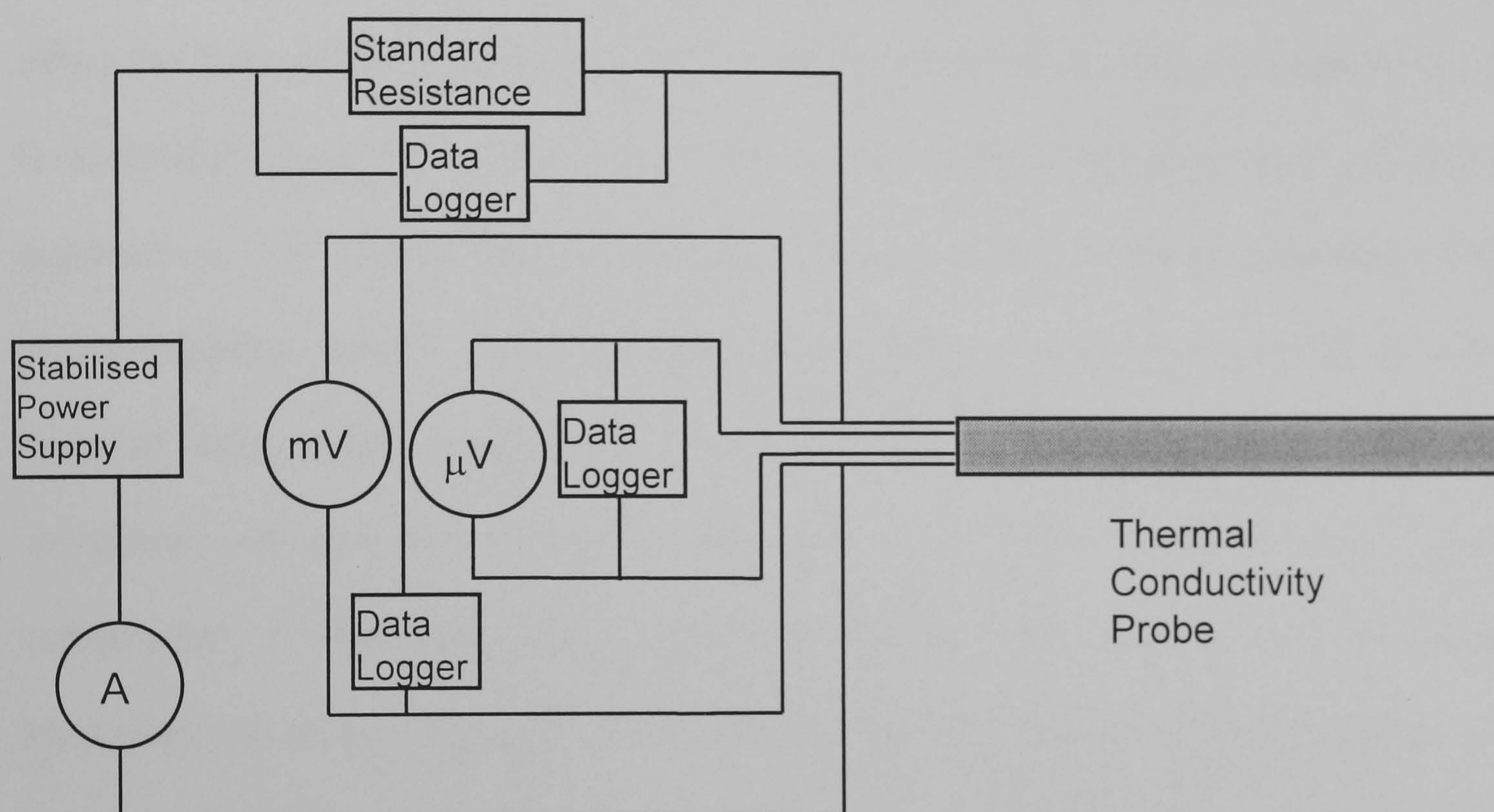


Fig 4.1, Diagram (not to scale) of the probe and accompanying instrumentation.

As has been previously stated the simplicity, size and operation of the probe lend itself to the *in-situ* testing of cob walls. To ensure the accuracy of the measured thermal data:

- The contact thermal conductance, H , between the probe and the measured material must be good, that is, a value of H which is as high as possible.
- The initial temperature at the precise moment before the heater is switched on must be known.
- The confirmation of little variation of background and sample temperatures.

- The power supplied to the probe heater has to remain constant and stable.

Some of these criteria affect the design of the probe and any associated measurement and recording instrumentation. The probe design evolved as the parameters required by the technique were clarified during the work, (details of these changes can be found later in this chapter).

The three main variables that need to be recorded whilst carrying out measurements using the thermal probe technique are (i) the temperature of the probe before the heater is switched on, (ii) the temperature during the heating schedule and (iii) the power supplied to the probe heater over the whole period of the experiment. The first instrumentation used to measure and record these variables consisted of a Hewlett Packard data logger linked to a Hewlett Packard HP 85B personal computer. The command software and recorded data were saved onto magnetic tape. Due to a combination of hardware and software problems, this measurement and recording instrument could not be used to its full potential and another instrumentation set was developed.

The new measurement and recording equipment was based around a Geologger Datataker model 615. This instrument can record temperatures from a range of different thermocouple types at different time steps. Small electrical voltage values can also be measured and stored to ensure an accurate determination of the power delivered to the probe heater. This instrument was supplemented with several more conventional measurement devices such as mercury-in-glass thermometers and digital multimeters. These were used to check the accuracy and correct functioning of the Datataker and to give an alternative check on conditions before and after the test period.

The eventual goal of the testing programme was to ensure accurate and valid measurements are taken *in-situ*. It is hoped that the results from these tests will faithfully measure the thermal properties of the samples under field conditions. However, it needs to be verified that the test equipment can produce accurate data. Thermal values can be measured for materials with known thermal properties under controlled conditions using the laboratory equipment. Until this controlled laboratory work is carried out the results of any *in-situ* tests will be uncertain. Because of this an initial series of laboratory studies on suitable materials was undertaken.

The different material samples that were investigated under laboratory conditions were tested at two locations on the University Campus, a laboratory area within the School of Architecture and the Building Science Laboratory in the Smeaton Building. The laboratory situated in the School of Architecture is an internal room with a small roof light and no form of heating. Because of this it has a reasonably stable thermal environment and was suitable for the initial series of tests. (It was felt that as the eventual goal of the project was to produce accurate measurements in a changeable thermal environment that it would be unwise to use fully temperature controlled conditions). The Building Science Laboratory however, does have underfloor heating and some large areas of north facing glazing and so provides a thermal environment that varies, but not as much as external conditions. For a direct comparison between the variations of ambient temperatures and the internal probe performance, please view graphs 7.1 and 7.2 in chapter 7. Graph 7.1 shows the ambient temperature variation during a typical field experiment and the probe temperature for one thousand seconds after the probe heater is switched on. In this field experiment the probe is placed horizontally into a 600mm thick cob wall. Graph 7.2 shows the reader how the rise in probe temperature can be affected by the reduction in probe heater power. The probe temperature at a probe heater power of 0.16W can be seen to

be far more erratic than the higher probe heater powers.

Initial tests were performed within a well-insulated container following the advice of Hooper and Lepper (1950):

“ Any temperature gradients within the specimen prior to the start of a test must be avoided. This necessitates the allowance of a few minutes time to permit the instrument to attain temperature equilibrium with the specimen before a test can begin. Variation in the temperature of the surroundings of the specimen may also give rise to initial temperature gradients. These can be avoided by wrapping the specimen heavily with insulation sometime before a test is made. Larger specimens are less subject to this effect.”

Further studies were carried out in which the samples were left uninsulated, and allowed to vary in temperature much as a field sample would. However the field studies are to be carried out upon cob walls 620mm thick, probably matching the performance of larger specimens. In this case according to Hooper and Lepper the measurements will be “ less subject” to any variations in surrounding temperature.

This series of studies replicated the varying temperature conditions similar to those encountered when carrying out field measurements. It was logical then to use the Building Science Laboratory as a ‘stepping stone’ to using the field apparatus in the external environment.

The initial measurement series investigated materials with known thermal properties. These materials were also chosen to provide a good thermal contact between the probe and the test material. Viscous liquids and easily deformed solids of low thermal conductivity allow the probe to have good physical contact with the sample medium. The range of these materials and the preparations undertaken before carrying out any measurements are discussed in chapter 6. The materials were placed in an insulated container and left undisturbed for a period of 24 hours between each measurement. This minimised the effects of any outside influences and reduced the impact of any previous

heating schedule. The field testing equipment used the same Geologger 615 for data collection and was fitted with two probes. To enhance the degree of portability and robustness of the field equipment, a watertight case with appropriate seals for any cabling and access arrangements was used. Separate lead-acid batteries powered the logger and the probe heater circuits. The circuits for each of the two probes could be selected by using a rocker switch and the equipment had built-in displays to monitor power usage and to ensure that the batteries had sufficient charge to undertake the field measurements. Data was transferred using a laptop computer with the same communication software as the laboratory based equipment.

Probe Development

The first probes used were based upon those developed by Dr Batty at the University of Cranfield. As previously mentioned, the probe wall was made from stainless steel tubing 0.067m long. Within this tube the heater and thermocouple were positioned. Ranges of measurements were undertaken using this configuration, but the results appeared to give inaccurate values for the thermal diffusivity of the test materials. It was felt that an improvement in thermal contact, that is a larger value of the probe thermal conductance, H , or better still a known value of the thermal contact was needed. To this end, the work of three groups, Banaszkiwicz, et al, (1997), Highgate and Mole, (1967) and Clarke & Kingston, (1950) were followed, (see chapter 3). These authors advocated that a heatsink material can provide a superior thermal contact between the surfaces of a measurement device and the sample. To provide such an improvement a silicon based heatsink compound was used to fill the interior of some of the probes. A number of holes in which the probes were inserted were also filled with heatsink compound. Two types of heatsink compound were used. The first was a silicon based compound manufactured by Electrolube, called HTSP, having a conductivity of $2.9 \text{ Wm}^{-1}\text{K}^{-1}$. The second material used

was produced by Dow Corning Ltd having a conductivity of $0.9 \text{ Wm}^{-1}\text{K}^{-1}$. The results of the unfilled and filled probes and holes can be viewed in chapter 6 and 7.

To allow the use of Blackwell's analysis of a radial heat flow condition for an infinite region of one material, bounded by a hollow cylinder, (see chapter 5, the 'rate analysis') a second thermocouple was attached to the outer surface of the probe wall. This enabled an analysis of the rate of change of temperature with time, with respect to short times when the probe was heated and then the heat flowed from the probe into the sample. Values for the thermal capacity of the probe, mc and the thermal resistance between the probe heater and the specimen H can be found .

The results of the laboratory and field studies using the equipment described within this chapter and the analysis outlined in chapter 5 can be viewed in chapters 6 and 7 respectively.

Chapter 5

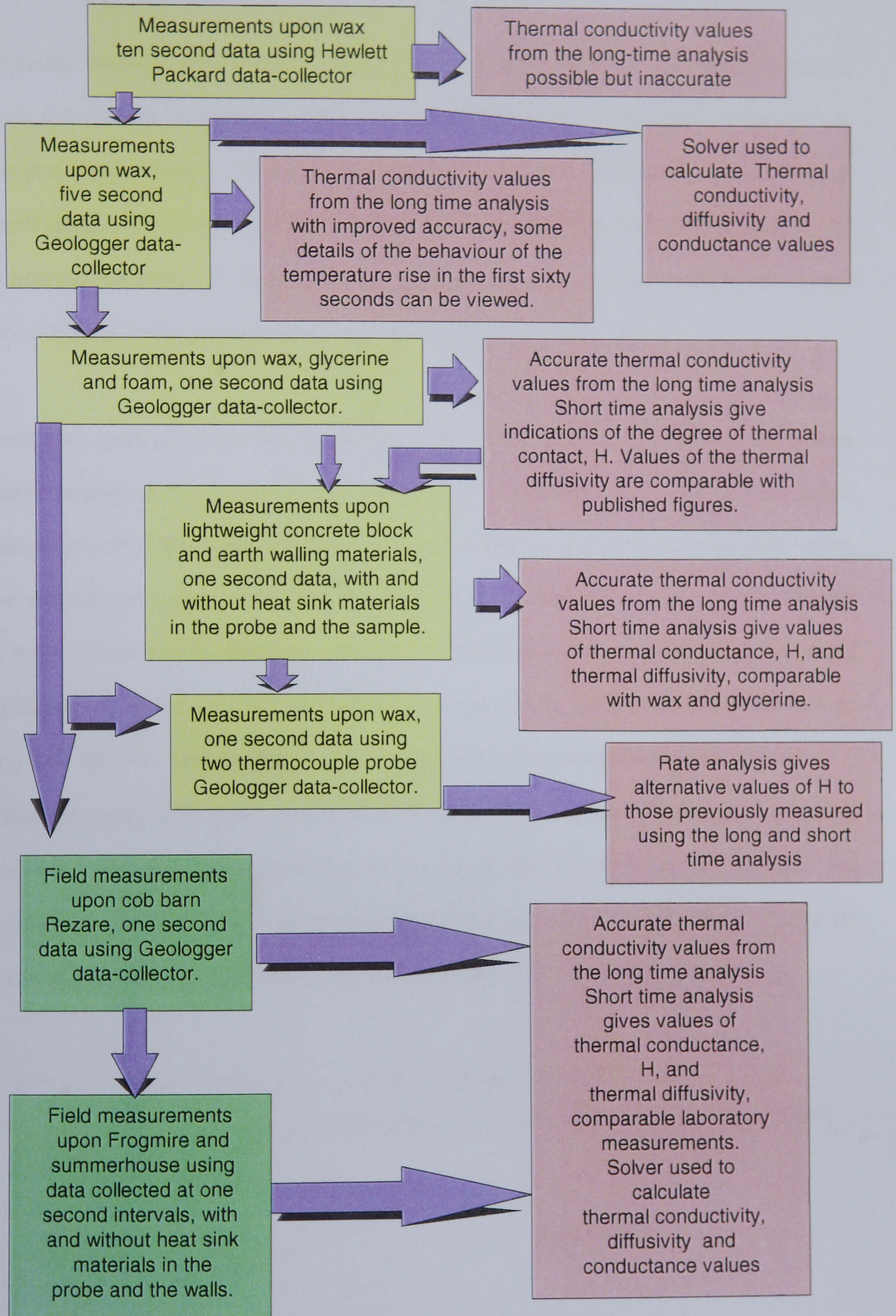
Measurement Theory.

The field studies are the main goal of this work, i.e. to visit a real cob wall, collect a set of data and use a number of well tried and tested routines to establish the wall's thermal conductivity and diffusivity with confidence. To reach this goal has involved some years developing the time dependent thermal probe technique. This development has advanced on two fronts. The first concerns the quality and quantity of the data (and a number of different specimens have been studied), while the second concerns the data handling routines used. These routines obtain the thermal conductivity and diffusivity and have been refined and expanded. Presenting this complex tale has its own difficulties, but the reader whose experience of this study may be limited, has an even more difficult task. In order to help the author and reader the following flowchart, figure 5.1 (over-page), was produced. This shows how both the experimental procedures and the methods of analysis have evolved chronologically.

The determination of thermal constants, λ and α of building materials by using a probe technique has been researched by a number of authors. (See chapter 3). Most investigators have concentrated upon the use of the technique to find the thermal conductivity of their specimens. However, according to Blackwell, (1954) the technique will also give values for the thermal diffusivity. If the density of a sample is known, the thermal capacity may be calculated from the diffusivity. These values, the thermal conductivity, λ and heat capacity, c , are important variables that will allow the building material to be modelled as part of a thermal simulation. This will reveal an accurate picture of the material's thermal behaviour under a range of simulated conditions.

Fig 5.1, Summary of Laboratory and Field Measurements.

Chronology: The earliest data is at the top of the page, the latest at the bottom.
 Key to colours: Pink = Analysis, Yellow = Laboratory measurements, Green = Field Measurements.



To accurately measure these thermal variables under both laboratory and field conditions Blackwell (1954) has suggested modifications to the original expression developed by Carslaw and Jaeger (1947). The major modifications allow; (i) the probe to be represented as a continuous line source of heat, and (ii) the contact resistance between the probe and the boundary of the sample is to have a finite value. Previously it is assumed that this contact resistance is zero, or the probe thermal conductance, H , to be very large.

Blackwell also concluded that two solutions of this heat flow from the probe as a time dependent function of the probe temperature would be necessary. Most investigators in this field before and after Blackwell had only investigated data at 'large times'. Blackwell states that the inclusion of contact resistance at the probe/test material boundary complicates the 'large time' solution and that the thermal contact resistance would be best found independently. A solution at short times, but still subject to the same boundary conditions as the long time solution, was proposed by Blackwell and will be described in this chapter. If λ is the thermal conductivity of the specimen, $\text{Wm}^{-1}\text{K}^{-1}$, α is the thermal diffusivity of the studied material, m^2s^{-1} , H is the outer conductivity of the probe, $\text{Wm}^{-2}\text{K}^{-1}$, Q is the heat supplied per unit length of probe, Wm^{-1} , the elapsed time of the measurement is t seconds and r_0 is the probe radius, m , then Blackwell states that the long time solution can be expressed as;

$$\theta = (Q/4\pi\lambda l) \{ \ln(4\alpha t / r^2) - \gamma + 2\lambda/rH + (r^2/2\alpha t) [\ln(4\alpha t / r^2) - \gamma + 1 - (\alpha mc/\pi r^2 l \lambda) (\ln(4\alpha t / r^2) - \gamma + 2\lambda/rH)] + \text{other terms } (r^2/\alpha t)^2 \}$$

.....Equation 1.

This reduces to

$$\theta = A [\ln t + B + (1/t) (C \ln t + D)] \quad \dots\dots \text{Equation 2.}$$

(When $\frac{1}{t_1^2}$ is very small or the term $O\left(\frac{r_o^2}{\alpha t_1}\right)^2$ can be neglected)

The four constants A,B,C and D of equation 2 have values:

$$\begin{aligned} A &= Q/4\pi l\lambda \\ B &= \ln(4\alpha/r^2) - \gamma + 2\lambda/rH \\ C &= (r^2/2\alpha)[1 - \alpha mc/\pi r^2 l\lambda] \quad \text{and} \\ D &= (r^2/2\alpha) [\ln(4\alpha/r^2) - \gamma + 1 - B\alpha mc/\pi r^2 l\lambda] \end{aligned}$$

where m = mass per unit length of the probe, Kgm⁻¹,

c = specific heat capacity of the probe, JKg⁻¹K⁻¹.

The analysis methods are now described in sequence. Each description uses a typical set of experimental data to illustrate the data handling.

Long time analysis, (t ≅ 150 to >1000 seconds, measurement time suggested by Blackwell and reinforced by experimentation shown in chapter 6).

For the long time solution the contribution of the term $\frac{1}{t_1}$ within the expression; $\theta = A [\ln t + B + (1/t) (C \ln t + D)]$ becomes negligible. Under this condition, the use of the above expression with experimental data yields a value for the thermal conductivity from term A,

since; $\theta_2 - \theta_1 = Q/4\pi\lambda \ln(t_2/t_1) \dots \text{Equation 3}$

or, a graph of the rise in probe temperature versus the natural logarithm of the elapsed time has a linear asymptote of slope $\frac{Q}{4\pi\lambda}$. Thus, if the power dissipated per unit length, Q is known, then the thermal conductivity λ can be determined. However, this relationship only exists assuming the probe behaves as a continuous line-source of heat of infinite length surrounded by an infinite medium. This assumption can be inaccurate and the effects of the finite radius of the probe and finite dimensions of the specimen have been considered by Vos, (1955). If the probe has a radius of r_0 , m, and the specimen has a thermal diffusivity α , m^2s^{-1} , then the time, t , seconds must satisfy the condition; $\frac{4\alpha t}{r_0^2} > 50$ or $t > \frac{50 r_0^2}{4\alpha}$...**Equation 4.**

The first effect described by Vos, equation 4, termed the r_0 effect, gives the delay in elapsed heating time associated with a probe of given diameter, before the linear section described by equation 3 is observed.

The second effect is associated with the finite dimensions of the sample. Vos describes a reflection effect that is concerned with the possible disturbance to the results of an experiment by the reflected heat wave travelling back to the probe from the nearest boundary of the specimen. According to Vos, the boundary effects become significant if;

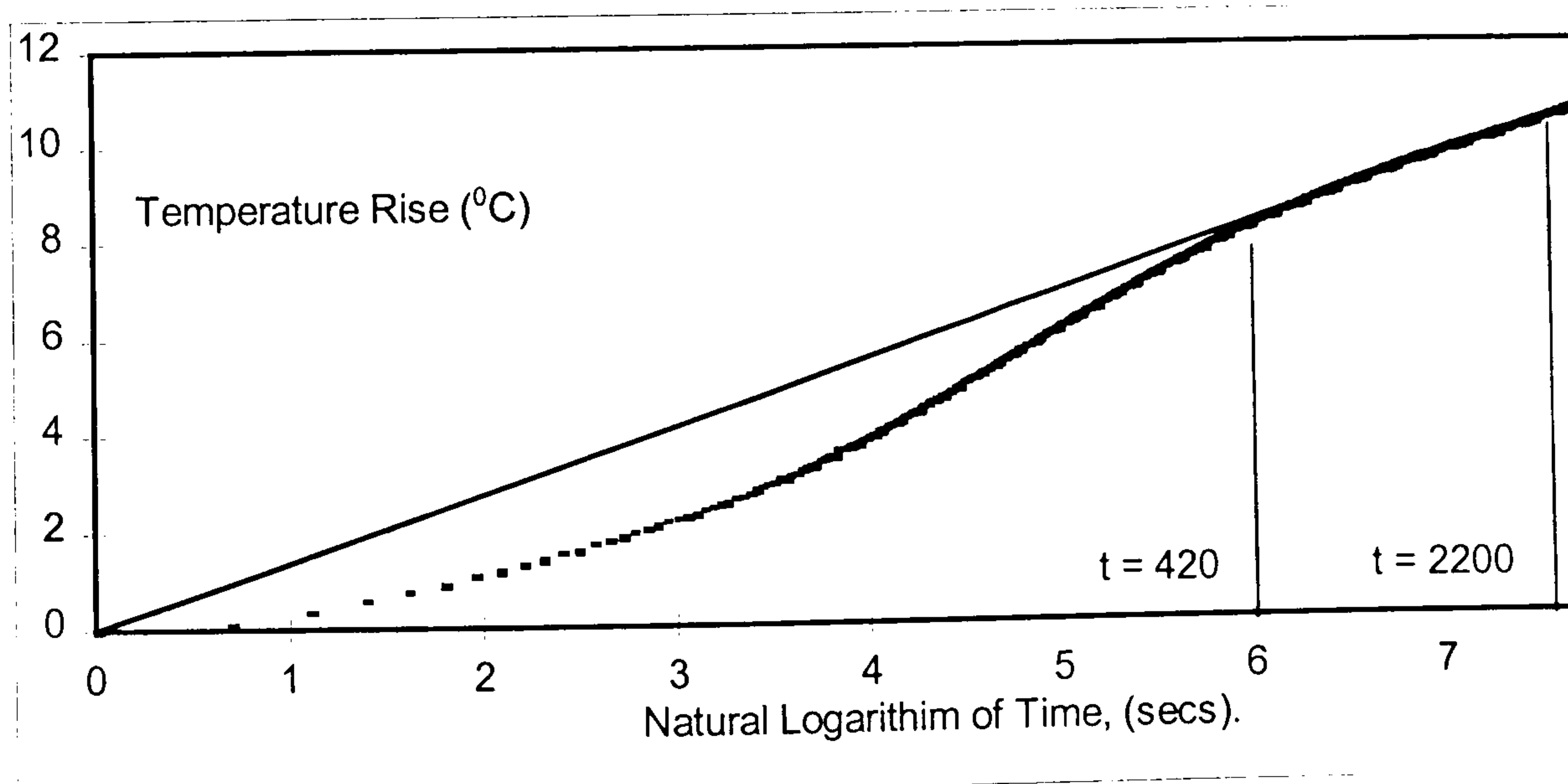
$$4\alpha t/r_0^2 > 0.6 \dots \text{Equation 5,}$$

Thus, to ensure that the results from the tests are unaffected by inappropriate heater durations and reflections from the specimen boundary, the test probe and samples need to conform to equations 4 and 5. The Vos criteria are not totally consistent in their published form and we will return to these two tests later in the discussion,

With the assumption that the two effects described by Vos have not unduly effected the long time results, the thermal conductivity may be found, see graph 5.1. However, the thermal diffusivity and ultimately the specific heat capacity of the sample are also required. To obtain the value of the thermal diffusivity from term B in the long time equation, equation 2.

Blackwell judges that the value of the parameter $\frac{2\lambda}{r_o H}$ needs to be very small, that is H is large and so the thermal contact resistance is appropriately small. The value of the thermal diffusivity may also be calculated if the value of H is known. This value of H can be obtained from both Blackwell's 'rate' studies and 'short time' analysis. Again, these two methods of analysis will be considered in more detail later.

Returning to the long time analysis, to illustrate this technique a typical set of results is shown in graph 5.1. Here the temperature rise of the probe ($\theta_2 - \theta_1$) is plotted against the natural logarithm of the elapsed time in a sample of phenolic foam. The linear portion extended from $\ln t = 6$ up to $\ln t = 7.7$ or from a time $t \cong 400$ seconds to $t \cong 2200$ seconds as was apparent by eye. A regression analysis of this region of the data gave the conductivity range stated below graph 5.1, from term A of the Blackwell long time equation.



Graph 5.1, shows typical long time behaviour, phenolic foam.

This study of phenolic foam has given maximum and minimum thermal conductivity values of 0.0283 and 0.0281 $\text{Wm}^{-1}\text{K}^{-1}$ with a mean value of $0.0282 \pm 0.003\text{Wm}^{-1}\text{K}^{-1}$. This value is approximately 12% smaller than the value given by the supplier, British Petroleum (0.032 $\text{Wm}^{-1}\text{K}^{-1}$).

This experiment was carried out with an air filled probe with a single central internally located thermocouple mounted at the centre of the probe, as described in chapter 4. The values for the thermal conductivity of the phenolic foam are described in more detail in chapter 6 and the implications of these results discussed in chapter 8.

Using the restrictions that Vos stated to the phenolic foam example, where $\alpha = 1.55 \times 10^{-8} \text{m}^2\text{s}^{-1}$ and $r_0 = 1.35 \times 10^{-3} \text{m}$, then the delay in time before the linear section and the assumptions of the probe theory hold true is ; $50 \times (1.35 \times 10^{-3})^2 / (4 \times 1.55 \times 10^{-8})$, which is 1470 seconds. The major part of the line used to calculate the conductivities is formed from data measured at times greater than 1470 seconds. Thus, the results from this long time analysis should accord with the thermal probe theory. However, part of the linear section of the curve does start before $t=1470$ seconds, at approximately $t=420$ seconds. If this time period is used in equation 4 the thermal diffusivity obtained is $5.424 \times 10^{-8} \pm 5.4 \times 10^{-9} \text{m}^2\text{s}^{-1}$ approximately 4 times larger in magnitude than the known value.

Short Time Analysis

In order to determine the probe to specimen thermal conductance, H, Blackwell, (1954) derived the small time or short time approximation;

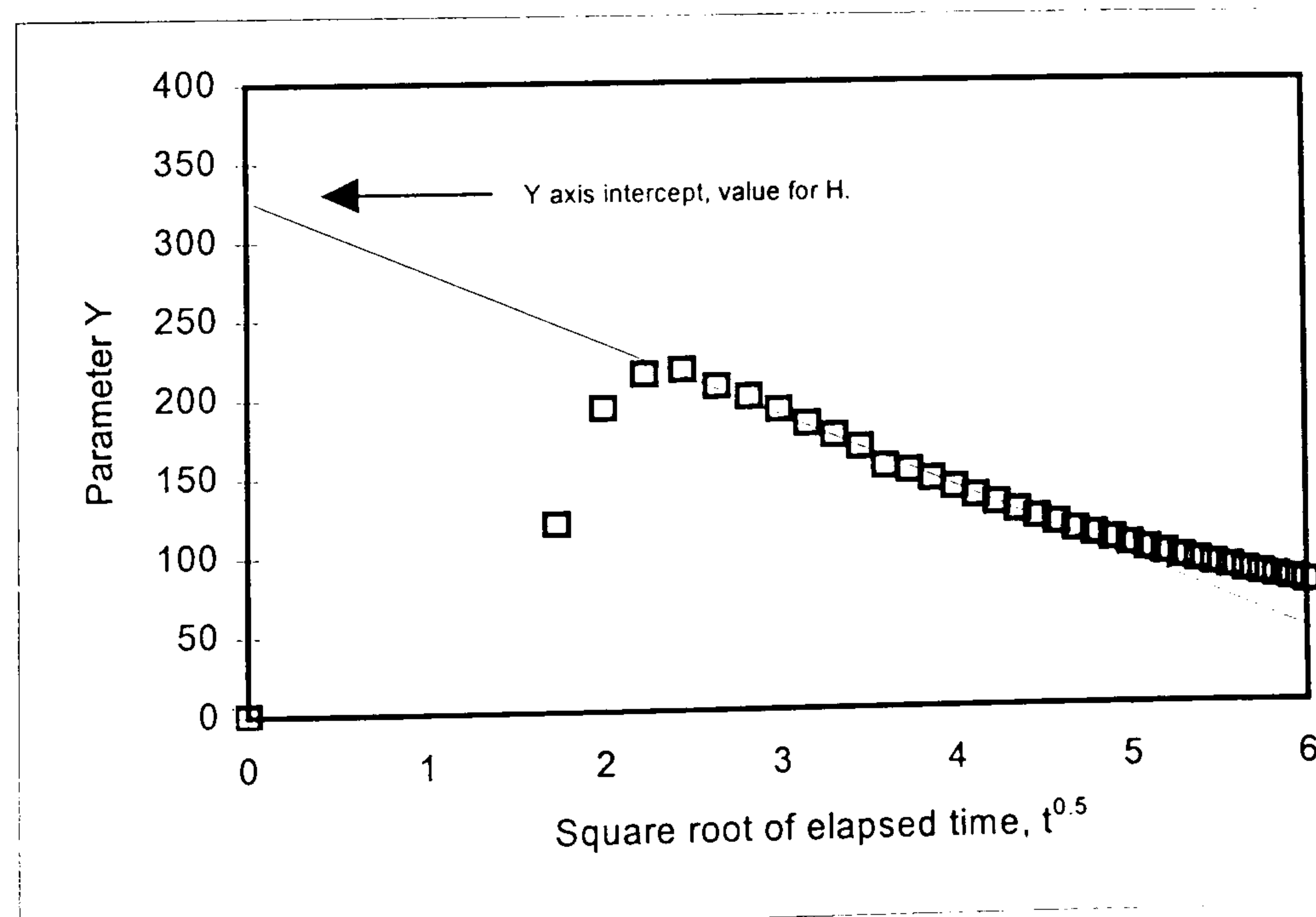
$$Y = ((mc/\pi r_0)(1/t^2))(t - (r_0 - r_1)^2/6\alpha_p - mc\theta/Q)$$

$$\approx H - ((16 H^2 \alpha^{0.5})/15\pi^{0.5}\lambda)t^{0.5} \dots \text{Equation 6}$$

where m is the mass per unit length of the probe, kgm^{-1} , c is the specific heat capacity of the probe, $\text{Jkg}^{-1}\text{K}^{-1}$, r_0 is the external radius of the probe, m , r_1 is the internal radius of the probe, m , α_p is the thermal diffusivity of the of the probe material, m^2s^{-1} , α is the thermal diffusivity of the specimen, m^2s^{-1} , Q is the heat supplied per unit probe length per unit time, Wm^{-1} and H is the outer conductivity of the probe, $\text{Wm}^{-2}\text{K}^{-1}$,

If the parameter Y is plotted against $t^{0.5}$ at short times t , a straight line should result, with an intercept H and a slope proportional to the square root of the thermal diffusivity. Blackwell points out that at very short times, say over the first few seconds, this behaviour will not be observed.

The value of the probe conductance (H), found from this short time solution, will be compared with values determined using the rate studies, presented in the next section. The value of H may be used to establish the physical 'fit' or contact conductance of the probe in the specimen. To illustrate this calculation the following example shows the short time analysis carried out upon a sample of cobblock using a probe and sample hole filled with the heat-sink material HTSP.



Graph 5.2, shows a typical short time analysis for cob block with HTSP heat sink material in the sample hole and in the probe.

Graph 5.2 shows Blackwell parameter Y plotted as a function of the square root of the heating time. A linear section exists between $t^{0.5}$ values of approximately 2.4 and 4.6, or between 6.0 seconds and 20 seconds. This gives an intercept on the Y -axis of approximately $327 \text{ Wm}^{-2} \text{ K}^{-1}$. As seventeen data points form the linear portion of the plot it can be assumed that equation 6 describes the data over this section of the experimental time scale. The repeatability of this analysis technique can be assessed by viewing the many similar curves in chapters 6 and 7.

The short time analysis is very sensitive to the correct initial temperature and time and this is again demonstrated in chapters 6 and 7. For this reason, the initial probe heater start time must be known precisely and data acquisition is required once every second.

To calculate the thermal diffusivity, which will in-turn allow the thermal capacity to be found, the thermal conductivity has to be known. Separate results from each experiment are shown in chapter 6.

Rate Analysis

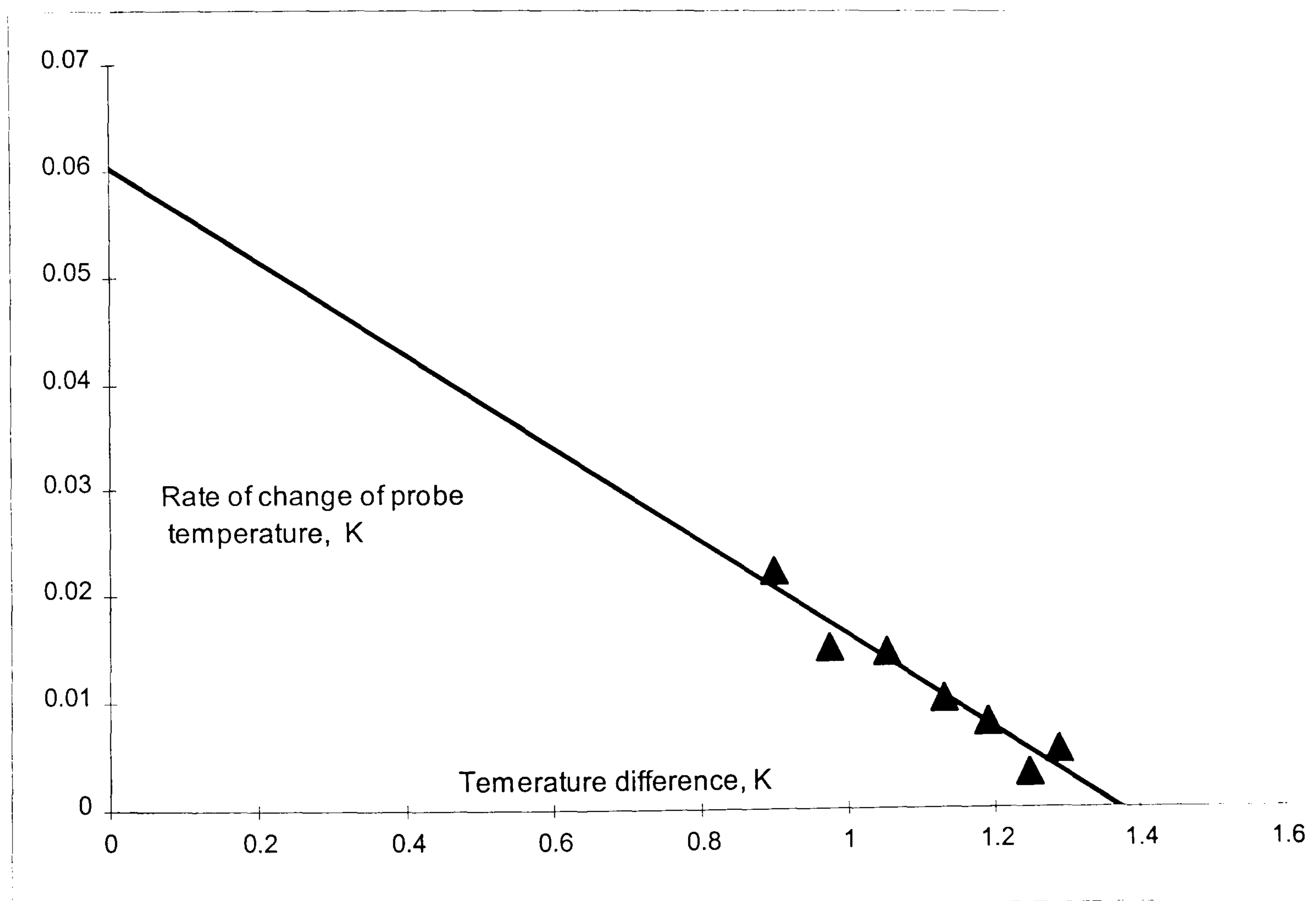
Blackwell's analysis begins with a differential equation and his argument runs; a probe of thermal capacity mc , is placed in a specimen and supplied with constant power, W . The temperature at the centre of the probe is θ_1 and just outside the probe and in the specimen the temperature is θ_2 . If the thermal conductance between these two temperatures is H , (that is between the probe and the specimen), then the rate of heat gain by the probe must be equal to the rate of energy arrival W minus the rate of heat loss to the specimen. Therefore, for a long cylindrical probe of length l and radius r we can write:

$$mc \frac{d\theta_1}{dt} = W - H 2\pi r l (\theta_1 - \theta_2), \dots \text{Equation 7}$$

(neglecting any end effects).

Please note: Q has been used in equation 6, where Q is the heat supplied per unit probe length per unit. It was felt that as Blackwell has already used these terms, it was easier to use W to equal the rate of energy arrival, where $W = Ql$.

A graph of $d\theta_1/dt$ against $(\theta_1 - \theta_2)$ has a slope of $H2\pi r l/mc$ and an intercept of W/mc . Since the values of W, r and l are known, then both mc and H can be determined. The following graph, graph 5.3, shows the rate analysis applied to an experiment carried out upon paraffin wax, using a probe without any heat sink material within the probe. The numerical results are shown in table 5.1 and further details are described in chapter 6.



Graph 5.3, shows the rate of change of probe temperature as a function of probe to specimen temperature difference $(\theta_1 - \theta_2)$.

Slope	-0.0439
Intercept	0.0601
Mean Power, W.	0.1041
Thermal Capacity of Probe, mc, JK ⁻¹	1.732
Probe Conductance, H, Wm ² K ⁻¹	136

Table 5.1, shows the results from the rate analysis of wax, runcode W2ts2600

These numerical values may then be compared and contrasted with the results of other measurements. For example, using the Blackwell short time studies, the parameter H can be compared with H found from the rate analysis and the iterative solutions described below. This may be seen within chapters 6 and 7 depending upon whether the measurements were undertaken in the laboratory or *in-situ*.

Iterative Solutions.

The early data gathering routines were programmed into the data logger with ten and later five-second intervals between each record of probe temperature, heater voltage and current. The ten and five-second data is sufficient for the interpretation of long time measurements. However, these relatively long time intervals between each data records make it difficult to accurately describe the behaviour of the rate of heat loss from the probe during the initial stages of any of these experiments. A further problem encountered with the early work was that the temperature record immediately before the heating took place was not reliably known for a long enough period, (because of the 5-10 seconds interval between each measurement), so that an accurate value of the initial start temperature was not available. This meant that the short time analysis could not be reliably applied to this data and therefore the 'short time' probe conductance and diffusivity could not be accurately determined. Therefore, to allow the calculation of more accurate results using the existing imperfect data

and to investigate the use of quicker retrieval methods, an iterative optimisation tool, Solver, part of the tools in Microsoft Excel was used.

Solver is an optimisation and resource allocation tool that involves the use of successive trials or iterations. During each iteration Solver uses a new set of values to recalculate a solution using constraints and a series of decision variables. The Solver routine was used to compare a set of temperature data from the internal thermocouple at the centre of the probe with theoretically predicted probe temperature rise data produced using the equation:

$$\theta = A [\ln t + B + (1/t) (C \ln t + D)] \quad \dots \text{Equation 2}$$

An appendix, Appendix A has been included to give a coherent explanation of how Solver works and to describe how Solver has been used to predict α , λ and H. The appendix gives details of the theory behind the probe technique and the principle of the Solver routine. The Solver model that was used, how the spreadsheet was set up and the potential problem of errors in the experimental data is also explored.

The first Solver routine used the terms A and B and therefore concentrated upon the longer time sections of the measured data, because at long times the terms containing $1/t$ are assumed to become very small.

Later in this chapter the solver routine will use all four constants of equation 2, that is A, B, C, and D. These will be used to explore the possible fit of the theoretical curve to the measured data at shorter times. Solver2 and Solver4 will be employed to distinguish between the applications, where Solver2 employs constants A and B and Solver4 uses all four constants, A, B, C and D.

Each calculation produced a set of theoretical temperatures using a range of values for thermal conductivity, thermal diffusivity and the conductance between the probe wall and the test specimen. These values were pre-defined within part of an excel spreadsheet using a number of choices, some larger and some smaller than an optimum value. The range of values of the three required parameters were based upon published data and previously measured values. The Solver was allowed to undertake a series of iterations over a 100-second period using a Pentium Personal Computer. Each iteration aimed to minimise the sum of the difference between the measured probe temperature (θ_m) and the theoretical probe temperature (θ_r), using the following equation;

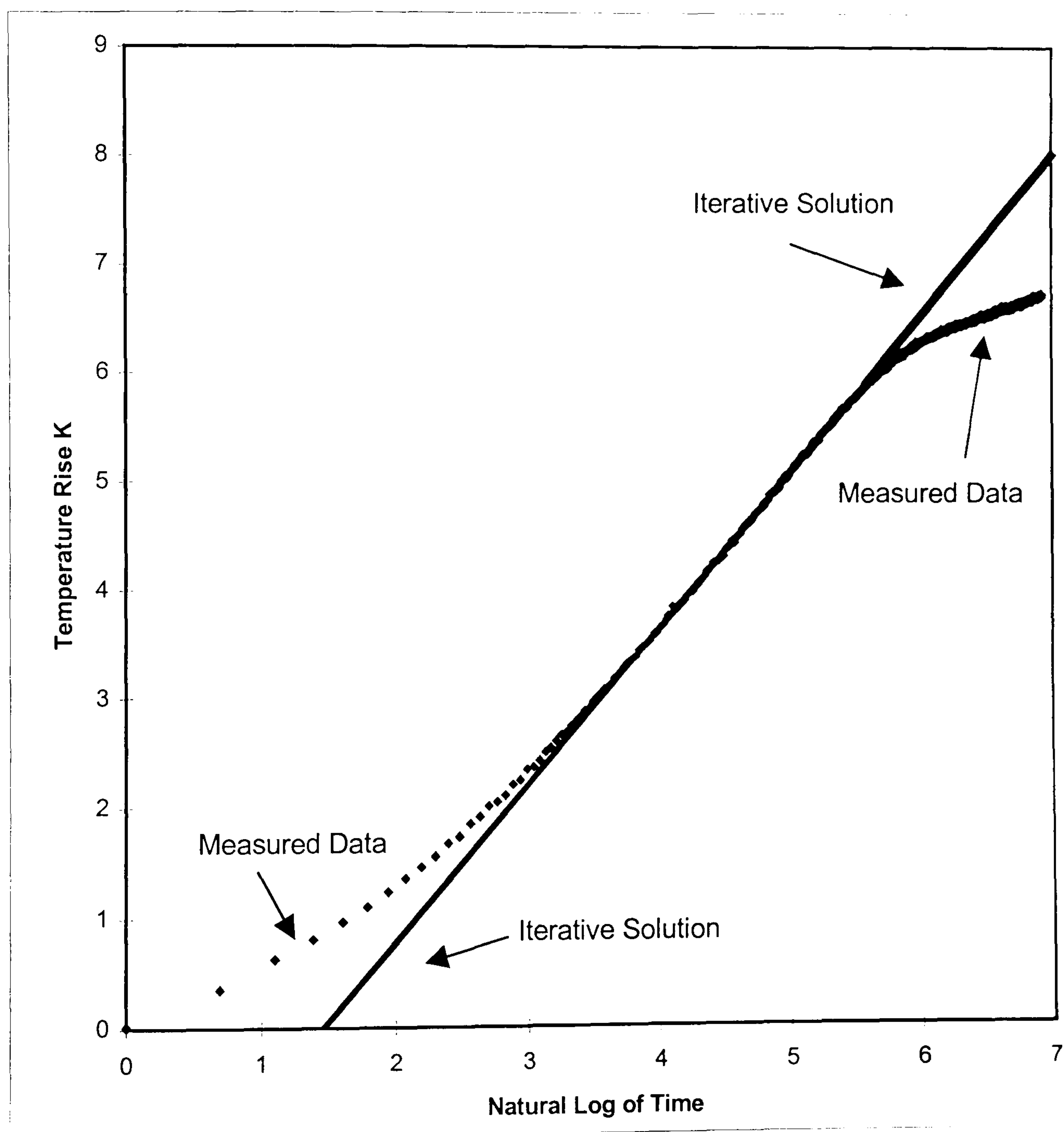
$$\text{Sum of differences} = [\sum(\theta_m - \theta_r)^2]^{0.5} = 0$$

In most instances the Solver carried out a series of iterations and obtained the optimum value for each of the variables α , λ and H that allowed the calculated temperature rise against the natural logarithm of time to closely fit the measured data within a 100 second iteration calculation time period. Occasionally the number of iterations required to achieve a good match meant that the time period needed was a little over 100 seconds, but this was rare. The time taken for the analysis, both in preparation for the analysis and carrying out the calculation process was therefore found to be less than was required for the 'traditional' calculations, mentioned earlier. However, as a Fortran routine maybe more traceable and transparent, a future development in this direction is intended. An example of the results of the process can be seen over the next pages, ultimately showing the iterative results for the three main variables compared with values from measured and published sources. The

iterative analysis for this example was undertaken using a range of variables for each thermal property of glycerine.

Thermal Conductivity $\text{Wm}^{-1}\text{K}^{-1}$	Thermal Diffusivity, m^2s^{-1}	Probe Conductance $\text{W m}^{-2} \text{K}^{-1}$
.30	9.5×10^{-8}	310

Table 5.2, shows a typical range of variables used for Solver2.



Graph 5.4, shows theoretical and measured data, Solver2, glycerine.

The graph 5.4 shows the iterative solution describing the experimental data from about 35 seconds up to about 250 seconds.

Data source	Thermal Conductivity $\text{Wm}^{-1}\text{K}^{-1}$.	Thermal Diffusivity m^2s^{-1}	Probe Conductance $\text{W m}^{-2} \text{K}^{-1}$
Published data.	0.292 (Glazmaier and Ramirez, 1985)	9.10×10^{-8}	N/A
	0.314 (Maqsood, et al, 1994).	1.11×10^{-7}	N/A
Rate Analysis, Long Time Analysis and Short Time Analysis	0.291	5.2×10^{-8}	308
Solver 2 data	0.288	5.9×10^{-8}	390

Table 5.3, shows the results for the published and measured values of thermal conductivity, thermal diffusivity and probe conductance for glycerine, compared with those obtained using Solver2.

The information in table 5.3 shows that the use of conventional analysis techniques and iterative methods give good agreement. The long time analysis of the measured data provides a thermal conductivity value for glycerine 0.6% smaller than the Glazmaier and Ramirez (1985) results and 7.5% smaller than the value obtained by Maqsood et al (1994). The values obtained from the Solver method vary from the published values for the thermal conductivity by up to 8%. Some published thermal diffusivity data, Glazmaier and Ramirez, (1985), Maqsood et al, (1994) is approximately half as small as the short time analysis results. The Solver2 analysis gave results that were again less accurate than the short time analysis undertaken upon the measured values. The Solver2 thermal diffusivity of 6.0×10^{-8}

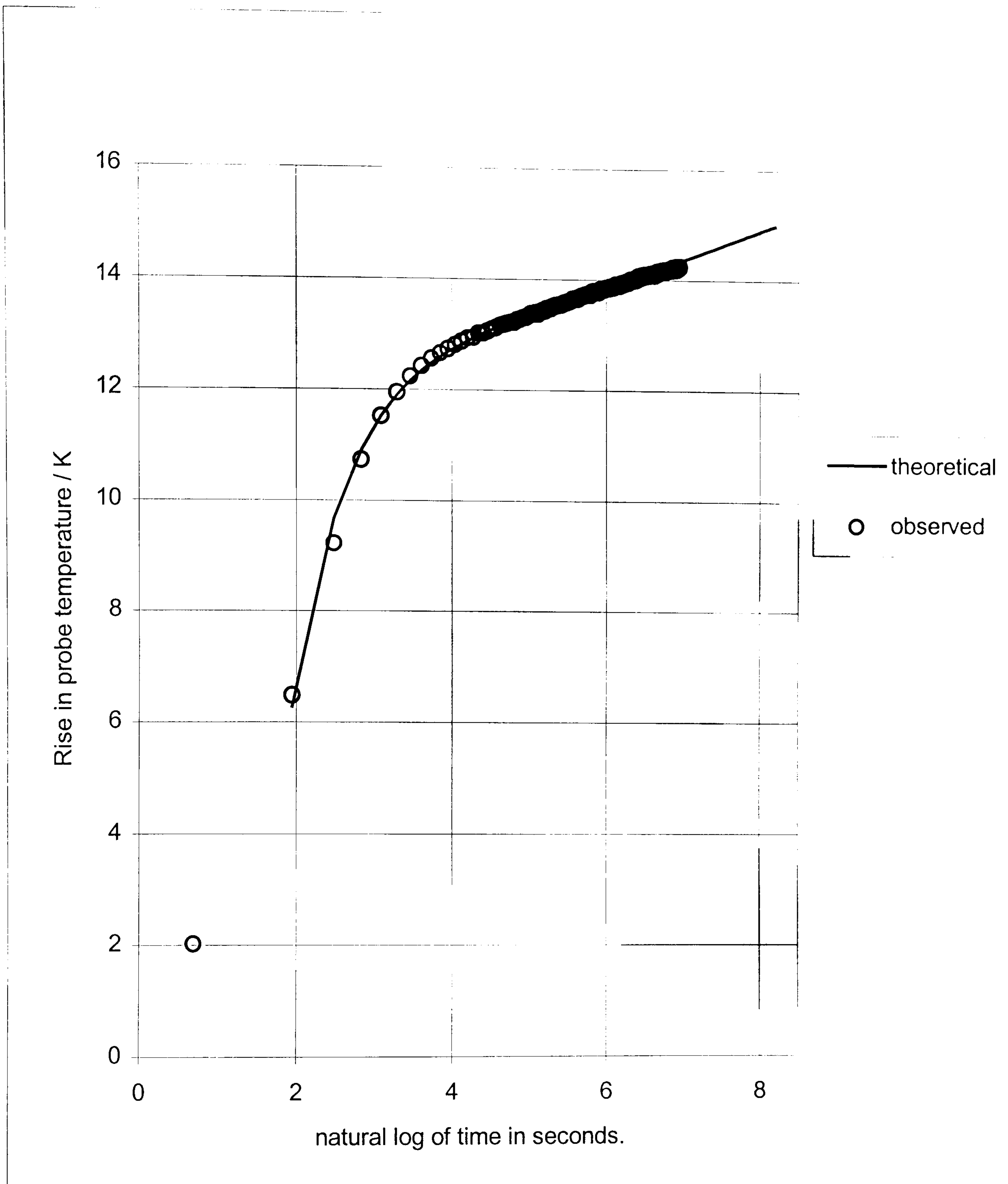
m^2s^{-1} is approximately 20 times smaller than the published value. Further examples of the Solver analysis can be viewed in chapters 6 and 7.

The predicted temperature rise θ_r was initially calculated by Solver2 using only terms A and B of the first equation formulated by Blackwell. A second Solver analysis, called 'Solver4', was undertaken using all four terms A, B, C and D to predict θ_r from earlier times. The two terms C and D are used with the term $1/t$, and therefore at long times became insignificant. However, the iterative solution also endeavours to predict the early time-period of the behaviour of the temperature rise of the probe. If the two missing terms C and D are used within the theoretical calculation, the predicted curve matches the measured data more closely, especially during the first tens of seconds of the data collection. The following example shows the iterative solution compared with θ_r for a cobblock. The iterative analysis uses variables for each thermal property and the routine again sought the minimum sum of the theoretical and measured differences in probe temperature rise, or more correctly the square root of the temperature differences squared.

Thermal Conductivity $\text{Wm}^{-1}\text{K}^{-1}$	Thermal Diffusivity m^2s^{-1}	Probe Conductance $\text{W m}^{-2} \text{K}^{-1}$
0.82	2×10^{-8}	90

Table 5.4, shows the range of variables used with Solver4 on cobblock data.

A graph showing the measured data (circles) and the Solver4 data, the theoretical rise in probe temperature (black line) both as a function of $\ln(t)$ is shown overleaf;



Graph 5.5, shows an Iterative solution using Solver4, coblock, showing theoretical and measured data for an air filled probe.

It can be seen that the predicted rise in temperature described the experimental data from a few seconds to beyond 1000 seconds.

To recap, the analysis of the experimental results has involved a number of separate data handling routines and these can be summarised as follows:

1. Long time analysis using terms $A + B$ in the first Blackwell equation, Equation 1.
2. Using Blackwell short time parameter Y for the determination of H , Equation 6.
3. Determination of α using H and intercept from 1, above.
4. Rate analysis using the short time data to ascertain mc and H for the probe.
5. Solver2 routine using only terms A and B of the first Blackwell equation, Equation 1.
6. Solver4 routine using A , B , C and D in the first Blackwell equation, equation 1 so that a larger time window may be described.

Not all of the analysis methods are applicable to all of the results. For example, the initial single thermocouple work, and the limited data collection experiments, will require an iterative analysis. The dual thermocouple studies and the later experiments employ the rate analysis as well as the long and short time analysis. An analysis regime is detailed in chapter 10, which suggests an order of use for each of the handling routines.

The results and details of the corresponding measurements are described in chapters 6 and 7. A standard format is used to aid the reader's appreciation of the results. As this format does repeat the analysis methods, the reader may want to concentrate upon the summary

tables situated throughout each sample report once the significance of the analysis methods is apparent.

Chapter 6

Laboratory measurements and results.

Before the thermal probe technique could be used upon cob walling, the validity of the technique had to be confirmed. The question concerning the unknown value of the thermal contact between the probe and the specimen needed to be resolved. Once this was clarified the technique could be used with confidence upon cob and other unbaked earth walling materials. A series of calibration experiments were undertaken on four different materials with known thermal properties, paraffin wax, glycerine, phenolic foam and a lightweight aerated concrete block. These materials allowed the probe to maintain a good thermal contact with each sample and had well known and predictable thermal properties. Once the probe performance had been studied and confirmed using these materials, cob and other unbaked earth walling materials were investigated. The initial experimental work was carried out under laboratory conditions described in this chapter and progressed to *in-situ* studies, which are described in chapter 7.

As previously discussed in chapter 4, the majority of the laboratory studies were carried out in a room within the University of Plymouth's Hoe Centre site. The room had no source of heating, was surrounded on all sides by other inhabited spaces and obtained natural lighting from a skylight over-shadowed by other buildings. Any changes in the thermal environment of the room were due to the ingress of cooler or warmer air from other parts of the building, thus any sudden variation of the temperature and the moisture content of the sample was minimised. However, the laboratory based measurements were intended as the precursor to an *in-situ* investigation and so it would have been inappropriate to test the samples within a completely controlled environment. The layout and specification of the equipment used is described in chapter 4.

Before each material could be studied confidently, the influence of the power dissipated per unit length $Q \text{ Wm}^{-1}$ had to be assessed. A stabilised power supply was used to ensure constant values of Q and the probe temperature rise was recorded using the methodology described in chapter 4. The power used was adjusted until the rise in temperature of the probe was large enough not to be unduly influenced by any variations in the surrounding thermal environment. The overall rise in probe temperature during the measurements will affect moisture movement within the sample and so the rise in probe temperature was monitored. This final temperature rise could also have a detrimental effect upon the materials that the probe is constructed from. In practice, it was found that overall temperature rises of less than 2 degrees Celsius were unacceptable because they were influenced by ambient temperature variations, see graphs 7.2 and 7.3 in chapter 7. For the reduction of moisture migration and continued integrity of the probe, it was felt that rises in temperature of more than 20 degrees should be avoided if possible. In general, all the experimental work employed rises in probe temperature of between 2°C and 15°C, depending on the thermal properties of the material being measured.

The measurement sequence started by initiating the logger recording system. The initial probe temperature was recorded for a period before the probe heater current was switched on. The data-logger measured the elapsed time, the heater potential difference, the standard resistance potential difference, (for the heater current), and the temperature rise of the thermocouple situated within the probe. Each experimental run used a series of trial measurements to ensure the heater power was tailored to suit the specimen and its thermal properties. This normally required some trial runs.

The data logged using the Geologger was downloaded to a personal computer and into an Excel spreadsheet where it was analysed. A graph of the rise in probe temperature against the natural logarithm of time was displayed to allow a visual inspection of the quality of the results. This enabled the appropriate region of the data to be selected and then used to calculate the thermal conductivity of the material. Because of the

experimental uncertainties in the temperature and power data, the initial thermal conductivity value is given within a range of possible values, mean, maximum, and minimum figures. In this way, the reliability of the data was assessed. Values for the thermal conductivity in any summary tables in this chapter and chapter 7 are mean values unless stated otherwise.

Individual studies of various specimens, ranging from paraffin wax to samples of unbaked earthen materials.

A number of different materials were studied. Initially, the studies of paraffin wax were used to gain confidence in the technique before moving to a specimen with uncertain or unknown thermal properties. The specimens were each studied in turn, following the route shown in the summary of laboratory measurements, flow chart 5.1 (chapter 5). We will now look at the results for paraffin wax, glycerine, phenolic foam and lightweight aerated concrete block.

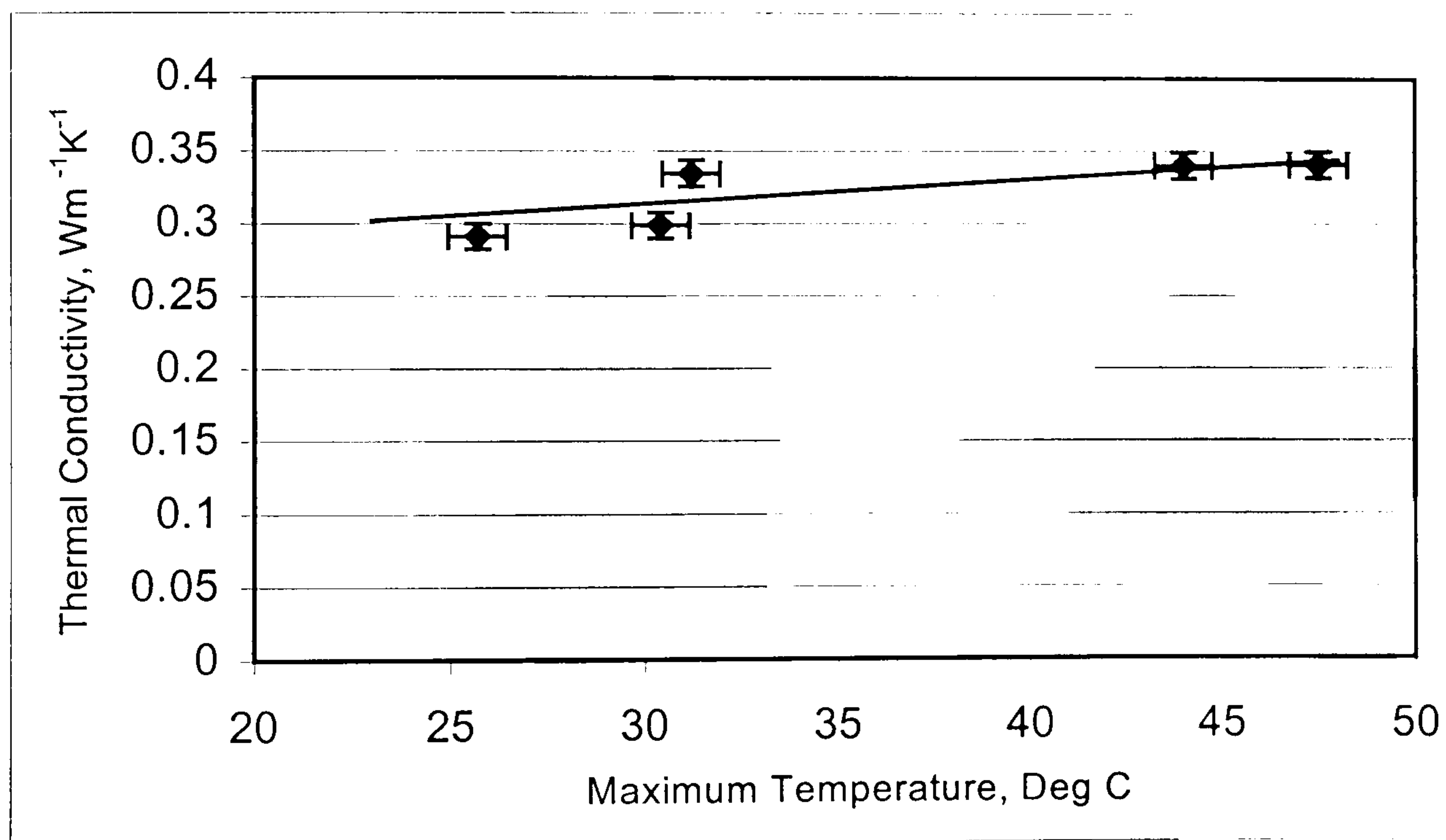
Paraffin Wax.

Paraffin wax, thermal conductivity $0.251 \text{ Wm}^{-1}\text{K}^{-1}$ and diffusivity $9.25 \times 10^{-8} \text{ m}^2\text{s}^{-1}$ and had already been used by Cranfield University to calibrate and demonstrate the reliability of their probes (Batty, 1984). Paraffin wax allowed the probe to be set into the material thus establishing a high thermal contact conductance between the probe and the specimen. Much of the initial measurements pre-dated the later probe modifications using heatsink compounds and twin thermocouples, as described in chapter 4. The initial work on wax used an air-filled probe with a single internal thermocouple. Table 6.1 shows a summary of the results of this early work.

Material	run no	Thermal Conductivity $\text{Wm}^{-1}\text{K}^{-1}$	Power (Watts)	Max temp ($^{\circ}\text{C}$)
wax	5	0.298	0.108	25.7
wax	6	0.299	0.179	30.4
wax	7	0.329	0.192	31.2
wax	8	0.341	0.499	44
wax	9	0.339	0.602	47.5
Mean value		0.320 ± 0.02		

Table 6.1 Summary of long time analysis results for initial study of paraffin wax with single thermocouple and air filled probe.

The mean value of thermal conductivity shown in table 6.1 is approximately 28% greater than the figure quoted by Batty, 1984. This high value maybe due in part to an increase in measured thermal conductivity with temperature. This relationship can be seen from graph 6.1. Although the measured thermal conductivity of the wax does rise with increase in temperature, the trend is gradual and not quite as steep as shown here.



Graph 6.1, shows the variation of measured thermal conductivity of paraffin wax with maximum probe temperature.

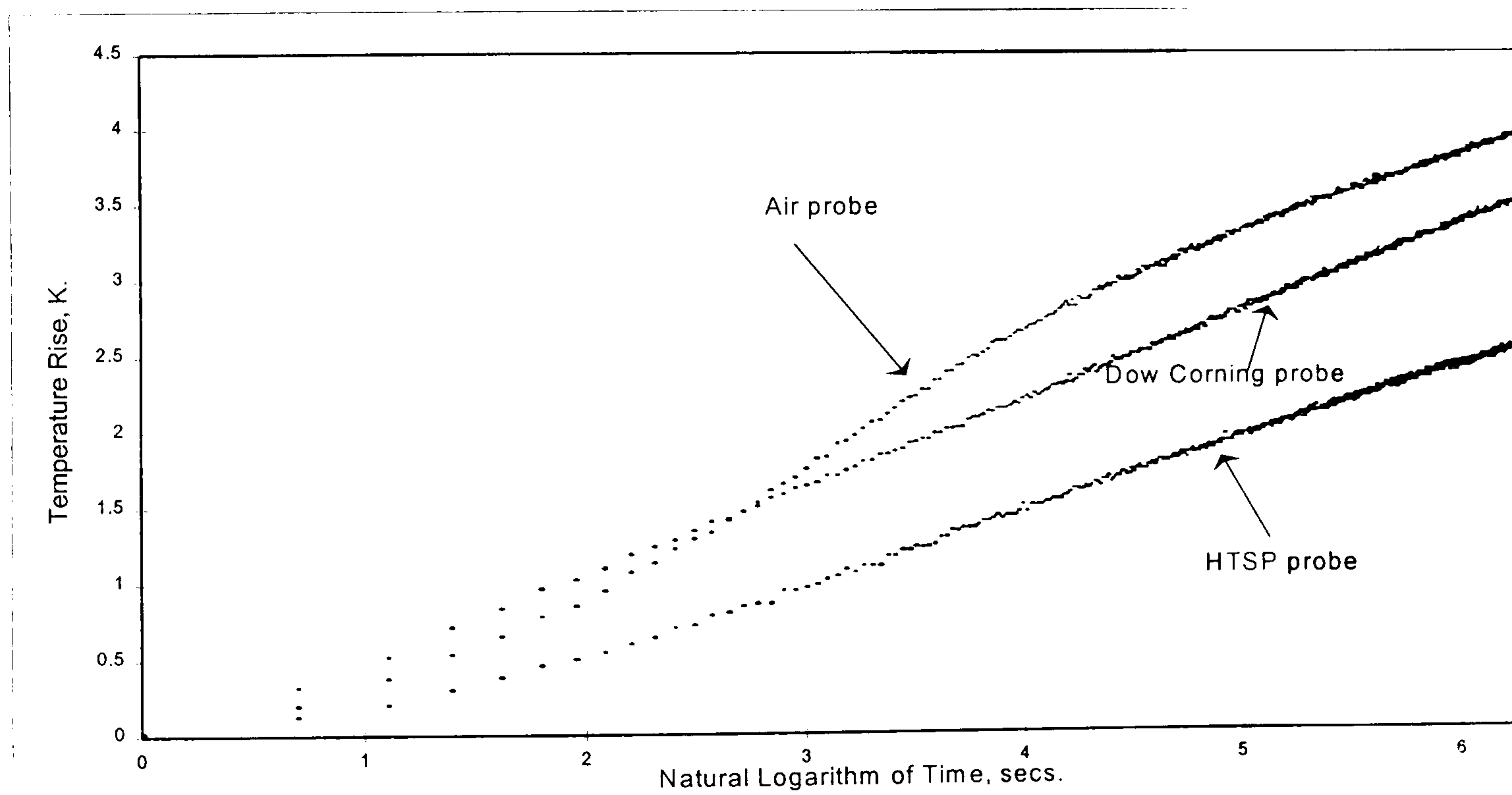
This variation in the value of the measured thermal conductivity of wax and the 28% larger value than determined by Batty, do question the possible effects that the probe conductance may be having. Previous authors have often assumed that H is large and

the term $2\lambda/r_0H$ in B of the initial Blackwell equation 2, can be ignored. If the value of H is assumed, say $5000 \text{ Wm}^{-2}\text{K}^{-1}$, then for paraffin wax with a probe radius, r_0 of 0.0013m the term $2\lambda/r_0H$ is 0.092 which is small compared with Euler constant, γ , (0.5772). Compare this with H having a value of $100 \text{ Wm}^{-2}\text{K}^{-1}$, the term $2\lambda/r_0H$ is 4.59 , which is 8 times bigger than γ and therefore significant. However, if the value of H is known and taken as $80 \text{ Wm}^{-2}\text{K}^{-1}$ the thermal diffusivity, (α) can be calculated as $2.2 \times 10^{-7} \text{ m}^2\text{s}^{-1}$. This value of α , using the later more accurate measured data, is consistent with published values. Therefore, It may be concluded that for the later data only, for measurements on paraffin wax, that a probe thermal conductance of $80 \text{ Wm}^{-2}\text{K}^{-1}$ is acceptable and can be used in calculating the thermal diffusivity.

However, the early data measured using a probe without heat sink compound in paraffin wax with 5 and 10 second time intervals between data collections, gives values for the calculated thermal diffusivity, α , that are very inconsistent. To underline this problem which is associated with the $2\lambda/r_0H$ term, a further calculation using an assumed H value of $80 \text{ Wm}^{-2}\text{K}^{-1}$ in equation 2 has been undertaken using the data from the early wax measurements. This method gave a range of values of α from 1×10^{-6} to $4.65 \times 10^{-6} \text{ m}^2\text{s}^{-1}$, a range of over 10^{13} . This degree of variation is unacceptable and therefore another method is needed to establish reliable values of the probe conductance and hence thermal diffusivity. This prompted using Blackwell's short time analysis to establish a more reliable figure for the thermal diffusivity of wax and the other materials by measuring the probe conductance H. The short time analysis, as reported in chapter 5, requires data to be sampled at one-second intervals rather than the five or ten-second-time interval that was sufficient for processing the long time data. The start of the heating period had to be accurately known. As the initial data was recorded at ten then five-second intervals, a new series of experiments were initiated incorporating these changes. The ten then five-second data was now used as a basis to obtain accurate values of the thermal diffusivity and other thermal variables using an iterative process.

Other changes to the technique involving the use of heat sink materials and twin thermocouples were introduced to the experimental programme as the work evolved. The next series of results show the effects of these changes. To aid the reader the study of each material is organised in a similar way. The long time analysis is used to determine the thermal conductivity of the sample, the short time studies provide the probe thermal conductance, H , and the thermal diffusivity of the sample, α . If the probe has used twin thermocouples, the short time rate method can be used. Finally, many of the samples that used five or ten second intervals between data collection, use the Solver iterative process to endeavor to establish λ , H , and α . Using this order of analysis, here are the later results for paraffin wax.

Graph 6.2 shows the long time behaviour of three probes with different fillings. The first is the simple air filled probe, and may be compared with probes containing either Dow Corning or Electrolube HTSP heatsink material.



Graph 6.2, shows the long time behaviour of twin thermocouple probes in Wax with various 'fillings'.

The temperature rise measured for the air probe is higher than either of the heat sink filled probes. The heat sink filled probes show a more effective heat transfer to the

paraffin wax, remembering that the probes are heated with similar but not identical powers.

Table 6.2 shows a summary of the second study results for the thermal conductivity of paraffin wax using more frequent data collection techniques, two thermocouples and heat sink filled probes. The values obtained from these studies give an average thermal conductivity of $0.261 \text{ Wm}^{-1}\text{K}^{-1}$. This compares favourably with the previously stated value determined by Batty of $0.251 \text{ Wm}^{-1}\text{K}^{-1}$ and is far better than the first series of measurements reported earlier.

Runcode	Power, Watts.	Thermal Conductivity, $\text{Wm}^{-1}\text{K}^{-1}$	Probe 'Filling'
wx2t1100	0.05	0.170	no sink in probe
wx2t1400	0.20	0.195	no sink in probe
wx2t1600	0.26	0.244	no sink in probe
wx2t1700	0.14	0.247	no sink in probe
wx2t1800	0.11	0.235	no sink in probe
		0.218 ± 0.03	Mean value
w2ts2100	0.50	0.284	Dow-Corning probe Filling
w2ts2200	0.31	0.269	Dow-Corning probe Filling
w2ts2600	0.10	0.252	Dow-Corning probe Filling
w2ts2800	0.06	0.264	Dow-Corning probe Filling
		0.267 ± 0.01	Mean value
sw2t0302	0.07	0.354	HTSP Probe Filling
sw2t0303	0.10	0.264	HTSP Probe Filling
sw2t0403	0.21	0.282	HTSP Probe Filling
sw2t0502	0.15	0.266	HTSP Probe Filling
sw2t0503	0.52	0.289	HTSP Probe Filling
sw2t0802	0.28	0.273	HTSP Probe Filling
sw2t1802	0.39	0.272	HTSP Probe Filling
sw2t2202	0.47	0.280	HTSP Probe Filling
		0.285 ± 0.03	Mean value
		0.261 ± 0.03	Overall Mean

Table 6.2, summary of long-time thermal conductivity, paraffin wax, twin thermocouple probes.

Using this time dependent thermal probe technique the thermal diffusivity may be found in several different ways. If the probe conductance is assumed to be very large, then the term containing $1/H$ in equation 2 (using only terms A and B) can be assumed to be small enough to disregard and so α can be found. Secondly, the slope from Blackwell's short

time analysis can be used to find α from equation 6. Finally, if the value of H is known from Blackwell's short time analysis then this value of H may be used in the original long time equation, equation 2 and a further value for α can be found.

Table 6.3 shows a summary of the short time analysis for paraffin wax with twin thermocouples and different probe sheath fillings. Here, the Blackwell short time method gave values of H and α .

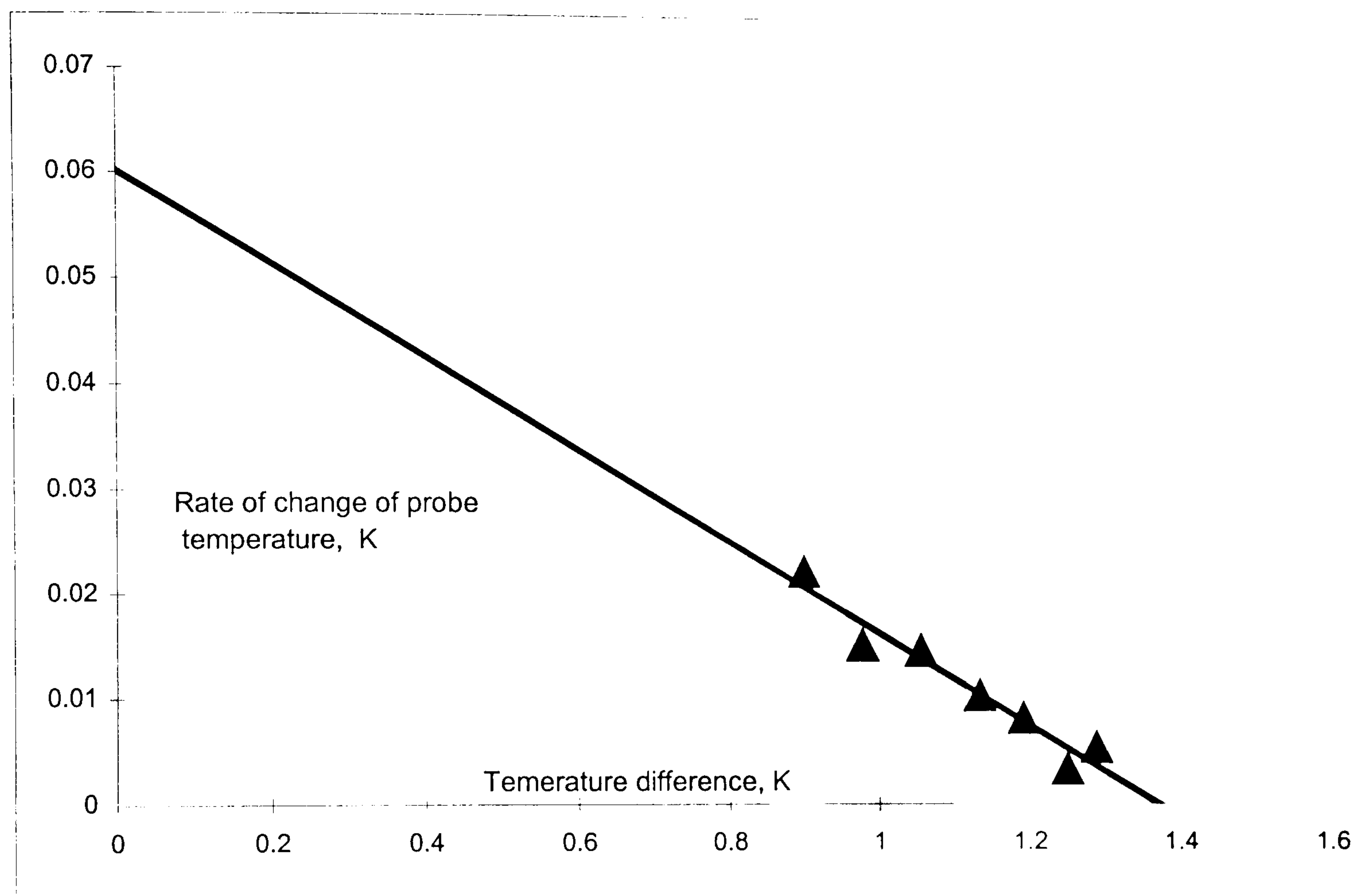
run code	'H' Probe Conductance, $Wm^{-2}K^{-1}$	Diffusivity m^2s^{-1}	Probe 'Filling'
wx2t1100	88	1.03×10^{-7}	no sink in probe
wx2t1400	83	1.43×10^{-7}	no sink in probe
wx2t1600	87	2.17×10^{-7}	no sink in probe
wx2t1700	86	2.25×10^{-7}	no sink in probe
wx2t1800	84	2.07×10^{-7}	no sink in probe
	85.6	$1.79 \times 10^{-7} \pm 5.3 \times 10^{-8}$	mean values
w2ts2100	104	2.55×10^{-7}	Dow-Corning probe Filling
w2ts2200	95	2.31×10^{-7}	Dow-Corning probe Filling
w2ts2600	101	2.08×10^{-7}	Dow-Corning probe Filling
w2ts2800	80	2.22×10^{-7}	Dow-Corning probe Filling
	95	$2.29 \times 10^{-7} \pm 1.97 \times 10^{-8}$	mean values
sw2t0302	128	1.73×10^{-7}	HTSP Probe Filling
sw2t0303	135	8.93×10^{-8}	HTSP Probe Filling
sw2t0403	150	9.77×10^{-8}	HTSP Probe Filling
sw2t0502	137	9.54×10^{-8}	HTSP Probe Filling
sw2t0503	152	1.01×10^{-7}	HTSP Probe Filling
sw2t0802	152	9.02×10^{-8}	HTSP Probe Filling
sw2t2202	142	1.03×10^{-7}	HTSP Probe Filling
	142.3	$1.07 \times 10^{-7} \pm 2.9 \times 10^{-8}$	mean values

Table 6.3, summary of the short time results, paraffin wax, twin thermocouple probe.

The average thermal diffusivity from this analysis is $1.07 \times 10^{-7} m^2s^{-1}$ (HTSP filled probe). Compared with the published value of $9.62 \times 10^{-8} m^2s^{-1}$ (Carslaw and Jaeger, 1947) the measured value is approximately 10% larger. This is viewed as a considerable improvement over the first results, which used data measured at 5 and 10 second intervals for paraffin wax.

As the short time studies' measurements were made using a probe with two thermocouples, the rate analysis may now be undertaken upon this data. The rate studies on paraffin wax were undertaken with the probes having two thermocouples, one at the

centre, mounted on the heater, the second on the exterior giving θ_1 and θ_2 respectively. The analysis of the rate of heat flow with time from the probe into the wax can be undertaken. It can be recalled that the graph of $d\theta_1/dt$ versus $(\theta_1 - \theta_2)$ should be linear from about 10 seconds up to about 60 seconds, while the heat flow initially warms the probe and the wax immediately in contact with the probe. Graph 6.3 shows the results of the rate analysis upon paraffin wax.



Graph 6.3, shows a typical rate analysis of paraffin wax runcode W2ts2600.

Slope	-0.0439
Intercept	0.0601
Mean Power, W.	0.1041
Thermal Capacity of Probe, mc, JK ⁻¹	1.732
Probe Conductance, H, Wm ² K ⁻¹	136

Table 6.4, shows the results of the rate analysis for paraffin wax runcode W2ts2600. Over the first minute of the heating schedule a straight line was observed for $d\theta_1/dt$ versus $(\theta_1 - \theta_2)$ as suggested by the theory. The probe thermal capacity mc is determined which is a function of the mass and specific heat capacity of the probe wall, heater,

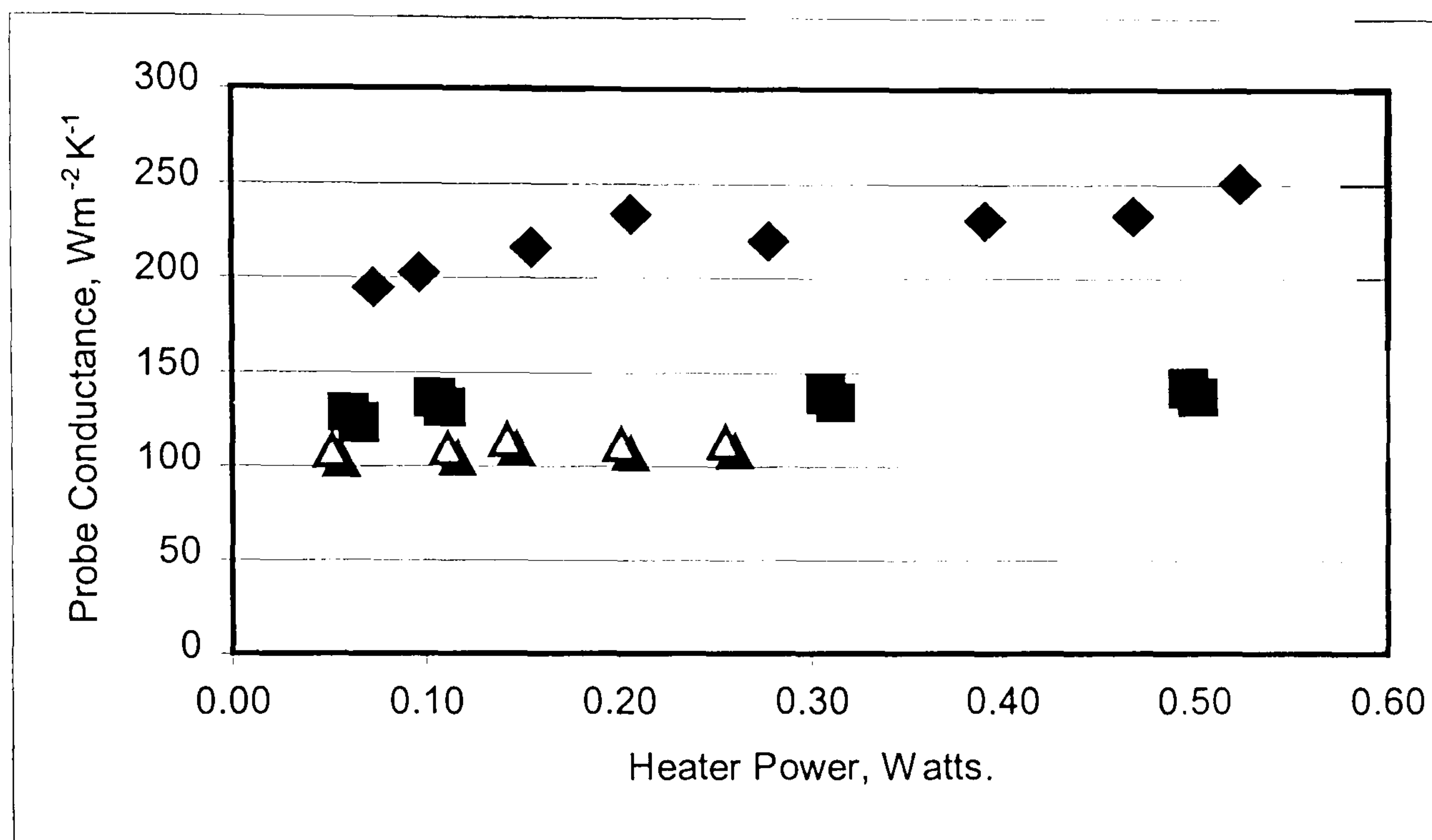
thermocouple, end caps and, when included, the probe filling. The probe contact conductance, H , between the centre of the probe and the external surface is also measured. This data allows a number of unknown variables to be established and gives a valuable check against much of the previously measured data. The use of this rate method represents a significant step forward towards using the probe method to accurately measure the thermal properties of materials both *in-situ* and in the laboratory.

Table 6.5 shows a summary of the results of the rate analysis for paraffin wax with twin thermocouples and different probe sheath fillings. The measured values for the probe conductance, H do vary from those found using the short time analysis, but do follow the same trend. The value of the probe thermal capacity, mc , is larger for the probes using heatsink compound. The HTSP heatsink compound is the more dense material, thus would be expected to have a higher mc value. However, as can be seen in table 6.5, the mc values for HTSP compound are slightly less than the less-dense Dow-Corning material. This may in part be due to the higher viscosity of the HTSP heat sink material and the associated difficulties in completely filling the probe with heat sink material.

run code	Power, Watts.	Probe Conductance H , $Wm^{-2}K^{-1}$	mc $Jkg^{-1}K^{-1}$	Probe 'Filling'
wx2t1100	0.05	107.8	0.681	No sink in probe
wx2t1400	0.20	111.7	1.024	No sink in probe
wx2t1600	0.26	112.8	0.843	No sink in probe
wx2t1700	0.14	113.9	0.962	No sink in probe
wx2t1800	0.11	109.6	1.135	No sink in probe
w2ts2100	0.50	142.0	1.408	Dow-Corning probe Filling
w2ts2200	0.31	139.2	1.544	Dow-Corning probe Filling
w2ts2600	0.10	136.1	1.732	Dow-Corning probe Filling
w2ts2800	0.06	128.1	1.907	Dow-Corning probe Filling
sw2t0302	0.07	194.9	1.242	HTSP Probe Filling
sw2t0303	0.10	202.7	1.137	HTSP Probe Filling
sw2t0403	0.21	234.1	1.200	HTSP Probe Filling
sw2t0502	0.15	216.0	1.087	HTSP Probe Filling
sw2t0503	0.52	250.5	1.120	HTSP Probe Filling
sw2t0802	0.28	219.6	1.098	HTSP Probe Filling
sw2t1802	0.39	231.2	1.069	HTSP Probe Filling
sw2t2202	0.47	233.2	1.067	HTSP Probe Filling

Table 6.5, summary of rate analysis studies on paraffin wax.

These studies were undertaken on paraffin wax while the experimental and analysis routines were being developed. The reader is reminded of the chronological progression of the work shown in flow chart 5.1. This may mean that more uncertainty may exist within the results for wax than for some of the later measurements. Because of these uncertainties, doubts were raised concerning the reliability of the value of the probe conductance.



Diamonds = HTSP filled probe. Squares = Dow-Corning filled probe. Triangles = air filled probe.

Graph 6.4, shows the probe conductance, H , from the rate analysis, variation with heater power, paraffin wax.

Graph 6.4 shows the increase in probe conductance, (H), with the use of different heat sink materials. All the probe conductance values measured show little variation with increases in heater power thus relieving some of the earlier doubts in this area.

The experience from the first laboratory measurements did lead to a number of modifications to the thermal probe technique. These modifications allowed the technique to progress, allowing more representative values of λ and H , which in turn allowed a more confident calculation of α . The use of heat sink material has given a more stable probe thermal conductance value, which appears to be independent of different heater powers. The inclusion of a second thermocouple situated on the exterior of the probe gives the

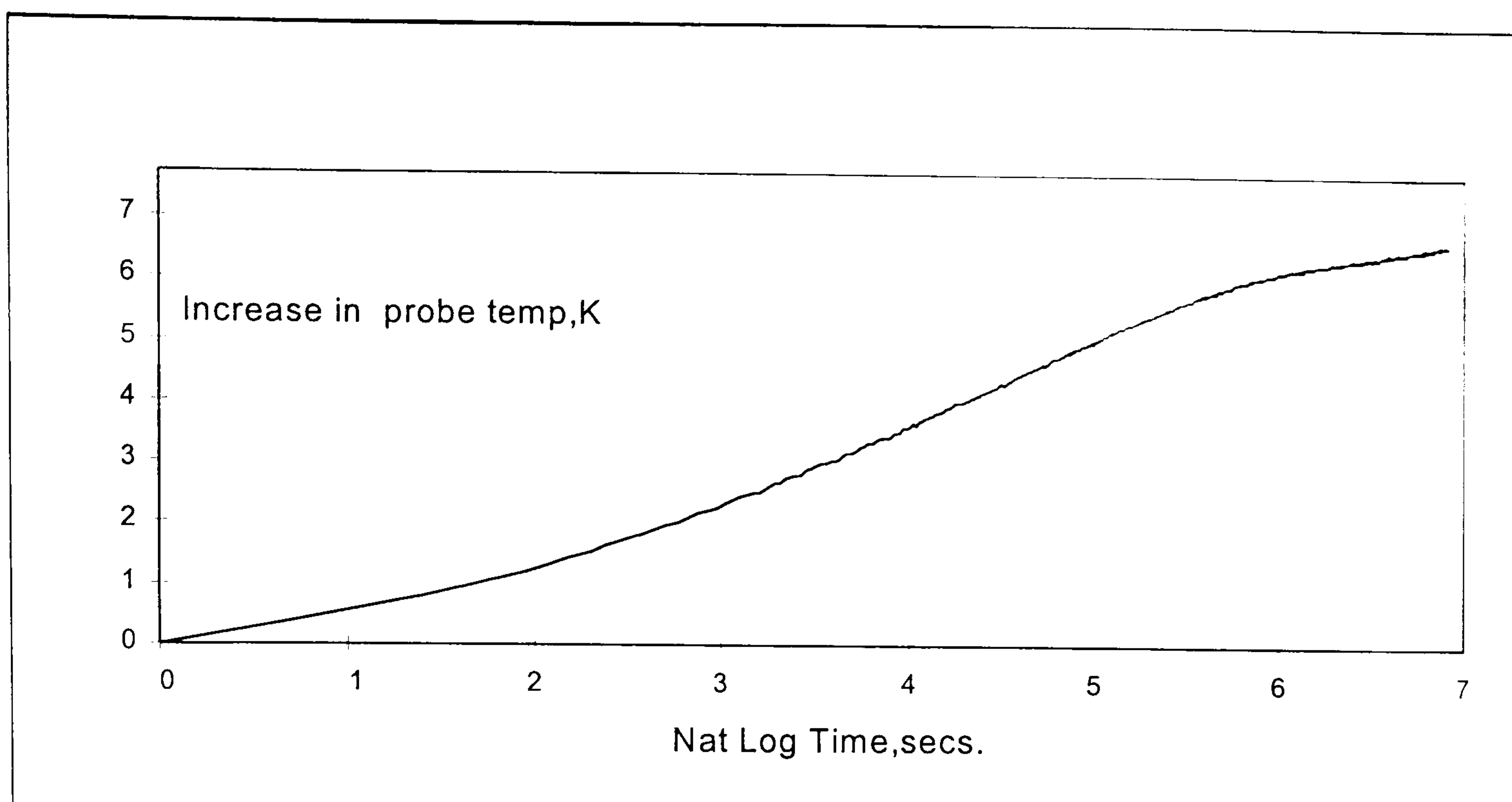
opportunity to measure H and then to calculate α values from a different section of data. This enables a valuable check upon the long time and short time results.

Glycerine

The next development was to study a specimen that would have an inherently high value of probe to specimen contact conductance, H . Glycerine, (sometimes referred to as Glycerol), $C_3H_8O_3$, was chosen as a suitable specimen because, as a liquid, it would provide better thermal contact than that achieved when inserting a probe into a drilled hole in a solid sample. Glycerine has also been studied by other researchers in the past (Maqsood et al, 1994), (Glazmaier and Ramirez, 1985) and the values of thermal conductivity and diffusivity are well known.

This point in the work coincided with the introduction of the 1 second intervals in the data collection, but before the twin thermocouples. This means that the data concerning the rise in temperature at short times is of better quality than the previous data, but the short time rate studies cannot be performed.

Graph 6.5 shows the rise in probe temperature as a function of the natural logarithm of time when the probe was placed in a flask of glycerine. The graph shows a rise in temperature of about 6K. Two linear sections can be seen, the first between $\ln t = 3.5$ (approximately 35 seconds) and $\ln t = 5.5$ (approximately 250 seconds). A second is apparent between $\ln t = 5.7$, (approximately 300 seconds) and greater than $\ln t = 6.8$ (approximately 900 seconds).



Graph 6.5, shows the long time behaviour, glycerine,

A possible reason for the difference in slope between the two linear sections can be the reflection of the heat from the boundary of the glycerine with its container back to the probe. If the analysis technique described by Vos is used then the time for the reflected wave is approximately 270 seconds. This matches with the change in slope at $\text{Int.} = 5.7$ or approximately 300 seconds. However, it is possible that stronger convection currents are carrying away more heat.

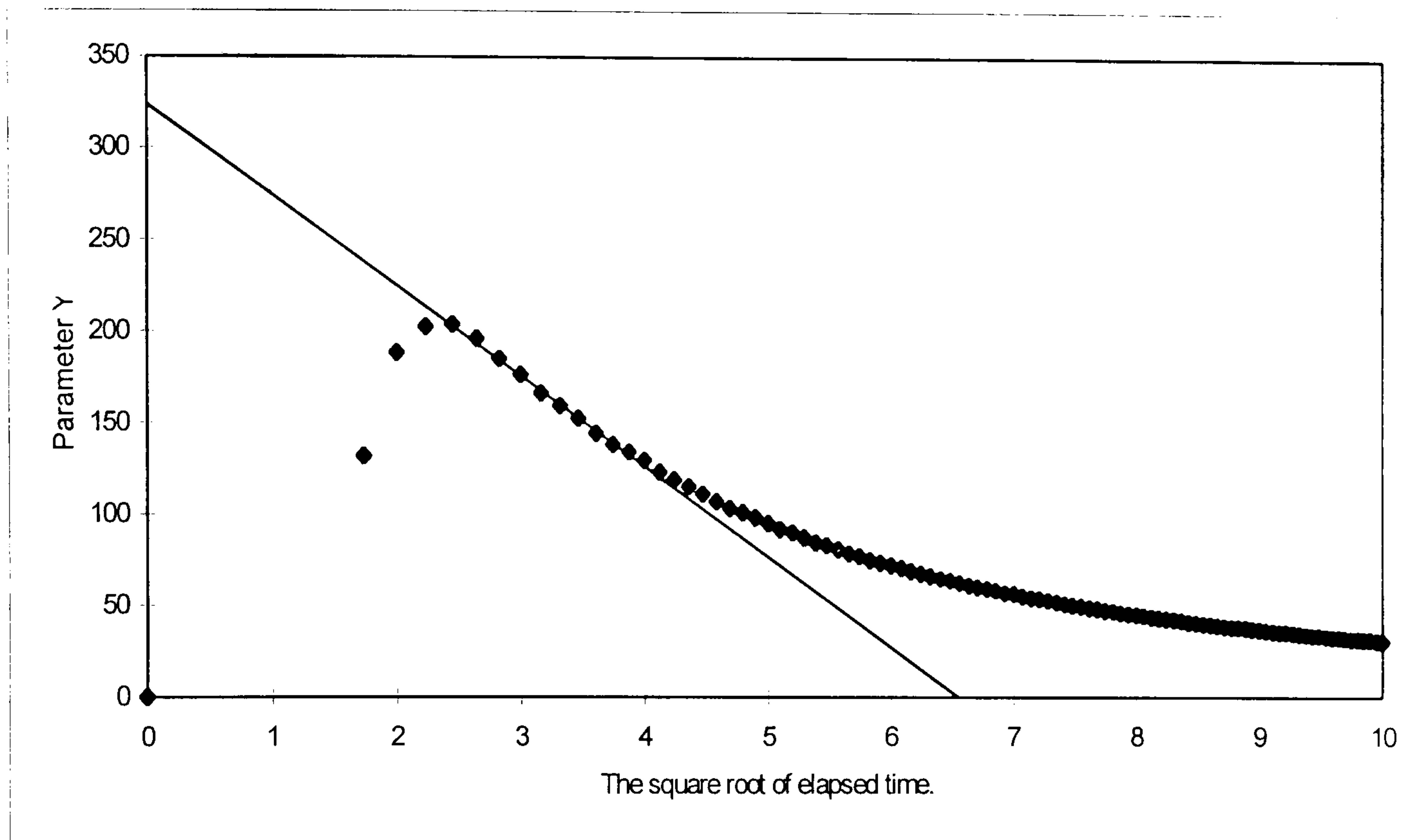
Using the long time analysis and the slope of the straight section of graph 6.3 ($\text{Int.} = 3.5$ (approximately 35 seconds) and $\text{Int.} = 5.5$ (approximately 250 seconds)) the value of the average thermal conductivity is $0.307 \text{ Wm}^{-1}\text{K}^{-1}$, the maximum value is $0.309 \text{ Wm}^{-1}\text{K}^{-1}$ and the minimum value is $0.303 \text{ Wm}^{-1}\text{K}^{-1}$.

Run code	Power, Watts.	Thermal Conductivity $\text{Wm}^{-1}\text{K}^{-1}$
gly9998	0.34	0.291
gly11998	0.34	0.288
gly8998	0.34	0.307
gly10998	0.34	0.287
Mean Value		0.293 ± 0.009

Table 6.6, summary of the long time results for the glycerine studies.

The long time analysis of the measured data provides a mean thermal conductivity value for glycerine of approximately 0.6% smaller than Glatzmaier and Ramirez, (1985), $0.292 \text{ Wm}^{-1}\text{K}^{-1}$ and approximately 7.5% smaller than the value obtained by Maqsood et al, (1994), $0.314 \text{ Wm}^{-1}\text{K}^{-1}$.

The Blackwell short time analysis of the data for glycerine is shown in graph 6.6.



Graph 6.6 shows the Blackwell short time analysis parameter Y against root t for glycerine.

The intercept on the Y-axis gives a value of the thermal probe conductance. The value obtained is $324 \text{ Wm}^{-1}\text{K}^{-1}$, quite high, which was as expected for a viscous liquid in good thermal contact with the exterior surface of the probe.

run code	'H', Probe Conductance $\text{Wm}^{-1}\text{K}^{-1}$	Diffusivity m^2s^{-1}
Gly9998	303	2.21×10^{-6}
Gly11998	287	2.41×10^{-6}
Gly8998	325	2.16×10^{-6}
Gly10998	317	2.48×10^{-6}
Mean values	308 ± 16.7	$2.26 \times 10^{-6} \pm 1.3 \times 10^{-7}$

Table 6.7, summary of the Blackwell short time results, glycerine.

The measured values for the thermal diffusivity of glycerine obtained here are larger than published data, $1.1 \times 10^{-7} \text{ m}^2 \text{ s}^{-1}$, (Maqsood A. *et al*, 1994), $0.967 \times 10^{-6} \text{ m}^2 \text{ s}^{-1}$ (Glatzmaier and Ramirez, 1985). As only four separate measurements were undertaken for this part of the study, the quality of results may be improved by further study. However, in comparison with the magnitude of the values for the thermal diffusivities calculated in the earlier tests, there is some improvement.

Phenolic foam

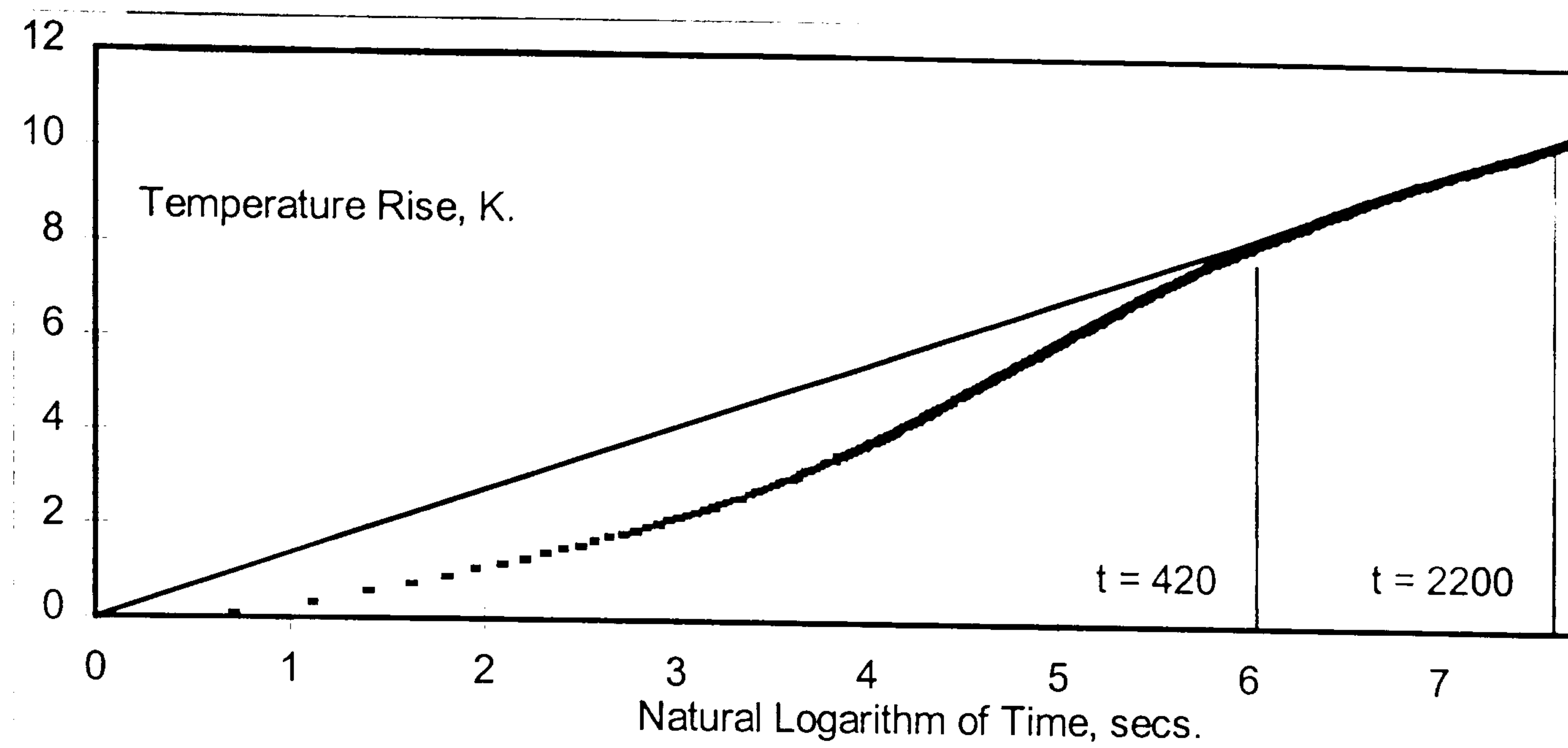
Phenolic foam was selected for two reasons. Firstly, the foam is a material with a very low thermal conductivity, the portion of the foam that is in very close proximity to the probe has similar thermal properties to the air that will surround the probe in any drilled hole. Secondly, the foam is neither a viscous liquid, such as glycerine, or a malleable solid similar to paraffin wax and does give the probe technique a chance to 'interrogate' a solid with quite different thermal characteristics. Phenolic foam has a structure that allowed objects that are long compared with their width to be rigidly held when inserted into the material and yet the material contact per unit area is relatively small. It is therefore expected that the contact conductance will be small. The foam had been tested at British Petroleum research facilities and its thermal conductivity was known to be $0.032 \text{ Wm}^{-1}\text{K}^{-1}$. Two studies of this foam were undertaken. The first set were characterised by Olidat codes and used an air filled probe and ten second interval data collection. The second set were characterised by Ksfoam codes and used heat sink filled probes with one second data collection. The Olidat measured values for the thermal diffusivity of the foam using this data gave an average value of $9.43 \times 10^{-8} \text{ m}^2\text{s}^{-1}$. When this value is compared with British Petroleum's data regarding phenolic foam, the measured value is 200 times smaller than the published data. Although this is obviously unacceptable, the error is not as large as the factor of more than 10,000 that was experienced when paraffin wax was first studied. It is felt that this magnitude of error is in part due to the lower thermal conductivity of the phenolic foam. The material that is surrounding the probe is of a similar

thermal conductivity to the surrounding air and therefore provides a similar barrier to the passage of heat from the probe. This in turn, will provide a more homogeneous sample to be measured, reduce the effects due to dissimilar materials placed around the probe and may help with the retrieval of representative values for the foam's thermal diffusivity. The thermal conductivity values shown in table 6.8 have an average value of $0.0277 \text{ Wm}^{-1}\text{K}^{-1}$. This value is approximately 14% smaller than the established figure. This may be due to heat transfer by convection and radiation across the small air gaps and not by conduction as is assumed in the theory. In addition, the probe may also not fit snugly in the foam as was assumed.

Material	run no	Thermal Conductivity $\text{Wm}^{-1}\text{K}^{-1}$	Power, Watts	Thermal Diffusivity $\text{m}^2 \text{s}^{-1}$
olidat	5	0.0302	0.132	7.7×10^{-8}
olidat	4	0.0222	0.108	1.69×10^{-7}
olidat	6	0.0282	0.153	5.62×10^{-8}
olidat	7	0.0303	0.153	7.48×10^{-8}
Mean value		$0.0277 \pm 3.8 \times 10^{-3}$	0.136 ± 0.02	$9.4 \times 10^{-8} \pm 5.0 \times 10^{-8}$

Table 6.8, summary of long time results, phenolic foam, single thermocouple and air filled probe.

Graph 6.7 shows the typical long time behaviour of phenolic foam in a second series of experiments, with KSfoam codes with one-second data collection and heat sink filled probes.



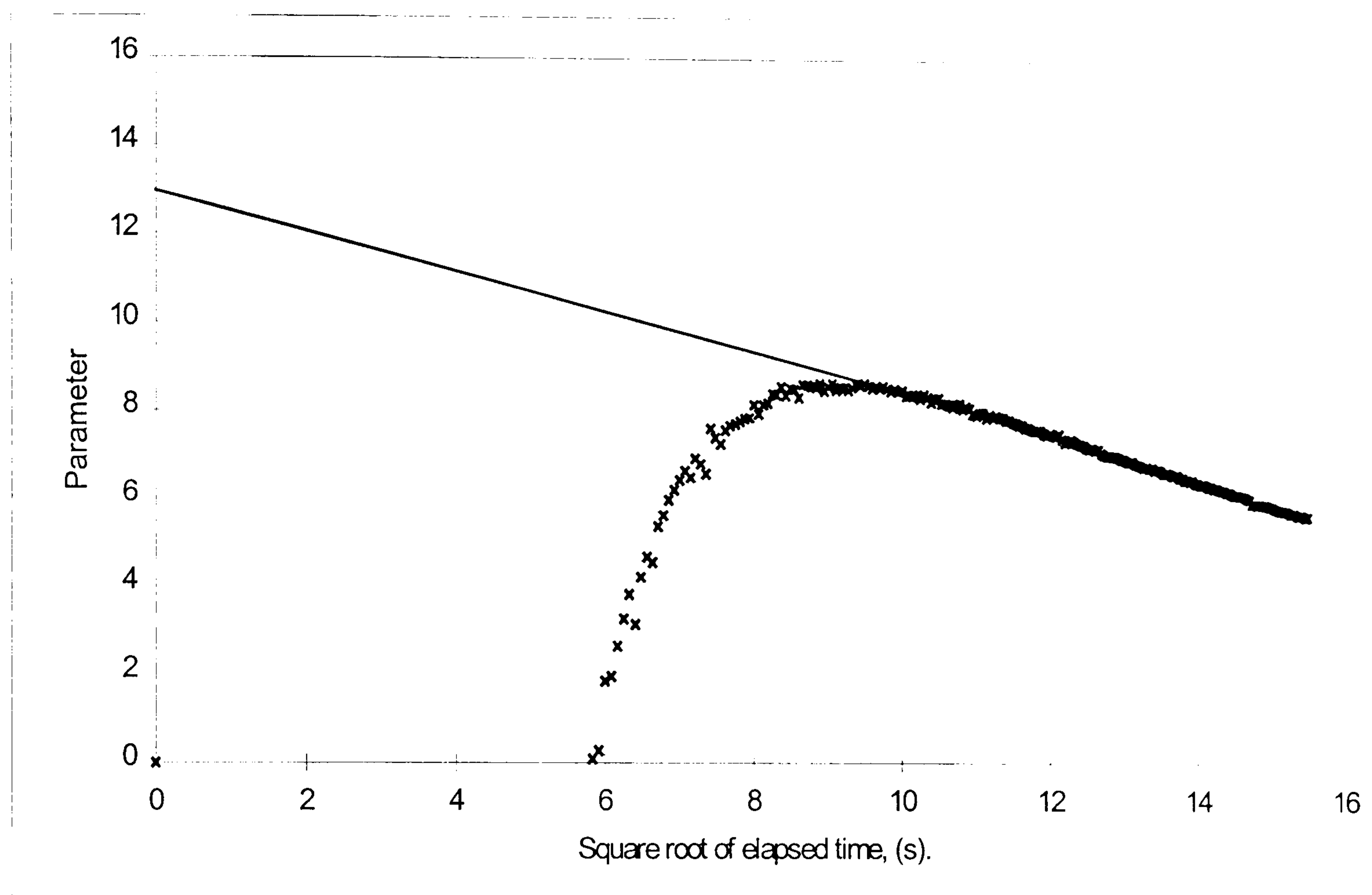
Graph 6.7, shows a typical long time result, phenolic foam.

As can be seen in graph 6.7 the increase in temperature is approximately 10K achieved in approximately 2000 seconds. To achieve a similar temperature rise in paraffin wax a heater power of more than 0.1W was required, thus reflecting the considerably lower thermal conductivity of the phenolic foam. The long time analysis of the results contained in graph 6.7 gave a range of thermal conductivities of 0.0282 to 0.0281 $\text{Wm}^{-1}\text{K}^{-1}$ with a mean value of 0.0282 $\text{Wm}^{-1}\text{K}^{-1}$. This compares favourably with the published value of 0.032 $\text{Wm}^{-1}\text{K}^{-1}$. Table 6.9 shows a summary of the second series of long time studies of phenolic foam. These measurements were undertaken because of the small number of values captured for the first foam measurements and the uncharacteristic values obtained using a lower probe heater power in run olidat4.

Run code	Power, Watts	Thermal Conductivity $\text{Wm}^{-1}\text{K}^{-1}$
KSfoam	0.02	0.0297
KSfoam2	0.07	0.0286
KSfoam3	0.03	0.0271
KSfoam4	0.03	0.0357
KSfoam5	0.03	0.0289
KSfoam6	0.03	0.0262
KSfoam7	0.03	0.0296
KSfoam8	0.03	0.0267
KSfoam10	0.05	0.0282
KSfoam11	0.05	0.0279
Mean value		0.0288 \pm 0.003

Table 6.9, summary of long time results, phenolic foam with HTSP heat sink filled probe.

The average measured thermal conductivity is $0.0289 \text{ Wm}^{-1}\text{K}^{-1}$, 10.7% lower than the $0.032 \text{ Wm}^{-1}\text{K}^{-1}$ the figure given by British Petroleum. To determine the thermal diffusivity of this sample, the Blackwell short time routine was used. A graph of Blackwell Y versus the square root of the elapsed heating time is shown in graph 6.8. The linear section of the graph extends from approximately 100 seconds to beyond 200 seconds.



Graph 6.8, shows a typical short time analysis for phenolic foam .

The intercept on the Y-axis gives a value of the thermal probe conductance. The value obtained is $12.96 \text{ Wm}^{-1}\text{K}^{-1}$, quite a low value as was expected. Table 6.10 shows a summary of the short time analysis of the KSfoam second series of studies carried out upon phenolic foam.

run code	Probe Conductance, H, Wm ² K ⁻¹ .	Thermal Diffusivity m ² s ⁻¹
Ksfoam	17.77	1.56 X 10 ⁻⁸
Ksfoam2	13.33	3.06 X 10 ⁻⁸
Ksfoam3	12.96	1.47 X 10 ⁻⁸
Ksfoam4	15.40	2.20 X 10 ⁻⁸
Ksfoam5	11.67	1.50 X 10 ⁻⁸
Ksfoam6	12.01	1.36 X 10 ⁻⁸
Ksfoam7	10.66	1.33 X 10 ⁻⁸
Ksfoam8	12.31	1.40 X 10 ⁻⁸
Ksfoam10	13.11	1.55 X 10 ⁻⁸
Ksfoam11	13.37	1.52 X 10 ⁻⁸
Mean Value	13.26	1.69 X 10 ⁻⁸ ± 5.4 x 10 ⁻⁹

Table 6.10, summary of the short-time results, phenolic foam.

As previously stated the thermal diffusivity may be found in three different ways. If the probe conductance is assumed very large, then the term containing $1/H$ in equation 2 (using only terms A and B) can be assumed to be small enough to disregard and so α can be found. Secondly, the slope from Blackwell's short time analysis can be used to find α from equation 6. Finally, if the value of H is known from Blackwell's short time analysis then this value of H may be used in the original long time equation, equation 2 and a value for α can be found. The values for the thermal diffusivity shown in table 6.10 were found from Blackwell's short time analysis and average $1.69 \times 10^{-8} \text{ m}^2\text{s}^{-1}$. This is nearly 10 times smaller than published values for similar foam, (see table 6.13A). The average measured values for 'H' the probe conductance is $13.26 \text{ Wm}^2\text{K}^{-1}$, low compared to the values that were obtained from other test materials. However, the thermal conductivity values do give a good correlation with the figure from B.P. It is possible that the probe was not completely filled with heat sink material or the heat sink material had changed due to its proximity to the probe heater. Further work is required in these areas.

Lightweight Concrete Block.

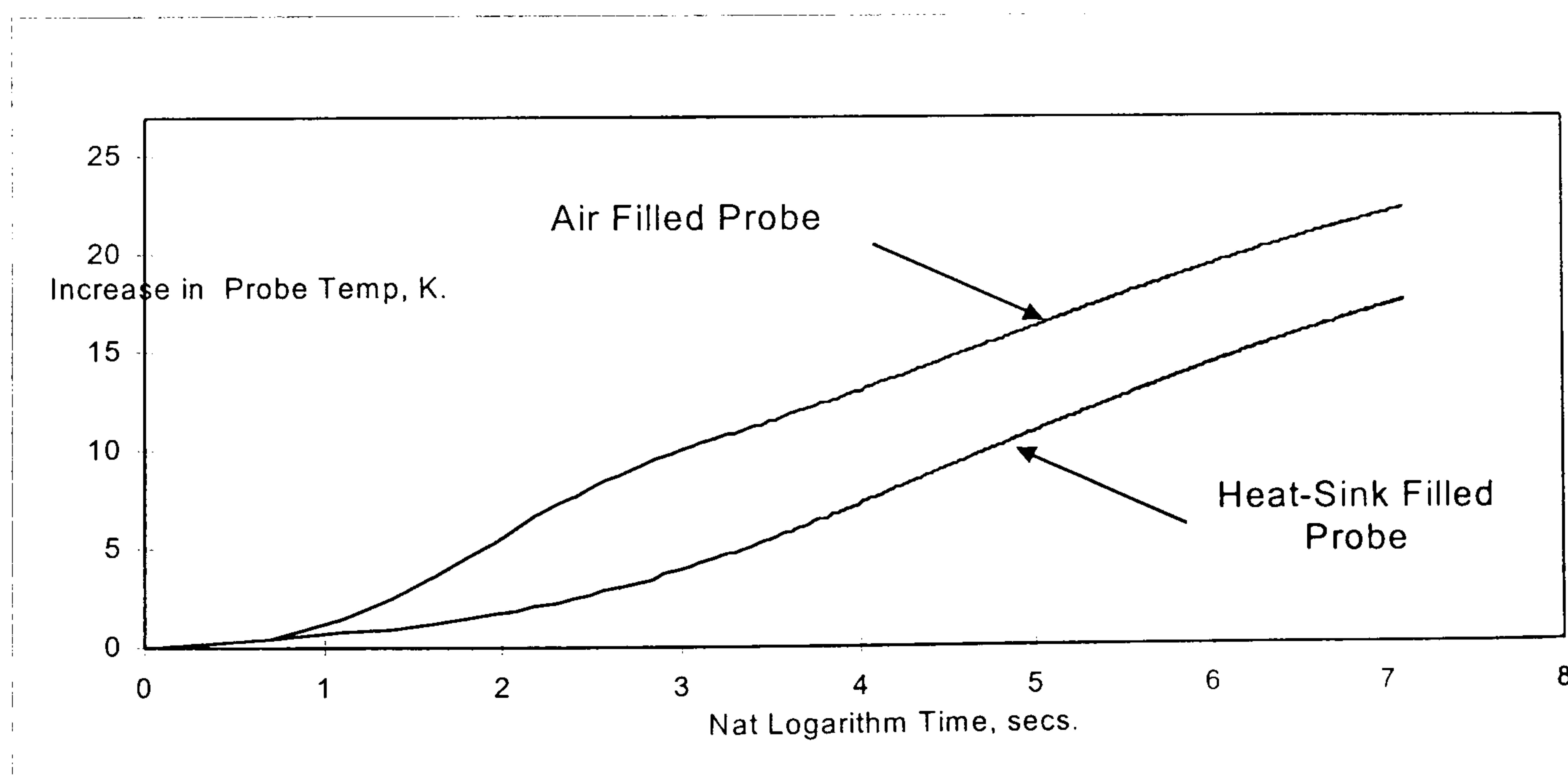
To allow a comparison with a solid material of known thermal properties, but with the material characteristics closer to unbaked earth walling, a lightweight aerated concrete block was next selected for study. Two holes were drilled in a Durox superblock made

from lightweight aerated concrete and a probe was placed in each hole. The first probe was an original type and air filled, while the second had a HTSP heatsink filling. The first series of experiments were carried out without heat sink material in the holes in the block, followed by a series with the silicon-based heatsink material inserted in the holes. During the second series of experiments using HTSP heatsink material, different probe types were used in each hole. It is important to make clear the various experimental cases. The following table shows the reader the various combinations of probe, hole and heat sink.

Hole Number	Graph 6.9	Graph 6.10
Hole 1	Air filled probe	Heat sink filled probe
Hole 2	Heat sink filled probe	Air filled probe

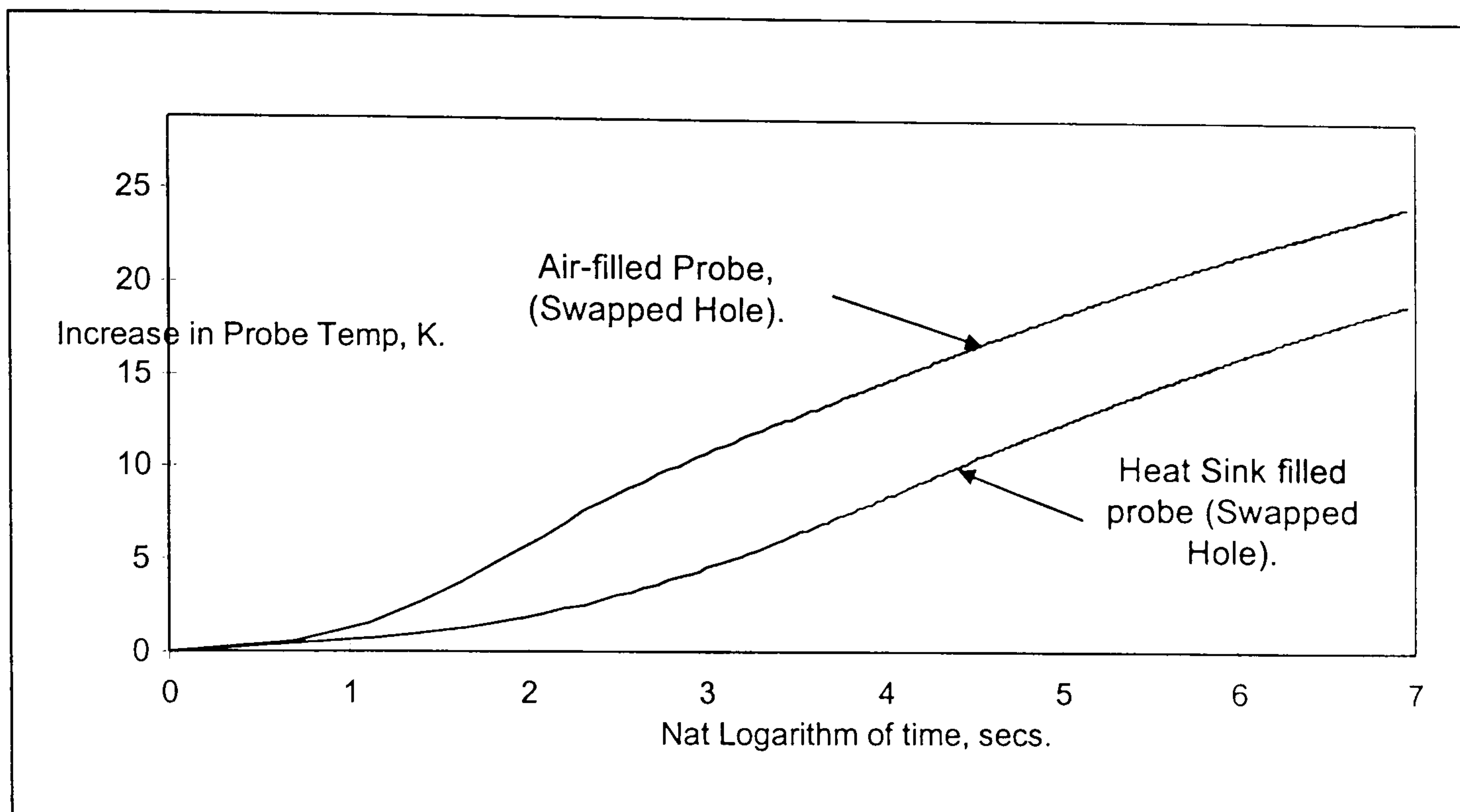
Table 6.11, shows the location of the different probe types for the lightweight aerated concrete block studies illustrated in graphs 6.9 and 6.10.

Graph 6.9 shows the difference in behaviour of the two probes, where, as usual, the rise in probe temperatures is plotted as a function of the natural logarithm of time. The probe with heat sink filling shows a noticeably lower over-all temperature rise and slower response than that of the air-filled probe. Both of the holes for the measurements shown in graph 6.9 were filled with HTSP heat sink compound.



Graph 6.9, shows the long time behaviour of an air-filled probe and heat-sink filled probe in lightweight aerated concrete block.

Graph 6.10 shows the effect of interchanging the probes again with heat sink in the holes in the lightweight aerated concrete block. As can be seen the shape of the lines and the temperature rise for each probe are unique to the probe and not a characteristic of the test material.



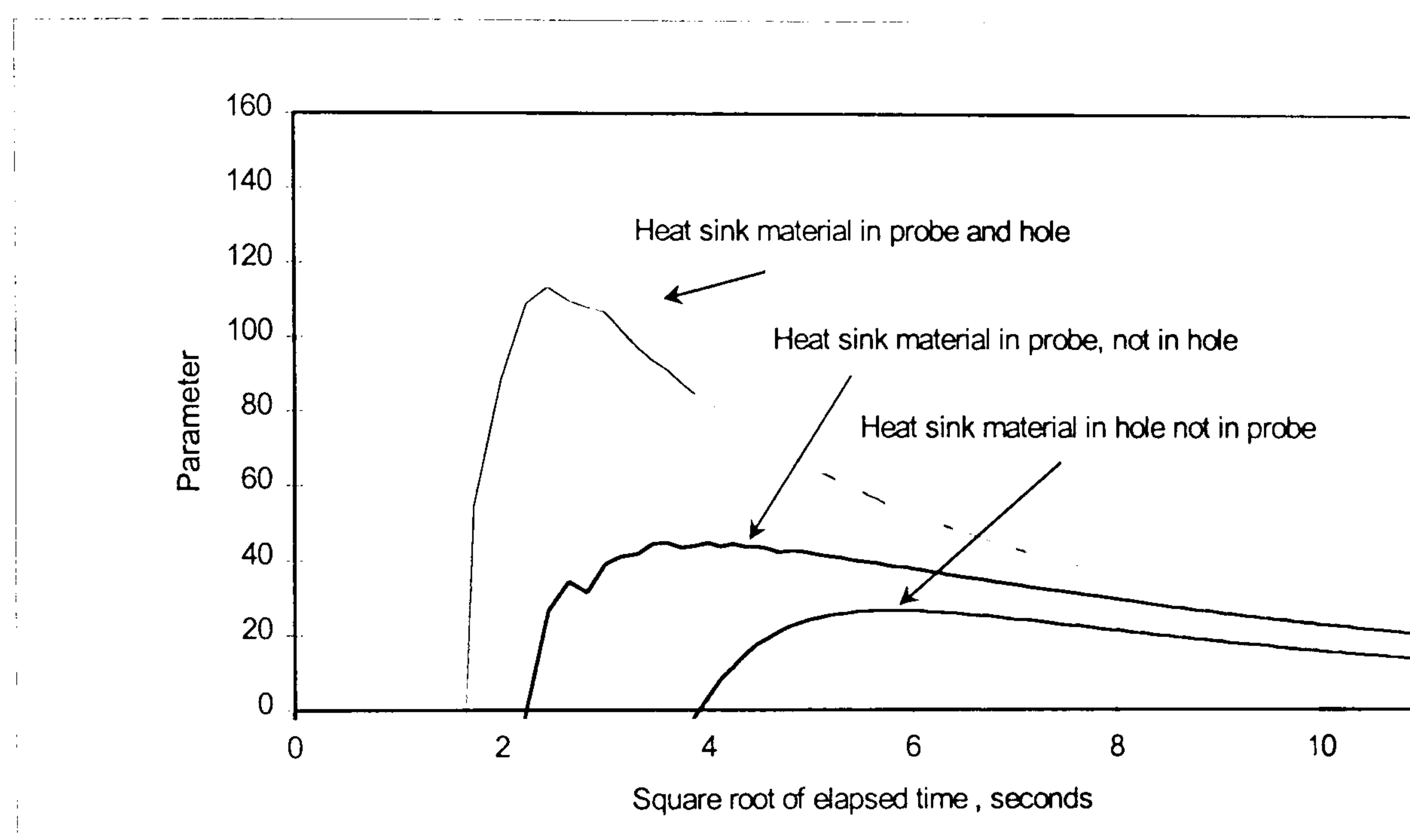
Graph 6.10, shows the long time behaviour of the probes shown in graph 6.9, interchanged in a lightweight aerated concrete block.

Table 6.12 shows a summary of the long time analysis results undertaken upon the aerated concrete block using probes with and without heat sink compound filling and with or without heat-sink compound in the block test holes.

run code	Power, Watts.	Thermal Conductivity $Wm^{-1}K^{-1}$	Probe condition (sink material = HTSP heat sink compound).
thp1711	0.33	0.13	sink in probe, not in block
thp1911	0.33	0.12	sink in probe, not in block
thp11511	0.36	0.12	sink in probe and block
thp11411	0.36	0.12	sink in probe and block
thp11311	0.36	0.12	sink in probe and block
thp11211	0.37	0.12	sink in probe and block
thp11011	0.37	0.13	sink in probe and block
thp21111	0.37	0.15	sink in block not in probe
Mean Value		0.126 ± 0.01	

Table 6.12, summary of the long time results of the laboratory studies of lightweight aerated concrete block.

The measured conductivity representing the heat sink in the hole within the lightweight block, but not in the probe, was higher than the other measurements. However, the thermal conductivities measured by using heat sink material in the probe and the hole of the block did return values that were very close in magnitude to the manufacturers figure of $0.12 \text{ Wm}^{-1}\text{K}^{-1}$, (Durox). To confirm the long time analysis values and to establish a figure for the probe thermal conductance, H, the short time analysis was used. Several short time analysis curves representing the effect of different positions of heat sink compound upon the results from a lightweight concrete block are shown in graph 6.11.



Graph 6.11, shows the short time behaviour in a lightweight aerated concrete block, heat sink material in probe and hole.

run code	Probe Conductance, H, $\text{Wm}^{-2}\text{K}^{-1}$	Diffusivity m^2s^{-1}	'Probe Condition' (sink material = HTSP heat sink compound).
thp1711	46.73	2.32×10^{-8}	sink in probe, not in block
thp1911	59.92	4.35×10^{-8}	sink in probe, not in block
thp11511	133.11	2.15×10^{-8}	sink in probe and block
thp11411	134.05	2.05×10^{-8}	sink in probe and block
thp11311	149.85	2.26×10^{-8}	sink in probe and block
thp11211	151.11	2.45×10^{-8}	sink in probe and block
thp11011	155.85	3.30×10^{-8}	sink in probe and block
thp21111	45.61	1.28×10^{-7}	no sink in probe but in block
Mean Value (sink in probe)		$2.44 \times 10^{-8} \pm 5.0 \times 10^{-9}$	

Table 6.13, summary of short-time results, lightweight aerated concrete block.

A summary of the studies of the four materials, wax, glycerine, foam and lightweight aerated concrete block that were undertaken to demonstrate the acceptability of the technique under laboratory conditions can be seen in table 6.13A. The measured values more or less agree with the published data. To move cautiously to the *in-situ* work and to act as a stepping stone, the next series of laboratory studies involve three different types of earth walling material.

Material	Measured Values		Published Values	
	Mean Thermal Conductivity $\text{Wm}^{-1}\text{K}^{-1}$	Mean Thermal Diffusivity m^2s^{-1}	Mean Thermal Conductivity $\text{Wm}^{-1}\text{K}^{-1}$	Mean Thermal Diffusivity m^2s^{-1}
Paraffin Wax	0.261 ± 0.034	$1.07 \times 10^{-7} \pm 2.9 \times 10^{-8}$	0.251	9.62×10^{-6}
Glycerine	0.293 ± 0.009	$2.26 \times 10^{-6} \pm 1.3 \times 10^{-7}$	0.292-0.314	$0.967 \times 10^{-7} - 1.1 \times 10^{-7}$
Phenolic Foam	0.029 ± 0.003	$1.69 \times 10^{-8} \pm 5.4 \times 10^{-9}$	0.032	1.00×10^{-7}
Lightweight Concrete	0.126 ± 0.01	$2.44 \times 10^{-8} \pm 5.0 \times 10^{-9}$	0.12	2.0×10^{-7}

Table 6.13A, summary of the measured results and published values of thermal properties of paraffin wax ,glycerine, phenolic foam and lightweight concrete measured during the laboratory studie

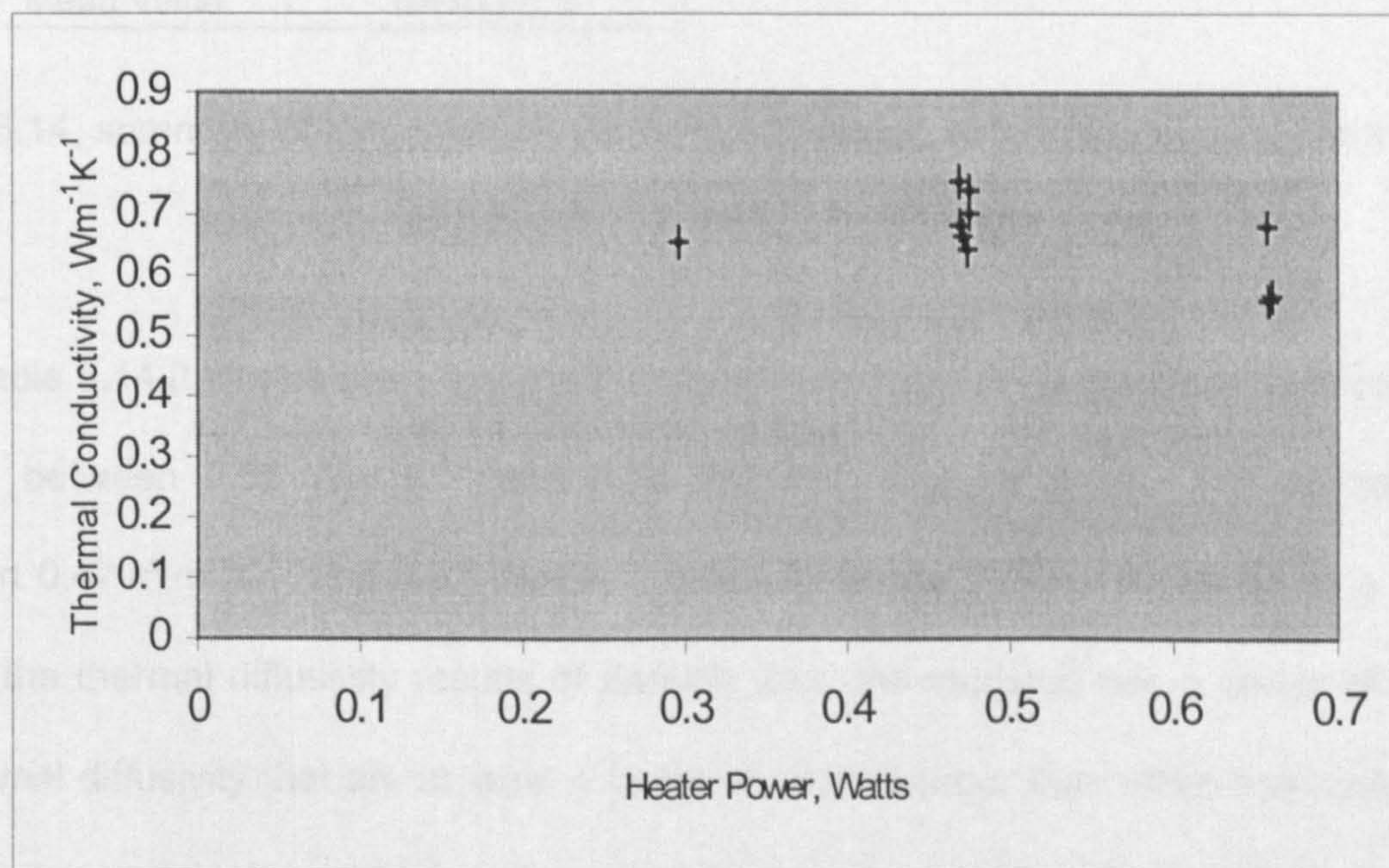
Earth Walling Materials

Three earth walling materials were tested in the laboratory. Mud and stud, (which will be called mudstud), wychert and cob blocks which together represent a cross section of the unbaked earth walling materials that are available in the UK. Mudstud is an infill material, wychert a monolithic material and cob blocks are a hybrid material. Details of these materials may be found in the glossary situated at the beginning of this thesis. The materials were tested using the same procedures outlined in chapter 4. Heat sink compound was used in the final studies in an effort to improve the thermal contact between the probe and the specimen. It was hoped that these measurements would bridge the gap between the laboratory and *in-situ* measurements.

Mudstud.

The first walling sample to be studied was a panel of mudstud prepared for Beech Farm, donated by John Heard, (the chairman of ICOMOS (International Committee for the Study and the Conservation of Earthen Architecture) in the UK), from his native Lincolnshire. The sample measured approximately 125mm x 500mm x 400mm and allowed several holes to be drilled without the danger of the holes interfering with any of the results. This panel was placed within a well-insulated container and the probe and specimen were allowed to reach thermal equilibrium before each study.

The first measurements undertaken upon the mudstud sample used a ten-second-time interval for data collection, rendering this information only useful for long time analysis and resulting in the thermal conductivity value. However, this data was useful to investigate the correct power range to be used for the probe heater.



Graph 6.12, shows the variation of thermal conductivity of mudstud with maximum temperature.

The thermal conductivity of mudstud is greater than either the paraffin wax or phenolic foam and so a higher heater power was required. To ensure that the use of different

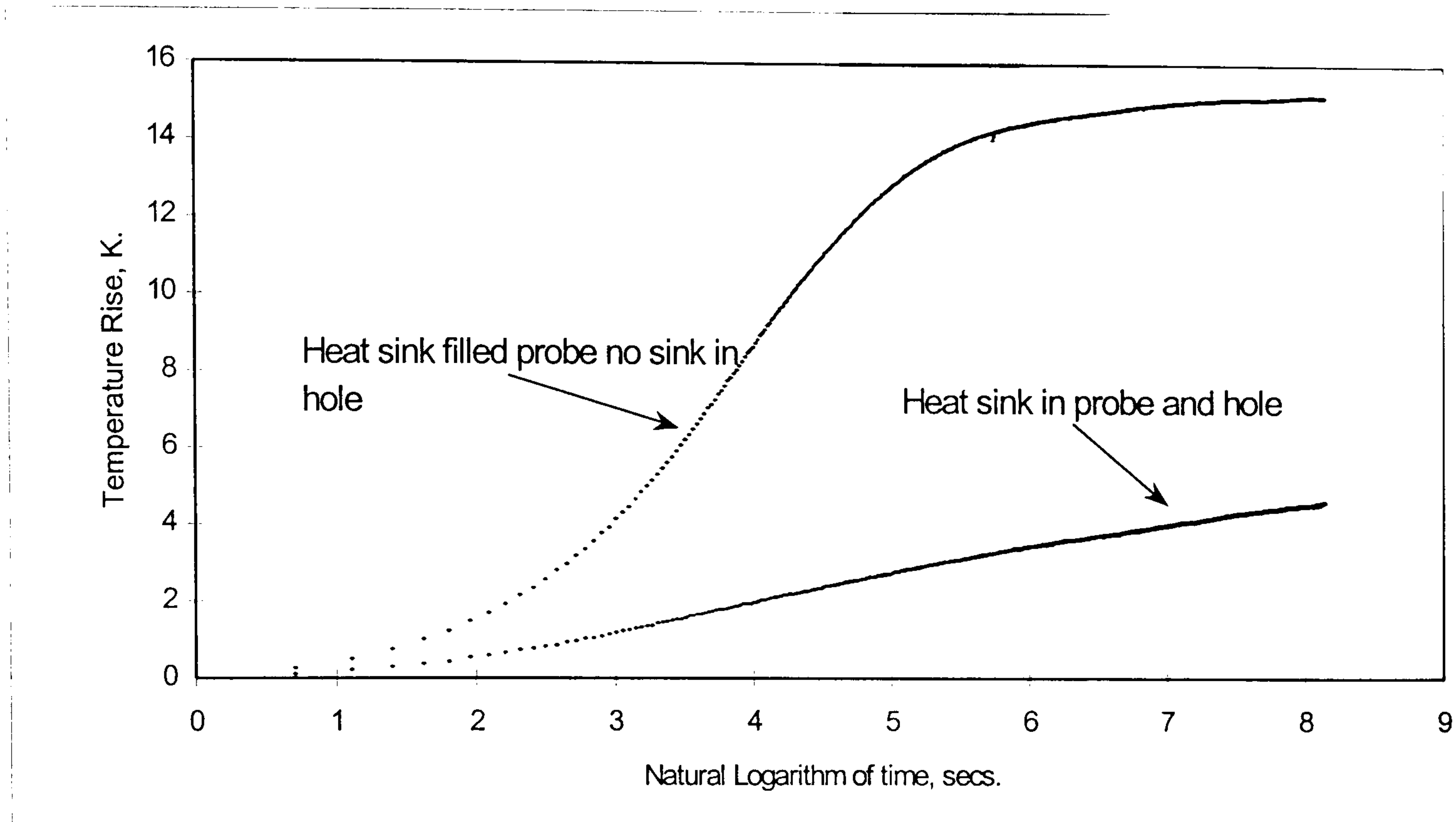
heater powers were not having an effect upon the results, three different power settings were used, ranging from approximately 0.2 Watts to 0.7 Watts. As can be seen in graph 6.12, the thermal conductivity values obtained from the long time analysis showed an even spread of values and appear to be unaffected by different heater power ranges. (However, the variations of ambient temperature have been shown to affect the results when using a heater power of less than 0.2 Watts in field conditions, (see chapter 7)).

Material	run no	Thermal Conductivity $\text{Wm}^{-1}\text{K}^{-1}$	Power, Watts	Mean temp, $^{\circ}\text{C}$	Thermal Diffusivity m^2s^{-1}
mudstud	1	0.655	0.296	30.5	0.415
mudstud	2	0.667	0.471	35.7	0.354
mudstud	3(2 r)	0.757	0.469	38.2	113.107
mudstud	3a	0.684	0.469	37.8	10.837
mudstud	4	0.644	0.474	39.1	2.733
mudstud	5	0.704	0.475	38.7	24.547
mudstud	6	0.741	0.475	39.1	101.054
mudstud	7	0.682	0.657	44.9	8.782
mudstud	8	0.566	0.660	47	0.803
mudstud	9	0.560	0.658	47.8	0.685
Mean Value		0.670 ± 0.06			

Table 6.14, summary of long time results for initial studies on mudstud walling with single thermocouple and air filled probe.

From table 6.14 it can be seen that the thermal conductivity of mudstud remains plausible varying between $0.56 \text{ Wm}^{-1}\text{K}^{-1}$ and $0.75 \text{ Wm}^{-1}\text{K}^{-1}$ compared with the estimates of between $0.47 \text{ Wm}^{-1}\text{K}^{-1}$ and $0.93 \text{ Wm}^{-1}\text{K}^{-1}$ given by Minke (1994). However, in a similar way to the thermal diffusivity results of paraffin wax, the mudstud has a series of values for thermal diffusivity that are at least a factor of 10,000 larger than other best estimates. Similar changes in the experimental procedure to those used for paraffin wax were introduced to allow a closer investigation of the behaviour of the probe in relation to its 'fit' in the mudstud sample. The modified procedure used heat sink material, a data collection interval of one second and at a later stage, a probe with twin thermocouples (see chapter 4, development of the technique).

Graphs 6.13 and 6.14 show the results of the long time and short time analysis using probes with heat sink material both in the probe and hole.

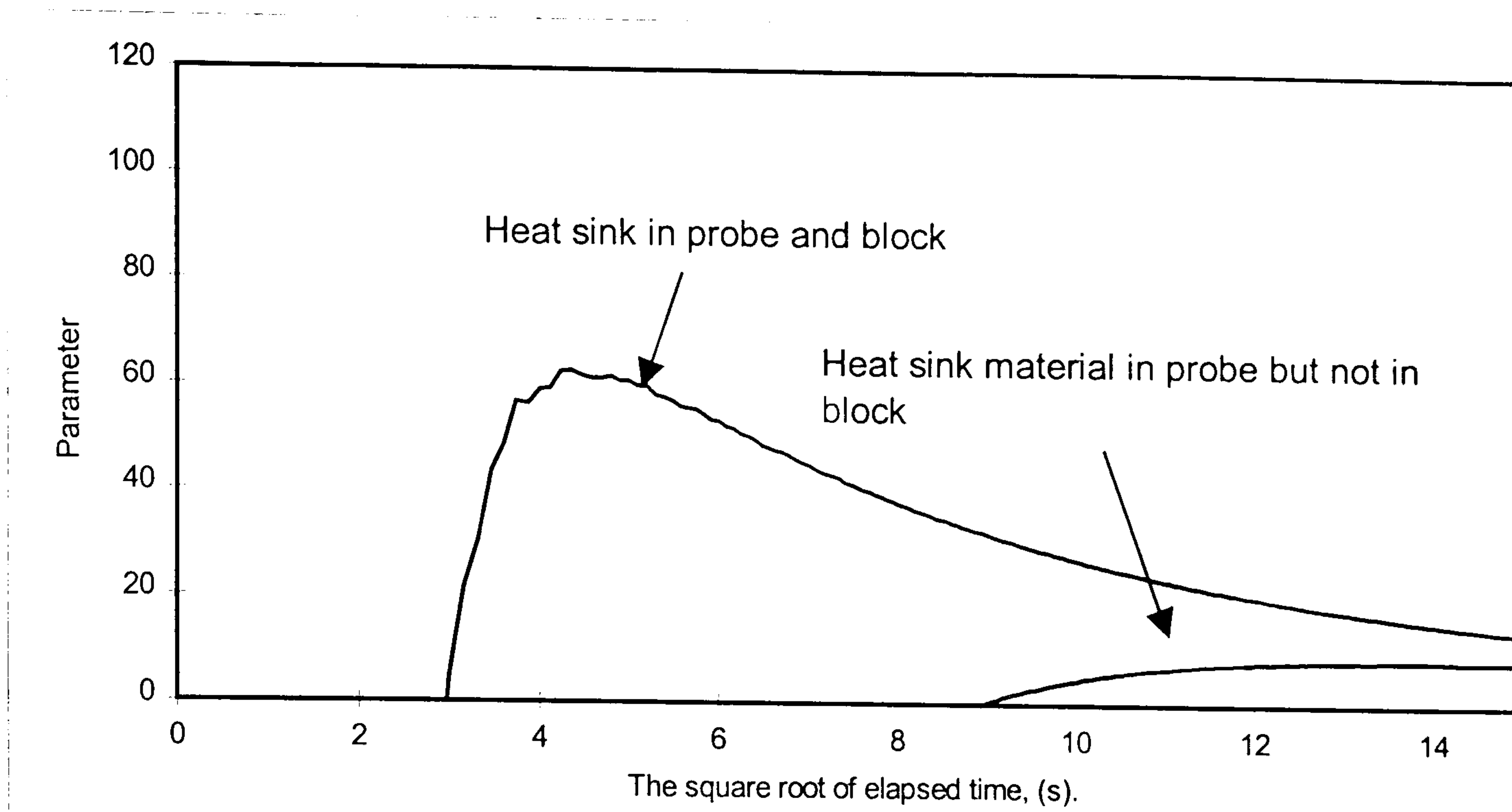


Graph 6.13, shows the long time behaviour of mudstud block with heat sink material.

The curves shown in graph 6.13 are similar in shape to those in graphs 6.9 and 6.10. This indicates that the introduction of heat sink materials are having a similar effect upon the mudstud block to that found in the lightweight aerated concrete block. The summary of long time results can be seen in table 6.15, where the value of the thermal conductivity is reduced when heatsink compound is used both in the material and in the probe.

run code	Power (Watts)	Thermal Conductivity $Wm^{-1}K^{-1}$	Probe Condition (sink material = HTSP heat sink compound).
ms2s0400	0.296	0.634	HTSP in Probe
ms2s3000	0.287	0.729	HTSP in Probe
ms2t0700	0.291	0.519	HTSP Probe and Hole
ms2t1000	0.285	0.598	HTSP Probe and Hole
Mean (last two values)		0.558 ± 0.055	

Table 6.15, summary of the long time results of the laboratory studies, mudstud.



Graph 6.14, shows the short time analysis, mudstud.

Graph 6.14 shows the higher peak for the short time analysis carried out upon the heat sink filled probe using a hole with heat sink material. Table 6.16 shows that a HTSP filled probe placed in the sample had a conductance of about $10 \text{ Wm}^{-1}\text{K}^{-1}$, while the filled probe in a filled hole had a probe conductance of $100 \text{ Wm}^{-1}\text{K}^{-1}$, ten times larger.

run code	Probe conductance $\text{Wm}^{-2}\text{K}^{-1}$	Thermal Diffusivity m^2s^{-1}	Probe Condition (sink material = HTSP heat sink compound).
ms2s0400	10.70	1.65×10^{-6}	HTSP in Probe
ms2s3000	8.74	1.14×10^{-7}	HTSP in Probe
ms2t0700	101.65	4.49×10^{-7}	HTSP Probe and Hole
ms2t1000	99.79	6.03×10^{-7}	HTSP Probe and Hole
		$5.26 \times 10^{-7} \pm 1.08 \times 10^{-7}$	Mean (last two values)

Table 6.16, summary of short-time results, mudstud.

The short time results for the probe conductance, H in mudstud are considerably smaller than the H values measured using the rate analysis shown in table 6.17. However, the increase in the probe conductance values are mirrored in the rate analysis. The increase in the value of mc when the probe is surrounded by heatsink compound as well as being filled with heatsink material, does suggest that the external heat sink material is being included in the mc value of the probe. This can also be seen in table 6.21 where the results of the rate studies upon wychert are summarised.

run code	Power (Watts).	Probe conductance $Wm^{-1}K^{-1}$	mc, JK^{-1}	Probe Condition (sink material = HTSP heat sink compound).
ms2s0400	0.296	351.0	0.993	HTSP in Probe
ms2s3000	0.287	328.7	0.969	HTSP in Probe
ms2t0700	0.291	542.4	1.586	HTSP Probe and Hole
ms2t1000	0.285	531.9	1.727	HTSP Probe and Hole

Table 6.17, summary of rate analysis studies on mudstud.

The long and short time results for mudstud concurs with thermal values of similar materials. For example, according to the CIBSE guide, 1985 brickwork used in the inner leaf of a cavity wall has a thermal conductivity of $0.62 Wm^{-1}K^{-1}$ and a thermal diffusivity of $4.65 \times 10^{-7} m^2s^{-1}$. Whilst according to the Chemical Rubber Corporation (CRC) handbook, Lide, 1996, the thermal conductivity of dry sand is $0.33 Wm^{-1}K^{-1}$. Dry sandy soil has a thermal diffusivity of $2.0 \times 10^{-7} m^2s^{-1}$ and $3.3 \times 10^{-7} m^2s^{-1}$ when it has a moisture content of 8%, (Carslaw and Jagaer, 1947). The mean value of the thermal diffusivity of mudstud is $7.04 \times 10^{-7} m^2s^{-1}$. However, this value drops to $5.26 \times 10^{-7} m^2s^{-1}$ if a mean is taken of the two readings taken with HTSP material in the hole and in the probe.

Wychert.

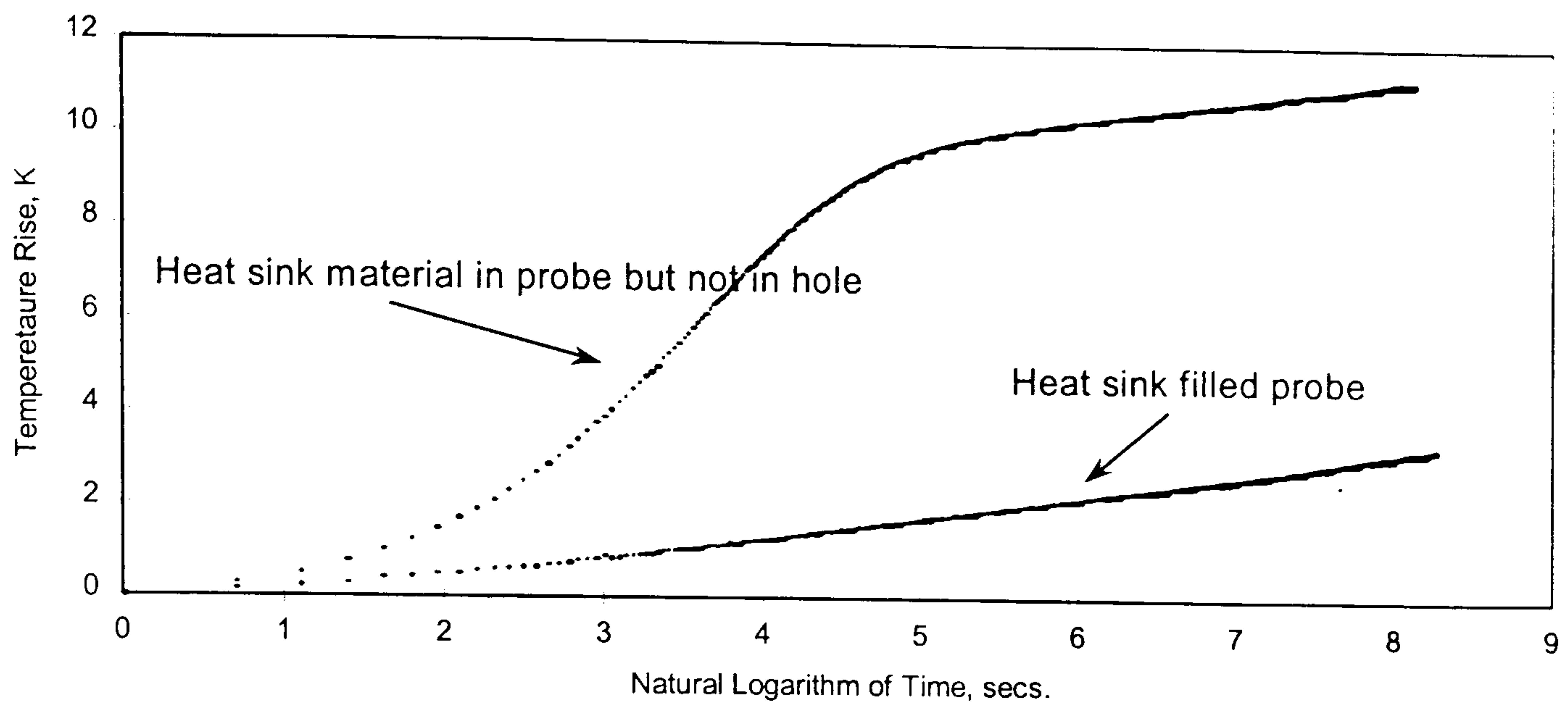
The second unbaked earth walling material studied was wychert, which is produced in a similar way to rammed earth, or pise de terre (see chapter 1). Wychert originates in Buckinghamshire and is composed of lime-rich subsoil. The measurement procedure was identical to that used for the mudstud sample, again containing the sample within an insulated container and delaying probe heating for 24 hours to allow the sample to reach thermal equilibrium. The range of heater power was found to be identical to the range required for the mudstud sample, confirming that the thermal properties of these two samples were similar. The wychert sample, however, had a higher thermal conductivity with a mean value indicated in the summary table 6.18 of $0.72 Wm^{-1}K^{-1}$.

Material	run no	Thermal Conductivity Wm ⁻¹ K ⁻¹	Power, Watts	Mean temp, °C
wychert	1	0.737	0.656	48.1
wychert	2	0.690	0.659	49.0
wychert	3	0.674	0.667	45.4
wychert	4	0.679	0.668	45.9
wychert	5	0.710	0.670	48.4
wychert	6	0.666	0.673	51.0
wychert	7	0.727	0.672	50.4
wychert	8	0.705	0.674	50.6
wychert	9	0.712	0.692	51.4
wychert	10	0.738	0.689	48.4
wychert	11	0.700	0.335	34.9
wychert	13	0.691	0.341	35.2
wychert	14	0.728	0.399	38.3
wychert	15	0.700	0.340	35.3
wychert	16	0.891	0.182	28.3
wychert	17	0.707	0.209	29.2
wychert	18	0.691	0.211	29.3
wychert	19	0.719	0.215	28.8
Mean Value		0.715 ± 0.048		

Table 6.18, summary of long time results for initial studies on wychert with single thermocouple air filled probe.

The first results for wychert obtained using data collection at a time interval of 10 seconds are shown in table 6.18. As can be seen the thermal conductivity values are similar to those obtained from the long time analysis of the mudstudd walling samples. A further five measurements were undertaken using the later reinforcement of heat sink material in the probe.

Graph 6.15 shows two long time studies on wychert. The first study used a heat sink filled probe, the second had heat sink also in the hole. This second case showed the reduced rise in probe temperature associated with higher rates of heat transfer from heater to specimen.

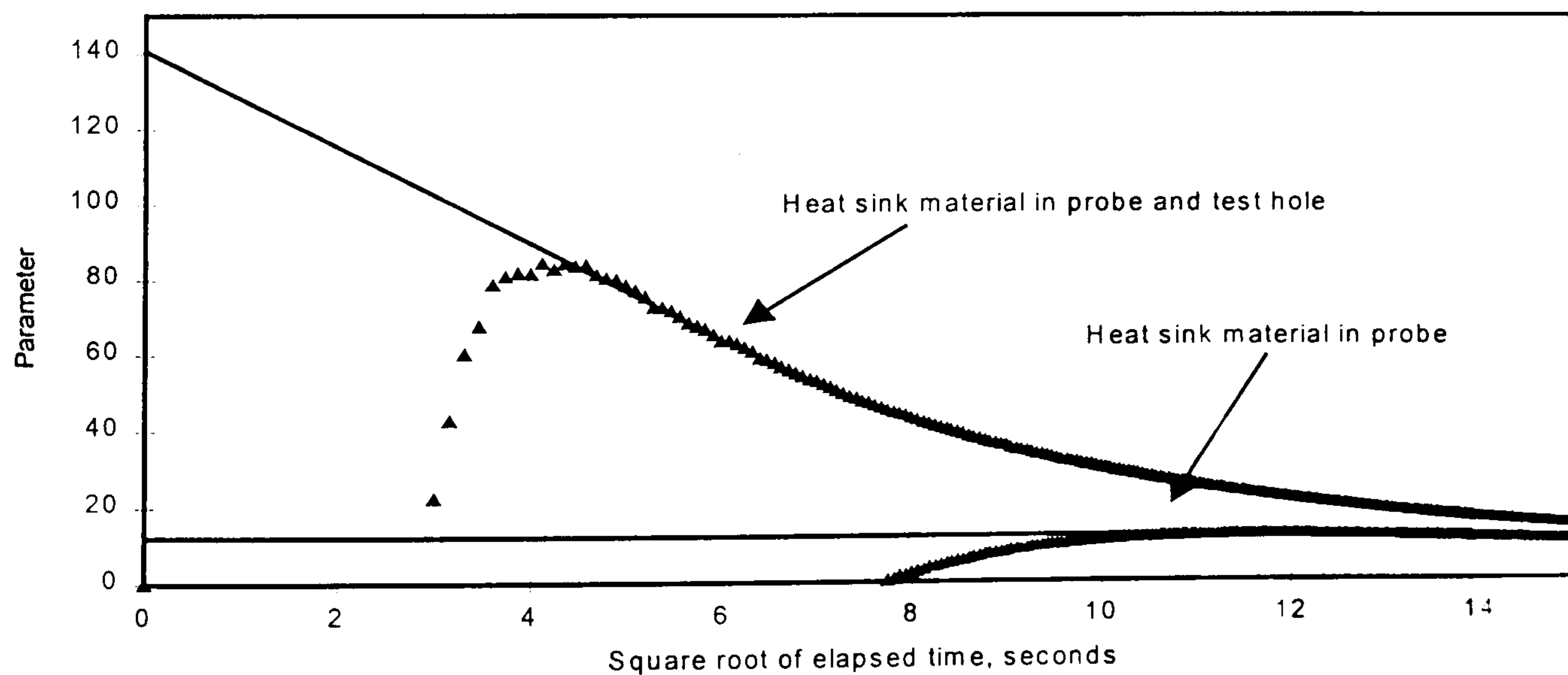


Graph 6.15, shows the typical long time behaviour of wychert, HTSP heat sink in the probe and in the hole.

run code	Power, Watts	Thermal Conductivity $Wm^{-1}K^{-1}$	Probe Condition (sink material = HTSP heat sink compound).
1905	0.289	0.721	HTSP probe and hole
2005	0.280	0.670	HTSP probe and hole
2105	0.286	0.754	HTSP probe and hole
2204	0.274	0.698	HTSP probe
2304	0.293	0.730	HTSP probe
Mean Value		0.715 ± 0.03	

Table 6.19, summary of the long time analysis of the laboratory studies of wychert.

The mean measured thermal conductivity of wychert is $0.715 Wm^{-1}K^{-1}$, similar to the measurements undertaken without heat sink material in the probe.



Graph 6.16 shows a short time analysis. Wychert, HTSP heat sink material in the probe and in the hole.

run code	Probe conductance $\text{Wm}^{-1}\text{K}^{-1}$	Thermal Diffusivity m^2s^{-1}	Probe Condition (sink material = HTSP heat sink compound).
2204	18.26	3.23×10^{-6}	HTSP probe
2304	18.64	3.51×10^{-6}	HTSP probe
1905	94.67	7.82×10^{-7}	HTSP probe and hole
2005	140.07	5.09×10^{-7}	HTSP probe and hole
2105	139.75	6.69×10^{-7}	HTSP probe and hole
Mean Value		$5.89 \times 10^{-7} \pm 1.17 \times 10^{-7}$	

Table 6.20, summary of short-time results, wychert.

The short time analysis undertaken upon wychert gives a mean value of $1.74 \times 10^{-6} \text{ m}^2\text{s}^{-1}$ for the thermal diffusivity. This value is twice as large as the figure for mudstud. However, if the two 'good' runs using the probes with HTSP heat sink material in both the hole and the probe are analysed the mean is then $5.89 \times 10^{-7} \text{ m}^2\text{s}^{-1}$. This figure compares more favourably with a value of $5.26 \times 10^{-7} \text{ m}^2\text{s}^{-1}$ measured for mudstud in the same conditions.

The rate analysis for wychert does confirm that the probe conductance, H, does increase with the addition of heatsink compound to the sample hole. However, as table 6.21, shows the higher values for H are approximately six times larger than the H values suggested by the short times studies shown in table 6.20. The value of mc increases in a very similar way to the increase noted in the results for the rate analysis for mudstud in table 6.21. It is felt that the increase in the value of mc is connected with the addition of heatsink material in the sample hole around the probe. The additional heatsink material around the probe may influence the rate method by contributing additional mass and specific heat to the probe. For this case, the mc value of the probes is almost doubled by addition of heatsink compound to the sample hole. Again, further carefully controlled additional work is required on the role of the heat sink material.

run code	Power, Watts.	Probe conductance $Wm^{-1}K^{-1}$	mc, JK^{-1}	Probe Condition (sink material = HTSP heat sink compound).
rate2204	0.274	135.1	0.928	HTSP in probe
rate2304	0.293	134.62	0.934	HTSP in probe
rate2005	0.280	673.9	1.648	HTSP in probe and hole
rate2105	0.286	668.2	1.999	HTSP in probe and hole

Table 6.21, summary of rate analysis studies on wychert.

Cob Block

A cob block manufactured from a compressed mixture of subsoil and straw into the dimensions of a standard concrete block, 440mm X 210mm X 100mm, was studied in a manner identical to the previous work on mudstod and wychert. The results of the long time studies upon cob blocks, which used heat sink material in and around the probe, can be seen in table 6.22. The standard cob block was, as previously stated, a mixture of subsoil and straw, the subsoil being drawn from a valley near Tedburn St Mary in mid Devon. A variation of the cob block was produced by the addition of waste lambs wool, added to improve the working properties of the block. The addition of wool allowed a more cohesive mix prior to placing in any moulds and reduced the amount of straw needed. According to Graham Fielding, (The Cob Construction Company), the waste wool sometimes gave the finished blocks an improved resistance to impact damage and utilises a locally produced waste material. Blocks of this type were studied to compare their thermal properties with the values of the ordinary cob blocks made by adding straw to the subsoil.

The first results for cob block were obtained using data sampling at time intervals of 10 seconds and are shown in table 6.22. As can be seen, the mean thermal conductivity value, ($0.74 Wm^{-1}K^{-1}$), is similar to those obtained from the long time analysis of the mudstod, ($0.67 Wm^{-1}K^{-1}$) and wychert, ($0.72 Wm^{-1}K^{-1}$) samples.

Material	run no	Thermal Conductivity Wm ⁻¹ K ⁻¹	Power, Watts
cobblock	1	0.700	0.675
cobblock	2	0.757	0.697
cobblock	3	0.740	0.685
cobblock	4	0.777	0.337
cobblock	5	0.716	0.338
cobblock	6	0.746	0.338
cobblock	7	0.703	0.211
cobblock	8	0.671	0.207
cobblock	9	0.744	0.207
cobblock	10	0.762	0.205
cobblock	11	0.698	0.208
cobblock	12	0.739	0.207
cobblock	13	0.756	0.338
cobblock	14	0.746	0.340
cobblock	15	0.734	0.339
cobblock	17	0.779	0.681
cobblock	18	0.793	0.681
cobblock	19	0.800	0.682
Mean Value		0.742 ± 0.035	

Table 6.22, summary of long time results for initial studies of cob block with single thermocouple air filled probe.

The long time thermal conductivity for the cobblocks showed no noticeable variation with different heater power values. For example, a low heater power of 0.207W gives a thermal conductivity of 0.744 Wm⁻¹K⁻¹, very similar to a thermal conductivity of 0.740 Wm⁻¹K⁻¹ for a heater power of 0.685W, three times as large. The long time results for cobwool are displayed in a similar way in table 6.23.

Material	run no	Thermal Conductivity Wm ⁻¹ K ⁻¹	Power (Watts)	Probe Condition (sink material = HTSP heat sink compound).
Cobwool	1	0.798	0.289	HTSP sink in probe and block
Cobwool	2	0.752	0.288	HTSP sink in probe and block
Cobwool	3	0.722	0.287	HTSP sink in probe and block
Cobwool	4	0.611	0.293	HTSP sink in probe not in block
Cobwool	5	0.476	0.294	HTSP sink in probe not in block
Cobwool	6	0.518	0.296	HTSP sink in probe not in block
Mean		0.646 ± 0.13	0.291 ± 0.003	

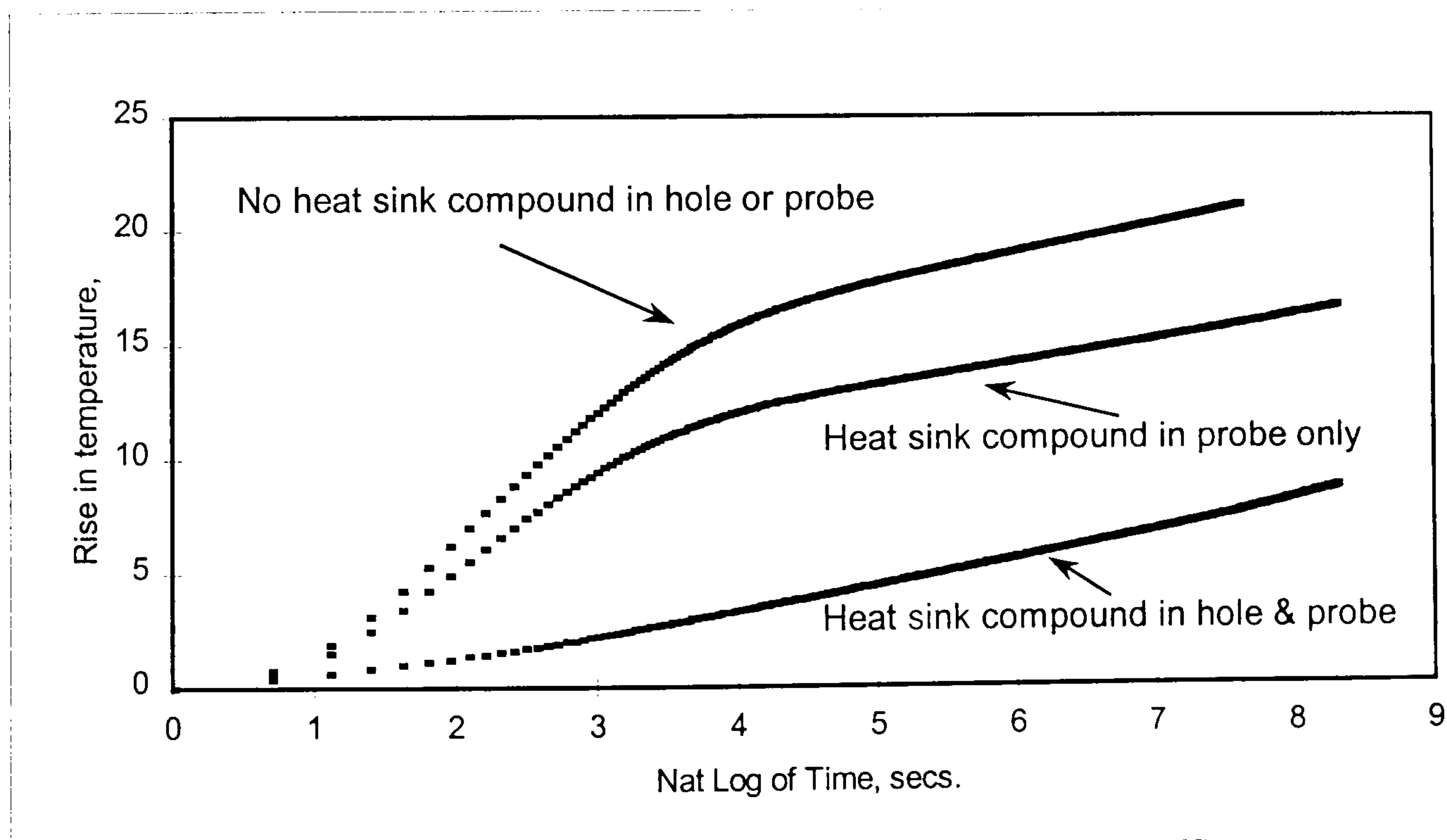
Table 6.23 summary of long time results for initial studies of cobwool with single thermocouple air filled probe.

The effect of inserting wool into a cob block appears to have reduced the mean thermal conductivity from 0.742 Wm⁻¹K⁻¹ to a value of 0.646 Wm⁻¹K⁻¹. Although the measured

values are erratic and the reduction in thermal conductivity is not large, the difference does appear to warrant further studies concerning the thermal properties of this material. Perhaps this further work could focus upon using more quantifiable ingredients and a more extensive series of measurements for both the cobblocks and cobwool blocks..

Following the pattern established in the earlier studies of paraffin wax, mudstud and wychert samples, the later studies of the cob blocks incorporated the improvements to the technique.

A cob block constructed with typical amounts of straw, was studied using HTSP heat sink modified probes. (The assessment of the straw content was undertaken by a visual inspection assessed by experienced operatives from the Cob Construction Company). HTSP heat sink compound was used in the probe and in the test hole. It was anticipated, much as for the earlier studies on various materials, that the influence of the heat sink compound would improve the thermal contact between the probe and the test material. The following graph shows the long time behaviour of a probe placed in holes with heat sink material.



Graph 6.17, shows the long time behaviour of cob block, combinations of heat sink material in the probe and the hole.

It can be seen that Graph 6.17 shows that the use of heat sink compound has reduced the overall temperature rise of the experiments.

Runcode	Thermal Conductivity $\text{Wm}^{-1}\text{K}^{-1}$	Probe Condition. (sink material = HTSP heat sink compound).
cob1278	0.35	sink in probe sink in hole
cob1268	0.39	sink in probe sink in hole
cob2288	0.38	sink in probe sink in hole
cob4188	0.35	sink in probe sink in hole
cob4198	0.34	sink in probe sink in hole
cob238	0.47	sink in probe no sink in hole
cob0317	0.34	sink in probe no sink in hole
cob3118	0.41	sink in probe no sink in hole
cob1	0.34	no sink in either
cobblk1.3	0.31	no sink in either
cbblk1.4	0.34	no sink in either
Mean Value	0.368 ± 0.04	

Table 6.24, summary of the long time results, second series of measurements upon cob blocks

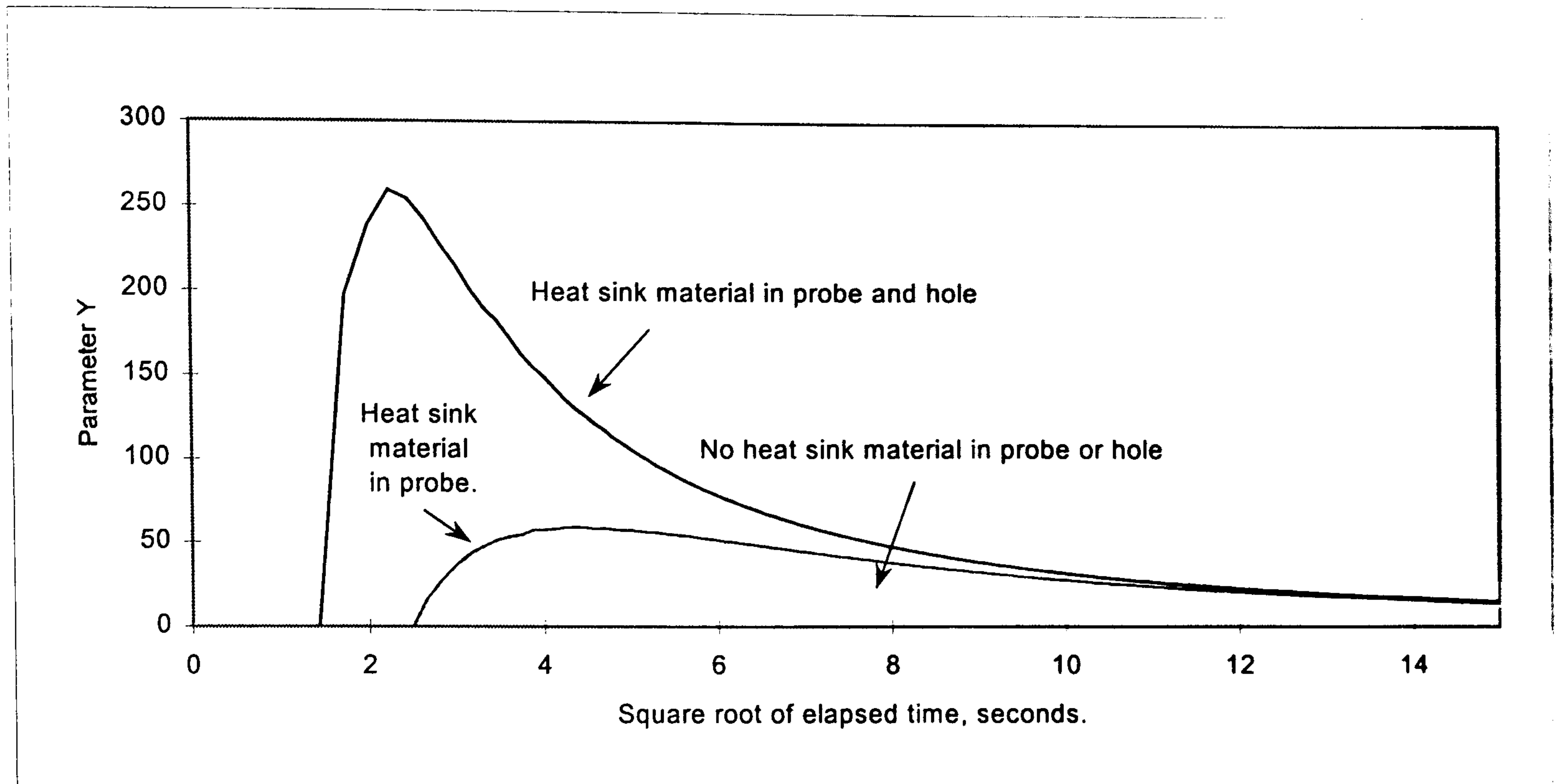
The second series of experiments undertaken upon cobblocks gave a much lower thermal conductivity when using the long time analysis, $0.368 \text{ Wm}^{-1}\text{K}^{-1}$ against $0.742 \text{ Wm}^{-1}\text{K}^{-1}$ for the earlier measurements without heatsink materials and at 5 and 10 second data collection intervals. A similar investigation was undertaken upon a cobwool block with similar reductions in the thermal conductivity values, as can be seen summarised in table 6.25.

Runcode	Thermal Conductivity $\text{Wm}^{-1}\text{K}^{-1}$	Probe Condition. (sink material = HTSP heat sink compound).
cwool1205long	0.390	HTSP sink in probe and block
cwool1305long	0.366	HTSP sink in probe and block
cwool1705long	0.359	HTSP sink in probe and block
cwool2604long	0.370	HTSP sink in probe NOT in block
cwool2704long	0.373	HTSP sink in probe NOT in block
cwool2804long	0.334	HTSP sink in probe NOT in block
Mean	0.365 ± 0.018	sink in probe nosink in hole

Table 6.25, summary of the long time results for cobwool blocks.

The long time results for cobwool show that there is a reduction in the thermal conductivity value, but not as large as experienced when comparing the results of the first measurements.

The Blackwell short time analysis of the data obtained for coblock4 gave a graph of the term Y against the square root of elapsed time as shown in graph 6.18.



Graph 6.18, shows the short time analysis of cob blocks with heat sink material in various positions.

The following table, table 6.26 shows the results from the short time analysis of the cob blocks.

Runcode	Probe Conductance, H , $Wm^{-1}K^{-1}$	Thermal Diffusivity m^2s^{-1}	Probe Condition, (sink material = HTSP heat sink compound).
cob1	31.96	9.08×10^{-7}	no sink in either
cobblk1.3	31.04	4.47×10^{-7}	no sink in either
cbblk1.4	33.46	8.79×10^{-7}	no sink in either
cob238	32.00	1.02×10^{-6}	sink in probe, no sink in hole
cob0317	31.81	9.25×10^{-7}	sink in probe, no sink in hole
cob3118	91.53	3.02×10^{-7}	sink in probe, no sink in hole
Mean Value	51.78	$7.46 \times 10^{-7} \pm 3.90 \times 10^{-7}$	Mean value of sink in probe
cob1278	315.00	6.67×10^{-7}	sink in probe & in hole
cob1268	327.00	7.97×10^{-8}	sink in probe & in hole
cob2288	412.93	5.96×10^{-8}	sink in probe & in hole
cob4188	307.14	7.22×10^{-8}	sink in probe & in hole
cob4198	298.30	6.95×10^{-8}	sink in probe & in hole
Mean Value	332.67	$6.95 \times 10^{-8} \pm 7.3 \times 10^{-9}$	
Mean of all α Values		$4.65 \times 10^{-7} \pm 4.1 \times 10^{-7}$	

Table 6.26, summary of the short-time results, cob blocks.

As can be seen from these results in table 6.26 the probe Conductance, H, increases by a factor of approximately 8 with the application of the heat sink compound. The measured

thermal diffusivity becomes smaller by factors of between 2 and 7. From the long time analysis of cobblocks the mean thermal conductivity of $0.368 \text{ Wm}^{-1}\text{K}^{-1}$ is considerably smaller than that found for either mudstud or wychert. However, as previously stated, a published thermal conductivity of dry sand is $0.33 \text{ Wm}^{-1}\text{K}^{-1}$ (Lide,1996) and as the measured value for cobblock is similar to this figure it is felt that this mean value is probably acceptable. This is also likely as the density of the cobblocks were less than the samples of mudstud or that for wychert. The thermal diffusivity values do vary between different combinations of sink and probe. The mean of all of the values, $4.7 \times 10^{-7} \text{ m}^2\text{s}^{-1}$, compares reasonably well with the α of mudstud, $7.04 \times 10^{-7} \text{ m}^2\text{s}^{-1}$, but is smaller than the α value of wychert, $1.74 \times 10^{-6} \text{ m}^2\text{s}^{-1}$.

Run Number	Probe Conductance, H	Thermal Diffusivity m^2s^{-1}	Probe Condition, (sink material = HTSP heat sink compound).
1	16.40	1.13×10^{-6}	HTSP sink in probe not in block
2	12.02	1.02×10^{-6}	HTSP sink in probe not in block
3	13.73	9.01×10^{-7}	HTSP sink in probe not in block
	42.15	1.02×10^{-7}	Mean Value
4	165.59	1.52×10^{-7}	HTSP sink in probe and block
5	160.04	1.35×10^{-7}	HTSP sink in probe and block
6	146.70	1.22×10^{-7}	HTSP sink in probe and block
	157.44	$1.36 \times 10^{-7} \pm 1.5 \times 10^{-8}$	Mean Value

Table 6.27, summary of the short-time results, cobwool blocks

As for the cobblock short time results, the increase in H with the addition of heatsink material in the sample hole is evident in the summary of cobwool results, see table 6.27. The size of the probe conductance is less than the comparable figures of the cobblocks. The figures for the thermal diffusivity, α , for cobwool blocks using heatsink material both in the probe and in the sample hole are uniform and give a mean short time thermal diffusivity value of $1.36 \times 10^{-7} \text{ m}^2\text{s}^{-1}$. The figures for the cobwool block α when the probe is placed in the sample hole without heatsink material are more variable. A series of rate analysis were then carried out using data from a cobwool block using the twin thermocouple probe previously used to measure the samples of paraffin wax, mudstud and wychert.

A summary of these results is shown in table 6.28.

Run Number	Probe Conductance, H Wm ⁻² K ⁻¹	mc JK ⁻¹	Probe Condition, (sink material = HTSP heat sink compound).
1	703.2	1.998	HTSP sink in probe and block
2	686.9	2.554	HTSP sink in probe and block
3	721.3	2.094	HTSP sink in probe and block
		2.212 ± 0.29	Mean Value
4	133.8	0.961	HTSP sink in probe not in block
5	308.2	0.962	HTSP sink in probe not in block
6	326.5	0.985	HTSP sink in probe not in block
		0.969 ± 0.013	Mean Value

Table 6.28, summary of the rate analysis studies, cobwool blocks.

The probe conductance figures, H, are in a comparable way to the previous rate studies results, larger than those resulting from the short time analysis. In addition, in a similar way, the trend of H values increase in magnitude when the heatsink compound is used in the sample hole and the probe. The probe thermal capacity, mc figures also show a similar rise in magnitude when heatsink material is used around the probe.

Conclusion

The results from these laboratory-based studies are very encouraging. The four initial materials studied, paraffin wax, glycerine, phenolic foam and lightweight concrete block confirmed that four pieces of information, the thermal conductivity, diffusivity, probe thermal conductance and in some cases, the mc of the probe can be determined. The use of the technique upon unbaked earth building materials has proved to be successful, allowing the measurement of the main thermal properties described in the aims of this study. The analysis technique that has yet to give realistic thermal values is the rate method. The trends suggested by the other studies are mirrored in the results of the rate analysis, but the actual magnitudes of H given by the rate analysis are consistently higher. The table below gives a summary of the thermal values determined using the present techniques. The values shown are mean figures and using the HTSP heat sink material gave more plausible results for the first four sample materials.

Material	Measured Values		Published Values	
	Mean Thermal Conductivity $Wm^{-1}K^{-1}$	Mean Thermal Diffusivity m^2s^{-1}	Mean Thermal Conductivity $Wm^{-1}K^{-1}$	Mean Thermal Diffusivity m^2s^{-1}
Paraffin Wax	0.261 ± 0.034	$1.07 \times 10^{-7} \pm 2.9 \times 10^{-8}$	0.251	9.62×10^{-8}
Glycerine	0.293 ± 0.009	$2.26 \times 10^{-6} \pm 1.3 \times 10^{-7}$	0.292-0.314	$0.967 \times 10^{-7} - 1.1 \times 10^{-7}$
Phenolic Foam	0.029 ± 0.003	$1.69 \times 10^{-8} \pm 5.4 \times 10^{-9}$	0.032	1.00×10^{-7}
Lightweight Concrete	0.126 ± 0.01	$2.44 \times 10^{-8} \pm 5.0 \times 10^{-9}$	0.12	2.0×10^{-7}
Mudstud	0.558 ± 0.055	$5.26 \times 10^{-7} \pm 1.08 \times 10^{-7}$	There are no published values for these materials.	
Wychert	0.715 ± 0.048	$5.89 \times 10^{-7} \pm 1.17 \times 10^{-7}$		
Cobblock	0.368 ± 0.04	$4.65 \times 10^{-7} \pm 4.1 \times 10^{-7}$		
Cobwool	0.365 ± 0.018	$1.36 \times 10^{-7} \pm 1.5 \times 10^{-8}$		

Table 6.29, summary of mean thermal conductivity and diffusivity values from published values and the laboratory work.

The thermal conductivities of the first four materials, paraffin wax, glycerine, phenolic foam and lightweight aerated concrete, concur with published values to a reasonable extent. The mean value for the thermal conductivity of paraffin wax is 3.9% larger than the published value (Batty, 1984). Phenolic foam's measured thermal conductivity is 9.6% smaller than the figure from British Petroleum, whilst glycerine's is between 0.6% and 7.5% smaller than published data (Glatzmaier and Ramirez, 1985); (Maqsood et al, 1994). The lightweight concrete studies gave a thermal conductivity as 4.8% larger than the manufacturers' figures, (Durox blocks). The thermal diffusivities measured for each material do not follow such a close agreement as the thermal conductivity values. However, the level of agreement is felt to be considerably closer than for the original thermal diffusivity measurements. With this degree of agreement and the consistency of the results in table 6.29, it is felt that the measured thermal values for the unbaked earth walling materials, mudstud, wychert and cobblocks, are representative and *in-situ* measurements may now begin with confidence. The next chapter, chapter 7, displays the results of the field studies carried out using the field apparatus described in chapter 4.

Chapter 7

Field Testing

Some authors have advocated the use of transient hot wire probes for the testing of various materials in 'field' conditions. (Hooper and Lepper, 1950; Blackwell, 1954; Batty et al, 1984). One recent research programme has been identified that has suggested the probe technique could have a field use, (Banaszkiewicz, M. et al.1997). This involves the unique conditions encountered when measuring the thermal properties of materials of other planets or natural satellites.

To determine the thermal properties of cob buildings in Devon, *in-situ* measurements of cob walling are essential. Cob walls vary in their construction depending upon their location, social standing, use and the cob mason that constructed the walls. The variation takes the form of different straw contents, degrees of compaction and therefore, differences in density. Other differences occur due to diverse soil types that may be prevalent in the area surrounding the wall or building, giving rise to geographical differences in cob walling. The surfaces of some cob walling were left bare and un-rendered requiring the use of smaller aggregate in the mix for aesthetic purposes. Buildings and stand-alone walling that were to be rendered, or that were of sufficiently low status, such as agricultural buildings, could employ a cob mix with larger sizes of aggregate. All of these factors will influence the thermal properties of the cob walling produced.

To establish a range of thermal properties of unbaked earth walling a series of studies were undertaken upon buildings and structures in a number of locations. To facilitate this experimental programme a modified version of the laboratory apparatus was prepared and installed within a weatherproof cabinet (see fig 7.1). The modifications included twin 12V DC power supplies that allow the data logger and probe heater to operate

independently of any external power supplies. The logger, heater control system and 12V DC power supplies were housed in a weatherproof case incorporating weather resistant connectors to the probes and other external thermocouples. This gave the opportunity to take measurements at a wide range of external and internal locations and use a number of different buildings and free-standing walls for the field tests.



Figure 7.1, Field equipment in cob barn, Rezare.

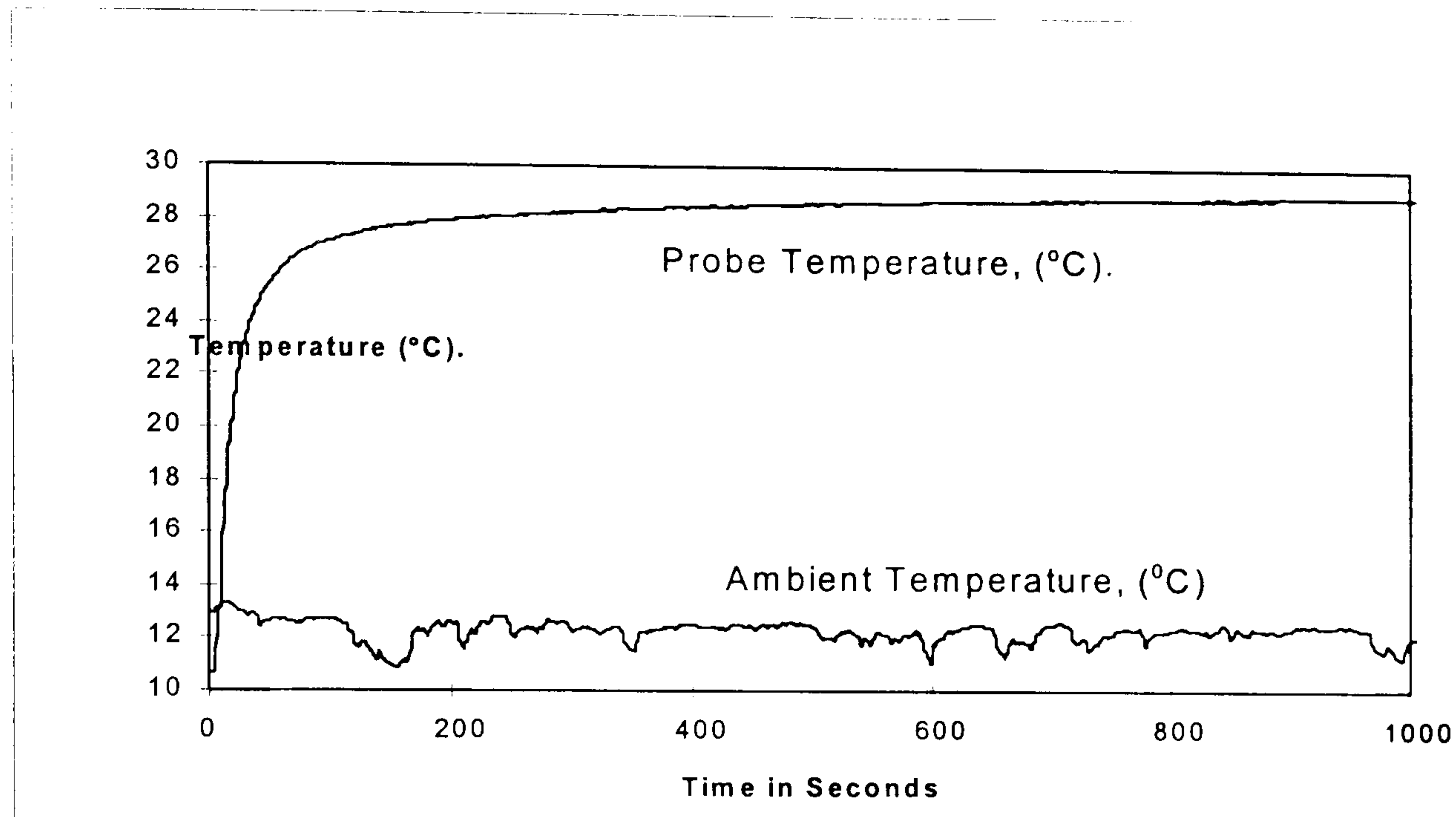
To verify the performance of the field testing apparatus, a number of laboratory based trials were carried out within the Building Science Laboratory situated within the University's Smeaton Building (see chapter 4).

Once the initial measurements had been successfully carried out and sufficient correlation had been found between the laboratory equipment and the field equipment, the field studies began. The field equipment was moved to a number of buildings and structures whose walls were made in part or wholly of unbaked earth.

During the fieldwork, measurements were made of the ambient temperature to give a comparison against the measured probe temperatures, using thermocouples and mercury

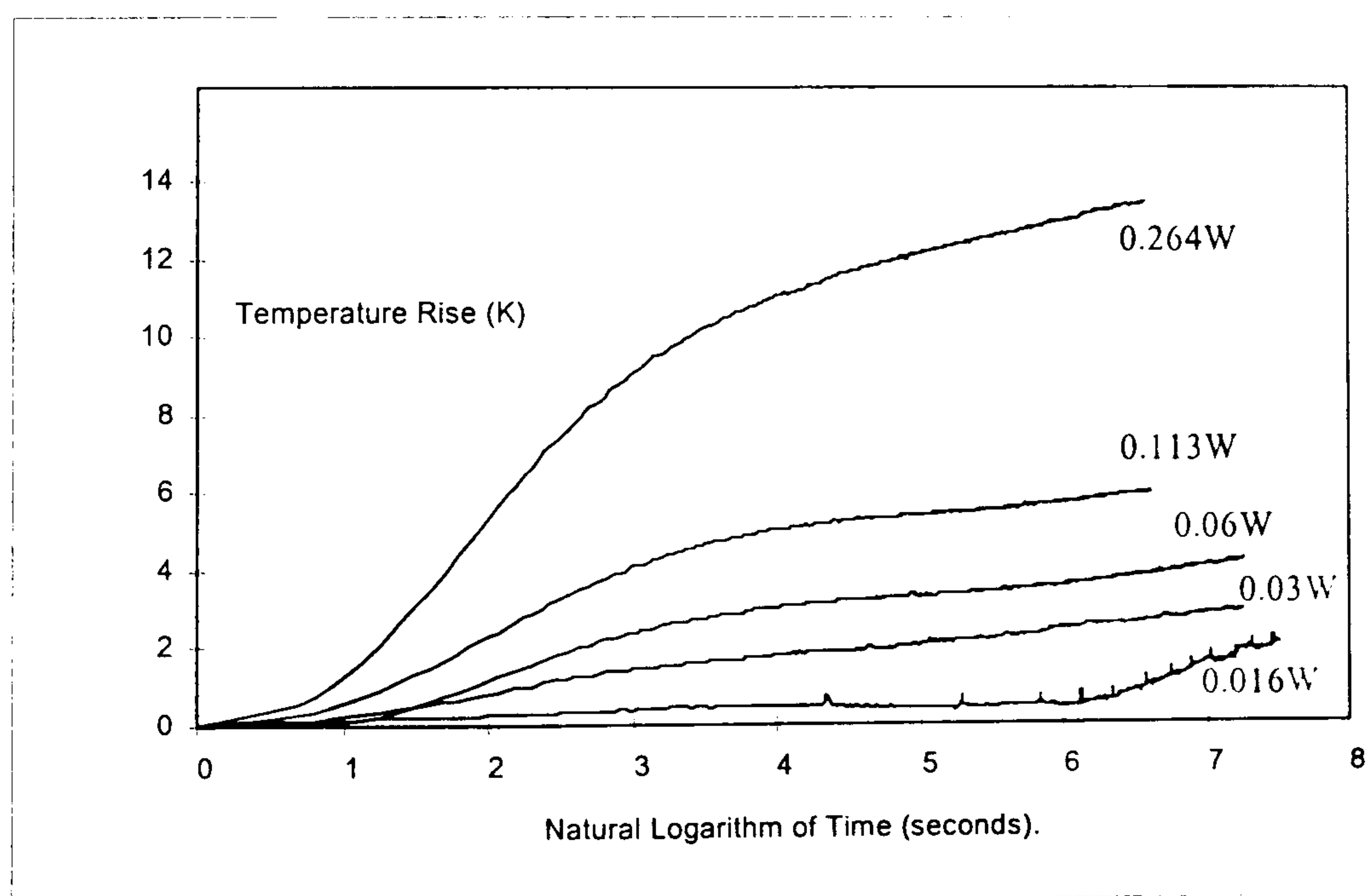
in glass thermometers.

Graph 7.1, shows the probe temperature variation together with the ambient temperature variation during a typical field experiment. As can be seen the temperatures recorded by the probe are unaffected by any external temperature variations.



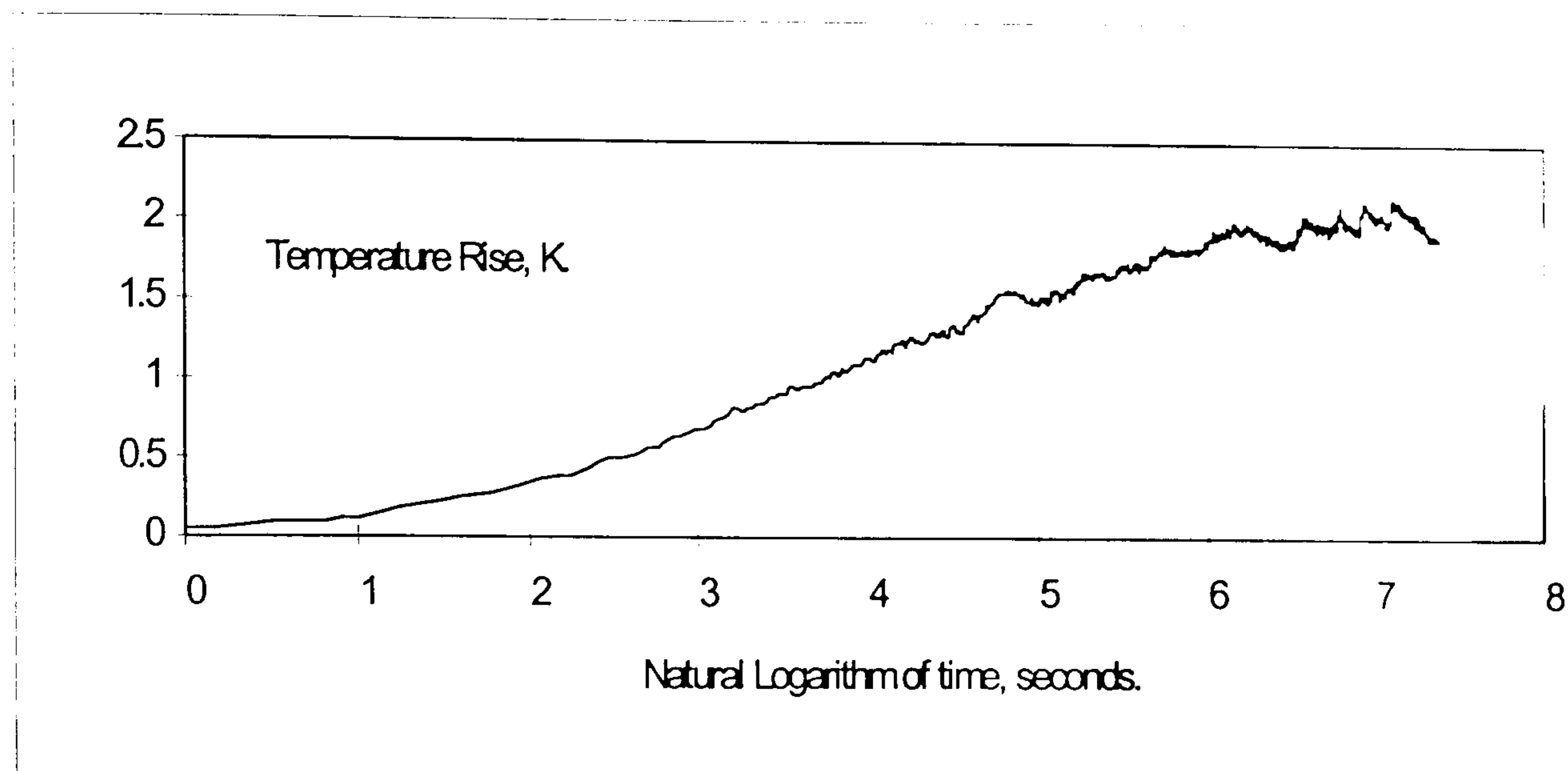
Graph 7.1, shows the ambient and probe temperature variations during a typical field test.

Ranges of different power settings were also tried to test the influence of probe heater power upon the long-time temperature rises. It is true that with small rises in probe temperature, of between 1 – 1.5°C, fluctuations in ambient temperature have an influence upon the results.



Graph 7.2, shows a range of long-time analysis curves obtained using different stabilised heater power settings.

A series of variations, particularly the natural logarithm of time of beyond 4, in line 5, can be seen. This effect is more apparent if the scale for the probe temperature rise is increased. The effects can now be seen more easily. (Graph 7.3).



Graph 7.3, shows the rise in probe temperature fluctuating at low probe heater power settings.

This information established the minimum power setting for the probe heater for the use in *in-situ* tests. It was decided that a power of 0.3W (total power supplied to the probe heater) was sufficiently high to produce measurements that were relatively unaffected by external influence. This power usually produced a rise in temperature of about 10 to 12K. The use of even higher heater power was felt to increase the probability of moisture migration from the probe site.

The next sections of this chapter describe the sample buildings and the measurements on three cob walled structures that were made available for study. Each building presents an opportunity to study a different form of walling, with different aspects of construction and cob characteristics. They range from a barn constructed from 'lower quality' cob to a more substantial structure located in a geologically different area. A modern cob-block structure was also tested.

Field Study One Cob barn Rezare near Launceston, grid reference SX359793

The study was carried out upon the walls of 150-year-old cob barn situated north of Rezare and south of Launceston. The barn was structurally sound, had a replacement profiled metal roof and was in need of some minor repairs to the internal part-flooring. Although, as can be seen in Figure 7.2, the cob walls were overgrown with ivy, the structure and moisture content of the interior of the cob appeared to be unaffected.



Figure 7.2, Cob barn, Rezare.

The area of the barn wall to be studied was situated on the upper storey, with measurements made at a point on the internal face of the north wall. The barn measures approximately 10m long by 5m wide and has cob walls of height varying between 2.0m and 2.4m built on a stone plinth. The stone plinth varies in height depending upon the slope of the ground. Because of the barn's close proximity to a fast flowing stream, the lower parts of the structure are sometimes flooded in the winter months and all readings were taken at sufficient height above this level to reduce any effects upon the conductivity measurements.

A hole of the same dimensions as the probe was drilled into the wall and the probe inserted, taking care not to jeopardise the thermal contact between the probe wall and the sides of the drilled hole. The external end of the probe, where the current and potential

leads to the heater, and thermocouple emerged, was covered with some expanded polystyrene foam insulation to reduce the influence of any changes in ambient thermal factors upon the readings taken by the probe.

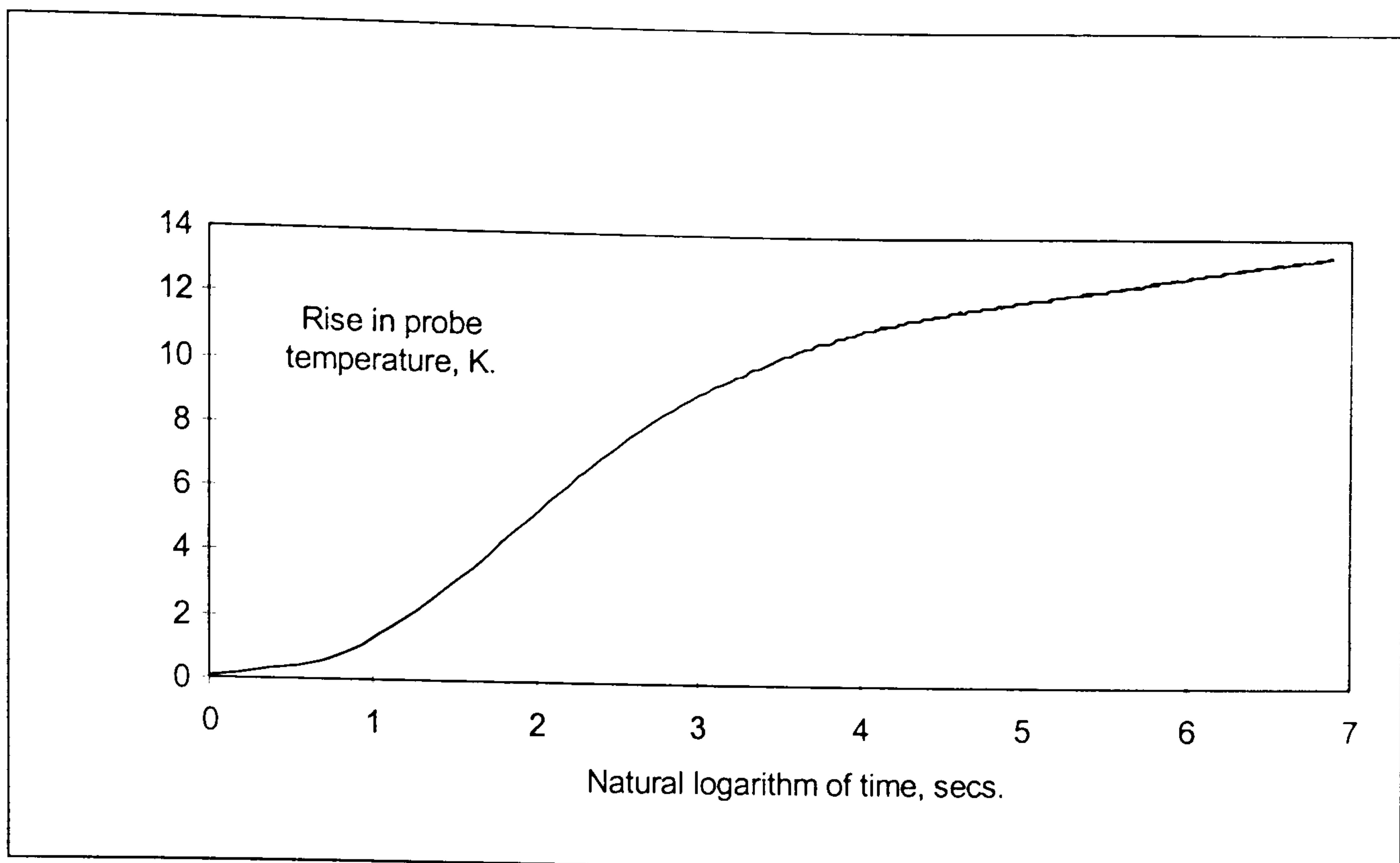
The cob walls were approximately 500mm thick and so any thermal effects on the probe from the exterior were reduced by the large amount of cob material between the probe and the outside environment. A number of runs were carried out in the manner previously described in this chapter and in chapter 4. The measurements were taken with 24 hours between each run. Each data collection run was given a runcode, in this case using the prefix 'Mike', (the owner of the barn). Several of the measurements associated with two of the runcodes were in error due to a malfunction of the field apparatus. This is the reason for the exclusion of runcodes Mike2 and Mike4 in the following tables and graphs.

This series of measurements were intended to gain a feel for data collection on real walls. The probe used was not filled with heat sink material as this programme of work was undertaken before the technique had been perfected. Because of this the analysis of these results is restricted. However, the measurements form the basis of some interesting approximate thermal values achieved using the iterative solution, Solver2 in Excel.

run code 'Mike'. Cob Barn	Power (Watts)	Temperature Rise (°C)	Time for test (seconds)
Mike 1	0.266	12.2	1450
Mike 3	0.265	13.45	981
Mike 5	0.265	12.62	783
Mike 6	0.263	13.47	719

Table 7.1, summary of the Rezare studies.

A plot of the rise in probe temperature versus the natural logarithm of elapsed time is shown in graph 7.4.



Graph 7.4, shows a typical long time behaviour, field study, Rezare.

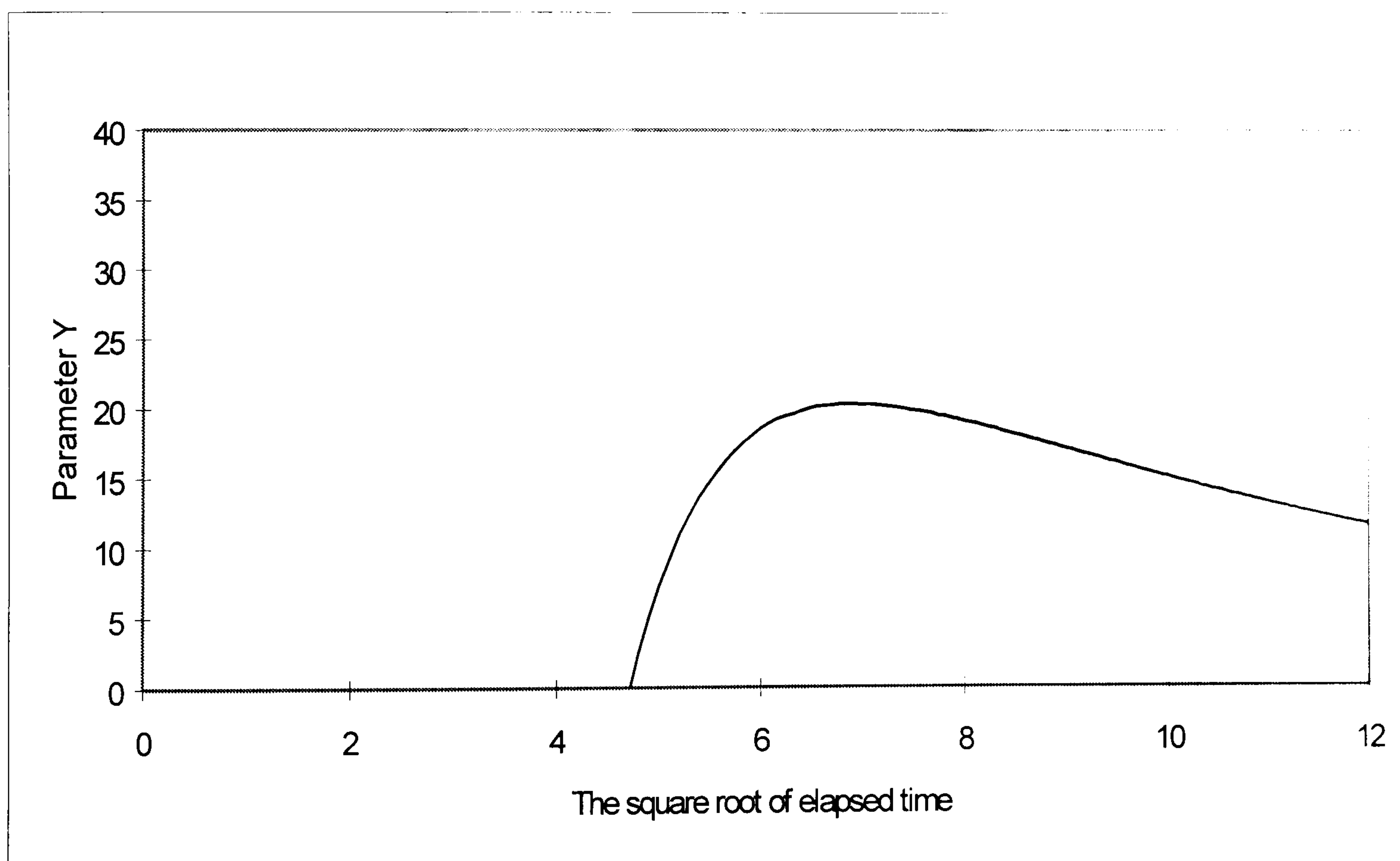
As can be seen in graph 7.4, the long time curve follows a similar shape to that discussed in chapter 5 and observed in Chapter 6. The curve shows a shallow 's' shape flattening to a straight line over a time period of 100 to 1000 seconds, or natural logarithm of time 4.5 to 7. A regression analysis was undertaken over this time range to determine the slope and intercept of the straighter section of the curve.

Taking into account the variation in power supplied to the probe heater and in the slope of the line in graph 7.4, the following thermal conductivities for the cob wall in Rezare were calculated using the long time analysis described earlier. The mean value of the measured thermal conductivity of the cob wall at Rezare shown in graph 7.4, is $0.417 \text{ Wm}^{-1}\text{K}^{-1}$, the maximum value $0.421 \text{ Wm}^{-1}\text{K}^{-1}$ and the minimum value $0.412 \text{ Wm}^{-1}\text{K}^{-1}$. This gives a probable variation of the mean value $\pm 2\%$, which is encouraging given the constraints associated with these field studies. However, the overall mean thermal conductivity for the Rezare cob was $0.6 \text{ Wm}^{-1}\text{K}^{-1}$ with a spread of $\pm 60\%$. This may be in part due to variations in cob moisture content and because the field apparatus was being used for the first time outside of the laboratory.

run code	power, Watts	Mean Thermal Conductivity $\text{Wm}^{-1}\text{K}^{-1}$	Thermal Diffusivity, m^2s^{-1}
Mike 1	0.2657	0.98	6.29×10^{-6}
Mike 3	0.2645	0.42	4.78×10^{-10}
Mike 5	0.2649	0.63	2.57×10^{-10}
Mike 6	0.2633	0.36	1.46×10^{-9}
	Mean	0.47 ± 0.14	(omitting Mike 1)

Table 7.2, summary of the long time analysis results Rezare field study.

Short time analysis using equation 6 was undertaken following the procedure described in chapter 5. This analysis focuses upon the data from the early part of the run, and concentrates upon the first 150 seconds of the elapsed time. The graph 7.5 shows that Blackwell parameter Y plotted against the square root of elapsed time. A linear section is clearly seen between about 50 and 100 seconds, ($t^{0.5} = 7$ to $t^{0.5} = 10$)



Graph 7.5, shows a short time analysis, Rezare.

The intercept on the Y axis gives a value of the thermal probe conductance, H. The value obtained is from graph 7.5 is $35.5 \text{ Wm}^{-1}\text{K}^{-1}$. Using this value of H and the slope of the line in graph 7.5, the thermal diffusivity was calculated. Table 7.4 shows the summary of

thermal values.

run code	Probe Thermal Conductance, H, $\text{Wm}^{-2}\text{K}^{-1}$	Thermal Diffusivity m^2s^{-1}
Mike1	40.24	6.07×10^{-6}
Mike3	35.35	1.92×10^{-6}
Mike 5	35.57	2.82×10^{-6}
Mike6	35.60	9.20×10^{-7}
Mean	36.70 ± 2.4	$2.93 \times 10^{-6} \pm 2.0 \times 10^{-6}$

Table 7.3, Summary of the short-time analysis results, Rezare.

The mean value of the probe conductance was $36.7 \text{ Wm}^{-1}\text{K}^{-1}$, while the mean thermal diffusivity for Rezare cob was $2.9 \times 10^{-6} \text{ m}^2\text{s}^{-1}$. As previously stated the probe and the sample holes used for the Rezare measurements did not contain any heat sink compound. This has been reflected in the low thermal probe conductances, H. As the reader will recall, the highest short time analysis values for the probe conductance were achieved during the measurements on glycerine in the laboratory and these gave an H of about $300 \text{ Wm}^{-2}\text{K}^{-1}$, (see chapter 6). Values of approximately $35 \text{ Wm}^{-2}\text{K}^{-1}$ compare well with probe conductance values of about $30 \text{ Wm}^{-2}\text{K}^{-1}$ measured in cobblocks in the laboratory, (see chapter 6).

The thermal diffusivity values shown in table 7.3 do vary a great deal. If an average of these values is taken, the resulting figure, $2.93 \times 10^{-6} \text{ m}^2\text{s}^{-1}$ is high compared to laboratory measurements undertaken on other unbaked earth materials. However, these values do come from a probe without any heatsink compound either in the probe itself, or in the sample hole. The thermal contact between the probe and the cob would be poor.

To explore these field measurements further, the iterative Solver2 routine was used to determine values for the thermal conductivity, the thermal diffusivity and the thermal conductance between the probe and the specimen wall. The range of values of λ , α and H to be tried are shown in table 7.4. The theoretical rise in temperature was predicted using the two constants A and B in the equation, and the Solver2 routine generated the solution shown in the table 7.5.

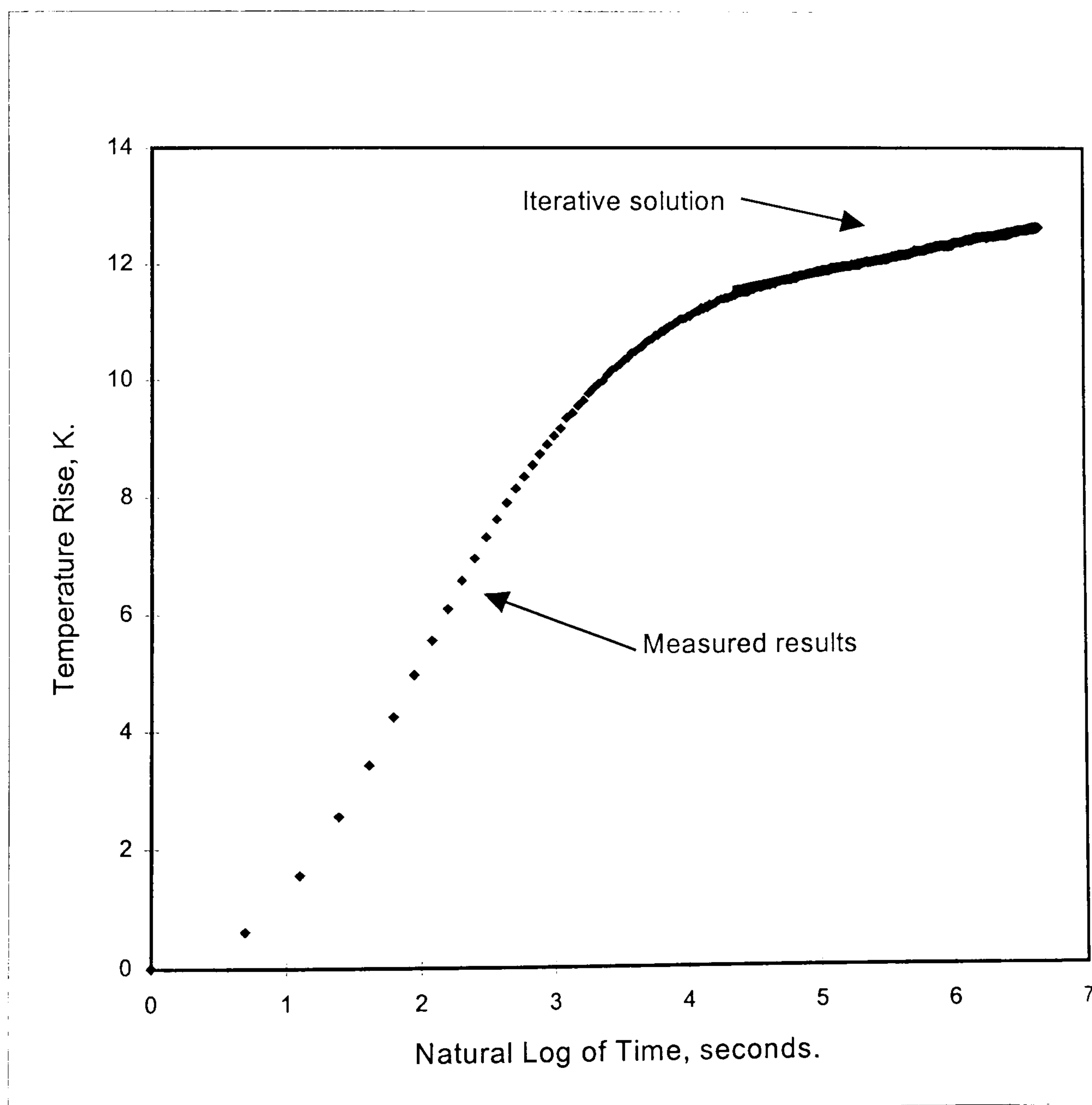
Thermal Conductivity, $\text{Wm}^{-1}\text{K}^{-1}$	Thermal Diffusivity m^2s^{-1}	Probe Thermal Conductance $\text{W m}^{-2}\text{K}^{-1}$
0.64	0.2×10^{-7}	34

Table 7.4, shows the input values of the three parameters for Solver2 routine.

Thermal Conductivity, $\text{Wm}^{-1}\text{K}^{-1}$	Thermal Diffusivity m^2s^{-1}	Probe Thermal Conductance, H, $\text{W m}^{-2}\text{K}^{-1}$
0.65	1.00×10^{-8}	41.8

Table 7.5 shows typical Solver2 results for Rezare cob.

The above values compare well with measured values obtained in the laboratory, For example the value of H , $42 \text{ W m}^{-2}\text{K}^{-1}$ matches up to approximately $32 \text{ W m}^{-2}\text{K}^{-1}$ for the measurements taken in the laboratory using cob blocks.



Graph 7.6, shows Solver2 results, Rezare field study.

run code	Thermal Conductivity $\text{Wm}^{-1}\text{K}^{-1}$	Thermal Diffusivity, m^2s^{-1}	Probe Thermal Conductance, H $\text{W m}^{-2}\text{K}^{-1}$
Mike 1	0.43	8.50×10^{-7}	69.4
Mike 3	0.40	1.02×10^{-7}	62.5
Mike 5	0.65	1.00×10^{-8}	41.8
Mike 6	0.36	1.05×10^{-8}	41.7

Table 7.6, summary of the values generated by the Solver2 iterative routine for Rezare cob.

The values obtained from Solver2, shown in table 7.6, match well with the values obtained by the long time measurements shown in table 7.2. The measured thermal conductivity for Mike 5 and 6 from table 7.2 are 0.63 and 0.36 $\text{Wm}^{-1}\text{K}^{-1}$ respectively. The Solver results for Mike 5 and 6 are 0.65 and 0.36 $\text{Wm}^{-1}\text{K}^{-1}$ respectively, which are very close indeed. The results for Mike 1 and 3 are less encouraging and do show less agreement. As expected, the thermal diffusivity results are not well matched, but still give a better correlation than the early results of the first laboratory measurements presented in chapters 5 and 6. The Solver analysis method, therefore, appears to be providing a good check against the long time analysis results, much as was experienced with the laboratory experiments. The Solver routine also has the advantage of being less time consuming than following separate calculations.

Field Study Two Cob block summerhouse, Bovey Tracey, grid reference SX816784.

This study was undertaken on cob blocks making up the structural walls of a partially completed summerhouse. The summerhouse is single storey and has dimensions of 2.5m long, 1.5m wide and approximately 2.0m high. The unbaked earth section of the wall varies from 1.2m to 1.4m high, founded upon a stone and concrete plinth approximately 0.8m in height. At the time of data collection the roof structure had not been completed and the walls were protected with temporary boarding to prevent rain damage. The walls were built from cob blocks using soil rich in clay from the Tedburn St Mary area close to Exeter. The majority of the blocks used wheat straw as their fibre content. A range of

similar blocks was studied under laboratory conditions, (see chapter 6).

A similar procedure to that undertaken for field study 1 at Rezare was adopted for Bovey cob, the probe was shielded with insulation and a 24-hour period was allowed between runs. The initial power values were based upon those used for the original laboratory based work, described in chapters 4 and 6, and the variations in heater power investigated, as mentioned earlier in this chapter. The first measurements that were undertaken were inconclusive.

When a second series of experimental runs were carried out on the Bovey cob summerhouse, the use of heat sink compound had been developed in the laboratory. This enabled a combination of field measurements to be carried out using a heatsink compound in different combinations of filled and unfilled probe and hole. Here it was intended to vary the thermal contact between the probe and the specimen and it was hoped that these different experimental conditions would give an insight into the effect of changing the probe thermal conductance, H. The runcodes for these tests were sup1 and sup2.

run code Summerhouse	power, Watts	Temperature Rise, K.	Duration, seconds	Probe Condition (Heat sink compound = HTSP heat sink material)
sup21012	0.366	14.71	1246.00	no heatsink compound in probe or hole
sup21212	0.367	12.38	1317.00	no heatsink compound in probe, sink in hole
sup11012	0.362	11.92	1265.00	heatsink compound in probe, no sink in hole
sup11212	0.362	7.78	1304.00	heatsink compound in probe and hole

Table 7.7, summary of the Summerhouse measurement series.

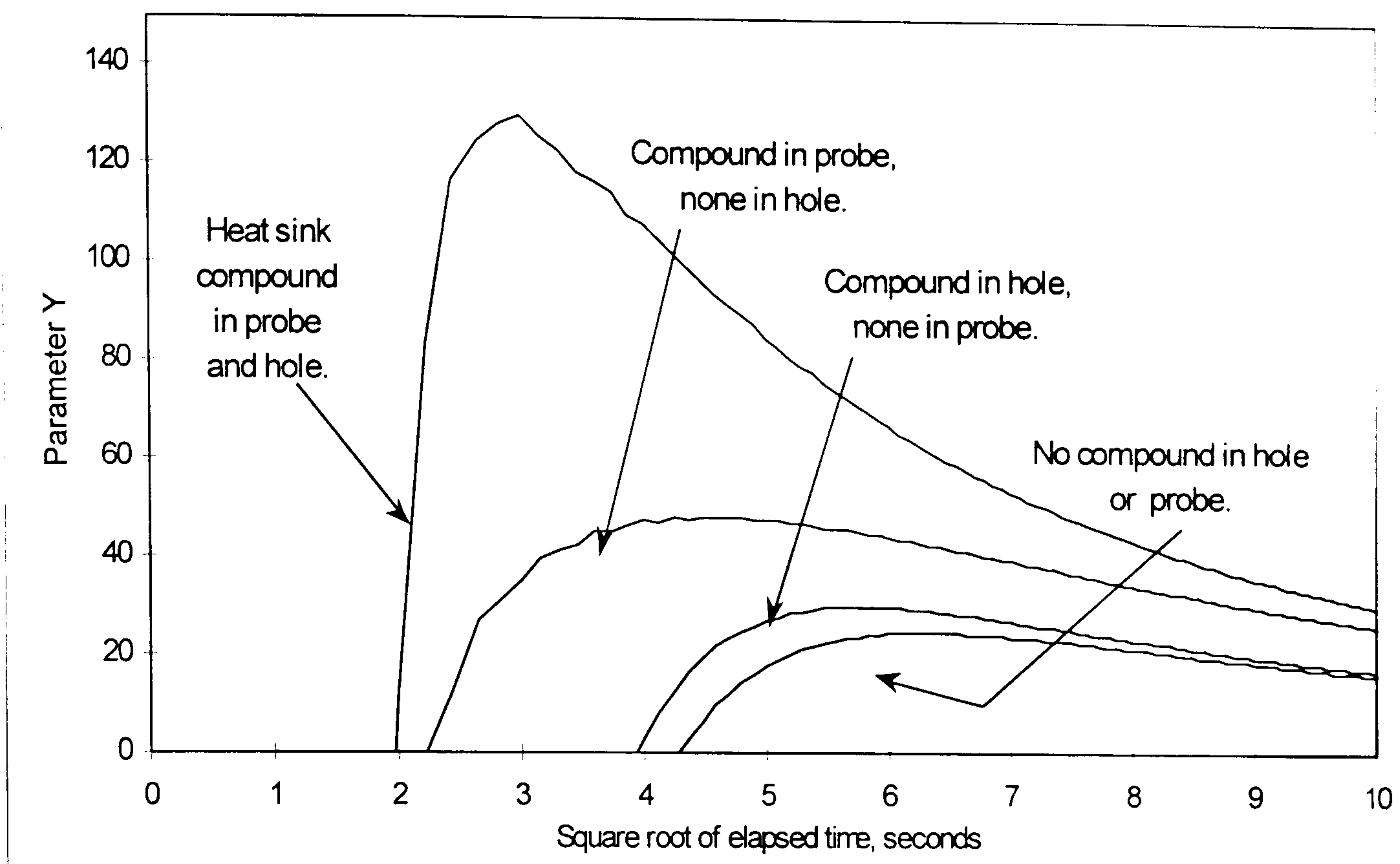
Table 7.7 gives details of the probe heater powers and associated temperature rises. This table also gives the duration of elapsed times and more importantly, the locations of the heat sink compound used in the field studies on Bovey cob.

run code	power, Watts	Thermal Conductivity $\text{Wm}^{-1}\text{K}^{-1}$	Probe Condition, (where sink = HTSP heat sink material).
sup21012	0.366	0.89	no sink in either
sup21212	0.368	0.86	no sink in probe sink in hole
sup11012	0.362	0.37	sink in probe no sink in hole
sup11212	0.362	0.38	sink in probe sink in hole
	Mean	0.38 ± 0.007	(of sink in probe values)

Table 7.8, shows a summary of the long time results for the Bovey studies.

A comparison may be made between the cob blocks that were studied in the laboratory and those that were placed in the structure of the Bovey summerhouse. These blocks were all manufactured at the same time and blocks were randomly selected to be studied in the laboratory, the remaining blocks were used in the Bovey summerhouse walls. As can be seen in table 7.8, the use of heat sink compound has reduced the measured *in-situ* thermal conductivity values. This is the reverse of the observed trend in measured thermal conductivity values in the laboratory. However, when heat sink compound is used in both the probe and the sample hole, the mean thermal conductivities are very similar, $0.36 \text{ Wm}^{-1}\text{K}^{-1}$ in the laboratory and $0.38 \text{ Wm}^{-1}\text{K}^{-1}$ *in-situ*. It could be debated that the heat sink compound may be unduly influencing these results and possibly accounting for the very similar values. But, as discussed in chapter 5, the long time results should address the sample material a reasonable distance from the probe site and thus away from any influence of the heat sink material.

The short time analysis was carried out on these Bovey cob measurements in the same way as before. Some of the holes that were drilled to receive the probe also had heat sink material placed in them to improve the thermal contact between the probe and wall. As can be seen in the following graph, graph 7.7, this variation in the experimental conditions had an effect upon the shape of the short time curves illustrated.



Graph 7.7, Short time analysis, showing the effects of introducing heat-sink material within the probes and test holes for Bovey cob.

The short time analysis gave results for the Bovey cob for probe thermal conductance, H , and thermal diffusivity. Table 7.9 shows the increase in probe/material conductance, H , due to the addition of heat sink material and the corresponding reduction in thermal diffusivity.

run code	Probe Thermal Conductance, $W m^{-2}K^{-1}$	Thermal Diffusivity, m^2s^{-1}	Probe Condition, (where sink = HTSP heat sink material).
sup21012	40.13	4.61×10^{-6}	no sink in either
sup21212	50.93	3.67×10^{-6}	no sink in probe sink in hole
sup11012	72.99	3.18×10^{-7}	sink in probe no sink in hole
sup11212	198.04	1.30×10^{-7}	sink in probe sink in hole
	Mean	$2.24 \times 10^{-7} \pm 1.32 \times 10^{-7}$	(of sink in probe values)

Table 7.9, shows the short time results for Bovey cob.

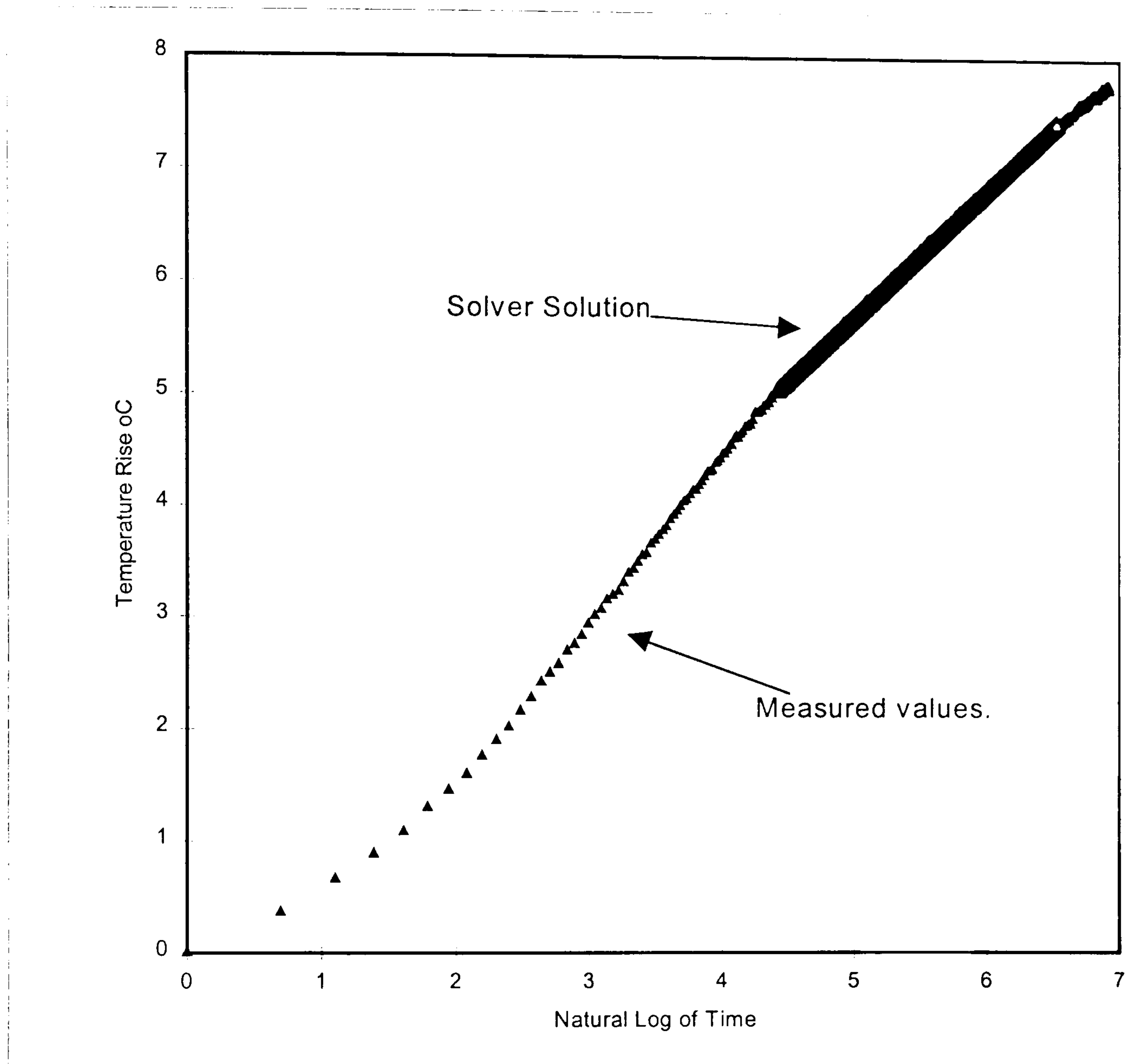
The short time curves illustrated in graph 7.7 show the same general behaviour as those produced from the analysis of the laboratory based measurements made on similar earth materials, such as mudstud, (graph 6.14), wychert, (graph 6.16). The measured probe conductance gradually increases with the addition of heat sink material and this pattern is also found in the laboratory measurements, (see tables 6.16, 6.20, 6.27).

As for the long time results, a comparison may be made between the short time results for the cob blocks that were studied in the laboratory and those that were placed in the structure of the Bovey summerhouse. As previously stated these blocks are all very similar in material content and manufacture. The average probe thermal conductance, H , in the laboratory was $332.67 \text{ W m}^{-2}\text{K}^{-1}$, and in the field, $198 \text{ W m}^{-2}\text{K}^{-1}$, both measurements used heat sink material in the probe and the hole. The thermal diffusivity results from the laboratory studies, $6.95 \times 10^{-8} \text{ m}^2\text{s}^{-1}$ are generally lower than the value obtained from the field studies, $1.3 \times 10^{-7} \text{ m}^2\text{s}^{-1}$. The difference in the values of H , may partially account for the different thermal diffusivity values between two very similar earth materials. This difference may have been compounded because only one *in-situ* measurement was taken with heat sink material both in the probe and the hole. It is suggested that future work could concentrate upon the use of identical or similar samples studied in laboratory and field conditions to investigate the differences observed in this part of the thesis.

As a precursor to using the iterative process, the thermal values that had been previously found using the long and short time analysis were used to try to match a theoretical probe temperature versus time solution to the measured values. As two possible different 'straight' regions were identified within the short time analysis graph this meant that two possible values for the probe conductance, H were suggested. The two values for H encountered when analysing sup11212 were used in the solver analysis to ascertain which H value gave a better fit with the measured data. For example, for the laboratory studies on cob blocks, runcode 11212 short time analysis could give two values for the probe conductance, $198 \text{ W m}^{-2}\text{K}^{-1}$ for the steeper and earlier part of the short time curve and $54 \text{ W m}^{-2}\text{K}^{-1}$ for the later and longer part. To help distinguish between these two values of H , and indicate which value was correct, solver was used twice with these two values. Using the following values shown in table 7.10, the graph 7.8 was produced.

Thermal Conductivity, $\text{Wm}^{-1}\text{K}^{-1}$	Thermal Diffusivity m^2s^{-1}	Thermal Conductance $\text{W m}^{-2}\text{K}^{-1}$
0.38	0.8×10^{-7}	198

Table 7.10, shows the thermal values for Excel Solver2 demonstrated in Graph 7.8, H of 198.



Graph 7.8 shows the measured values matched against the Solver2 values with a probe conductance of $198 \text{ W m}^{-2}\text{K}^{-1}$, Bovey cob.

Graph 7.8 shows that the solver solution using an H value of $198 \text{ W m}^{-2}\text{K}^{-1}$ is in agreement with the measured data. This suggests that the earlier part of the short time analysis graph should be used to establish H, the probe conductance value. Earlier the better, bearing in mind Blackwell's comments on this approximate method. This early part of the curve can vary in length, but periods of less than 150 and preferably 100 seconds from the first measurement should be used. Once the appropriate order of magnitude of H had been

established using the short time analysis, then a range of values of the thermal conductivity, thermal diffusivity and probe conductance can be suggested for the parallel iterative solution. Turning now to the field studies of these cob blocks and to explore the Bovey cob data further, the iterative solution using Solver2 was used to propose values for the thermal conductivity, the thermal diffusivity and the thermal conductance between the probe and the test wall. The results of these Solver2 applications are shown in table 7.11.

run code	Thermal Conductivity, $\text{Wm}^{-1}\text{K}^{-1}$	Thermal Conductance $\text{W m}^{-2}\text{K}^{-1}$.	Thermal Diffusivity, m^2s^{-1}
sup21012	0.86	49.6	9.97×10^{-9}
sup21212	0.91	54.8	1.03×10^{-9}
sup11012	0.48	83.4	5.83×10^{-8}
sup11212	0.38	240.0	7.06×10^{-8}
Mean Values	0.65 ± 0.26	107 ± 89	$3.5 \times 10^{-8} \pm 3.5 \times 10^{-8}$

Table 7.11, summary of the Solver2 results for Bovey cob, series 2.

If the values of thermal conductivity, λ , diffusivity, α , and probe conductance, H , of Bovey cob obtained by using Solver2, are compared with the long time and short time analysis for probes with varying use of heat sink compound, the resulting tale is complex. It is easiest to indicate where the different methods of analysing the results show good and poor matches. To begin, the thermal conductivity, λ , obtained from the long time analysis and Solver2 show the same reduction in magnitude due to the introduction of heat sink compound. This can be seen by viewing tables 7.8 and 7.11. For example, runcode sup21012, $0.89 \text{ Wm}^{-1}\text{K}^{-1}$ (long time analysis), $0.86 \text{ Wm}^{-1}\text{K}^{-1}$ (Solver2), no heat sink compound in either probe or wall reduces to that measured in runcode sup11212, $0.38 \text{ Wm}^{-1}\text{K}^{-1}$ (long time analysis), $0.38 \text{ Wm}^{-1}\text{K}^{-1}$, (Solver2), heat sink compound both in probe and wall. In addition, the magnitudes of the thermal conductivity values are very similar. However, although the thermal diffusivity values obtained from the short time analysis show a difference between the using and not using heat sink compound, the short time diffusivity figures decrease whilst the Solver2 diffusivity figures increase.

The Bovey cob thermal conductances, H , values measured by the short time analysis are in the most part mimicked by those produced from Solver2. Low values for H where no heat sink material is used, $40 \text{ W m}^{-2}\text{K}^{-1}$ (Short time analysis), $50 \text{ W m}^{-2}\text{K}^{-1}$ (Solver2) and much higher values when heat sink material is used in both the probe and wall, $198 \text{ W m}^{-2}\text{K}^{-1}$ (short time analysis), $240 \text{ W m}^{-2}\text{K}^{-1}$, (Solver2).

Although the figures for H and λ are in reasonable agreement, the variation of the thermal diffusivity α values does cause some doubt about the results from either the short time analysis or the Solver2 results and this can be seen by viewing the standard deviations for λ , α and H . The values suggested by Solver are however, still considerably closer to likely or guessed values than the initial laboratory measurements as described in chapters 5 and 6.

Field Study Three Cob barn/stable, Frogmire, Sandford, near Crediton, Devon, grid reference SS825015.

The third study building is built from a different soil to that already studied and it forms part of a complex of buildings with a well documented history just north of Crediton in Mid-Devon. The buildings date from the late sixteenth century and have been dated from various architectural features by Maggie Ford, (Ford, Unpublished). The building has cob walls made from the local soil based upon red sandstone and has a lower clay content than the cob summer house blocks, or the cob in the barn near Launceston. The wall is an internal wall facing north with very little temperature variation due to solar gain. The wall is about 2.5m high, 550mm thick with the two test probes used placed 1 and 2m vertically up the face of the wall from the floor and insulated from the ambient air in the usual way. For the study at Frogmire the holes drilled in the wall initially didn't contain any heat sink compound. The later tests used heat sink compound in the sample holes to improve the thermal contact between the probe and the specimen. The second series of runs will allow

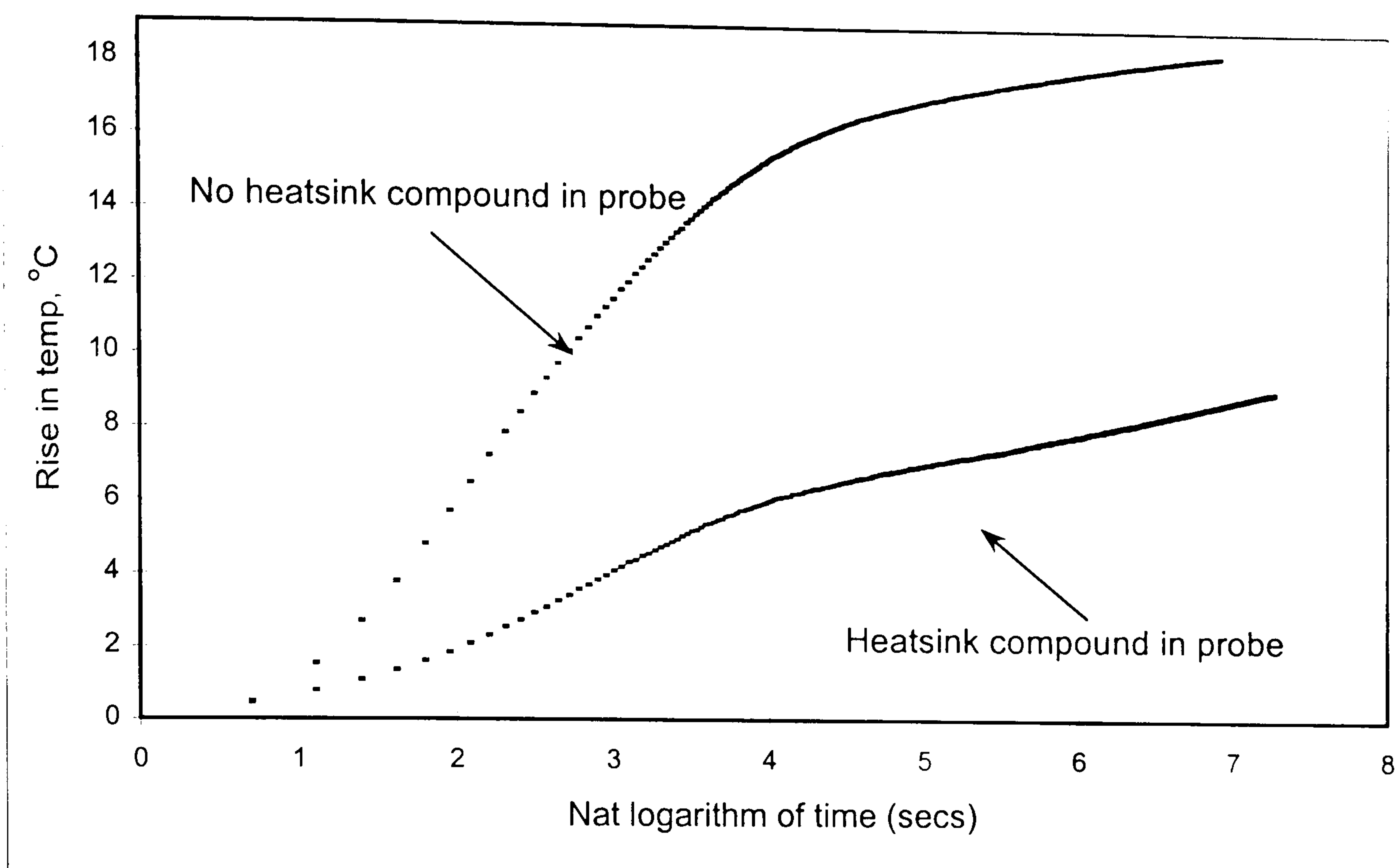
a comparison of the different results anticipated from different H values. Table 7.12, indicates the probe heater powers and distribution of heat sink material.

run code	power, Watts	Probe Condition, (Heat sink compound = HTSP heat sink material).
fgp2810	0.364	no heatsink compound in probe or hole
fgp2910	0.363	no heatsink compound in probe or hole
fgp2a810	0.365	no heatsink compound in probe or hole
fgp2a910	0.364	no heatsink compound in probe or hole
fgp1810	0.358	heatsink compound in probe, no sink in hole
fgp1910	0.357	heatsink compound in probe, no sink in hole
fgp1a810	0.357	heatsink compound in probe, no sink in hole
fgp1a910	0.353	heatsink compound in probe, no sink in hole
fgp22210	0.362	heatsink compound in hole but not in probe
fgp22310	0.363	heatsink compound in hole but not in probe
fgp2211	0.359	heatsink compound in hole but not in probe
fgp1211	0.355	heatsink compound in probe and hole
fgp12210	0.358	heatsink compound in probe and hole
fgp12310	0.359	heatsink compound in probe and hole

Table 7.12, summary of the heater power and probe conditions for the measurements undertaken at Frogmire.

Typical long-time behaviour of the measurements is shown in graphs 7.9 to 7.11 and table 7.13 presents the thermal conductivity values after the long time analysis.

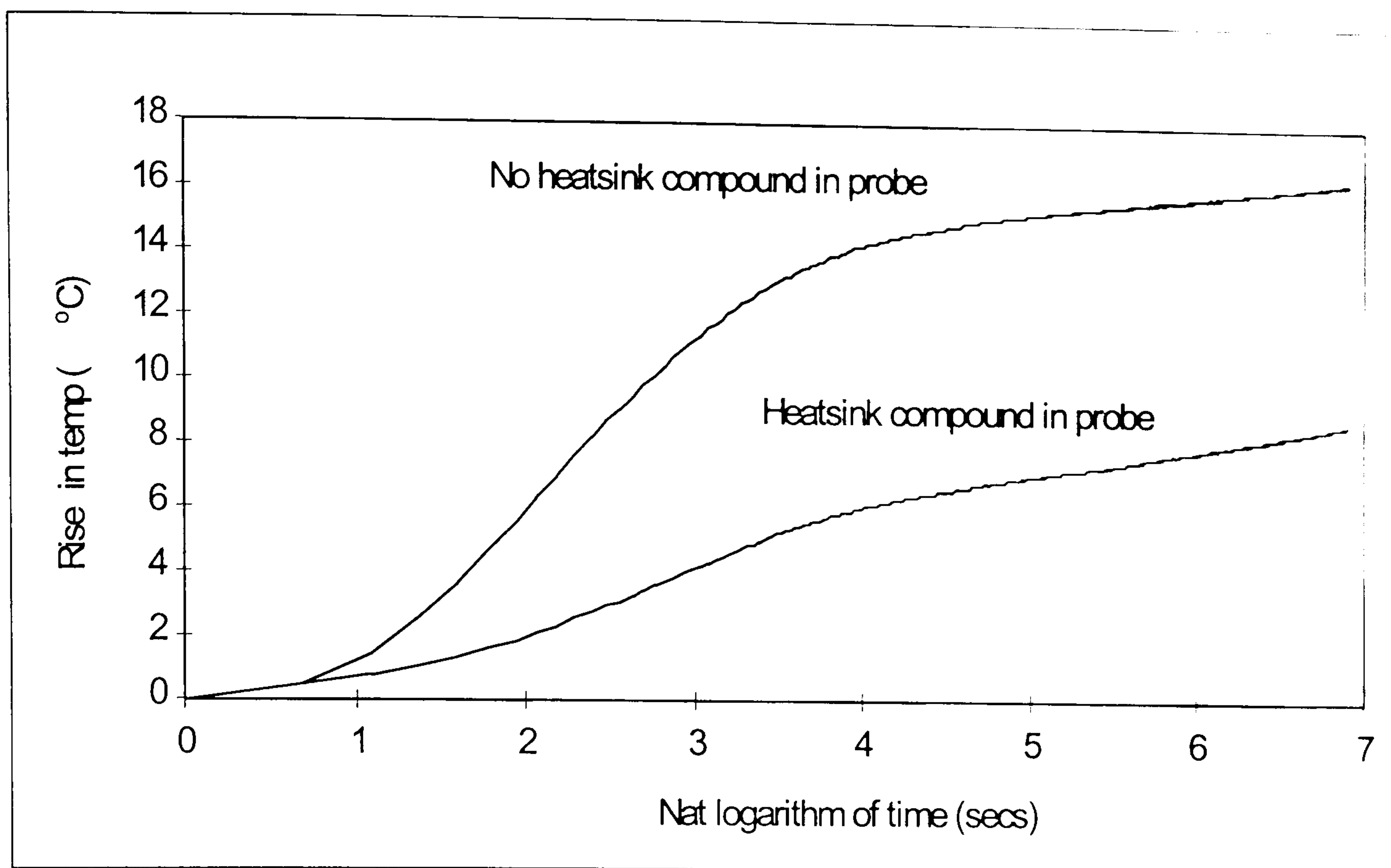
Initially two probes were inserted into drilled holes in the north facing internal wall. Neither of these holes were filled with heat sink compound. One of the two probes contained heat sink compound. The second probe, without heat sink material, showed a larger rise in temperature.



Graph 7.9, shows the long time curves for two probes each with different fillings.

Frogmire.

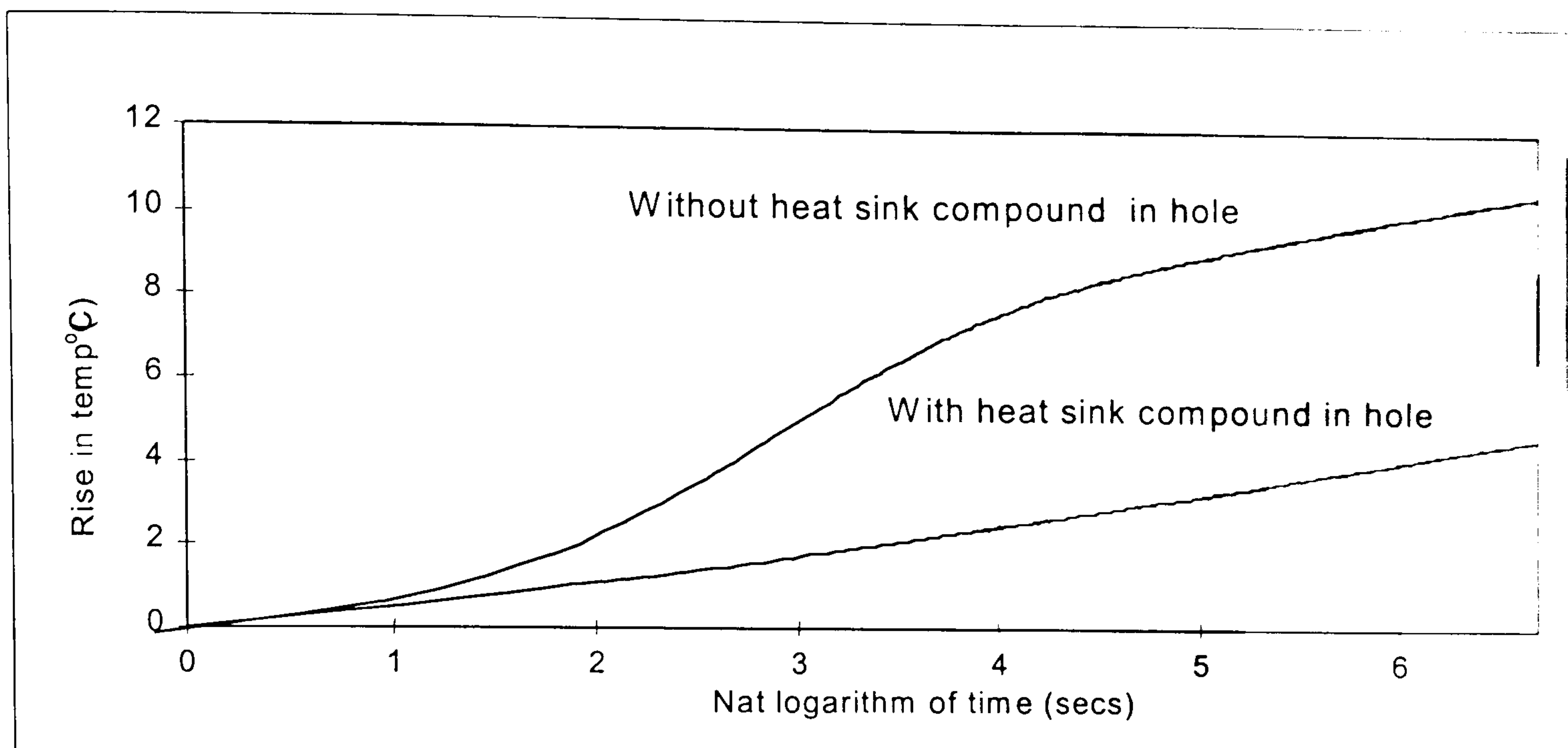
To investigate the effects of any variations in probe and in material surrounding the holes in the wall, the probes were interchanged. Further measurements were taken in an identical manner to the previous measurements. It was hoped that the curves that were produced would highlight any differences or similarities in the wall material around the holes and probe behaviour. Graph 7.10 shows the results of the interchanged probes between the original holes shown in graph 7.9 and clearly the two sets exhibit very similar behaviours.



Graph 7.10, shows the long time behaviour for air filled interchanged probes, Frogmire.

In graph 7.9 the curves are almost identical to those in graph 7.10. Thus the shapes of the curves are as a result of the differences in probe design and not influenced to a great extent by the different thermophysical properties that might be exhibited by any changes in the wall material. This bears out the findings of a similar experiment undertaken upon the laboratory measurements of the lightweight aerated concrete block described in chapter 6.

Once a pattern of temperature rise within the probes had been established, the holes were filled with HTSP heat sink compound in the same way as before. The graph 7.11 and the table 7.13 show the results of these modified runs. It can be seen that the overall temperature rise has been reduced for both the unfilled probe and filled probe when compared to the tests carried out on holes without sink material placed in probe.



Graph 7.11, shows a probe filled with heat sink compound, sample hole with and without heat sink compound, long time behaviour, Frogmire.

The range of values of thermal conductivity for the Frogmire study can be noted from the summary in table 7.13.

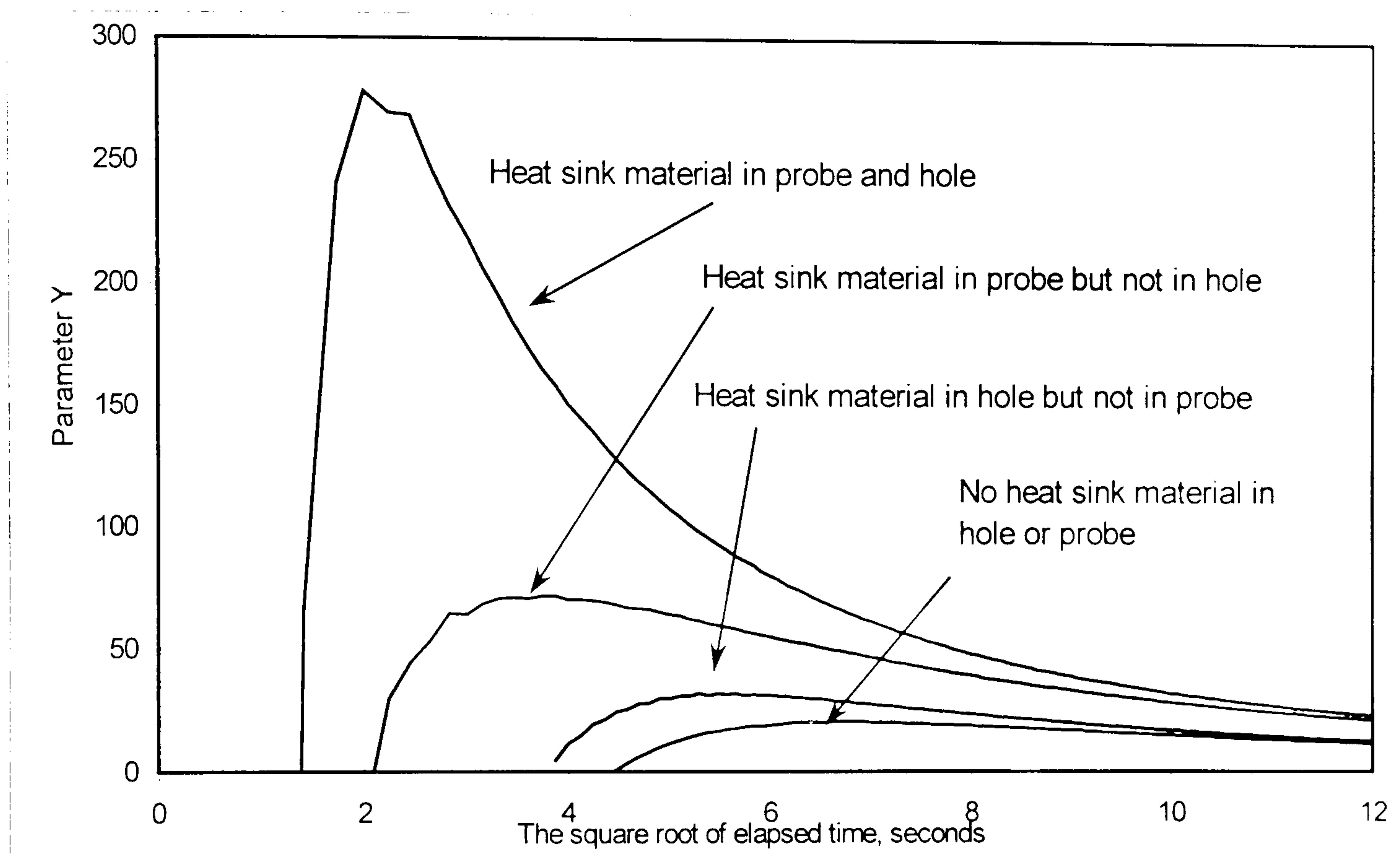
run code	power, Watts	Thermal Conductivity $Wm^{-1}K^{-1}$	Probe Condition, (sink material =HTSP heat sink compound).
fgp2810	0.364	0.64	no sink in either
fgp2910	0.363	0.64	no sink in either
fgp2a810	0.365	0.75	no sink in either
fgp2a910	0.364	0.69	no sink in either
fgp1810	0.358	0.46	sink in probe, no sink in hole
fgp1910	0.357	0.47	sink in probe, no sink in hole
fgp1a810	0.357	0.55	sink in probe, no sink in hole
fgp1a910	0.353	0.49	sink in probe, no sink in hole
fgp2211	0.359	0.57	no sink in probe sink in hole
fgp1211	0.355	0.47	sink in probe sink in hole
fgp12210	0.358	0.49	sink in probe sink in hole
fgp12310	0.359	0.50	sink in probe sink in hole
	Mean	0.50 ± 0.04	(of sink in probe values)

Table 7.13, a summary of the long time results, Frogmire

The values of thermal conductivity contained in table 7.13 show a considerable variation from the highest, $0.75 Wm^{-1}K^{-1}$ to the lowest $0.47 Wm^{-1}K^{-1}$. However, the last series of measurements to be taken, using sink material in both the probe and the sample hole, do

show a consistency with the thermal conductivity varying only between 0.47 and 0.50 $\text{Wm}^{-1}\text{K}^{-1}$.

The short time analysis was carried out upon the Frogmire measured data in the same way as before. As can be seen in graph 7.12, and much as for the Bovey summerhouse measurements, the distribution of heat sink material has produced the range of now familiar short time analysis curves.



Graph 7.12, shows the short time analysis, different heat-sink fillings in probes, Frogmire.

From the graph 7.12 the values of the thermal conductance, the intercepts on the Y axis, give a range of values of H varying between $33.95 \text{ Wm}^{-2}\text{K}^{-1}$ and $428 \text{ Wm}^{-2}\text{K}^{-1}$. The curves show a difference in height exemplifying the changes in the value of H. As previously discussed the intercept from the curves should be taken in the early period of the straighter section of the curve, preferably below 100 seconds. A summary of the short time analysis can be seen in table 7.14.

run code	Probe Thermal conductance $\text{Wm}^{-2}\text{K}^{-1}$	Diffusivity, m^2s^{-1}	Probe condition (sink material =HTSP heat sink compound).
fgp2810	33.92	3.07×10^{-6}	no sink in either
fgp2910	33.69	3.09×10^{-6}	no sink in either
fgp2a810	33.95	4.20×10^{-6}	no sink in either
fgp2a910	33.85	3.58×10^{-6}	no sink in either
fgp1810	103.80	3.62×10^{-7}	sink in probe, no sink in hole
fgp1910	103.27	3.49×10^{-7}	sink in probe, no sink in hole
fgp1a810	104.33	4.73×10^{-7}	sink in probe, no sink in hole
fgp2211	219.61	1.46×10^{-7}	no sink in probe sink in hole
fgp1211	62.00	6.74×10^{-7}	sink in probe sink in hole
fgp12210	52.00	5.59×10^{-7}	sink in probe sink in hole
fgp12310	428.02	1.01×10^{-7}	sink in probe sink in hole
		$3.31 \times 10^{-7} \pm 1.81 \times 10^{-7}$	Mean value of probes with HTSP compound in hole and in probe, (omitting fgp1211)

Table 7.14, summary of the short time results, Frogmire.

The results shown in table 7.14 show a gradual increase of the probe conductance as the heatsink material is placed in the probe and in the hole. However, the results for fgp1211 and fgp12210 do not follow this pattern. The thermal diffusivity was also reducing in size except for these results. It is assumed that in some way the probe had become loosened in the sample hole and resulted in the reduced contact and therefore affected the results. For runcode fgp2211 the probe thermal conductance appears to be higher than might be expected using a probe without heatsink material inside the probe.

The thermal diffusivity values shown in table 7.14 show a reduction of about a factor of 10 when the heat sink compound is added to the probe. Further heat sink material that is added to the sample holes appears to have variable effects upon the thermal diffusivity, much as for the variation in the thermal conductance values. The mean thermal diffusivity value that is quoted in table 7.14 is made up from all of the heat sink related thermal diffusivity measurements except runcode fgp1211 which, as stated previously seems to have been affected by an external influence. The mean value of the thermal diffusivity of

the cob at Frogmire, $3.31 \times 10^{-7} \text{ m}^2\text{s}^{-1}$ is under twice as small as the thermal diffusivity measurements undertaken in the laboratory upon mudstud, ($5.26 \times 10^{-7} \text{ m}^2\text{s}^{-1}$), wychert, ($5.89 \times 10^{-7} \text{ m}^2\text{s}^{-1}$), and cobblock, ($4.65 \times 10^{-7} \text{ m}^2\text{s}^{-1}$). It can be seen that if the trend shown by the majority of results holds true, the addition of heatsink compound does give a more reliable and representative value for the thermal properties of Frogmire's cob walls.

In a similar way to the field studies at Rezare and Bovey Tracey, an iterative solution was used to propose values for the thermal conductivity, the thermal diffusivity and the thermal conductance between the probe and the wall.

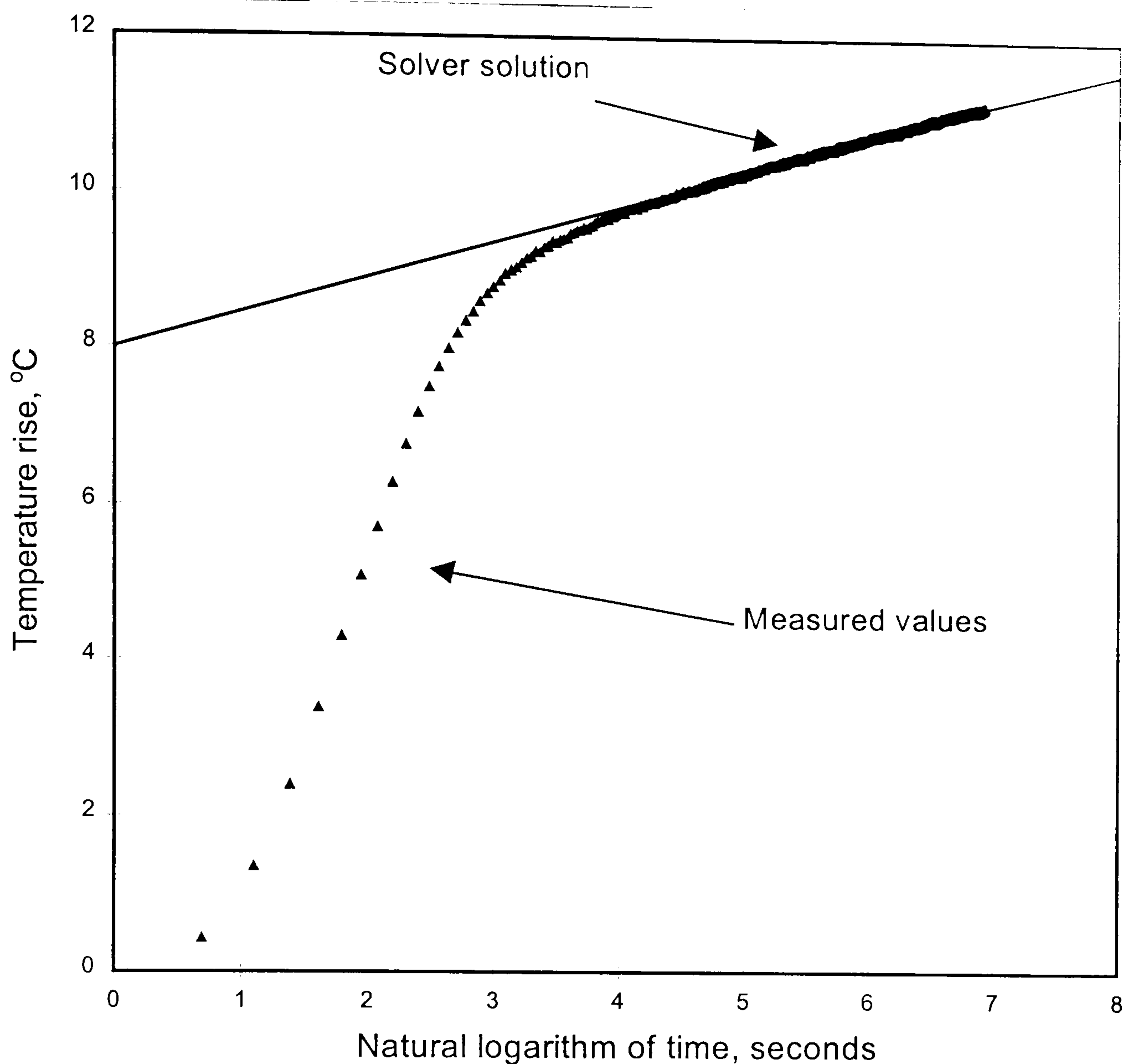
Using the following input values shown in table 7.15 for Solver2, then the graph 7.13 and the corresponding thermal values of Frogmire cob in table 7.16 were produced.

Thermal Conductivity, $\text{Wm}^{-1}\text{K}^{-1}$	Thermal Diffusivity m^2s^{-1}	Thermal Conductance $\text{W m}^{-2}\text{K}^{-1}$
0.99	1.9×10^{-7}	95

Table 7.15, shows the values used in Solver2 to generate Table 7.16.

Thermal Conductivity, $\text{Wm}^{-1}\text{K}^{-1}$	Thermal Diffusivity m^2s^{-1}	Probe Thermal Conductance, $\text{W m}^{-2}\text{K}^{-1}$
0.936	1.827×10^{-7}	76.596

Table 7.16, shows the chosen values using Solver2.



Graph 7.13, shows Solver2 solution against measured data for Frogmire cob.

run code	Probe Condition (sink material =HTSP heat sink compound).	Conductivity $Wm^{-1}K^{-1}$	Diffusivity, m^2s^{-1}	Probe Thermal Conductance, $Wm^{-2}K^{-1}$
fgp2810	no sink in either	0.74	8.20×10^{-8}	44.1
fgp2910	no sink in either	0.75	9.20×10^{-8}	44.0
fgp2a810	no sink in either	0.90	8.80×10^{-9}	43.7
fgp2a910	no sink in either	0.75	9.27×10^{-8}	44.5
fgp1810	sink in probe, no sink in hole	0.52	6.51×10^{-8}	158.0
fgp1910	sink in probe, no sink in hole	0.46	3.70×10^{-8}	132.0
fgp1a810	sink in probe, no sink in hole	0.55	5.46×10^{-8}	132.0
fgp2211	no sink in probe sink in hole	0.95	7.63×10^{-8}	74.0
fgp1211	sink in probe sink in hole	0.48	1.55×10^{-8}	275.0
fgp12210	sink in probe sink in hole	0.53	1.25×10^{-8}	264.0
fgp12310	sink in probe sink in hole	0.51	1.30×10^{-8}	268.0

Table 7.17, summary of Solver2 results for Frogmire cob.

The correlations between the suggested thermal conductivity values from Solver2 against the measured values show a good match for some of the measurements. Some thermal

conductivities were predicted with a small difference, fgp2810, $0.74 \text{ Wm}^{-1}\text{K}^{-1}$ Solver2 and $0.64 \text{ Wm}^{-1}\text{K}^{-1}$ measured. Others were predicted with no difference, fgp1a810, $0.55 \text{ Wm}^{-1}\text{K}^{-1}$ Solver2, $0.55 \text{ Wm}^{-1}\text{K}^{-1}$, measured. The pattern of the magnitude of the probe thermal conductance, H, shown in table 7.14 is repeated in the suggested values from Solver2 in table 7.17. The probe thermal conductance for fgp2810, measured using the short time method is $34 \text{ Wm}^{-2}\text{K}^{-1}$, whilst the Solver2 value for H for the same runcode is $44.1 \text{ Wm}^{-2}\text{K}^{-1}$, a reasonable agreement. The larger figure for H measured for runcode fgp12310, $428.02 \text{ Wm}^{-2}\text{K}^{-1}$ is again similar to the Solver2 value of H, $440 \text{ Wm}^{-2}\text{K}^{-1}$. However, runcode fgp2211 which uses heat sink material in the hole, but not in the probe, has a measured H value of $219.61 \text{ Wm}^{-2}\text{K}^{-1}$, which is much larger than the H value found using Solver2, $74 \text{ Wm}^{-2}\text{K}^{-1}$. The measured H values for fgp1211 and fgp12210 are unexpectedly low whilst the fgp12310 measured H value is unexpectedly high. This is contrasted with the Solver2 H values for these in-situ measurements which are remarkably stable in comparison.

Whilst the values found using the short time analysis for H and λ are generally similar to the solver2 values, the thermal diffusivity values are different. The α values from the short time analysis show, except for runcode fgp1211, a gradual reduction with the use of heat sink compound, first in the probe and then in the probe and in the hole in the wall. Solver2 α values also show a reduction with the use of heat sink compound, and generally are about 10 to 100 times smaller. Solver2 appears to be able to predict the λ and H values with more certainty than values of α .

Conclusion

The field experiments used the improvements in the original thermal probe technique perfected in the laboratory to measure the thermal properties of the cob walling at the three field-study sites. The Rezare, Bovey Tracey and Frogmire results from the long and short time analysis gave values similar to those achieved in the laboratory. The Solver2

iterative values were in broad agreement with the trend of the measured results if possible, more applicable to the prediction of the values of λ and H .

The results shown in table 7.18 are the first to be published concerning unbaked earth buildings in the UK and provide a starting point for the further analysis of buildings of this type throughout the West Country and elsewhere.

Field Study Building	Thermal Conductivity $\text{Wm}^{-1}\text{K}^{-1}$, λ	Thermal Diffusivity, m^2s^{-1} , α
Cob Barn, Rezare	0.47 ± 0.14	$2.93 \times 10^{-6} \pm 2.0 \times 10^{-6}$
Cob Block Summer house Bovey Tracey	0.38 ± 0.007 (mean, sink in probe)	$2.24 \times 10^{-7} \pm 1.32 \times 10^{-7}$
Cob Building, Frogmire	0.50 ± 0.04 (mean, sink in probe)	$3.31 \times 10^{-7} \pm 1.81 \times 10^{-7}$

Table 7.18, summary of the best values using the long and short time methods.

In general, the value of the thermal conductivities that are comparable to other published accounts have a $+/- 2\%$ to $+/- 5\%$ error, the thermal diffusivity values vary more, depending upon the material measured and the measurement technique used.

These results along with the results from the laboratory measurements are discussed in a more global sense in Chapter 8.

Chapter 8

Discussion.

This chapter summarises the work completed and discusses the results from the laboratory and field studies in relation to the main objective of the investigation outlined in the introduction. This objective can be summarised as the application of a time dependent probe technique to measure the thermal conductivity and diffusivity of cob walls in Devon.

The main aim of the study required the collection of thermal conductivities and diffusivities of existing Devon cob. To achieve this it was considered that the measurement technique must satisfy five criteria; (i) the technique must be non-destructive, (ii) it must not influence the material being measured, (iii) must give representative values for both the thermal conductivity, (λ), and the thermal diffusivity, (α), (iv) should be rapid and affordable and (v) allow *in-situ* testing.

A search was undertaken to discover a technique that could measure the thermal conductivity and thermal diffusivity of cob walling which would comply with the above criteria. This narrowed the range of suitable measurement types to time-dependent techniques as these allowed the simultaneous evaluation of both the thermal conductivity and thermal diffusivity of the specimen or sample.

The chosen time dependent measurement method uses a probe small enough to cause minimum disturbance to the sample. The technique also relies upon a very short measurement time and employs a low heater power, reducing the moisture migration from the measurement site. This will, in turn, reduce the possibility of unrepresentative readings.

The thermal probe technique is also the only technique that is robust, whilst remaining portable, thereby being suitable for the field studies.

Previous researchers had developed a range of different time dependent measurement probes each with characteristics suited to different measuring environments. The probe developed by Batty, (Batty et al, 1984) provided this investigation with the basis of an instrument that fulfils the previously mentioned criteria, small, fast, reliable, robust and inexpensive.

This probe was first used in laboratory studies utilising a logging system to automatically record the electrical power of the probe heater and the probe internal temperature, accurately timing each event. This work, through a series of experiments on different materials, enabled confidence to be gained before turning to the fieldwork. The same probe system was modified after a series of laboratory-based familiarisation and feasibility studies were conducted into a portable measurement system. This system was employed to measure the thermal properties of three cob buildings, each representing a different type of cob wall.

Probe Conductance

Much of the development of the probe focused upon the acquisition of representative values for both the thermal conductivity and diffusivity of the various samples. To this end, the interface between the probe and the test material was closely investigated. The probe conductance, the value of the degree of thermal contact between the external surface of the probe sheath and the specimen, was deemed vital to allow the representative measurement of the thermal conductivity and thermal diffusivity. Other researchers (Blackwell, 1954), believed the probe conductance, H , had to be large to allow the accurate assessment of the

thermal diffusivity. However, Blackwell also suggested that a more accurate assessment of the value of the thermal diffusivity can be obtained if the probe thermal conductance, H is known. To enable the determination of H , the behaviour of the rise in probe temperature at short times, over the first minute or so of the heating schedule was investigated and a 'short time' solution derived by Blackwell was used to analyse the results. This procedure allowed values of H to be determined and these were used to establish the magnitude of the thermal diffusivity of the samples studied in both the laboratory and fieldwork.

Various ways of improving the thermal contact between the probe and the test material were tried. These included the use of materials that theoretically would naturally establish good thermal contact with the probe. Paraffin wax was first used as standard for the probe studies, by Batty, to measure the reproducibility of its thermal conductivity. It was chosen because, if the wax was allowed to solidify around the probe, the thermal contact between probe and wax would be good. The laboratory measurements undertaken in this study suggest that a typical thermal conductance value of paraffin wax to the exterior of the probe is approximately $85 \text{ Wm}^{-2}\text{K}^{-1}$ using an air filled probe. This figure increased when heat sink compound was used inside the probe and this is described in more detail later in this chapter in the section entitled, Heat Sink Material and Improvements in H .

Glycerine, a viscous liquid, was felt to give the probe the best chance of maintaining good physical contact between the probe and material. A series of measurements on glycerine helped build confidence in the technique. Glycerine gave the author a useful indicator to the probable maximum value of the thermal conductance of the probe to specimen interface, H , of approximately $300 \text{ Wm}^{-2}\text{K}^{-1}$. It was felt that if any measurements of H for other materials, or different test procedures that were close to this figure then they would be approaching an

optimum value. This should be compared with H values found for the probe in wax of about $85 \text{ Wm}^{-2}\text{K}^{-1}$.

A second analysis method used the 'rate' equation (Blackwell, 1954), to measure a value for H and to provide a measured value of the thermal capacity of the probe. This method relies upon the use of a second thermocouple attached to the external surface of the probe. Measurements were then possible which gave a direct indication of the flow of heat between the probe heater and the sample, at very early stages in the heating schedule. The use of this second external thermocouple was the most recent development of the probe and only therefore used in the recent laboratory studies. The results from the rate studies showed that over the first minute of the heating time a straight line was observed for $d\theta/dt$ vs Δt as suggested by Blackwell. This confirmation of Blackwell's theory allowed the measurement of a number of different thermally related properties. The probe thermal capacity, (mc), was determined, a function of the mass and specific heat capacity of the probe wall, heater, thermocouple, end caps and when included, the probe filling. The probe contact conductance, H, between the centre of the probe and the sample surface is also measured.

The values for H using this rate method were, for the most part, in agreement with the trend exhibited by the values of H calculated from the Blackwell short time analysis method. For example, the Blackwell short time mean value for H, paraffin wax is $85.6 \text{ Wm}^{-2}\text{K}^{-1}$ for an unfilled probe, $95 \text{ Wm}^{-2}\text{K}^{-1}$ for a Dow-Corning filled probe and a probe with Electrolube High Temperature Silicon Paste, (HTSP) filling, H is $142 \text{ Wm}^{-2}\text{K}^{-1}$. This can be compared with the rate mean values of H of $109 \text{ Wm}^{-2}\text{K}^{-1}$ for an unfilled probe, $134 \text{ Wm}^{-2}\text{K}^{-1}$ for a Dow-Corning filled probe and $223 \text{ Wm}^{-2}\text{K}^{-1}$ for a probe with a HTSP filling. Both series of mean values of H increase, but the rate studies generally give values that are approximately 30% larger. It is unclear why the trends predicted by these two techniques have a relatively good match, but

the actual figures disagree. A range of reasons including poor thermal contact of the external thermocouple could be responsible. Clearly more work, both theoretically (concerning the reliability of the rate results), and experimentally (using the thermocouple probes in the field), is required in this area of twin thermocouple probes.

Some disagreement was apparent between the values measured using the rate method and the long and short time techniques. Despite this, it is felt that the use of the rate method represents a significant step forward towards using the time dependent probe technique to accurately measure the thermal properties of materials both *in-situ* and in the laboratory. Procedures and probe designs that are necessary to protect the external thermocouple from damage when the probe is inserted into real cob walls during field conditions have not been established. However, further studies will enable the design of a robust probe using two thermocouples to be produced. Then the probe thermal capacity mc and a second probe conductance value, H can be measured in the field, as part of a routine data collection exercise. The collected rate data can be compared with thermal values obtained from other analysis techniques.

Heat Sink Material and Improvements in H

The short time and the rate analysis methods were used to investigate the use of heat sink materials to improve the thermal contact between the probe and the test material. Both the short time and rate analysis techniques demonstrated that the heat sink compound improved the thermal contact between the probe and the test material. Degrees of improvement of thermal contact were recorded in a range of combinations of air-filled and sink filled probes with and without sink filling placed in the sample hole. This is exemplified by the short time results for cob block, where the mean H value for an unfilled probe is $32 \text{ Wm}^{-2}\text{K}^{-1}$, while for

the HTSP filled probe H is $92 \text{ Wm}^{-2}\text{K}^{-1}$ and the filled probe and hole have a mean H of $332 \text{ Wm}^{-2}\text{K}^{-1}$. The final figure describing the mean H of the filled probe and sample hole is in agreement with the mean H measured for glycerine, $307.94 \text{ Wm}^{-2}\text{K}^{-1}$. For all the sample materials the greatest increases in probe thermal conductance were experienced when both the probe and the sample hole were filled with heat sink material. The heat sink material with the higher thermal conductivity, HTSP, $\lambda = 2.9 \text{ Wm}^{-1}\text{K}^{-1}$, gave the higher values of H. The Dow Corning heat sink material, $\lambda = 0.9 \text{ Wm}^{-1}\text{K}^{-1}$, gave mean H values of between $95 \text{ Wm}^{-2}\text{K}^{-1}$ and $134 \text{ Wm}^{-2}\text{K}^{-1}$ whilst the HTSP heat sink material, gave values between $142 \text{ Wm}^{-2}\text{K}^{-1}$ and $223 \text{ Wm}^{-2}\text{K}^{-1}$ for H.

During the fieldwork the possibility of the results being affected by the inhomogeneity of the specimen immediately surrounding the probe were examined. During the studies two probes were inserted into two separate holes approximately 400mm apart. (It was felt that this distance would effectively isolate the material of each of the test holes). Neither of these holes were filled with heat sink compound. One of the two probes contained heat sink compound. On interchanging the two probes, further data was collected in an identical manner to the previous measurements. (Results are reported in full in chapters 6 and 7). The shape of the long time curves were attributable to the probe, high temperature rise for the air filled probe and low rise for the heat sink filled probe. This remained the case when the probes were interchanged, thus proving that the results were typified by the probe design, even when surrounded by cob material in a different part of the wall. The results of these runs also confirmed that the different heat sink material combinations were having a direct effect upon the thermal conductance and this was not attributable to any arbitrary variations in the composition of the wall material.

One of the most dramatic improvements in the representative nature of the data was exemplified by the measured values of thermal diffusivity. As the thermal diffusivity is calculated using an equation in which the value of logarithmic α and reciprocal H functions are combined, small changes of the variables, such as the thermal conductivity, λ , and H will create large variations in the value of α . Because of this, the accurate determination of α is difficult using the methods used in this study. However, the introduction of heat sink compound material has reduced the variation of the thermal diffusivity, α . Initially α ranged over 10^{13} orders of magnitude for the five and ten second interval data. Later α values of $1.07 \times 10^{-8} \text{ m}^2\text{s}^{-1}$ (HTSP filled probe in paraffin wax), were obtained within 10% of the published value of $9.62 \times 10^{-8} \text{ m}^2\text{s}^{-1}$ (Carslaw and Jaeger, 1947). It is felt that the improvements in the thermal contact provided by the careful use of small amounts of heat sink material provide more representative values of thermal conductivity and thermal diffusivity of the specimens. It is assumed that the heat sink material can bridge any small air gaps experienced when inserting the probe into the sample. This is particularly pertinent to field studies when ideal conditions for measurement are less likely. The thermal conductivity values determined for most of the samples, when using heat sink material, remained relatively unaltered in comparison with the studies undertaken without any heat sink material. This is unsurprising as the thermal conductivity measurements are obtained using a long time-period analysis. The long time-period analysis depends upon observations of data representing the volume of the specimen at several centimetres away from the probe with its thin layer of heat sink material. Future work could involve the use of large diameter test holes with considerably increased quantities of heat sink material to investigate the degree of influence brought about by the introduction of a 'third' material. It is envisaged that part of this further study may place a heater and thermocouple, without an outer sheath, into a hole filled with different heat sink materials.

The Long time Solution and Potential Errors

The thermal conductivity of the materials used in the laboratory and field studies was determined using a long time solution first proposed by Carslaw and Jaeger and refined by Blackwell. The long time solution assumes the temperature rise of the interior of the probe will be a linear function of the natural logarithm of the elapsed time. After approximately 250 seconds, depending upon the material being measured, the line does become straight and the slope of this region was used to assess the thermal conductivity of the sample. A boundary reflection effect, following Vos, (1955), could influence the probe temperature to an extent if $\frac{4\alpha t}{b^2} > 0.6$ (equation 5), where the specimen boundary is 'b' from the probe, t is the length of the period of heating, and α is the thermal diffusivity of the specimen. For a sample of thermal diffusivity of $3 \times 10^{-7} \text{ m}^2\text{s}^{-1}$, which is a typical value from the many field measurements, then for an experiment with a duration of approximately 1000 seconds, the centre of the probe was required to be at least 44mm from the nearest boundary of the specimen. All the laboratory and field boundary to probe distances were large enough so that this reflection effect would be negligible. However, it must be borne-in-mind that, as stated in chapter 5, the presentation by Vos of his results is vague.

As the specimens in the field work were relatively large and inhomogeneous, any results for the region close to the probe, that is those obtained from relatively short time periods (250-400 seconds), are likely to be unrepresentative of the larger regions of the specimen. As a result of this, long time measurements mostly rely upon the analysis of time periods of over 400 seconds. This allows enough time to pass for the heating effect of the probe to be influenced by the volume of sample beyond the immediate vicinity of the test hole.

The long time curves of temperature rise against the natural logarithm of time showed distinctive patterns for each different material tested. The overall temperature rise varied with

each change in the position of heat sink material used in the probe and the sample hole. Heat sink material both within the probe and in the hole allowed the heat from the probe heater to be efficiently transferred to the sample. Thus, overall temperature rises were appreciably lower than in those studies carried out with a similar power level and in an identical material. Insulating materials logically provided curves that had large temperature rises for only low levels of power input to the probe heater.

Solver studies.

Initial experimental data was collected at a logging time-interval of five and ten seconds. This, as described in chapter 5, did not give sufficient detail during the initial 40 to 60 seconds of each run to allow a meaningful short time analysis to be attempted. The related problem of not knowing the exact start of the run, or exactly when the probe heater current was switched on compounded this. These two problems affected the prediction of the probe thermal conductance, H . If the value of H was uncertain, then the reliability of the measured value of the thermal diffusivity of the specimen was uncertain. To try to make use of this incomplete data, an optimisation routine, Excel Solver was utilised. The Solver2 routine was used to predict the values of the thermal conductivity, λ , thermal diffusivity, α and probe thermal conductance, H , from the early 5 and 10 second data using the first two terms of equation 2. The Solver2 thermal values were a good match for the later better quality data processed in the usual way. The good matches, when achieved, allowed a further reference to judge the quality of measured values found from other analysis methods. A guide to the use of Solver in this work can be found in the appendix. As the Solver routine is not as transparent as a similar Fortran routine it would be advantageous to compare Solver results with a similar

Fortran routine. Further iterative techniques using Fortran routines and Genetic Algorithms to establish more traceable data are planned.

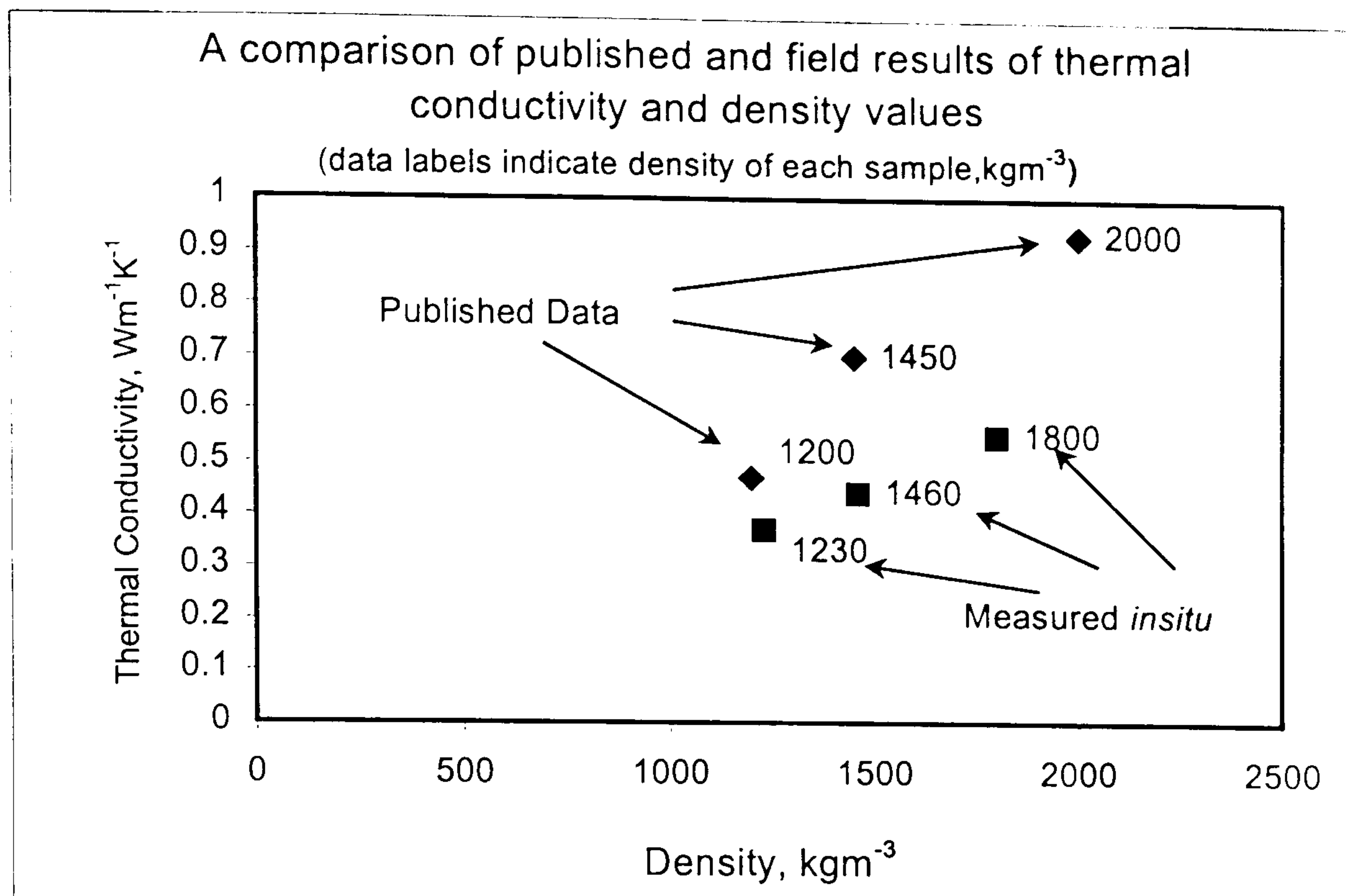
Thermal Characteristics for use in Thermal Modelling.

Using a series of mean values obtained from the data measured from the field tests, the following table has been produced. Here the thermal conductivity and diffusivity for the typical cob samples measured *in-situ* are shown. With suitable values of the density of the cob samples, the specific heat capacity has been determined, since $c = \lambda/\alpha\rho$.

Thermal Values		Field Study Locations		
Property	Units	Rezare	Bovey Tracey	Frogmire
Density of cob	kgm ⁻³	1460	1230	1800
Thermal Conductivity	Wm ⁻¹ K ⁻¹	0.47 ± 0.14	0.38 ± 0.007 (mean, sink in probe)	0.50 ± 0.04 (mean, sink in probe)
Thermal Diffusivity	m ² s ⁻¹	2.93 × 10 ⁻⁶ ± 2.0 × 10 ⁻⁶	2.24 × 10 ⁻⁷ ± 1.32 × 10 ⁻⁷	3.31 × 10 ⁻⁷ ± 1.81 × 10 ⁻⁷
Specific Heat Capacity	Jkg ⁻¹ K ⁻¹	110	1343	923

Table 8.1, summary of the thermal properties of the field test results.

The values in table 8.1 can be compared to the published data, (Minke, 1994) illustrated in table 2.1, chapter 2. Graph 8.1 shows this comparison.



Graph 8.1, shows a comparison of the field measurements with published data indicating various thermal conductivities at different densities.

It can be seen that the published thermal conductivities are generally higher than the field data obtained in this work. However, the rise in thermal conductivity with an increase in the value of density is similar for both sets of results. Taking into account the variability of the samples and the use of different analysis techniques for each set of results, the discrepancy is acceptable. Clearly, with a larger number of field results, more definite conclusions can be made. The specific heat capacity for the cob at Rezare was determined from studies that did not use any heatsink compound during the measurements and so it is of little surprise that because of the high thermal diffusivity figure, the specific heat capacity is unrealistically low. However, the two measurements carried out using heat sink compound do give specific heat capacities which are realistic and form the basis of values that will be used in thermal simulations. The chosen values were a thermal conductivity of $0.5 \text{ Wm}^{-1}\text{K}^{-1}$ and a specific heat capacity of $1000 \text{ Jkg}^{-1}\text{K}^{-1}$ as these two figures were felt to match the thermal properties of the final and most realistic study, Frogmire. The cob walls at Frogmire were measured

towards the end of the experimental programme and used heatsink compound both in the probe and in the hole. The cob was also from a historical building, rather than from a more recent construction. However, as cob is a variable material the figures were adjusted to come to a compromise between the figures of Frogmire, Rezare and Bovey Tracey.

The cob wall construction used in the simulation comprised 600mm of cob bounded by layers of render and plaster, as described in chapter 9. This construction has a thermal transmission value of $0.82 \text{ Wm}^{-2}\text{K}^{-1}$, considerably higher than the current value allowed by the building regulations. At this point the suppositions of Gooch can be discussed. In chapter 2, Gooch is quoted concerning the possible thermal transmission value of a modified 625mm-cob wall nearing a value of $0.35 \text{ Wm}^{-2}\text{K}^{-1}$. If this is the case, the extra insulative value contributed by the modifications discussed in chapter 2 would have to contribute an improvement of $0.47 \text{ Wm}^{-2}\text{K}^{-1}$. If the cob wall was modified with woodshavings (as suggested in chapter 2), let us assume that woodshavings have a thermal conductivity of $0.06 \text{ Wm}^{-1}\text{K}^{-1}$, slightly higher than cork board ($0.043 \text{ Wm}^{-1}\text{K}^{-1}$) and about the same as fibre insulating board, (Smith et al, 1994). The woodshavings would then give a modification that would be represented by a thickness of shavings of approximately 130mm. However, if the reader views the results of the thermal simulations which compares the thermal performance of the timber framed building, constructed to modern building regulations, to the almost identical model but built with cob walls, it becomes clear that the issue of matching the thermal transmission values may not necessarily be of great benefit.

These models and the results from the simulations are described in chapter 9.

Conclusion

The techniques perfected during the laboratory and field studies and the representative values for the thermal conductivity and diffusivity allow more accurate dynamic thermal simulations to be undertaken. This will, in turn, allow the valid comparison of simulations prepared by previous authors modelling earth-sheltered buildings with the thermal behaviour of Devon's cob buildings. Further comparisons can be made with the thermal behaviour of a virtually identical building built to modern thermal regulations. Much of the anecdotal evidence presented in chapter 1 and 2, concerning the beneficial thermal characteristics of Devon cob and other earth buildings can be assessed in the light of the results of the thermal simulations. Chapter 9 presents a summary of the results of these simulations and conclusions are drawn.

Chapter 9

Thermal Modelling and Results.

This chapter begins by reviewing the existing research completed previous to this study relating to the modelling of earth as part of, or surrounding, buildings. In doing so, the findings of this research can be compared with the conclusions drawn from the thermal modelling of a cob building. To allow the reader to compare the thermal behaviour of a cob building with that of a modern dwelling, a second model, a timber framed dwelling, is simulated with identical conditions to those used for the cob model. The preparation of these two building models, one of cob and another constructed to the current thermal elements of the building regulations is described. Finally the results of thermal performance simulations using these models are presented and discussed.

Previous research involving computer modelling of the thermal behaviour of buildings with unbaked earth structural elements is very limited. However, a number of papers have been published concerning the use of earth sheltered buildings. An earth-sheltered structure uses earth as an outside covering. Normally this will require the building to have a separate inner layer, which is intended to fulfil the normal functional requirements, such as structural integrity and waterproofing. Because of this, the earth sheltered or earth bermed buildings (see glossary), will behave much as an extension of the ground around the structure in question. The outer earth layer will mostly follow the ground's temperature profile and moisture content. This is obviously very different from the position of a typical unbaked earth wall, which will be isolated from the ground by a plinth and so have a moisture content far below that of the earth in the ground. The wall will also, because of its far smaller dimensions, be unlikely to be able to damp out as much of the variations in ambient temperature as the earth berm of an earth-sheltered building. Although earth is used to surround buildings of this type, it tends to supplement the existing structure and provides extra material to influence the interior thermal environment. Buildings made with

cob walls share some of the features of earth sheltered buildings, such as thermal mass, due to the large volumes of material involved. However, the results of such models are likely to vary due to the previously mentioned increased moisture content of the soil surrounding earth-sheltered buildings. The earth used in earth sheltered buildings is separated from the internal environment by the structure of the building, in contrast with cob dwellings, whose thermal mass is in direct contact with the internal environment. Cob walls are relatively uniform in nature with a well-known range of constituents and regular dimensions. Soil used in earth sheltered buildings can vary in consistency and dimensions. However, as earth sheltered buildings do have some performance characteristics that could be similar to dwellings with cob walls it is relevant to review some previously published material.

The heating, ventilation and air conditioning related energy consumption of earth sheltered single storey office buildings and dry-storage warehouses were investigated using computer simulation by G. Meixel et al (1981). A range of buildings in various locations in the United States were modelled and an increase in the extent of earth sheltering indicated a significant reduction in the energy requirements and peak energy demand. Earth integrated farm buildings in relation to energy conservation were investigated by Lloyd Jones (1983). This publication concentrates upon the energy savings possible due to the reduced internal-external temperature profiles in winter conditions. Bligh & Willard (1985) investigated the value of the thermal conductivity used to model earth-contact buildings. By using finite element thermal analysis software similar to that used in this study, it was found that the value used for the thermal conductivity in any model has a significant effect on the calculated thermal performance of a building. The modification of the surface of the earth surrounding an earth integrated building is discussed by B. C. Jayashankar (1989). The paper focuses upon shading, wetting, insulating and glazing with clear plastic sheets and blackening the earth layers that surround a partially sunken room. These measures were investigated in three different

Indian climate types using analytical calculations and reduced scale models. A range of predicted hourly temperature variations were tabulated for each of the treatments in the appropriate climate type and recommendations for each were cited. Krarti and Claridge (1990) discuss the environmental and energy conserving advantages of earth sheltered structures. This paper states:

' The high heat capacity of the soil and its thermal insulation value greatly attenuate ambient temperature variations at the surfaces of an earth sheltered building and somewhat reduce the total energy flows across the envelope of such buildings.'

In summary, the previous research into earth sheltered or earth bermed buildings predicts an attenuation of ambient temperatures and that the thermal performance of any simulations is dependent on the thermal properties used in any model. The results of this research could provide further understanding of the thermal properties of unbaked earthen walling. However, as previously discussed, earth sheltered or bermed buildings normally have a surrounding earth layer that extends for several metres in thickness and vary in moisture content and composition. If this is compared to the reduced thickness of earth utilised in cob walls, often 500-650mm, the characteristics found in simulations of earth sheltered buildings may be apparent, but it is anticipated, with a corresponding reduction in their effect.

Two building models were thermally simulated with three aims: (1) to test the anecdotal evidence that exists (as the reader will recall from chapters 1 and 2), suggesting that cob buildings are cool in summer and warm in winter, (2) to compare the results from earth sheltered building studies and to investigate the thermal properties of cob buildings in Devon and (3) to explore the differences and similarities between the thermal performance of a modern domestic building with a more traditional cob walled house.

The Simulation Models.

The models used for the simulation were based upon a domestic scale building using two different forms of construction. The first used a modern form of construction of a timber frame for the main structural element of the building. All parts of the construction were compliant with the Building Regulations, Part L, Conservation Fuel and Power (DOE,1995). The second model utilised the same internal dimensions as the first model, but used cob for the walls. A rendered image of the simulation model can be seen in Figure 9.1.

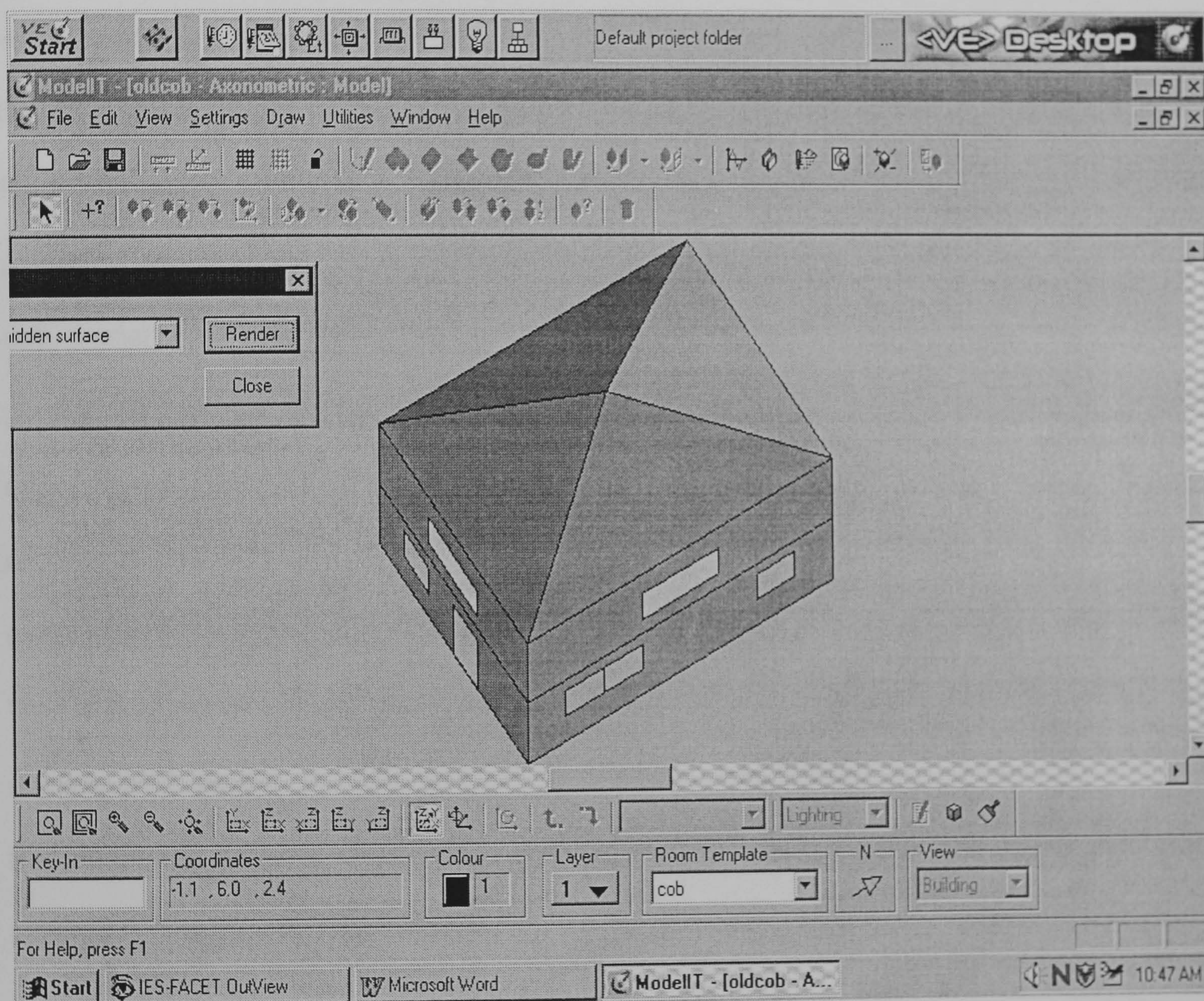


Figure 9.1, ModelIT CAD representation of the domestic model used for the two simulations.

Each model was two stories in height and had a building footprint of 48m² and a storey height of 2.2m. These are dimensions that were felt to be representative of a typical modern four-bedroomed detached dwelling. Both models had solid ground floors,

ceilings, doors and windows that conform to current building regulations. Both models used a modern roof design and modern materials. The roof was pitched and clad in concrete tiles. The upper floor ceiling was made from plasterboard and insulated to current building regulations using fibre insulation. It was noted that a thatch roof would have been more appropriate for the cob model, as thatch is the normal partner to cob in Devon. However, to enable a direct comparison of the two models it was felt that the roof had to be of identical construction and materials for both building models. (As an aside, the reader may be interested to know that thermal insulation values for thatch may also warrant thermal investigation using the time dependent thermal probe technique). The timber-framed model has a wall faced in 100mm brickwork, a 10mm air-gap, 60mm of fibre insulation bounded by structural plywood and finished internally with gypsum plasterboard. This construction has a thermal transmittance value of $0.45 \text{ Wm}^{-2}\text{K}^{-1}$. The cob model had walls of 600mm of cob finished internally and externally with layers of plaster and render respectively. (Cob walls, should be allowed to breathe in order to ensure a long life, (Keefe 1998)). Cement-based plasters and renders are therefore not recommended in practice and therefore lime-based materials have been used in the simulation for the cob model only.). The thermal conductivity value used for cob was $0.5 \text{ Wm}^{-1}\text{K}^{-1}$, a value chosen to represent the thermal conductivities measured in the field studies and shown in table 7.19. The cob wall construction has a calculated thermal transmittance, or U value, of $0.82 \text{ Wm}^{-2}\text{K}^{-1}$, considerably higher than the current value allowed by the building regulations.

The thermal-modelling package used was Apache Sim. part of the *Facet suite of software* produced by Integrated Environmental Solutions, (I.E.S. Ltd), Glasgow. The models were built-up using ModellT, a CAD-related design package, which allowed the assignment of each thermal property of the building materials (α , λ and ρ) and their associated dimensions. A profile of use, including quantities and occupation patterns of people, internal appliances, various building services and their frequency of use can be defined.

However, as mentioned previously, the aims of the simulation were to concentrate upon the use of two quite different building materials for the walls of the models. Because of this, it was felt prudent to simplify the building model as much as was practicable. To this end the models were programmed to be unheated and to be without lights, appliances or even occupants. In this way, it is hoped that the results from any simulations will readily show the thermal characteristics of each of the models. These models were then investigated under the influence of a one-year period of weather (based on Plymouth weather data), and their thermal performance displayed in the form of indoor air temperature versus time graphs.

The Simulation Results.

The simulation package, Apache Sim., uses dynamic thermal analysis to take into account the full effect of the storage capacity of the building materials that are used in a building model. The program does this by using finite difference techniques to model the transmission and storage of heat in the building fabric using defined time steps. The simulation results used a time step of 30 minutes.

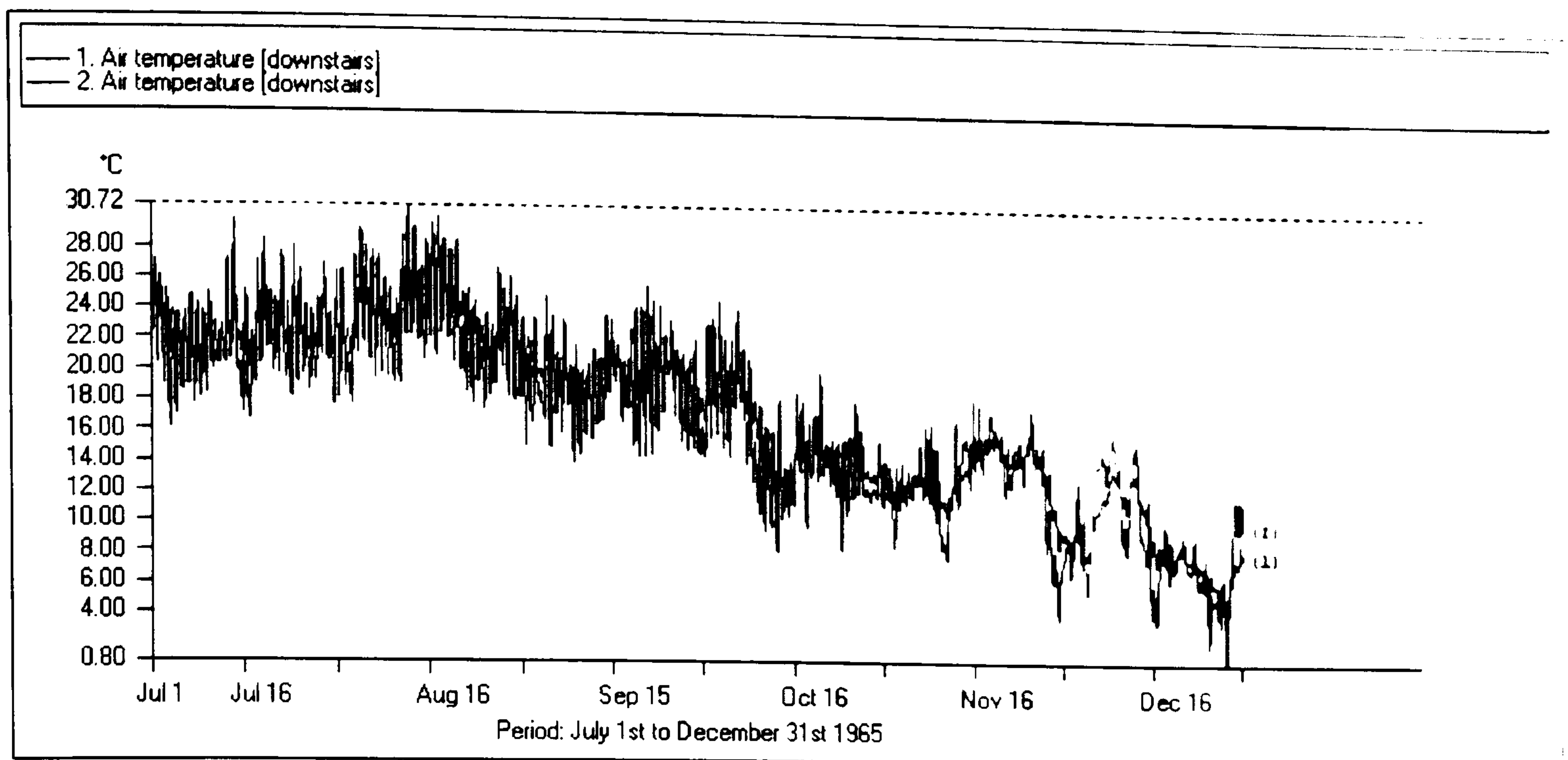
The weather data used was measured in Plymouth, but did date back to the nineteen sixties. It was felt that as long as the two models were subjected to the same external conditions and that the weather data was representative of the geographical area, the analysis of the results would be valid.

Apache Sim. results

The simulation results are organised to give the reader an insight into the differences in the internal air temperatures between the cob and timber framed models. Initially, the models were used in a simulation for six months covering a seasonal period between mid-summer and mid-winter. Secondly, the models were used in two shorter simulations, each of one month in duration, namely January and July.

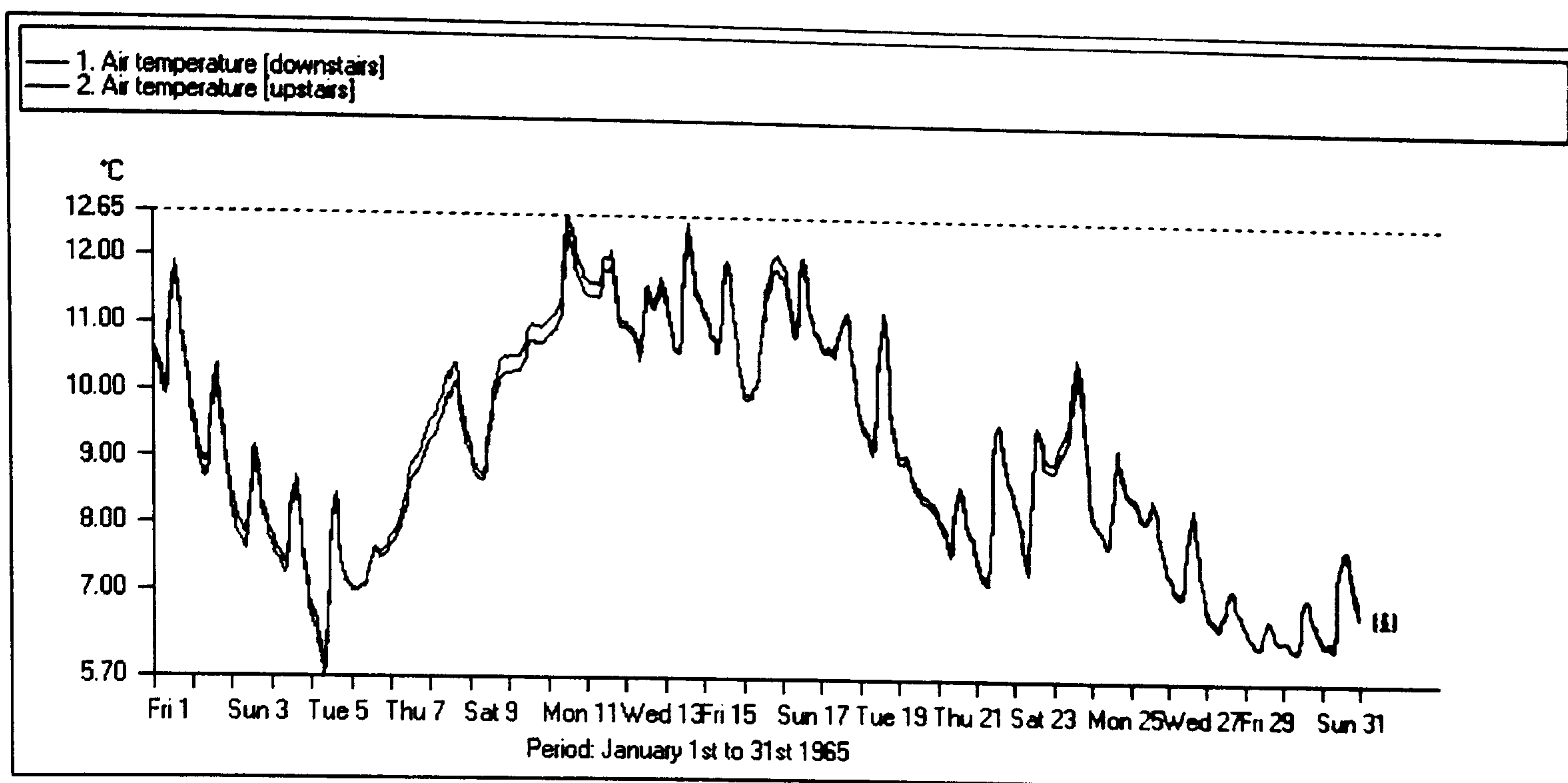
1, Black line = average downstairs air temperature, traditional cob building.

2, Red line = average downstairs air temperature, timber frame dwelling.



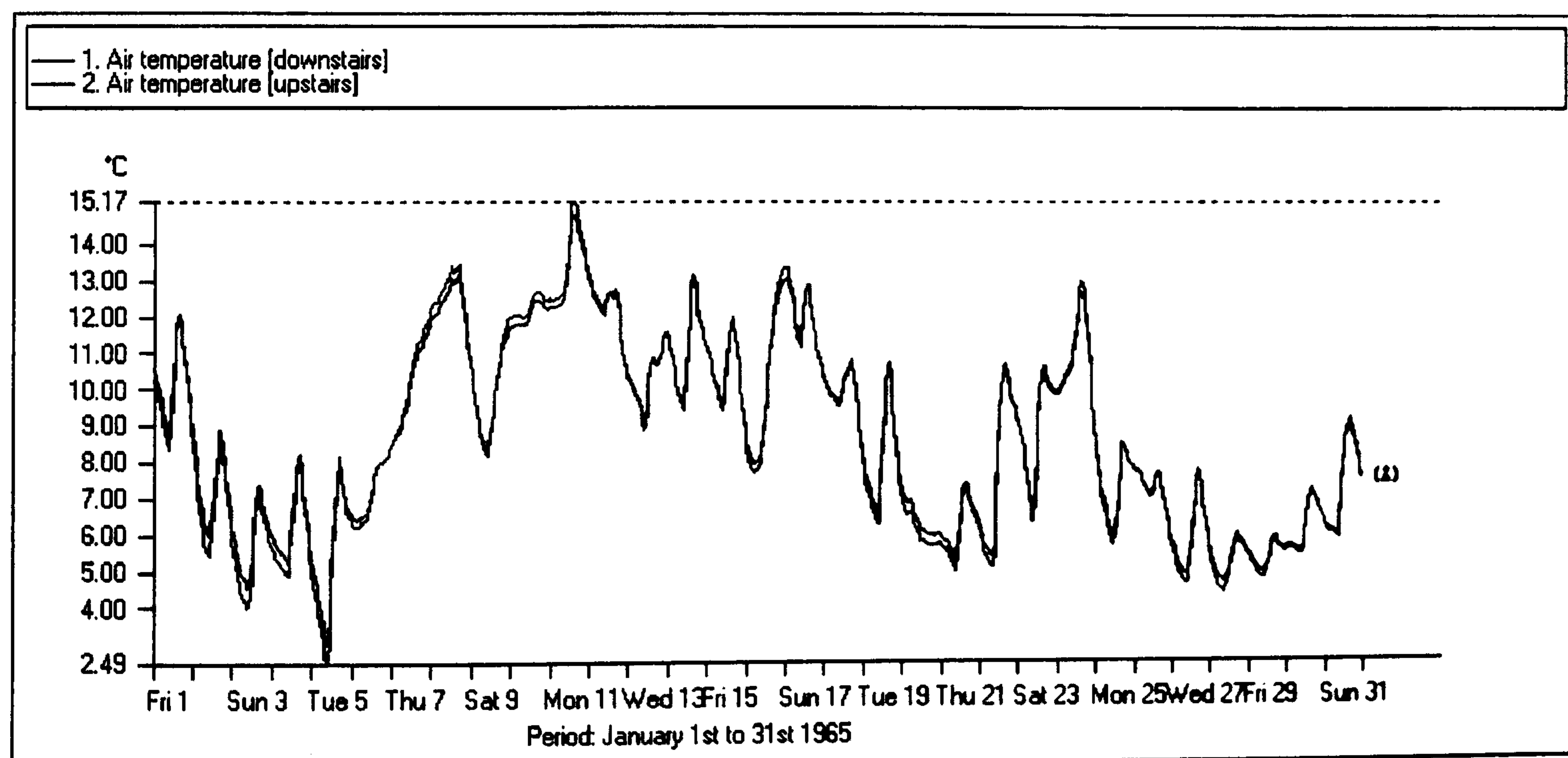
Graph 9.1, shows the internal downstairs air temperatures for the cob and timber frame models over a six month period.

The graph 9.1 shows the red line, representing the internal air temperature of the timber frame model, fluctuating either above or below the black line, the internal temperature of the cob model. The reader will have noticed that the internal temperatures represent the downstairs area of the model. From graphs 9.2, 9.3, 9.4 and 9.5, it can be seen that there is very little difference between the behaviour of the internal air temperature of the upper and lower stories of either the cob or the timber frame models. Because of this it is felt that by using downstairs internal air temperatures in graph 9.1 the results are representative and the interpretation of the results is considerably simplified.



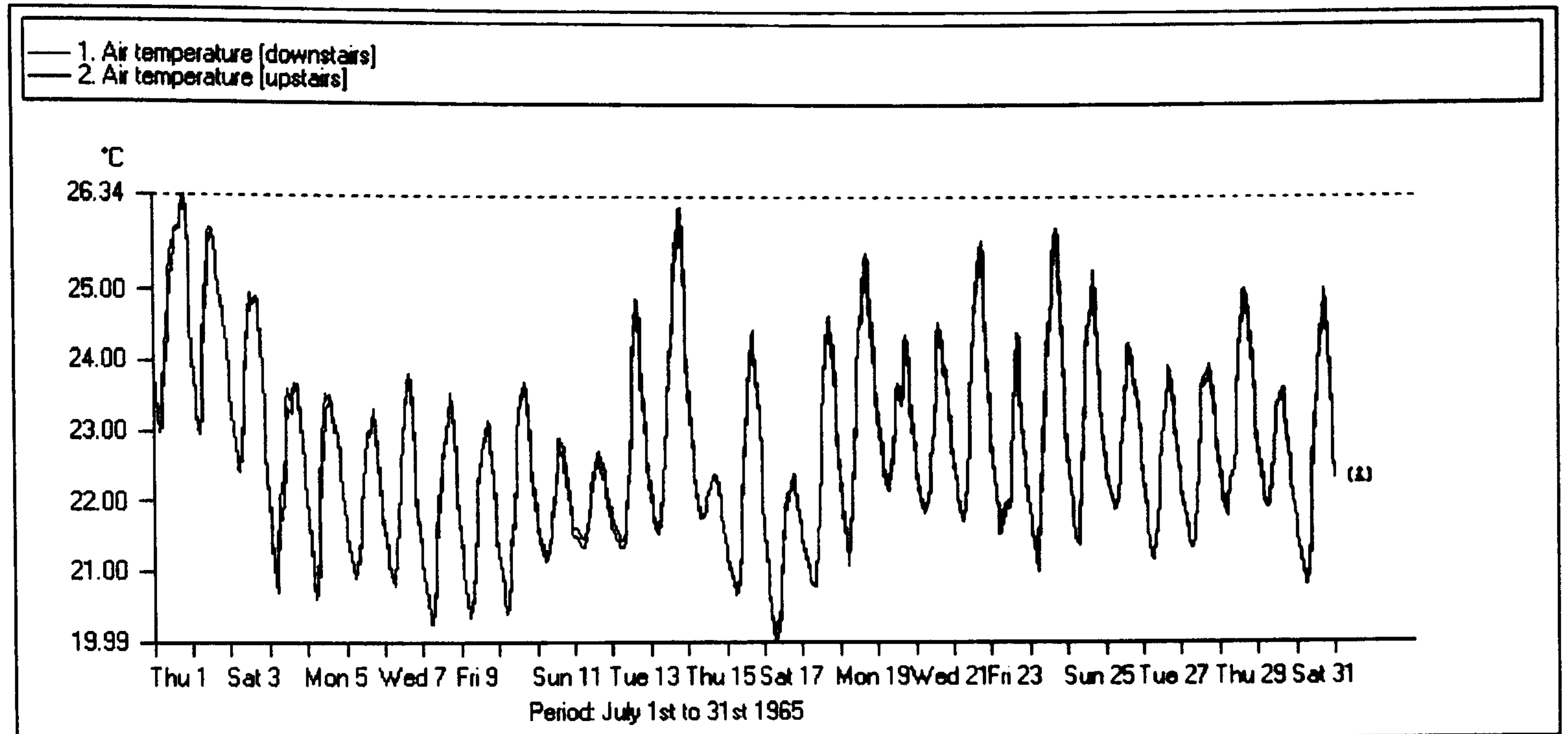
Graph 9.2, shows a comparison of upstairs and down stairs, January internal air temperatures for the cob model.

The winter average internal air temperatures for the cob model, shown in graph 9.2, vary between 12.4 °C and 5.9°C. It can also be seen that the upper and lower storeys have very similar internal air temperatures. The diurnal variations are approximately 1.5 to 2°C.



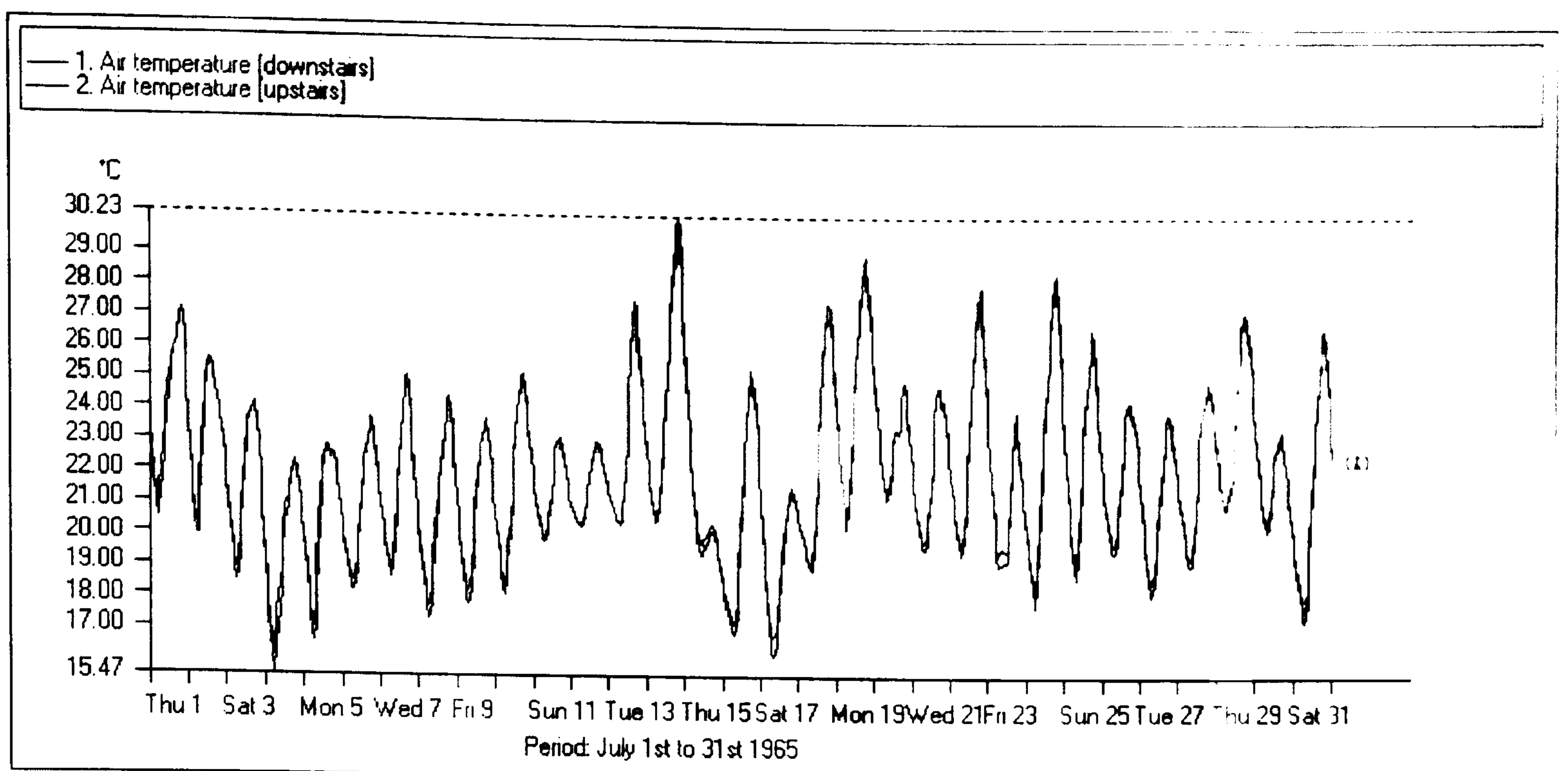
Graph 9.3, shows a comparison of upstairs and down stairs, January internal air temperatures timber frame model.

The variations in average internal winter temperature for the timber frame model vary between 14.82 °C and 3.03 °C, showing a larger range of internal temperatures than the cob model. The diurnal range varies more than the cob model, showing differences of up to 7 °C.



Graph 9.4, shows a comparison of upstairs and down stairs, July internal air temperatures for the cob model.

Much as for the winter studies, during the summer the average internal air temperatures of the upper and lower storeys of the cob model are very similar. The maximum internal air temperature is 26.26°C and the minimum is 20.14°C, so the range of highest to lowest temperatures is 6.12°C, which is very similar to that range found in the winter cob model, 6.51°C.



Graph 9.5, shows a comparison of upstairs and down stairs, July internal air temperatures, timber frame model.

The shape of the curves for the cob model in graph 9.5 is very similar to the curves described in graph 9.4 for the timber frame model. This is unsurprising as both models were simulated using the same weather data. However, the maximum average internal temperature of the timber frame model is 29.71°C, much higher than the maximum average internal temperature of the cob model. The minimum average internal air temperature of the timber frame model is 16.16°C, approximately 4°C less than the corresponding temperature in the cob model. Like the cob model, the range of highest to lowest temperatures in summer, 13.55°C, is similar to the maximum to minimum average internal temperature range in the timber frame model during the winter, 13.55°C. Summary data from the single month cob and timber frame simulations can be seen in table 9.1

Statistic	Traditional cob building, January internal air temperature (°C)	Timber frame dwelling, January internal air temperature (°C)	Traditional cob dwelling, July internal air temperature (°C)	Timber frame dwelling, July internal air temperature (°C)
Minimum	5.91	3.03	20.14	16.16
Maximum	12.42	14.82	26.26	29.71
Max - Min	6.51	11.79	6.12	13.55
Mean	9.08	8.71	22.73	22.05

Table 9.1, show a summary of the minimum, maximum and mean air temperatures from the two models simulated using Apache Sim.

As can be seen from table 9.1 the variation in temperatures between the cob building and the timber frame model are different. When identical weather data is used to simulate external conditions around each of the models, both give different internal temperatures. The range between the maximum and minimum air internal temperatures for the cob building is 6.51 °C in January and 6.12°C during July. The range between the maximum and the minimum temperatures for the timber frame model are wider, 11.79 °C in January and 13.55 °C during July. However, the mean average internal temperatures are quite similar when comparing winter to winter, 9.08 °C, (cob) 8.71 °C, (timber frame) and summer to summer figures, 22.73 °C, (cob), 22.05 °C (timber frame). Thus, if the mean of the average internal temperatures were quoted in an attempt to describe the thermal behaviour of the two models a reader might draw the conclusion that there was little difference between each model's thermal behaviour. A more accurate description of how each model behaves can only be seen if the ranges of temperature variation are taken into account. The previously quoted temperature range of about 6 °C for the cob model and about 12-13 °C for the timber frame model shows that the average internal air temperature remains more stable within the cob model. The difference in the stability of the thermal environment inside the models can only be attributed to the two different walling materials, as the simulation models are identical in all other aspects.

These findings do, in part, confirm the work carried out by Krarti & Claridge (1990), Jayashankar (1989), Meixel et al. (1981) and Lloyd-Jones (1983). Much as these authors suggest the temperature ranges described by the simulations of the cob model are much smaller than the timber frame model. As these average internal temperature variations are damped, this may, in part, also support the many pieces of anecdotal evidence indicating that cob buildings have an agreeable internal climate.

Chapter 10

Conclusions and Future Work.

Conclusions

This work has explored the application of a time dependent probe technique to satisfy five criteria: that the technique should be (i) non-destructive, (ii) must not influence the material being measured, (iii) should give representative values for both the thermal conductivity (λ) and thermal diffusivity (α), (iv) should be rapid and affordable and (v) should allow *in-situ* testing.

The aims of this investigation, as described in the introduction and commented upon in the discussion section of this thesis, have been achieved. For example, this work has demonstrated that the time dependent probe is appropriate for obtaining both the thermal conductivity and the thermal diffusivity properties of cob and other materials to an acceptable degree of accuracy.

Let us concentrate upon three of the criteria that this study set out to investigate, concerning the non-destructive, non-influential and affordable nature of the measurement system. The technique was felt to be unintrusive, allowing measurements to be taken without unduly affecting the walls integrity. The physical size of the probe was small compared with the size of typical specimens. The small size of the probe and the relatively inexpensive materials and equipment used in the measurement system also keep the cost of building such a system to a minimum. The technique uses low probe heater powers (the values used during field measurements were approximately 0.3W), this reduces the migration of moisture to a minimum and avoids the corresponding effects upon the value of the thermal conductivity of the specimen. However, it was found that

when probe heater power values of less than 0.03W were used the corresponding small rises in probe temperature made the results from the technique less certain and prone to influence by fluctuations in the ambient temperature. The short measurement times and relatively simple analysis techniques that have been developed allow the rapid identification of the thermal properties of a sample. However, although a measurement run may well only take approximately 2000 seconds, to ensure representative results, the sample will still need to be left undisturbed for a period of time, such as 24 hours, before any measurements may be made.

Another focus of this study, criteria (iii), is to secure representative values of thermal conductivity and diffusivity of the chosen specimens. The long time analysis technique, developed by Carslaw and Jaeger and then by Blackwell and Batty et. al., has been used to confirm the thermal conductivity of a range of materials in the laboratory. The laboratory measurements allowed the time dependent probe technique to be calibrated using materials of known thermal characteristics. Examples of the results from the long time analysis include measurement of the thermal conductivity of paraffin wax as $0.261 \text{ Wm}^{-1}\text{K}^{-1}$, against a published value of λ , of $0.251 \text{ Wm}^{-1}\text{K}^{-1}$ (Batty et. al., 1984). A lightweight concrete block had a measured thermal conductivity of $0.126 \text{ Wm}^{-1}\text{K}^{-1}$ compared with the manufacturer's figure of $0.12 \text{ Wm}^{-1}\text{K}^{-1}$. With this work completed, the study focused upon the evaluation of the thermal diffusivity in laboratory and field conditions.

As the reader will recall, the probe conductance, H , a value representing the thermal contact conductance between the probe and the material, had to be known to reproduce representative values of the thermal diffusivity of a sample. Several methods of confirming this vital element were established. The short time analysis first suggested by Blackwell (1954), was used, as far as the author is aware, for the first time, to measure H

for a range of materials in laboratory conditions. The value of the probe conductance was $50 \text{ Wm}^{-2}\text{K}^{-1}$ when a probe was placed into a hole in a lightweight aerated concrete block without any sink material used. This increased to approximately $150 \text{ Wm}^{-2}\text{K}^{-1}$ when a probe was placed in the same block but with heat sink material in the hole. An upper value of probe conductance was suggested by using a liquid as the specimen, a material that would theoretically be in good thermal contact with the probe. The probe conductance values for glycerine averaged approximately $300 \text{ Wm}^{-2}\text{K}^{-1}$, roughly double the H values used in the solid material with heat sink material, which, in turn, were double those measured in the solid sample without heat sink compound. Further measurements of H in a range of materials, with and without heatsink compound, replicated this pattern of results. Although preliminary in nature, these results give a better understanding of the magnitude of the thermal conductance between the probe and the sample material and allow the use of the second term in equation 2 chapter 5. This, in turn, allows the calculation of thermal diffusivity values, α , which before any established method for finding H was used, had to be estimated. The assumption that H is large in all instances has been shown by this work to be inappropriate.

To enable the analysis of earlier incomplete data, the Microsoft Excel Solver iterative routine was used. The Solver iterative method allowed the simultaneous calculation of H , α and λ for a single or twin thermocouple probe, using data taken at 1, 5 and 10-second intervals. The Solver routine was particularly helpful in obtaining values for the probe conductance, H , when the short time analysis method was unavailable in the earlier studies, when data was collected at 5 or 10-second time intervals. As an investigative tool Solver enabled a full analysis of the raw data that before would have had only limited value.

The investigation of methods to improve the probe's thermal conductance indicated that improvements in H can be achieved by the use of small quantities of heat sink compound. Corresponding improvements in the values of thermal diffusivity were observed. The first values of thermal diffusivity, α , were found from using an estimated H value in the B term of the long time equation, equation 2 in chapter 5. The resulting range of thermal diffusivity, α , of over 10^{13} was obviously unacceptable. The Blackwell short time analysis using the first 60 seconds of data recorded at one-second intervals combined with the use of heat sink compound gave more realistic thermal diffusivity values for the sample materials. Using this method and one second intervals between data collection, the thermal diffusivity values for paraffin wax gave a relatively stable value of $1.07 \times 10^{-7} \text{m}^2\text{s}^{-1}$, which although not a perfect match, compares well with the published value of $9.62 \times 10^{-8} \text{m}^2\text{s}^{-1}$, (Carslaw and Jaeger, 1947). The combination of the use of Blackwell short time analysis and the measurement of H , enable the time dependent probe technique to establish credible values for α , representing a significant achievement and increased scope for the use of this measurement method.

The final development of a thermal probe with twin thermocouples allowed the analysis of the heat flow across the boundary between the probe heater and the specimen. This new technique differed from the early studies since the probes had an additional thermocouple, the original at the centre of the probe as before and a second at the interface between the probe outer surface and the specimen. The analysis method used was termed the short time rate method, or rate method. The short time rate method was developed as another technique to find the probe conductance, H and hence the thermal diffusivity. A further variable, the probe thermal capacity, mc , is a function of the mass and the specific heat capacity of the probe, the heater, and thermocouples and can also be determined. Although many of the values, such as the value of the probe thermal conductance, found using the rate method were not in agreement with the short time

method, the general trends predicted by the rate method were very similar to those indicated by the short time method. It is felt that the rate method is a promising technique and with further work with carefully constructed twin thermocouple probes, will help to confirm and provide a valuable check upon many of the findings of the other analysis methods. To conclude the practical aspects of the time-dependent probe technique, here is a check list which summarises both the physical and analytical factors for an ideal measurement system. Following the many threads of this investigation and with the five criteria for the data collection system set by this study in mind, here is the ideal system.

1. A probe that has a large length to radius ratio and small wall thickness should be used, thus satisfying the requirement for an instrument that can be approximated as a line heat source. This will, as previously discussed, allow the technique to be non-destructive.
2. Probes with two thermocouples, one central and another placed on the outer wall of the probe surface should be used. This will allow the thermal capacity of the probe, and the probe to specimen conductance, to be determined and hence allow the specimen thermal conductivity and diffusivity to be measured with reasonable certainty.
3. A high conductivity material should be used to fill the probe and fill between the probe and the specimen to increase the value of the probe specimen conductance, H .
4. The technique has a data collection time interval of one second for a significant period of time, to ensure the required quality of the measured data. Data should be collected for at least 100 seconds before the heater power is switched on.
5. To allow for the different thermal properties of specimens, it is wise to undertake several trial runs using different heater powers to ascertain the optimum probe heater power to be used, corresponding to appropriate rises in temperature. These rises should be between 3 and 20K.

6. Enough data at one second or less intervals should be recorded to ensure that an accurate picture of the thermal performance of the specimen is mapped. It is recommended that the probe temperature versus time curve is followed for at least 3000 seconds, although not all of this data will be required to calculate the thermal properties of the specimen.
7. The Blackwell long-time method, using a graph of rise in probe temperature against the natural logarithm of elapsed time, should be used to give the thermal conductivity, λ , of the sample, using a suitable regression analysis.
8. The short-time rate method should be used to plot $d\theta_1/dt$ versus $(\theta_1 - \theta_2)$ to give the thermal capacity of the probe, mc , and the thermal conductance, H_r , between probe and specimen.
9. The Blackwell short-time method should be used to obtain another value of the probe-specimen conductance, H_b , for comparison with H_r .
10. The Microsoft Excel Solver iterative routine can then be used along with all four of the Blackwell long-time constants A,B,C and D in equation 2, chapter 5 to find H and α , with a range of H (H_r to H_b) and λ from item 7 using λ_{\max} and λ_{\min}^* as the range for λ .

* λ_{\max} and λ_{\min} refer to the thermal conductivities calculated using combinations of the highest and lowest values of long time line slope and heater power.

The final stage and the main focus of this study was to obtain *in-situ* representative thermal values of cob walls. A unique arrangement of measurement apparatus was developed which would allow the previous laboratory based technique to be portable and allow the measurement of thermal values in the field. After a series of trials using three different cob buildings, the technique was perfected to a point where reliable values of the thermal conductivity and diffusivity were measured. Building upon the developments from the previous laboratory measurements, appropriate heater power levels and the use of heat sink compounds were investigated. A series of values for the thermal conductivity and diffusivity were found to equate well with those available in published data (Minke

1994), which concerned similar materials (see table 8.1 and graph 8.1 in chapter 8). Measurements were undertaken to establish that different probes could be used in the same sample hole with almost identical results. This work has demonstrated that the time dependent probe technique, employing an accurate DC powered logging and heater power supply system and using appropriate safeguards will provide representative values for both the thermal conductivity and diffusivity of *in-situ* cob walls.

To help summarise the results of this work here is a table illustrating the findings of the measurement programme.

Material/Field study location	Measured Values		Published Values	
	Mean Thermal Conductivity $Wm^{-1}K^{-1}$	Mean Thermal Diffusivity m^2s^{-1}	Mean Thermal Conductivity $Wm^{-1}K^{-1}$	Mean Thermal Diffusivity m^2s^{-1}
Paraffin Wax	0.261 ± 0.034	$1.07 \times 10^{-7} \pm 2.9 \times 10^{-8}$	0.251	9.62×10^{-8}
Glycerine	0.293 ± 0.009	$2.26 \times 10^{-6} \pm 1.3 \times 10^{-7}$	0.292-0.314	$0.967 \times 10^{-7} - 1.1 \times 10^{-7}$
Phenolic Foam	0.029 ± 0.003	$1.69 \times 10^{-8} \pm 5.4 \times 10^{-9}$	0.032	1.00×10^{-7}
Lightweight Concrete	0.126 ± 0.01	$2.44 \times 10^{-8} \pm 5.0 \times 10^{-9}$	0.12	2.0×10^{-7}
Mudstud	0.558 ± 0.055	$5.26 \times 10^{-7} \pm 1.08 \times 10^{-7}$	There are no published values for these materials.	
Wychert	0.715 ± 0.048	$5.89 \times 10^{-7} \pm 1.17 \times 10^{-7}$		
Cobblock	0.368 ± 0.04	$4.65 \times 10^{-7} \pm 4.1 \times 10^{-7}$		
Cobwool	0.365 ± 0.018	$1.36 \times 10^{-7} \pm 1.5 \times 10^{-8}$		
Rezare	0.47 ± 0.14	$2.93 \times 10^{-6} \pm 2.0 \times 10^{-6}$		
Bovey Tracey	0.38 ± 0.007 (mean, sink in probe)	$2.24 \times 10^{-7} \pm 1.32 \times 10^{-7}$		
Frogmire	0.50 ± 0.04 (mean, sink in probe)	$3.31 \times 10^{-7} \pm 1.81 \times 10^{-7}$		

* Please note, the thermal conductivity figures for cobblock and cobwool have been shown with values to three decimal places unlike the other values. The differences between the measurements from these two materials are small and it is felt that it is informative for the reader to see that there is a difference in the two thermal conductivities.

Table 10.1, summary of the results from the laboratory and field studies.

This is a significant contribution; to our database of the properties of cob walls in Devon, to our understanding of the probe technique and to use in the gathering of field data. The thermal conductivity and diffusivity values obtained from the field studies were used in dynamic thermal simulations.

Using a dynamic thermal computer analysis program, Apache Sim., the predictions by previous authors, Meixel et al. (1981) and Krarti & Claridge (1990), of the damping effect of earth sheltered buildings upon ambient temperatures, were confirmed to be applicable to cob buildings. The comparison between a timber framed model building, prepared to current building regulations, and a similar cob building showed that the range of average internal temperatures of each model were different. The average winter and summer internal air temperatures of the timber frame model varied by between approximately 12 to 13.5°C compared with a difference of about 6°C with the cob model. This much reduced variation of average internal temperatures could be one of the reasons for the many anecdotal descriptions of cob building being warm in winter and cool in summer.

To summarise:

This work has demonstrated the feasibility of using the time-dependent thermal probe technique to measure the thermal properties of various building materials and to study cob walls in the field.

Crucial to this contribution was the development of a range of practical techniques and methods of analysis leading to the establishment of the probe thermal conductance, H . It has enabled the measurement of thermal diffusivity values that were previously reliant upon estimates of H , or the assumption that H was very large.

For the first time this work reports the results and methodology of a series of field studies regarding the measurement of the thermal conductivity and diffusivity of three Devon cob buildings.

These measurements, when used in a dynamic thermal simulation have confirmed the predictions of previous authors concerning the damping effects of earth structures.

Future Work

Some elements of this work, chiefly those pertaining to evolution of the probe technique including a range of different heat sink compounds and the perfection of a robust twin thermocouple probe, need to be developed to confirm the technique.

Another interesting avenue of research would be to repeat the theoretical derivation of the equation which describes the rise in probe temperature as a function of time. The aims here would be, to determine the $O(1/t^2)$ terms from equation 1 chapter 5, (as this has been neglected in this work) and also to explore the theoretical implications of filled probes. Since the solver routine generates better quality data with four constants, rather than with two, it is expected that further improvements would be possible if the $O(1/t^2)$ terms were included. In this way it is hoped that the agreement between published thermal conductivities and diffusivities and measured data can be further improved.

The three case studies undertaken as part of this study represent only a small number of the possible combinations of cob, soil and building type represented by the cob buildings of Devon. The time-dependent thermal probe technique can be used to undertake a comprehensive survey of the different varieties of Devon's cob buildings.

Other directions of future studies of these thermal properties may include the examination of the role of the moisture content on the thermal conductivity and diffusivity of materials in *in-situ* tests. Structural and thermal properties can be investigated in conjunction with varying straw and density values of cob and other unbaked earth walling systems. The broad effects of using the *in-situ* technique during summer and winter conditions can be investigated.

The technique has been developed into a novel tool which is useful for obtaining the two necessary thermal properties of cob walls. However, other materials used in the construction industry and other industries can benefit from the use of *in-situ* thermal measurements. *In-situ* studies undertaken upon materials that vary in density, homogeneity and other physical properties, will introduce different challenges to the existing field study arrangement. Further work can examine the suitability of the technique and develop solutions to problems encountered in the field.

Future results can then be fed-back into thermal simulations further improving the accuracy of the models used.

References.

Banaszkiewicz, M., Seiferlin, K., Spohn, T., Kargl, G., Komle, N., 1997 *Simultaneous measurement of the thermal conductivity and thermal diffusivity of unconsolidated materials by the transient hot wire method*. Rev. Sci. Inst. American Institute of Physics; Vol. 56, No 7, pp 4184-4190

Batty W. J., Probert S. D., Ball M, and O'Callaghan P. W., 1984 *Use of the thermal-probe technique for the measurement of the apparent thermal conductivities of moist materials*, Applied Energy, Vol. 18, pp 301-317.

Batty W. J., O'Callaghan P. W. and Probert S. D., 1984 *Assessment of the thermal-probe technique for rapid, accurate measurements of effective thermal conductivities*, Applied Energy, Vol.16, pp 83-113.

Blackwell, J., 1954 *A Transient-flow method for determining of thermal constants of insulating materials in bulk*, Journal of Applied Physics, Vol. 25, No 2, pp 137-144.

Bligh T. P. & Willard T. E., 1985 *Modelling the thermal performance of earth-contact buildings, including the effect of phase change due to soil freezing*, Computers & Structures, Vol. 21, No 1/2, pp 291- 318.

Buettner, K., 1955 *Trans Amer. Geophysics Un.*, Vol. 36, pp 827-30

Building Research Board. 1922 *Special Report 5: Building in Cob and Pise de Terre*. HMSO. (Overseas Building Note No 184, Stabilised Soil Blocks For Building.)

Bullard, E. C., Maxwell, A. E., and Reville, R., 1956 *Advanced Geophysics* Vol. 3 pp 153-81

CEBS, (Commonwealth Experimental Building Station), 1950 *Earth wall construction*, Notes on the science of building, No. 13, The building research liaison service, Sydney.

Carslaw H. S. and Jaeger, J. C., 1947 *Conduction of heat in solids*, 1st Ed. Oxford University Press, Oxford.

Carslaw H. S. and Jaeger, J. C., 1959 *Conduction of heat in solids*, 2nd Ed. Oxford University Press, Oxford.

Coventry, K., 2000, Straw contents and the structural implications upon cob, unpublished PhD Thesis, University of Plymouth,

CIBSE, (Chartered Institution of Building services Engineers), Guide A3. 1985 Thermal Properties of Building Structures, CIBSE, London.

Clarke, L. N. & Kingston, R. S. T., 1950 *Equipment for the simultaneous determination of thermal conductivity and diffusivity of insulating materials using a variable-state method*. Australian Journal of Applied Science Vol. 1.No 2, pp 172-87.

D'Eustachio, D. and Schreiner, R.E., 1952 *A study of a transient heat method for measuring thermal conductivity*. Transactions American Society of Heating and Ventilation Engineers: Vol. 58, No 1457, pp 331-42

DEBA (Devon Earth Building Association), 1996 October, *Cob and the Building Regulations*. Ed, Ley, T. and Widgery, M.

Devon Historic Buildings Trust, 1992 *The Cob Buildings of Devon, 1, Historic Building Methods and Conservation*. Devon Historical Buildings Trust .

D.o.E., 1995 UK Building Regulations, Part L, Conservation of Fuel and Power, HMSO, London.

E.D.S.L., Environmental Design Simulations Limited, 1989. T.A.S. Handbook.

Egeland, P., 1988 *Devon Cob and Thatch*. Devon Books, Exeter, Devon.

Facey, W., 1997 *Back to Earth. Adobe Building in Saudi Arabia*, Al-Turath in association with The London Centre of Arab Studies, Riyadh, pp 70-73

Ford, M., Unpublished *The Relevance of GIS in the Evaluation of Vernacular Architecture*, MPhil Thesis, University of Plymouth.

Fujii, M., Park,S.C., Tomimura,T., and Zhang,X., 1997 *A non-contact method for measuring thermal conductivity and thermal diffusivity of anisotropic materials*, International Journal of Thermophysics, Vol. 18, No 1 : pp 327-39

Glatzmaier, C. and Ramirez, F., 1985 *Simultaneous measurement of the thermal conductivity and thermal diffusivity of unconsolidated materials by the transient hot wire method*. Review of Scientific Instruments, Vol. 56, No 7, pp 1394-1398

Goldstein, 1932 Proceedings of the London Mathematics Society, No 34.

Gooch, B., 1990 *Vernacular Building: Thatched and Cob Cottages are Idyllic: True or False?* Architect and Surveyor, December.

Greer, M.J.A. 1996 The effect of Moisture content and Composition on the Compressive Strengths and Rigidity of Cob made from the Soil of the Breccia Measures near Teignmouth, Devon. PhD thesis, University of Plymouth.

Gustafsson, S. & Karawacki, E., 1979 *Transient hot strip method for simultaneously measuring thermal conductivity and thermal diffusivity of solids and fluids*. Nordic Symposium on Earth Heat Pump Systems, pp 55-61

Gustafsson, S., 1983 *Thermal properties of surface layers using pulse transient hot strip measurements*. 18th International Thermal Conductivity Conference, pp 553-64

Gustafsson, S. 1991 *Transient plane source techniques for thermal conductivity and thermal diffusivity measurements of solid materials*. American Inst. of Physics, Review of Scientific Instruments Vol. 62, No 3, pp 797-804

Gustafsson, M., Karawacki, E. and Gustafsson, S., 1994 *Thermal conductivity, thermal diffusivity and specific heat of thin samples from transient measurements with hot disk sensors*. American Inst. of Physics, Review of Scientific Instruments, Vol. 65, No 12, pp 3856-59

Highgate, D. and Mole, G., 1967 *A transient method of determining the thermal transmission properties of sand and other materials*, The Electrical Research Association Report No. 5231, Leatherhead.

Hooper, F.C. and Lepper, F.C., 1950 *Transient heat flow apparatus for the determination of thermal conductivities*, Transactions American Society of Heating and Ventilation Engineers: Vol. 56, pp 309-24.

- IES, Integrated Environmental solutions, 1999 Apache Sim. Operation Manual. Glasgow.
- Izhar-ul-Haq, M., 1991 *Simultaneous measurement of thermal conductivity and thermal diffusivity of rock-marbles using transient plane source (TPS) technique*, Heat Recovery Systems & CHP, Vol. 11, No 4, pp 249-254.
- Jayashankar B. C., Sawhney, R. L. and Sodha, M. S., 1989 *Effect of different surface treatments of the surrounding earth on thermal performance of earth integrated buildings*, International Journal of Energy Research, Vol. 13, pp 605-619.
- Jones, L., 1983 *Earth integrated farm buildings*, Concrete Construction, March, pp 229-33
- Karawacki, E. and Suleiman, B., 1992 *An extension to the dynamic plane source technique for measuring thermal conductivity and specific heat of dielectric solids*. American Inst. of Physics, Review of Scientific Instruments, Vol. 63, No 10, pp 4390-97
- Keefe, L. 1998. *An investigation into the Causes of Structural Failure in Traditional Cob Buildings*. M Phil thesis, University of Plymouth.
- Knox, A., 1978. *Living in the Environment*, Mullaya Publications, Victoria, Australia.
- Krarti, M. & Claridge, DE, 1990 *Two dimensional heat transfer from earth sheltered buildings*, Journal of Solar Energy Engineering, Vol. 112, pp 43-50.
- Lide, D. R. Ed, 1996 *CRC Handbook of Chemistry and Physics*, 77th edition, Chemical Rubber Corporation INC, CRC Press, Florida USA.
- McCann, JM. 1993 *Clay and Cob Buildings*. Shire Publications,

- Makowski, M. W. and Mochlinski, K., 1956 *Proc. Inst. Elect. Engrs.* Vol. A, No 103, pp 453-70.
- Mann, G., and Forsyth, F. G., 1956 *Modern Refrigeration*: Vol. 59, pp 188-91.
- Maqsood, A. *et al*, 1994 *Simultaneous Measurements of Thermal Conductivity and Thermal Diffusivity of Insulators, Fluids and Conductors Use the Transient Plane Source, (TPS) Technique.* International Journal of Energy Research, Vol. 18, pp 777-782.
- Mason, V.V., and Kurtz, M., 1952 *Trans. Amec. Inst. Elec. Eng.* Vol. 71, pp 623.
- Meixel, G.D. 1981 *Energy use of non-residential earth-sheltered buildings in five different climates*, The underground space conference and exposition, potential of earth sheltered and underground space. Chapter 43, pp 227-257.
- Minke, G., 1994 *Lehmbau - Handbuch, Der Baustoff Lehm und seine Anwendung*, Okobuch Verlag, Staufen bei Freiburg, pp 55-58.
- Minke, G., 1995 *Materialkennwerte von Lehmstoffen*, Bauphysik.
- Padfield, T., 1998 *Casting Mud in the Debate on Museum Environmental Standards*, <http://www.natmus.min.dk/cons/tp/mudbuf/mudbuf1.htm>
- Pearson, G. T., 1992 *Conservation of Clay and Chalk Buildings*, Donhead, London, pp 51-56.
- Sabuga, W. and Hammerschmidt, U., 1995 *A new method for the evaluation of thermal conductivity and thermal diffusivity from transient hot strip measurements*, International Journal of Thermophysics, Vol. 16, No 2, pp 557-65.

Sattel, G., 1980 *Determination of thermal conductivity and diffusivity of Rhinegraben-sediments with a new ring source device*, Advances in European Geothermal Research, 2nd International Seminar on the Results of EC Geothermal Research, pp 62-9.

Schleiermacher, A.L.E.F., 1888 *Wiedman Annalen Physik*, Vol. 34 pp 623.

Saxena, N.S., Joshi, S.R., Sarma, K. and Saksena, M.P., 1994 *Compositional dependence of thermal conductivity and thermal diffusivity of carbonate and silicate based rocks*, Indian Journal of Pure and Applied Physics, Vol. 32, pp 499-503

Skeib,G., 1950. *Z. Met.*, Vol. 4, pp 32-9.

Smith, B. J., et al, 1994 *Environmental Science*, Longman, London.

Smith, W. O. and Byres H. G., 1938 *Proc. Soil Sci. Soc. America*. Vol. 3, pp 13-19

Song, Y. W., Grob, U. and Hahne, E., 1993 *A new method for thermal diffusivity and thermal conductivity evaluation from transient hot-strip measurements*, Fluid Phase Equilibria, Vol. 88, pp 291-302.

Stalhane, B., and Pyk, S., 1931. *Ny method for bestamning av varmeledningskoefficienter*, Tekn. Tidskr, Vol. 61 No 28, pp 389-93.

Susa, M. and Nagata, K., 1993 *Thermal conductivity, thermal diffusivity and specific heat of slags containing iron oxides*, Iron & Steelmaking, Vol. 20 No 3, pp 201-03

Trotman, P., 1993. *Dampness in Cob Walls*, Devon Earth Building Association Seminar, Exeter, December 9th .

de Vries, D.A., 1952 *Meded. Landbhogesch., Wageningen* , Vol. 52, pp 1-72.

de Vries, D.A. and Peck A.J. ,1958 *On the cylindrical probe method of measuring thermal conductivity with special reference to soils*, Australian Journal of Physics. Vol. 11, pp 255-71.

Van der Held, E. F. M., and van Drunen,F.G., 1949 *Physica* pp 865-81.

Vilcu, R and Ciochina, A., 1981 *Absolute measurement of thermal conductivity and thermal diffusivity of liquids by classical procedure of the transient hot-wire method*, Revue Roumaine de Chimie Vol. 26, No 4, pp 527-37.

Volhard, F. and Westermarck, M., 1994. *Savirakentaminen - Kevytsavitekniikka*, RAK, Helsinki, pp 121-139.

Vos, B. H., 1955 *Measurements of the thermal conductivity by non-steady state methods*, Applied Science Res. , Section A, Vol. 5, pp 425-38.

Watanabe, H., 1997 *Accurate measurement of the thermal conductivity and thermal diffusivity of toluene and n-heptane*, International Journal of Thermophysics, Vol. 18, No 2, pp 313-25.

Wechsler, A. E., and Glaser, P. E., 1965 *Pressure effects on Postulated Lunar Materials*, Icarus, Vol. 4, pp 335-52

Weishaupt, J., 1940 *ForschArb. IngWes*, Vol. 11, pp 20-35.

Williams Ellis and J and E Eastwick-Field, 1947 *Building in Cob, Pise and Stabilised Earth*.
Country Life.

Woodside, W., 1958 *Probe for thermal conductivity measurement of dry moist materials*, Heating, Piping & Air Conditioning, Sept, 163-70.

Wright, A., 1980 *Craft Techniques for Traditional Buildings*, Batsford, pp 27-46.

Westermarck, M., 1997. *The manufacture and use of Nature-Based Building Materials as a Secondary Livelihood for Farmers*, Preliminary Research, 1st English Resume, Helsinki University of Technology, Faculty of Architecture, Research Unit for the Built Environment.

Yellott, J., 1975. *Solar Orientated Architecture*, The National Bureau of Standards, ASU, Tempe, Arizona, USA.

Bibliography – Books and Journals

Addy, SO. *The Evolution of the English House*, 1898, 2nd edition, (revised John Summerson, 1933).

Aslet, C. and Powers, A., 1986 *The National Trust book of the English house*, 1st edition Penguin Books, pp 53-63.

Ashurst, J. and N., 1983 *Practical Building Conservation*, English Heritage Technical Handbook Volume 2 : Brick, Terracotta and Earth, Gower Technical Press, pp 87-111 and 116-126.

Beacham, P., (Ed.). 1990 *Devon Building*, Devon Books, Exeter.

Blackwell, J.H., 1953 *Radial heat flow in regions bounded internally by circular cylinders*, Canadian Journal of Physics, Vol. 31, pp 472-479.

Blackwell, J.H., 1956 *The axial error in the thermal conductivity probe*, Canadian Journal of Physics, Vol. 34, pp 412-417.

Bondi, P. and Cali, M. 1974 *Rapid method for the measurement of the thermal diffusivity of rocks*, XIII International Conference on Thermal conductivity, pp 389-396.

Bouwens, D., 1994 *English mud-brick and mud building*, Context, No 34, Pub. The Association of Conservation Officers, pp 19-21.

Brown, R.J., 1979 *The English Country Cottage*, Robert Hale.

Brunskill, R.W., 1993 *Traditional buildings of Britain. an introduction to vernacular architecture*, 2nd edition, Gollancz, pp 89-91.

Chislett, H., 1995 *Gone to earth*, The Times Magazine, November 4th, pp50-51.

Ciochina, A. and Vilcu, R., 1983 *Transient hot wire method for absolute and simultaneous measurement of thermal conductivity and thermal diffusivity of fluids*, Revue Roumaine de Chimie Vol. 28, No 8, pp 795-804.

Doat, P., 1991 *Building with earth*, The Mud Village Society, 1st English edition, New Delhi, India.

Easton, D. 1996 *The rammed earth house*, Chelsea Green Publishing Company, Vermont.

Gillian, L. 1995 *Mud, Mud, Glorious Mud Devon Cob Houses*. Cottage and Castle, March, pp

29-33.

Graves, R.S. and Zarr, R.R., Editors, 1997 *Insulation materials, testing and apparatus*, 3rd volume, ASTM STP1320, pp 109-127, 141-151 and 337-354.

Houben, H. and Guillaud, H., 1994 *Earth Construction*, Intermediate Technology Publications.

Henry, K. and Coumou, K.G. 1991 *New direct measurement techniques for thermal conductivity, thermal diffusivity and specific heat capacity*, 19th Annual NATAS Conference , Boston, 23-26 September 1990, pp 129-134

Jackson, A.J., Adams, J. and Millar, R.C., 1978 *Thermal conductivity measurements on high temperature fibrous insulation by the hot wire method*. Thermal Transmission Measurements of Insulation, Tye, R.P. Ed., American Society for Testing and Materials, pp 154-171.

Jaeger J.C., 1959 *The use of complete temperature-time curves for determination of thermal conductivity with particular reference to rocks*. Australian Journal of Physics, Vol. 12, pp 203-217.

Jewson, N., 1913 Country Life Issue 22nd November.

Khoshtaghaza, M.H. et al, 1995 *Thermal diffusivity and thermal conductivity of alfalfa cube*, Canadian Agricultural Engineering, Vol. 37, No 4, pp 321-325.

Luo, J. and Stevens, R., 1997 *Thermal diffusivity/conductivity of magnesium oxide/silicon carbide composites*, Journal of American Ceramics Soc., Vol. 80, No 3, pp 699-705.

McHenry, P.G., 1989 *Adobe and rammed earth buildings*, University of Arizona Press, Chapters 11, 12, 15 and appendix a.

Munafo, P. and D'Orazio, M., 1997 *Hygro-thermic behaviour of earth-brick's masonries*, International Conference on Building Envelope Systems and Technology, Bath, April, pp 411-416.

Norton, J., 1986 *Building with Earth, A Handbook*. Intermediate Technology Publications.

Pradhan, P. R., 1991 *Temperature dependence of thermal conductivity and thermal diffusivity of some composites using the transient plane source technique*, International Journal of Energy Research, Vol. 15, pp 49-56.

Penn, C. 1999 *Old Cob Walls are right up to Date*, Western Morning News, October 18th, pp 27.

Price, W.L.V., 1983 *The calculation of thermal conductivity and thermal diffusivity from transient heating measurements*, Building and Environment, Vol. 18, No 4, pp 219-222.

Singe, R. et al, 1985 *Simultaneous measurement of thermal conductivity and thermal diffusivity of some building materials using the transient hot strip method*, Journal of Applied Physics, Vol. 18, No 1, pp 1-8.

Stubbs, 1954 *The Building Encyclopaedia*, Amalgamated Press, London.

Sumita, S. and Schumann, P., 1994 *Earth building today*, The Architects Journal, Sept, pp 48 - 50.

Vermat L.S., 1991 *Probe controlled transient method for simultaneous determination of thermal conductivity and thermal diffusivity*, Journal of Applied Physics, Vol. 26 No 2 pp 259-270.

Watanabe, H. 1996 *Accurate and simultaneous measurement of the thermal conductivity and thermal diffusivity of liquids using the transient hot-wire method*, Metrologia, Vol. 33, pp 101-115.

Watson and Harding (Ed.) 1994 *Out of Earth*, National Conference on Earth buildings, Dartington, Devon, University of Plymouth.

Watson and Harries (Ed.) 1995 *Out of Earth, II* National Conference on Earth buildings, Dartington, Devon, University of Plymouth.

Watt, J., 1994 *Mud glorious mud*, Perspectives, October, pp 53-56.

Webb, C., 1997 *Mud, mud glorious mud*, The Times, Saturday April 12, pp 8.

Woodside W. and Messmer, J. H., 1961 *Thermal conductivity of porous media. 1. Consolidated sands*, Journal of Applied Physics, Vol. 32, No 9, pp1688-1706

Bibliography – Web Pages.

Cob Builders Handbook www.cpros.com

Cob Code Project, www.deatech.com/natural/cobinfo.

Cob, Glorious Cob!, www.crofter.com/wotsit/wotsit_on_west_1213.html

Earth Architecture: an Overview, www.ran.org/ran

Earth Building and Their Repair, www.buildinfconservation.com/articles/masonry_earth

Earth Building Styles, www.Nzld.net/ebanz

Earth Sheltered Houses, www.eren.doe.gov/erec_factsheets_earth

Ecodesign, www.home.aone.net.au

Erec, www.eren.doc.gov

Natural Building systems, www.coopameriac.org

Sixth international conf, Terra, www.netstoreusa.com

Sustainable heating/cooling www.earthship/massandinulation

U.S. Icomos Newsletter www.icomos.org

APPENDIX A.

This appendix was added prior to the reproduction of the final thesis, and explores the background and application of the *Solver routine*, found in the Microsoft Office Excel 97 spread sheet package, which was used to determine the thermal properties of some of the samples studied in this work. This appendix has six sections; 1) Introduction, 2) a resume of the theory behind the probe technique, 3) Principle of the Solver routine, 4) the Solver model, 5) Setting up the spread sheet and Solver routine, and finally, 6) Some results with discussion and conclusions. The potential problem of errors in the experimental data is explored in section 7).

1. Introduction

By way of introduction to this discussion of the Solver routine, the section entitled, "Algorithm and methods used by Solver", to be found in the Excel help section, is reproduced as follows.

Microsoft Excel Solver uses the Generalised Reduced Gradient (GRG2) non-linear optimisation code developed by Leon Lasdon, University of Texas at Austin, and Allan Waren, Cleveland State University.

Linear and integer problems use the simplex method with bounds on the variables, and the branch-and-bound method, implemented by John Watson and Dan Fylstra, Frontline Systems, Inc. For more information on the internal solution process used by Solver, contact:

Frontline Systems, Inc., P.O. Box 4288, Incline Village, NV 89450-4288, (702) 831-0300

Web site: <http://www.frontsys.com>

Electronic mail: info@frontsys.com

Portions of the Microsoft Excel Solver program code are copyright 1990, 1991, 1992, and 1995 by Frontline Systems, Inc. Portions are copyright 1989 by Optimal Methods, Inc.

We would like to acknowledge with grateful thanks the efficient and rapid response of Tom Aird, Frontline Systems, who gave help and support in showing how to establish Solver routines, and clarified the terms and strategy used by the routine.

The present problem is classified as a non-linear unconstrained optimisation.

2. A resume of the theory behind the probe technique.

To introduce the Solver modelling studies, a brief resume of the theory behind the thermal probe technique is given below. This probe technique is being used to determine the thermal properties of earth walls found in many of Devon's buildings.

The time-dependent thermal probe technique employs a line heat source supplied with constant power Q (Watts). The probe has a mass m (kg), thermal capacity c_p ($\text{J kg}^{-1}\text{K}^{-1}$), a length L (m) with an external radius r (m). To minimise the error due to axial heat flow from the probe we followed Blackwell, and, as a result, the ratio of probe length to radius was in the region of 50. The probe is placed in a specimen with thermal conductivity λ ($\text{W m}^{-1}\text{K}^{-1}$) and thermal diffusivity α (m^2s^{-1}). This specimen is assumed to be of infinite extent and at a uniform initial temperature θ_i (C). Between the outer surface of the probe and the specimen there is a thermal contact conductance H ($\text{W m}^{-2}\text{K}^{-1}$). After careful measurement of the specimen's initial temperature, the power Q is switched on and the probe temperature θ (C), (measured by the E type thermocouple at the centre of the probe), increases with the elapsed time t in seconds. The rise in probe temperature $(\theta - \theta_i)$ C with time is recorded, and then analysed assuming the rise in probe temperature as a function of time is given approximately by the following expression, where γ is Euler's constant with a value 0.57722.

$$\theta = (Q/4\pi\lambda l) \{ \ln(4\alpha t / r^2) - \gamma + 2\lambda/rH + (r^2/2\alpha t) [\ln(4\alpha t / r^2) - \gamma + 1 - (\alpha mc/\pi r^2 l \lambda) (\ln(4\alpha t / r^2) - \gamma + 2\lambda/rH)] + \text{other terms } (r^2/\alpha t)^2 \} \quad 1$$

We have assumed that the “other terms with $(1/t)^2$ ” can be ignored, since as the time t increases this term will soon become negligible, and the rise in probe temperature as a function of time simplifies to;

$$\theta = A [\ln t + B + (1/t) (C \ln t + D)] \quad 2$$

$$\text{where } A = Q/4\pi l\lambda$$

$$B = \ln(4\alpha/r^2) - \gamma + 2\lambda/rH$$

$$C = (r^2/2\alpha)[1 - \alpha mc/\pi r^2 l\lambda] \quad \text{and}$$

$$D = (r^2/2\alpha) [\ln(4\alpha/r^2) - \gamma + 1 - B\alpha mc/\pi r^2 l\lambda]$$

This equation, equation 1, is described as non-linear since there is a term proportional to $(1/\lambda)$ times $\ln(\alpha)$.

3. The Solver routine and the principle behind this optimisation sum.

We have used the Microsoft Office Excel 97 Solver routine to determine values of the three unknowns, α , λ and H . In this thesis two different Solver routines have been studied. The first model used Solver2, a Solver routine with only the first two constants A and B in equation 2. Solver4 employs all four of the constants A , B , C and D in equation 2. In this appendix only the Solver2 routine will be explored. Solver4 requires knowledge of the probe thermal capacity mc_p , and this information is not readily available. We input a trial value for each of the three unknowns, α , λ and H . Solver2 uses an iterative process to find the minimum of the square root of the sum of the differences between experimental rise in probe temperature θ_e and the calculated, or trial, rise in probe temperature θ_t determined at the same elapsed time, all squared. In other words Solver2 looks for the minimum;

$$\text{Sum} = [\Sigma(\theta_e - \theta_t)^2]^{1/2} = 0$$

4. The Solver Model.

The table below gives the data that were used to create the model to compare with the experimental results using the Solver routine. The Solver routine is designed to optimise non-linear problems. Here we have a non-linear problem since there are products of the unknowns in the expression for the rise in probe temperature. The solutions sought are not constrained in anyway, we do not know the results at the start, and practically there are no reasons why any solution should lie in any particular region, except that the solutions should be positive and of appropriate physical magnitude. Solver is ideal for this application, and the limitations will be due to the theoretical temperature versus time expression and the experimental errors, not due to the Solver routine. We are therefore using Solver for an unconstrained non-linear optimisation.

Table of values used to construct the Solver model.

MATERIAL AND CODE		For Solver model	
Thermal conductivity	(Wm ⁻¹ deg ⁻¹)	λ	0.25
Thermal diffusivity	(m ² sec ⁻¹)	α	10 ⁻⁷
Probe contact conductance	(Wm ⁻² deg ⁻¹)	H	100
Power	(Watts)	Q	0.25
length of probe	(m)	L	0.065
Radius	(m)	r	0.0013

The Solver model uses a simplified equation for the trial temperature θ_t with the three unknowns λ , α and H expressed as ratios in x, y and z. Here, we write $x = 0.25/\lambda$.

$y = \text{Ln} (4 \alpha / (r^2)) / \text{Ln} (4 \cdot 10^{-7} / (0.0013)^2)$ and $z = 100 / H$. These variables x, y and z have values close to unity, and a form that simplifies the expression for θ , equation 1 above, that can now be written as:

$$\theta_t = AS^2x (\text{Ln} (t) + BS^2 y - 0.57722) + CS^2 z. \quad 3.$$

Here the constants have values;

$$AS2 = Q/\pi L = 1.224269,$$

$$BS2 = \text{Ln} (4 \cdot 10^{-7} / (0.0013)^2) = -1.441019, \quad \text{and}$$

$$CS2 = Q/(200\pi rL) = 4.70873.$$

Note that in the various studies, the values of the probe power, probe length and radius must be the relevant ones, and entered into the model.

5. Setting up the spread-sheet.

In the present Solver routine there are three named cells, say E20, F20 and G20, and initial guesses or trial values of x, y and z are placed in these cells, say $x = y = z = 1$.

The naming follows the path, Insert, Name, Define from the general tool bar in the Excel spread sheet. The values of θ_t are calculated as a function of time and the differences ($\theta_e - \theta_t$) are found. By squaring these differences the negative components can be made positive and the total sum of the differences squared can be found. Solver then seeks values of x, y and z that minimise the square root of this sum. It is then a simple matter to convert these values of x y and z back into λ , α and H. On calling the Solver routine, in the Tools drop down menu, the Solver parameters window appears, and the "Set target cell" allows the identification of the target cell, where the sum of the differences is to be minimised. Here the "Equal to" a "minimum" must be selected, and the "By changing cells" are identified as E20:G20, the initial trial values.

The routine was used in the default mode, that is with a maximum time 100 seconds, number of iterations 100, precision 10^{-6} , (tolerance 5%*), convergence 0.001 with tangent estimates, forward derivatives and Newton searches

* Only applies when constraints are imposed upon integers

The completed optimisation values are, when found, inserted back into their appropriate ratios, to find λ , α and H.

6. Discussions and conclusions.

For this appendix and to demonstrate the application of the Solver routine we studied SAE 10W-30 engine oil. The usual experimental system was used, and a viscose liquid ensured good thermal contact between probe and specimen. However, in a liquid convection currents soon become established and the conduction between probe and still specimen is no longer probable. However, the experimental data showed a linear plot between 20 and 100 seconds when the rise in probe temperature was plotted against the natural logarithm of the elapsed time. After about 130 seconds the rise in temperature was smaller for the same heat input suggesting that the heat is being transferred away from the probe more quickly due to the convection currents in the fluid. A regression analysis on this line gave the thermal conductivity as $0.146 \text{ Wm}^{-1}\text{K}^{-1}$. After a long time, some 1000 seconds the probe constant was calculated to be $68.5 \text{ Wm}^{-2}\text{K}^{-1}$, and the thermal diffusivity was $4.75 \cdot 10^{-8} \text{ m}^2 \text{ s}^{-1}$. On applying the Solver routine to the 20 to 100 second section of the data the thermal conductivity was $0.147 \text{ Wm}^{-1}\text{K}^{-1}$, the thermal diffusivity $1.07 \cdot 10^{-7} \text{ m}^2 \text{ s}^{-1}$ with the probe conductance $92.4 \text{ Wm}^{-2}\text{K}^{-1}$. We conclude that the conductivity is $0.147 \text{ Wm}^{-1}\text{K}^{-1}$, the thermal diffusivity is $7.73 \cdot 10^{-8} \text{ m}^2 \text{ s}^{-1}$ and the probe conductance $80.5 \text{ Wm}^{-2}\text{K}^{-1}$.

The book entitled, "Heat Transfer with applications", by Kirk D. Hagen, published by Prentice Hall in New Jersey, 1999, gives tables for the thermal properties of this oil. The experimental results were obtained at a mean temperature of 24.5C and at this temperature Hagen gives the following values the SAE 10W-30 engine oil, conductivity $0.136 \text{ Wm}^{-1}\text{K}^{-1}$ and diffusivity $8.51 \cdot 10^{-8} \text{ m}^2 \text{ s}^{-1}$. The long time regression analysis appears to under estimate the diffusivity, while the Solver routine over estimates this parameter.

7. Influence of errors in the temperatures

To enable the modelling studies to reflect some information on the Solver performance, the calculated temperatures were adjusted by the addition of random errors. The temperatures were produced so that they had the same degree of uncertainty as those determined in the laboratory.

First it is necessary to determine the uncertainty in the temperature measurements observed in the laboratory.

The recent studies on engine oil allowed an estimate of the standard deviations associated with the temperatures to be determined. For example, prior to switching on the heater current, the initial temperature was 16.845C with a standard deviation of 0.013C. Again, towards the end of this oil experiment the temperature had risen to 26.180C with a standard deviation of 0.012C. In the treatment of the results it is the rise in probe temperature that is used to determine the thermal properties. In this case the uncertainty in the rise temperature would have a range between a maximum of $26.180 + 0.012 - (16.845 - 0.013)$, or 9.360C, and a minimum of $26.180 - 0.012 - (16.845 + 0.013)$, or 9.336C. Expressed another way, we can say that the rise in temperature was found to be 9.348 ± 0.012 C. We would expect that over the course of the probe studies the range of useable rise temperatures would be from 4 to 18C, while the standard deviation in the measured temperatures would remain constant at 0.013C. In order to demonstrate the application of the Microsoft Office Excel 97 Solver routine, a probe specimen model will be used to generate temperature versus time curves. The Excel random number generator, $\text{Rand}() \cdot (b-a) + a$, will generate random numbers between a and b. This tool will be used to calculate errors to perturb individual probe rise-temperatures. Since the standard deviation only includes some 67% of the samples, and to allow for the random number generated temperatures to be optimistic, the assumed error will be $2 \cdot 0.012$ C or 0.024C. This means that the percentage errors in the probe rise temperatures will be 0.6% at 4C falling to 0.13% at 18C. As an example, for a theoretical rise temperature of 9C, then the modelled temperature would be given by the expression,

$\text{Rand()} * [9 + 0.024 - (9 - 0.024)] + (9 - 0.024)$

In a trial of this expression the first five of fifty temperatures generated were 9.017, 9.008, 8.979, 9.001, and 8.977C. Using the Descriptive Statistics package, in Excel, on these fifty temperatures gave the mean temperature as 8.9992C, with standard error 0.00169, standard deviation of 0.0119, with maximum and minimum temperatures of 9.024 and 8.977C respectively. The standard deviation obtained from these results of 0.0119C agrees well with the values previously determined for the oil data above of 0.013 and 0.012C. In the Solver modelling the example temperature of 9C, in the sum above, will be replaced by a probe rise-temperature Q calculated from the theoretical expression number 1.

Thermal probe, based upon a design by Cranfield University (Batty 1984).

